Brain-behaviour relationships and individual variability in cognitive and emotional processing

Inaugural-Dissertation

zur Erlangung des Doktorgrades der Mathematisch-Naturwissenschaftlichen Fakultät der Heinrich-Heine-Universität Düsseldorf

vorgelegt von

Nevena Kraljević

Düsseldorf, Juni 2025

aus dem Institut für Systemische Neurowissenschaften der Heinrich-Heine-Universität Düsseldorf
und
dem Institut für Neurowissenschaften und Medizin - Gehirn und Verhalten (INM-7) des Forschungszentrums Jülich.
Gedruckt mit der Genehmigung der
Mathematisch-Naturwissenschaftlichen Fakultät der
Heinrich-Heine-Universität Düsseldorf
Berichterstatter:
1. Prof. Dr. Simon Eickhoff
2. Prof. Dr. Gerhard Jocham
Tag der mündlichen Prüfung:

Eidesstattliche Erklärung:

Ich versichere an Eides Statt, dass die Dissertation von mir selbständig und ohne unzulässige fremde Hilfe unter Beachtung der "Grundsätze zur Sicherung guter wissenschaftlicher Praxis an der Heinrich-Heine-Universität Düsseldorf" erstellt worden ist. Die Dissertation hat in gleicher oder ähnlicher Form noch keiner anderen Prüfungsbehörde vorgelegen.

Düsseldorf, 12. Juni 2025	
Nevena Kraljević	

Table of Contents

1 AE	SSTRACT	<u> 7</u>
2 ZL	SAMMENFASSUNG	9
3 GE	ENERAL INTRODUCTION	11
<u> </u>	THE INTRODUCTION	<u> </u>
3.1	INDIVIDUAL DIFFERENCES IN BEHAVIOUR	12
3.1.1	COGNITION	12
3.1.2	AFFECT: EMOTION, SOCIAL COGNITION	13
3.2	Brain-Behaviour Relationships	14
3.2.1	STRUCTURAL MRI - GREY MATTER STRUCTURE	14
3.2.2	FUNCTIONAL MRI - FUNCTIONAL CONNECTIVITY	16
3.2.3	NEURAL CORRELATES OF COGNITION AND AFFECT	18
3.3	INFLUENCING FACTORS ON BRAIN-BEHAVIOUR RELATIONSHIPS	19
3.3.1	HERITABILITY	19
3.3.2	Prediction	
3.4	AIM OF THE STUDIES	21
4 S1	TUDY 1	າວ
7 31	001 1	<u></u> 20
<u>5 S1</u>	TUDY 2	<u>25</u>
6 SI	JMMARY AND GENERAL DISCUSSION	27
<u> </u>		£1
6.1	COGNITION AND AFFECT - INTEGRATED DIMENSIONS	
6.1.1	Brain Morphology and Heritability (Study 1)	28
6.1.2	FUNCTIONAL CONNECTIVITY AND PREDICTABILITY OF TASK STATES (STUDY 2)	29
6.1.3	COMPLEMENTARY RESULTS	29
6.2	LIMITATIONS AND OPPORTUNITIES	30
6.3	RELEVANCE AND IMPACT	32
6.4	CONCLUSION	33
7 RE	EFERENCES	35
. 111		<u></u>
8 AC	CKNOWLEDGEMENTS	45

1 Abstract

Human experience and behaviour is subject to multiple different mental processes, which can be separated into cognitive and socio-affective processes. Many studies investigate how experience and behaviour is linked to brain structure and function, and also how much influence can be attributed to our genetic makeup. However, little is known about how behavioural domains are subject to different influencing factors of inter-individual differences of the brain. In particular, how overlapping genetic influences exhibit in brain structure and which influence different functional task states drive in predictability of individual behaviour. Therefore, in my dissertation I investigated the phenotypic and genetic correlations of cognitive and affective traits and brain structure (cortical thickness, surface area and subcortical volumes; study 1). I further examined to what extent the correspondence of functional network priors and task states with behavioural target domains influenced the predictability of individual performance in cognitive, social, and affective tasks (study 2).

Using phenotypic correlation and heritability-analysis the first study investigated heritability and genes as influencing factors on inter-individual differences of the brain. Cognition revealed several associations with brain morphology, while trait affect revealed only few significant correlations with subcortical volumes and local cortical thickness, where it overlaps in left superior frontal cortex with cognition. Decomposing the phenotypic association into genetic and environmental components, revealed that the associations were accounted for by shared genetic effects between the traits. Using functional correlation and predictability of task states and network priors the second study investigated state- and network-specificity as influencing factors on brain-behaviour relationships, by predicting individual performance in cognitive, social, and affective tasks. Predictions from whole-brain FC were slightly better than those from FC in task-specific networks, and a slight benefit of predictions based on FC from task versus resting state was observed for performance in the cognitive domain.

With my dissertation I provide an integrative model of how cognition and affect relate to the human brain. By combining insights from structural anatomy, heritability modelling, and functional connectivity-based prediction, my results reveal that these traditionally distinct domains share common neural substrates. The superior frontal cortex has been identified as a heritable anatomical hub for both cognitive and affective traits. However, multivariate FC patterns during both task and resting states carried only moderate predictability of individual performance levels of cognition and socio-affective processes, manifesting nevertheless the influence of brain state and network dynamics in shaping individual behaviour. In sum, with these studies I replicated previous findings, but also extended insights into the interplay of cognitive and socio-affective processes with brain-behaviour relationships, and how different factors influence inter-individual differences in the brain.

2 Zusammenfassung

Menschliches Erleben und Verhalten unterliegt vielen verschiedenen mentalen Prozessen, die in kognitive und sozio-affektive Prozesse unterteilt werden können. In vielen Studien wird untersucht, wie Erleben und Verhalten mit der Struktur und Funktion des Gehirns zusammenhängen und welchen Einfluss genetischen Veranlagung spielen. Es ist jedoch nur wenig darüber bekannt, wie unterschiedliches Verhalten den verschiedenen Einflussfaktoren interindividueller Unterschiede des Gehirns unterliegt. Insbesondere, wie sich überlappende genetische Einflüsse in der Gehirnstruktur zeigen und welchen Einfluss verschiedene funktionelle Aufgaben auf die Vorhersagbarkeit des individuellen Verhaltens haben. In meiner Dissertation untersuchte ich daher die phänotypischen und genetischen Korrelationen von kognitiven und affektiven Merkmalen und der Hirnstruktur (kortikale Dicke, Fläche und subkortikale Volumina; Studie 1). Darüber hinaus habe ich untersucht, inwieweit die Übereinstimmung von funktionellen Netzwerken und Aufgabenzuständen die Vorhersagbarkeit der individuellen Leistung bei kognitiven, sozialen und affektiven Aufgaben beeinflusst (Studie 2).

Mit Hilfe phänotypischer Korrelationen und Heritabilitätsanalysen untersuchte die erste Studie die Heritabilität und Gene als Einflussfaktoren auf interindividuelle Unterschiede des Gehirns. Kognitive Prozesse zeigten mehrere Assoziationen mit Hirnstruktur, während Affekt nur wenige signifikante Korrelationen mit den subkortikalen Volumina und der lokalen kortikalen Dicke aufwies, wobei es im linken superioren frontalen Kortex Übereinstimmungen mit Kognition gab. Die Analyse der phänotypischen Assoziation in genetische und umweltbedingte Komponenten ergab, dass die Assoziationen durch gemeinsame genetische Effekte zwischen den Domänen erklärt werden konnten. Mit Hilfe der funktionellen Korrelation (functional connectivity; FC) und der Prädiktion von Aufgabenzuständen und Netzwerken untersuchte die zweite Studie die Zustands- und Netzwerkspezifität als Einflussfaktoren auf die Beziehungen zwischen Gehirn und Verhalten, indem sie die individuelle Leistung bei kognitiven, sozialen und affektiven Aufgaben vorhersagte. Die Vorhersagen aus der FC des gesamten Gehirns waren etwas besser als die aus der FC in aufgabenspezifischen Netzwerken. Für die Leistung im kognitiven Bereich wurde ein leichter Vorteil der Vorhersagen auf der Grundlage der FC aus dem Aufgaben- gegenüber dem Ruhezustand festgestellt.

In meiner Dissertation stelle ich ein integratives Modell vor, wie Kognition und Affekt mit dem menschlichen Gehirn zusammenhängen. Durch die Kombination von Erkenntnissen aus der strukturellen Anatomie, der Modellierung der Vererbbarkeit und der auf FC basierenden Vorhersage zeigen meine Ergebnisse, dass diese traditionell unterschiedlichen Bereiche gemeinsame neuronale Substrate aufweisen. Der superiore frontale Kortex wurde als vererbbarer anatomischer Knotenpunkt sowohl für kognitive als auch für affektive Merkmale identifiziert. Die multivariaten

FC-Muster sowohl im Aufgaben- als auch im Ruhezustand zeigten jedoch nur eine mäßige Vorhersagbarkeit des individuellen Leistungsniveaus bei kognitiven und sozio-affektiven Prozessen, was den Einfluss des Hirnzustands und der Netzwerkdynamik auf die Gestaltung des individuellen Verhaltens deutlich macht.

Zusammenfassend lässt sich sagen, dass ich mit diesen Studien nicht nur frühere Ergebnisse replizieren konnte, sondern um Erkenntnisse über das Zusammenspiel von kognitiven und sozio-affektiven Prozessen mit Gehirn-Verhaltens-Beziehungen erweitern konnte und darüber, wie verschiedene Faktoren interindividuelle Unterschiede im Gehirn beeinflussen.

3 General Introduction

Everyone is unique in experience, thought and behaviour, affect and cognition, but also brain structure and function. Understanding the link between the human brain, individual behaviour, thoughts and feelings, remains one of the greatest questions in neuroscience. Researching the link between brain and behaviour is a scientific pursuit that offers great potential for mental health and personalized medicine, by offering pathways to more precise diagnostic and therapeutic approaches. Therefore, investigating the human brain helps us to elucidate human inter-individual variability. Both within healthy individuals, and with regards to mental health and the treatment of brain disorders.

Human experience and behaviour is subject to multiple different mental processes. Roughly, these processes can be separated into cognitive and socio-affective processes. Many studies investigate how experience and behaviour is linked to brain structure and function, and how much influence can be attributed to our genetic makeup. However, little is known about how behavioural domains are subject to different influencing factors of inter-individual differences of the brain. In particular, how overlapping genetic influences exhibit in brain structure and which influence different functional task states drive predictability of individual behaviour.

There are various neuroscientific approaches in the quest to study human brain-behaviour relationships and to investigate how experience and behaviour is linked to brain structure and function: Some studies use electrophysiological methods, such as electroencephalography. Some use neuroimaging methods, such as structural magnetic resonance imaging (MRI), or functional imaging methods, such as functional MRI (fMRI). Some use genetic tools, such as genome-wide association studies or twin studies. Some use specific analytic tools, such as machine learning (ML) or predictive modelling, connectomics or network analysis, or functional decoding and meta-analytic annotation. But irrespective which are the chosen measures, in order to study behaviour, there need to be behavioural and psychometric measures. These can be conducted in tasks or in self-report questionnaires.

My dissertation focuses on the influencing factors of inter-individual differences of the brain, specifically, how genetic influences exhibit in brain structure, and how task states drive predictability of individual behaviour. For this, I will first elaborate on the specific behaviours investigated here – cognition and affect – and their relationship to the brain. Then, I will elaborate on heritability and functional task states, as influencing factors of inter-individual differences of the brain.

3.1 Individual differences in behaviour

Human behaviour is driven by different complex mental processes, that can be roughly separated into cognitive and socio-affective processes. Therefore, I decided to investigate cognition and affect as representations of human complex and rich behavioural variability. Despite covering only a fraction, they provide insight into how individuals perceive, interpret, and respond to their environment (Gross, 2015; Langner et al., 2018; Pessoa, 2008). As such, they serve as robust, multidimensional phenotypes for linking behaviour to underlying neural and genetic mechanisms.

3.1.1 Cognition

Cognition refers to mental processes involved in acquiring, processing, storing, and applying information. These processes include perception, attention, memory, language, reasoning, and executive control, including working memory, enabling individuals to interpret and respond to their environment. Intelligence is described as the capacity to carry out cognitive tasks effectively. It reflects how efficiently and flexibly cognitive processes are deployed, usually in novel or complex situations.

The human interest and contemplation about cognition and intelligence have a long history. A scientific approach on cognition dates back to the early nineteen hundreds, where Spearman framed the "general ability factor g" (Spearman, 1904). This was further investigated and developed by Cattel into two sub-constructs: crystallised and fluid intelligence (Cattell, 1943, 1963).

Crystallized intelligence refers to the ability to recognise and apply solutions through previously acquired knowledge and past experiences. It involves knowledge and skills accumulated over time, such as cultural and general knowledge. It can therefore improve with age, peaking in adult life, with only a slow decline until the age of 70 (Cattell, 1963; Hunt, 2001; Jones & Conrad, 1933; Salthouse, 2019).

In contrast, fluid intelligence refers to the ability to solve novel problems without relying on prior knowledge. Therefore, fluid intelligence is usually involved in tasks of non-verbal nature, such as solving mathematical or spatial problems. This involves quick, abstract, and flexible reasoning, as well as the ability to comprehend and manage multiple information simultaneously and manage the amount of information needed to solve the problem (Cattell, 1963). A core component of fluid intelligence is therefore working memory, the ability to maintain and update or manipulating relevant information (Baddeley, 2012; Hofmann et al., 2012; Little et al., 2014). On average, fluid intelligence reaches the maximum in ability in early adulthood and declines with age (Baltes et al., 1999; Jones & Conrad, 1933; Salthouse, 2019).

Crystallised and fluid intelligence are distinct but interconnected cognitive systems (Cattell, 1963; Tucker-Drob, 2009). The ability of fluid intelligence to solve novel

problems, reason abstractly, and adapt to new situations is required for acquiring and integrating new knowledge – which over time consolidates and contributes to crystallized intelligence. Furthermore, crystallized intelligence can support fluid intelligence by providing context and meaning. This bidirectional support is especially interesting, given that crystallised and fluid intelligence have different decline rates throughout life (Baddeley, 2012; Tucker-Drob, 2009).

Moreover, while working memory (WM) represents only one aspect of fluid intelligence, it has been shown to be a good proxy and representation for fluid intelligence (Colom et al., 2015). Furthermore, it has been investigated, that working memory capacity predict variation not only in fluid intelligence, but also crystallised intelligence (Alloway & Alloway, 2009; Martinez, 2019).

3.1.2 Affect: Emotion, Social Cognition

As a clear distinction between "emotion" and "affect" remains unresolved, the terms are often used interchangeably in the literature (Bradley & Lang, 2002; Pessoa, 2008; Salsman et al., 2013). Broadly, affect is a complex and multifaceted construct used to refer to emotional experience (Lindquist et al., 2012). Its elusive definition and inherently subjective, bodily nature makes it difficult to be measured in a standardized fashion (Nummenmaa et al., 2014). Therefore, measurement methods include self-reports, physiological indicators (such as heart rate or skin conductance), or the behavioural response to stimuli (Bradley & Lang, 2002). Nevertheless, in the assessment a distinction can be made between emotional processes and trait affect. On the one hand, affective traits can be assessed with self-reports, which are then divided into positive and negative traits. On the other hand, emotional processes, that pertain to identification and responding, can be assessed using tasks.

Trait affect is commonly measured through self-reports and divided into a positive and negative dimension, which are considered independent, instead of opposites. Hence, allowing both to be experienced at the same time (Diener & Emmons, 1984; Salsman et al., 2013). Positive affect includes emotions such as happiness, enthusiasm, and contentment, contributing to psychological well-being, including life satisfaction and a sense of purpose (Salsman et al., 2014). Conversely, negative affect includes emotions like anger, fear, and sadness, which can also manifest in varying intensities and are linked to negative self-evaluation or life dissatisfaction (Pilkonis et al., 2013; Salsman et al., 2013).

Emotion processing starts with a trigger and ends with a mental and behavioural response. Importantly, an emotional response can only be elicited with a relevant stimulus. Emotion processing refers to identifying, interpreting, and responding to emotional cues in oneself and others (Gross, 2015; Langner et al., 2018). It is closely linked to social cognition, which includes the understanding of others' thoughts and

feelings. It is crucial in engaging in effective social interactions, since it includes understanding both oneself and others as social beings.

Social cognition spans across both the cognitive and affective domain. Social cognition is linked to theory of mind, which is described as the ability to infer others' mental states, beliefs, intentions, and emotions. Theory of mind allows individuals to make sense of others' behaviour, predict and interpret social interactions and communicate effectively and appropriately in social settings (Bzdok et al., 2012; Salazar Kämpf et al., 2023; Wheatley et al., 2007).

Cognition and affect are essential behavioural domains, each representing distinct but interacting processes. Further, they each offer important insights into human individual behavioural variability. In sum, cognition includes attention, memory, reasoning and problem-solving. It is linked to information processing and goal-directed responses. Affect includes emotional states, responses and regulation, and is driven by reflexive, spontaneous responses. However, despite these distinctions, cognition and affect interact dynamically. Emotional states can bias decision-making, while cognitive appraisal can influence and regulate emotion processing. Furthermore, they are both influenced by internal and external stimuli (Langner et al., 2018; Pessoa, 2008). In my dissertation I aim to investigate these concepts both separately as well as their overlap.

3.2 Brain-Behaviour Relationships

To investigate the human brain and to link structure and function to behaviour, a lot of different neuroimaging modalities have evolved. The prerogatives of being non-invasive and in-vivo have been crucial for behavioural neuroscience. In my research I primarily focused on structural and functional MRI, while further using multivariate analyses comprised of heritability analyses and machine learning prediction.

3.2.1 Structural MRI - grey matter structure

Structural MRI captures the anatomy in a static, high-resolution image of the brain, while fMRI measures brain activity over time. Structural MRI takes advantage of the different densities of water content in the brain tissues. This is translated into images, where the different tissues and structures of the brain, such as grey and white matter, and cerebrospinal fluid can be distinguished. In my research I focused on grey matter structure. Grey matter can be found in the central nervous system, hence the spinal cord and the brain. It consists of neuronal cell bodies, dendrites, unmyelinated axons, astrocytes, oligodendrocytes, microglia and blood vessels. It plays a central role in sensory perception, motor control, and higher-order cognitive functions.

3.2.1.1 Cortical thickness and subcortical volume

Cortical thickness refers to the distance in millimetres between the white matter and the pial surface. The distance typically ranges between 1 and 4.5 millimetres (Fischl & Dale, 2000; Palomero-Gallagher & Zilles, 2019). Even though measuring the grey matter cortical thickness sounds simple, it is no small feat, since the pial surface is difficult to detect in standard MRI. Hence, (Fischl & Dale, 2000) developed with FreeSurfer an algorithm to estimate the grey and white matter boundary. This boundary representation is then deformed, with specific constrains, outward until the pial surface. From there, the distance to the white matter border at any point results in the cortical thickness (Fischl & Dale, 2000). This procedure requires both T_1 and T_2 weighted images to accurately map the grey matter as well as distinguish the pial surface from dura and blood vessels (Glasser et al., 2013).

Further, subcortical structures are neural formations in the basal brain, that have been shown integral in motor function, memory, and emotional and cognitive processing. They include deep grey matter structures and nuclei such as the thalamus, caudate, putamen, pallidum, hippocampus, amygdala, accumbens area, and ventral diencephalon. Similarly to cortical thickness, estimating the difference in tissue densities between subcortical structures and surrounding white matter, boundaries can be drawn and the subcortical volume can be calculated. Since the subcortical structures are integral in several behavioural processes, it is important to include them analogously to cortical thickness in brain–behaviour analyses.

3.2.1.2 Surface area

Surface area, understandably, refers to the surface of the cerebral cortex. It is intrinsically related to the cortical folding (gyrification). Therefore, most of the surface is hidden in the sulci (Chauhan et al., 2021), making it challenging to map out. Similar to cortical thickness and subcortical volume, the computation of surface area requires sophisticated processes. To automate and improve the delineation of the cortical surface, (Glasser et al., 2013) further enhanced the widely-used FreeSurfer pipeline for the Human Connectome Project (HCP) dataset (Fischl, 2012) used here. Both T_1 - and T_2 -weighted images are used to clearly define the white matter and pial surfaces and thereby the cortical ribbon. Following this ribbon, triangles are formed and summed to create a grid or mesh. This mesh transforms the cerebral cortex into a 2D sheet. This sheet can then be aligned to different spaces, such as the MNI surface space, to further allow for comparison between subjects.

Importantly, surface area is a morphological feature distinct from cortical thickness. It has been suggested that cortical thickness and surface area evolutionary developed independently (Geschwind & Rakic, 2013), are influenced by different genetic and environmental factors (Panizzon et al., 2009), and develop differently and

independently across the lifespan (Fjell et al., 2015; Hogstrom et al., 2013). Cortical thickness reflects neuronal density and dendritic arborization within a cortical column, while cortical surface area reflects the horizontal expansion of the cortical sheet and number of cortical columns. Therefore, it is important to look at them separately (instead of using cortical volume), as well as looking at them both, in order to understand the individual neural influences.

3.2.2 Functional MRI - functional connectivity

While structural MRI captures static images of the brain's anatomy by acquiring each brain slice once, functional MRI (fMRI) measures brain activity over time by repeatedly scanning the whole brain. fMRI is based on the effect, that active brain regions have increased metabolic demand, consuming more oxygen, resulting in an increased blood flow into the specific region. This vascular response results in a shift in the ratio of oxygenated to deoxygenated haemoglobin, producing the so-called Blood Oxygen Level Dependent (BOLD) contrast, which can be detected by the MRI scanner as changes in signal intensity. This alteration in regional blood oxygenation, the hemodynamic response, is observed over several seconds, with peaks at 3–5 seconds after a stimulus (Hillman, 2014).

To reliably capture these dynamics and acquire high-quality fMRI images, it is important to scan the brain with a repetition time shorter than the width of the hemodynamic response function. Additionally, shorter repetition time also improves artefact removal through e.g. physiological noise or head movement. Therefore, in the HCP high-resolution data with a repetition time of 0.72 seconds was acquired (Glasser et al., 2016). Further, spatial resolution is critical for accurately localizing BOLD signals and distinguishing between anatomical compartments such as grey matter, white matter, and CSF. Therefore, by acquiring functional data at 2 mm isotropic resolution, this further enables a precise location of the BOLD signal onto the cortex (Glasser et al., 2013, 2016). Despite significant technical differences between structural and functional imaging, acquired fMRI data can only be processed and analysed precisely by projecting the functional signals onto the structural surface reconstruction, providing an anatomically informed framework for analyses.

3.2.2.1 Resting-state and task-based FC

While the BOLD contrast is considered a proxy for neuronal activation, functional connectivity (FC) identifies correlations of activity between multiple regions of the brain. FC refers to the temporal (statistic) correlation of signal fluctuations between spatially distant regions, revealing distinct brain regions functioning in accordance, reflecting the functional integration of brain regions.

Since the brain is constantly active, the interactions between brain regions can be measured in the absence of tasks, hence during rest (resting-state FC), or during the performance of specific tasks (task-based FC). Resting-state FC captures BOLD signal fluctuations that occur in the absence of explicit tasks. It captures the intrinsic network structure of the brain, which have been shown to be stable and reproducible over time (Biswal et al., 1995). Commonly observed networks include the default mode network, frontoparietal network, dorsal attention network, and salience network (Biswal et al., 1995; Yeo et al., 2011). Resting-state FC is suggested to reveal baseline or "trait-like" properties of brain organization (Finn et al., 2015).

Task-based FC assesses connectivity patterns of functional coupling between brain regions in response to specific cognitive, emotional, or sensory tasks performed in the scanner. Task-based FC reflects context- or state-dependent networks, by task-evoked modulation of functional connectivity through increased coupling. While resting-state and task-based FC share common network architectures, task-based FC shows altered functional coupling in response to task demands (Cole et al., 2014; Shine et al., 2016).

Particularly resting-state fMRI (rs-fMRI) has gained popularity in recent years, due to its convenient application. It can be assessed quickly and easily for all parties involved. The low level of compliance simplifies measurement, making it especially popular in clinical populations, while additionally reducing costs. This lead to a high focus of research on resting state fMRI. As mentioned above, while there seems to be an overlap between resting-state and task-based activation, and even structural morphology, some resting-state fMRI research reveals rather low brain-behaviour relationships. However, both resting-state and task-based FC patterns are unique and can therefore be used to research inter-individual differences. Therefore, in my dissertation I compare and investigate different "states" (resting-state and different task-states) and their effect on predictability of individual behaviour.

FC can be assessed with seed-based correlation analysis or data-driven methods, such as independent component analysis (ICA) or graph-theoretical approaches. While each of these methods have their specific uses and advantages, data-driven methods pose the difficulty of interpretability, while also often being data-set specific. Thus, in my dissertation, I used seed-based correlation analysis. By using *a priori* regions of interest (ROIs), or seeds, it can be assumed, that the selected regions activate during certain tasks. *A priori* ROIs can be defined in a multitude of ways. Here, I defined specialised networks based on activation likelihood estimation (ALE) meta-analyses, and further used a data-driven approach, by delineating networks using general linear modelling (GLM) reflecting brain activation in the large HCP data sample during the tasks of interest. However, the question is whether it has to be exactly the task network that is related to a specific behaviour or whether interactions within other networks are also associated with behaviour.

3.2.3 Neural correlates of cognition and affect

While cognition is multifaceted, a consistent set of brain regions have been identified quite early due to lesion studies: the prefrontal and parietal cortices (Damasio et al., 1996; Rosenbaum et al., 2005; Scoville & Milner, 1957; Stuss et al., 2001). Damage to these regions lead to impaired executive functions. Then, Haier and colleagues showed a correlation between intelligence and gray matter volume in frontal, temporal, parietal, and occipital regions using voxel based morphometry (Haier et al., 2004), which has been supported in functional studies as well. In a large meta-analysis Basten et al. found supporting evidence of brain activation in the lateral prefrontal cortex, the medial frontal cortex, as well as the parietal and temporal cortex in intelligence. More specifically, they found the inferior frontal sulcus and gyrus, middle frontal and temporal gyrus, superior parietal lobule, and the pre-supplementary motor area to be consistently activated during tasks associated with cognition (Basten et al., 2015). Other meta-analyses focussing on working memory found, in addition to some of the aforementioned regions, the thalamus and basal ganglia to be involved (Rottschy et al., 2012).

A similar trajectory can be seen in how we came to understand which brain regions are critical for trait affect. Early lesion studies highlighted the importance of the amygdala, ventromedial prefrontal cortex (vmPFC), and insula in emotion processing and regulation, emotional experience, and decision-making involving affective valence (Adolphs et al., 1995, 1996; Bechara et al., 1999; Calder et al., 2000; Damasio et al., 1994). However, also frontal, temporal and parietal brain regions, as well as the anterior cingulate cortex, have been shown to be involved (Barbey et al., 2014; Hornak et al., 2003). The lesion-based evidence is also supported by structural und functional studies (Lindquist et al., 2012; Schmaal et al., 2017), which further found the prefrontal cortex, the thalamus and the periaqueducal gray to be involved (Kober et al., 2008; Lindquist et al., 2012). In particular relevant for emotion processing (or emotional face processing) are the already mentioned amygdala and insula. However, further active regions found in the limbic areas include the parahippocampal gyrus and the posterior cingulate cortex, and in the temporoparietal areas the parietal lobule and the middle temporal gyrus. Further involved are visual areas, such as the fusiform and lingual gyrus, the medial frontal gyrus, the putamen and the cerebellum (Fusar-Poli et al., 2009; Müller et al., 2018).

In sum, key brain regions in cognition are covered mainly by the multiple-demand and the cognitive control network. The multiple demand network includes the (posterior-medial) frontal cortex, insula, intraparietal sulcus, and inferior frontal sulcus. The cognitive control network includes the anterior cingulate cortex/pre-supplementary motor area, dorsolateral prefrontal cortex, inferior frontal junction, and posterior parietal cortex. In affect, the limbic system, including in particular the amygdala, with extensions to the prefrontal cortex, cingulate gyrus, thalamus, and hippocampus, have

been associated. These regions have been mainly based on lesion studies and group effect between task conditions. They therefore show, that these regions are consistently involved in these processes. However, to what extent they are associated with individual behavior is incompletely understood.

3.3 Influencing Factors on Brain-Behaviour Relationships

One of the main goals in behavioural neuroscience is to understand how the human brain works and how individual variability is driven. Several approaches can applied to try to elucidate this quest: heritability analyses can help explain how much of individual variability in brain structure or function is influenced by genes. Prediction can help us move beyond group averages. Finally, multivariate and multimodal analyses tie all modalities together and try to approach the brain as it is: an interconnected system.

3.3.1 Heritability

Heritability is a statistical estimate explaining what proportion of the variation in a given trait in a population is due to genetic variation. The variance (V) of a phenotype (P) within a population is composed of genotypic (G) and environmental (E) variance. Narrow-sense heritability (h^2), calculable with twin studies, refers to the proportion of phenotypic variance that is attributable to additive genetic variance V(A), and is estimated as $h^2 = V(A) / V(P)$ (Bruell, 1970; Nes & Roysamb, 2015). Research of genetic influences provides insights into the biological basis and possible influences in both healthy and diseased people. It helps us further understand the biological (genetic) constrains, while empowering us with the knowledge about potential environmental influence. This pertains to both the brain, as well as behavioural traits.

Thanks to heritability analyses based on twin studies, it has been analysed, that the majority of the human brain morphology is highly heritable (Jansen et al., 2015), but also, individually both cortical thickness and surface area revealed to be highly heritable in humans (Panizzon et al., 2009). Further, behavioural traits are heritable. Ranking at the top is cognition, which has been shown to be highly heritable (Krapohl et al., 2014; Plomin & Deary, 2015). In contrast, since affective traits are much more elusive and a clear delineation still of debate (Desmet, 2018; Gross, 2015), the research of heritability in these traits is much less consistent. Nevertheless, affective traits have been identified as heritable to some extent (Bouchard & Loehlin, 2001; Lykken & Tellegen, 1996), while some diseases associated with affective disorders show high heritability (Fernandez-Pujals et al., 2015; Kendall et al., 2021). Further, cognitive empathy or social cognition has also been shown to be heritable (Warrier et al., 2018).

Therefore, in the first study, I not only investigate the phenotypic association between cognition, affect and local brain anatomy, but also investigate the shared brain basis between cognition and trait affect and their genetic correlation. This enables me to investigate heritability as an influencing factor on brain–behaviour relationships in cognition and affect.

3.3.2 Prediction

For the most time, and laid out in the previous section, neuroscience relied on very specified lesion patients or large samples to establish brain-behaviour relationships. Through new insights this locationist approach is being challenged by the constructionist approach, which suggests an interaction between brain functional networks, instead of one specific location to be responsible for a specified function (Lindquist et al., 2012). In addition, we now have more (brain) data available, including large densely sampled datasets, such as the Human Connectome Project. Prediction with machine learning allows us to go beyond conventional statistics and make use of the large, complex and high-dimensional datasets. While conventional statistical approaches help us understand relationships between variables, they often rely on simplifying assumptions—such as independence, linearity, and low dimensionality—that may not reflect the true complexity of brain-behaviour relationships.

In contrast, predictive modelling and machine learning are able to handle high-dimensional, complex, and often nonlinear data, enabling the analysis and identification of distributed patterns across the brain that are informative at the level of individual behaviour. Therefore, the application of prediction in neuroscience offers the potential to further knowledge and the development of brain-based biomarkers for personalized medicine to inform diagnosis, prognosis, and intervention strategies on an individual level.

However, statistics allow an interpretable hypothesis driven approach to brain-behaviour relationships, while machine learning functions largely within a "black box". While the ability to handle complex data and potentially discover patterns with machine learning is a major strength, the models often lack interpretability, making it difficult to infer the underlying biological mechanisms driving the observed patterns.

Therefore, in my dissertation, I applied statistical models to achieve an interpretable and reduced feature space of brain data before applying different machine learning algorithms. Instead of relying on whole-brain data—and therefore omit biological interpretability—I yielded functional networks through different approaches: 1) Meta-analyses of networks activated through specific tasks, and 2) Definition of networks from high-powered and diversified task-fMRI studies. I then computed the functional connectivity within these network based on different task states and

analysed their predictability with regards to corresponding behaviour. By comparing FC derived from resting-state and task-based fMRI, and applying predictive modelling techniques, I can assess whether FC from behaviourally related states (e.g. FC from WM predicting WM) offer better predictive power than unrelated states (e.g. FC from WM predicting EMO).

This integrated approach allows not only to identify associations between brain regions and behaviour (statistical analysis), but also to determine whether these associations are genetically influenced (heritability analysis) and whether they are informative for predicting individual differences in behaviour (predictive modelling).

3.4 Aim of the studies

One main goal of neuroscience is to understand and gain deeper insights into brain function and organisation and to link it to behaviour. Many studies investigated how experience and behaviour is linked to brain structure and function, and also how much influence can be attributed to our genetic makeup. While there are many converging studies investigating cognition, there are inconclusive findings for affect, as well as their interplay. Further, little is known about how behavioural domains are subject to different influencing factors of inter-individual differences of the brain. In particular, how overlapping genetic influences exhibit in brain structure and which influence different functional task states drive predictability of individual behaviour.

Therefore, the first study focused on identifying a shared behavioural basis across cognition and affect and examined whether this convergence is mirrored in local brain structure. Here, I focused on structural morphometry such as cortical thickness, surface area, and subcortical volume. Finally, by analysing the heritability, I investigate if cognition and affect have shared genetic effects within behaviour and in brain morphology.

In the second study I move from structural anatomy to functional brain networks. Here, I investigate if individual differences in cognition (represented by working memory), emotion, and social cognition can be predicted from potential patters of FC. By comparing the predictability of FC derived from resting-state and task-based fMRI in different *a priori* networks, I can assess the influencing factor of task state and network specificity on brain-behaviour relationships. Further, by using *a priori* defined networks based on meta-analyses and large samples, I aim to improve interpretability of machine learning models.

With this dissertation I aim to investigate how inter-individual differences in cognitive and socio-affective processes are related to structural brain anatomy and functional connectivity. Further, I assess phenotypic and morphological heritability, as well as the predictability of task states and network specificity as influencing factors of brain variability.

4 Study 1

Behavioral, anatomical and heritable convergence of affect and cognition in superior frontal cortex

Nevena Kraljević^{1,2}, H. Lina Schaare^{1,7}, Simon B. Eickhoff^{1,2}, Peter Kochunov³, B. T. Thomas Yeo^{4,5,6}, Shahrzad Kharabian Masouleh^{1,2}, Sofie L. Valk^{1,2,7}

¹⁾ Institute of Neuroscience and Medicine (INM-7: Brain and Behaviour), Research Centre Jülich, Jülich, Germany

²⁾ Institute of Systems Neuroscience, Heinrich Heine University Düsseldorf, Düsseldorf, Germany

³⁾ Maryland Psychiatric Research Center, University of Maryland School of Medicine, Baltimore, Maryland, USA

⁴⁾ Department of Electrical and Computer Engineering, Centre for Sleep and Cognition, Centre for Translational MR Research, N.1 Institute for Health and Institute for Digital Medicine, National University of Singapore, Singapore, Singapore

⁵⁾ Athinoula A. Martinos Center for Biomedical Imaging, Massachusetts General Hospital, Charlestown, MA, USA

⁶⁾ NUS Graduate School for Integrative Sciences and Engineering, National University of Singapore, Singapore

⁷⁾Otto Hahn group Cognitive Neurogenetics, Max Planck Institute for Human Cognitive and Brain Sciences, Leipzig, Germany

NeuroImage (2021)

DOI: 10.1016/j.neuroimage.2021.118561

Impact Factor (2021): 7.4

Own contributions

Conception and design of study

Implementation, reviewing and adapting analysis code

Statistical data analysis

Interpretation of results

Preparing figures

Writing paper

Total contribution 70 %



Contents lists available at ScienceDirect

NeuroImage

journal homepage: www.elsevier.com/locate/neuroimage



Behavioral, Anatomical and Heritable Convergence of Affect and Cognition in Superior Frontal Cortex



Nevena Kraljević ^{a,b,1}, H. Lina Schaare ^{a,g,1,*}, Simon B. Eickhoff ^{a,b}, Peter Kochunov ^c, B.T. Thomas Yeo ^{d,e,f}, Shahrzad Kharabian Masouleh ^{a,b}, Sofie L. Valk ^{a,b,g,*}

- a Institute of Neuroscience and Medicine (INM-7: Brain and Behaviour), Research Centre Jülich, Jülich, Germany
- ^b Institute of Systems Neuroscience, Heinrich Heine University Düsseldorf, Düsseldorf, Germany
- ^c Maryland Psychiatric Research Center, University of Maryland School of Medicine, Baltimore, MD, USA
- ^d Department of Electrical and Computer Engineering, Centre for Sleep and Cognition, Centre for Translational MR Research, N.1 Institute for Health and Institute for Digital Medicine, National University of Singapore, Singapore
- ^e Athinoula A. Martinos Center for Biomedical Imaging, Massachusetts General Hospital, Charlestown, MA, USA
- ^fNUS Graduate School for Integrative Sciences and Engineering, National University of Singapore, Singapore
- g Otto Hahn group Cognitive Neurogenetics, Max Planck Institute for Human Cognitive and Brain Sciences, Stephanstr. 1A, Leipzig 04103, Germany

ARTICLE INFO

Keywords: Affect Cognition Heritability Frontal cortex Cortical structure Genetic correlation

ABSTRACT

Cognitive abilities and affective experience are key human traits that are interrelated in behavior and brain. Individual variation of cognitive and affective traits, as well as brain structure, has been shown to partly underlie genetic effects. However, to what extent affect and cognition have a shared genetic relationship with local brain structure is incompletely understood. Here we studied phenotypic and genetic correlations of cognitive and affective traits in behavior and brain structure (cortical thickness, surface area and subcortical volumes) in the pedigree-based Human Connectome Project sample (N=1091). Both cognitive and affective trait scores were highly heritable and showed significant phenotypic correlation on the behavioral level. Cortical thickness in the left superior frontal cortex showed a phenotypic association with both affect and cognition. Decomposing the phenotypic correlations into genetic and environmental components showed that the associations were accounted for by shared genetic effects between the traits. Quantitative functional decoding of the left superior frontal cortex further indicated that this region is associated with cognitive and emotional functioning. This study provides a multi-level approach to study the association between affect and cognition and suggests a convergence of both in superior frontal cortical thickness.

1. Introduction

The human cerebral cortex is implicated in multiple aspects of psychological functions, including cognitive abilities and affective experiences. Psychological traits and neuropsychiatric disorders have been reliably associated with interindividual variation in cortical macrostructure (Thompson et al., 2020). Moreover, variation in macroscale grey matter structure, such as in cortical thickness and surface area, is strongly driven by heritable and polygenetic influences (Grasby et al., 2020; Panizzon et al., 2009; Winkler et al., 2010). Affective and cognitive traits have also been shown to underlie genetic effects (Davies et al., 2011; Okbay et al., 2016; Zheng et al., 2016). However, to which degree trait affect, cognition, and brain structure share a genetic basis is incompletely understood.

Behavioral genetic studies have previously been conducted to assess heritability of habitual (i.e. trait) cognitive and affective processes. Using pedigree-based designs allows the assessment of genetic effects on a given phenotype by comparing monozygotic twins with other sibships and unrelated individuals (Almasy et al., 1997; Almasy and Blangero, 1998). Twin-based studies showed that cognitive abilities are largely influenced by genetic effects (Bartels et al., 2002; Davies et al., 2011; Kan et al., 2013; van Soelen et al., 2011; Wainwright et al., 2005). Affective traits have been investigated in genetic studies by using measures of positive and negative affect, as well as subjective well-being (Diener and Emmons, 1984; Lykken and Tellegen, 1996; Russell and Carroll, 1999; Salsman et al., 2013; Watson and Tellegen, 1985). These studies repeatedly found trait negative affect to be heritable, while trait positive affect was not related to genetic effects

^{*} Corresponding authors at: Institute of Neuroscience and Medicine (INM-7: Brain and Behaviour), Research Centre Jülich, Jülich, Germany. E-mail addresses: schaare@cbs.mpg.de (H.L. Schaare), s.valk@fz-juelich.de (S.L. Valk).

¹ These authors contributed equally to this work.

(Baker et al., 1992; Zheng et al., 2016). Conversely, Lykken and Tellegen (1996) showed that individual differences in subjective well-being were partly explained by genetic variation in several thousand middleaged twins. Along this line, Genome-Wide Association Studies (GWAS) reported various loci associated with subjective well-being (Okbay et al., 2016). These results emphasize a genetic basis of the variation in both cognition and some affective experiences.

Human brain structure also underlies genetic influences, as brain volume, cortical surface area and thickness have been found to be strongly heritable and to show a polygenetic architecture (Brouwer et al., 2014; Grasby et al., 2020; Panizzon et al., 2009; Winkler et al., 2010). Neuroimaging genetics studies demonstrated that associations between cognition and cortical thickness can be explained by shared genetic effects (Brans et al., 2010; Desrivières et al., 2015; Joshi et al., 2011; Shaw et al., 2006). Gene enrichment studies have further associated subjective well-being with differential gene expression in the hippocampal subiculum and with GABAergic interneurons, suggesting a genetic link between brain structure and affective traits (Baselmans et al., 2019). Moreover, shared genetic effects have been found to drive the association between neuroticism – a personality trait closely linked to negative affect – and surface area in the right medial frontal cortex (Valk et al., 2020).

Classically considered to be distinct entities, most neuroimaging studies to date investigated neural correlates of cognition and affect as separate constructs yielding inconclusive results. There is a multitude of evidence which suggests that general cognitive abilities are positively correlated with greater brain volume across the human lifespan (Oschwald et al., 2019). Using surface-based measures, individual differences in cognition have been related to prefrontal and parietal cortical thickness, though often with contradictory outcomes: Both positive correlations between cortical thickness and cognitive abilities (Karama et al., 2009; Narr et al., 2006; Shaw et al., 2006, Bajaj et al., 2018, Hanford et al., 2019), as well as negative correlations (Goh et al., 2011; Salat et al., 2002; Sowell et al., 2001; Van Petten et al., 2004) have been reported.

With respect to affective traits, neuroimaging studies have repeatedly shown that state and trait emotional processes correlate with activity, connectivity and anatomy of the brain (Atkinson et al., 2007; Brierley et al., 2004; LaBar et al., 1995; Lindquist et al., 2012; Rohr et al., 2015; Tsuchiya et al., 2009).

Recent theories emphasize the interplay and shared mechanisms of emotions and cognition in the human brain (Barrett, 2016; Pessoa, 2008): Emotions can both facilitate and impede cognitive function, depending on the context (Dolcos and Denkova, 2014; Okon-Singer et al., 2015). At the same time, cognitive processes are inherent in most aspects of emotional experience and regulation (Ochsner and Gross, 2005; Pessoa, 2008). This behavioral association is mirrored by overlapping brain networks associated with emotions (Barrett, 2016; Khalsa et al., 2018) and cognitive control (Langner et al., 2018; Pessoa, 2008). Thus, affective experience and cognitive abilities are inherently coupled in the human brain (Barrett, 2016; Pessoa, 2008). Yet, it remains unclear if this coupling reflects in neuroanatomical correlates and if cognition and affect share a genetic basis.

In sum, (1) cognitive abilities and their relation with brain structure are highly heritable; (2) affective experience is associated with brain function and structure and may also be driven by genetic factors, depending on the affect measurement; (3) there is a complex interrelation between affect and cognition in behavior and brain. However, whether cognition and trait affect have a shared genetic relation to brain structure is not known to date. We studied the relationship of cognition and affect in behavior and local brain structure and evaluated whether cognitive abilities and trait affective self-reports can be accounted for by shared genetic effects between behavior and brain. First, we evaluated the relation of cognition and trait affect on the behavioral level by conducting phenotypic correlation, as well as heritability analyses and genetic correlation in a large sample of healthy twins. Next, we assessed

cognition and affective traits in relation to cortical thickness, subcortical volumes and cortical surface area, to evaluate whether cognition and affect yield phenotypic and genetic correlations with local brain structure. We expected to observe that phenotypic associations of cognition and affect with brain structure can be explained by genetic correlations.

2. Materials and methods

2.1. Participants

The Human Connectome Project (HCP) is a publicly available data base. In this study, the Young Adult Pool was used, which comprised 1206 healthy individuals (656 women, mean age = 28.8 years, standard deviation (SD) = 3.7, range = 22–37 years). In total, there were 292 monozygotic (MZ) twins, 323 dizygotic (DZ) twins, and 586 singletons (additionally 5 missing values in zygosity information). After exclusion of individuals without brain structural (N = 93) or behavioral data (N = 20) relevant to this study, and participants with corrupted brain data (N = 4), our final sample comprised 1091 individuals, of which 592 were women. This sample included 274 MZ twins, 288 DZ twins, and 525 singletons (additionally 4 missing values in zygosity information). Its mean age, standard deviation and range remained the same as for the total HCP sample.

2.2. Ethics statement

Analysis of the HCP data has been approved through the local ethics committee of the University of Düsseldorf, Germany.

2.3. Data/code availability statement

To ensure reproducibility of this study using unrestricted and restricted data of the publicly available HCP dataset (www.humanconnectome.org), the code that has been used in our analyses can be found here: https://github.com/CNG-LAB/affect_cognition. As specified in the HCP Restricted Data Use Terms, investigator-assigned IDs of included participants will be shared upon publication of the study.

2.4. Behavioral measures

The cognitive and affective measures used in this study were selected in the data base of the HCP and derived from the National Institute of Health (NIH) toolbox for Assessment of Neurological and Behavioral Function® (neuroscienceblueprint.nih.gov). Composite scores from the cognition and emotion categories were used, while one category comprised several sub-domains (Table 1).

2.4.1. Cognition

The cognitive function composite score (total cognition) was assessed by averaging the fluid cognition composite score (fluid cognition) and the crystallized cognition composite score (crystallized cognition). As illustrated in Table 1, the fluid cognition score was obtained by averaging the scores of the Dimensional Change Card Sort Test, Flanker, Picture Sequence Memory, List Sorting, and Pattern Comparison measures. That is, fluid cognition is the combination of scores of executive function, inhibition and attention, episodic memory, working memory, and processing speed (Akshoomoff et al., 2013). The crystallized cognition score was obtained by averaging the scores of Picture Vocabulary and Oral Reading Recognition measures. That is, crystallized cognition consists of language in the sense of translation of thought into symbols and deriving meaning from text, as a reflection of past learning experiences (Akshoomoff et al., 2013; Gershon et al., 2013).

As cognition can be both conceived as a general factor (G), but at the same time crystallized and fluid cognition are differentiable, we investigated the general cognitive score (total cognition), as well as fluid and crystallized cognition.

Table 1Behavioral scores. Overview of composition of behavioral variables.

Category	Domain	Sub-domain	Test
Cognition	Fluid cognition	Executive function – cognitive flexibility	Dimensional Change Card Sorting (DCCS)
		Executive function - Inhibition and attention	Flanker
		Episodic memory	Picture Sequence Memory
		Processing speed	Pattern Comparison
		Working memory	List Sorting
	Crystallized cognition	Language	Picture Vocabulary
			Reading Recognition
Affect	Positive affect/psychological well-being	Life satisfaction	Self-report
		Meaning and purpose	
		Positive affect	
	Negative affect	Anger-affect	Self-report
		Anger-hostility	
		Fear-affect	
		Perceived stress	
		Sadness	

Table 2Behavioral variables. Mean, standard deviation, as well as minimum and maximum of each variable included in our analyses.

Variables	Mean	SD	Min	Max
Total Cognition	121.8	14.6	84.6	153.4
Fluid Cognition	115.0	11.6	84.5	145.2
Crystallized Cognition	117.7	9.9	90.4	154.0
Positive Affect	52.1	7.2	27.1	72.6
Negative Affect	48.7	6.8	30.9	78.8
Mean Affect	1.7	6.2	-19.6	20.8

2.4.2. Affect

To examine trait affect in this study, a composite measure of general affect was used, consisting of both positive and negative affect. Trait affect can be sub-divided into positive and negative traits, which are separable constructs that may be represented as one bipolar scale or two unipolar scales (Diener and Emmons, 1984; Russell and Carroll, 1999; Salsman et al., 2013; Watson and Tellegen, 1985). Positive affect, also known as psychological well-being, is characterized by the experience of pleasant feelings, such as happiness, serenity and cognitive engagement (Diener and Emmons, 1984; Salsman et al., 2014, 2013). We composed the construct of positive affect by averaging the scores from the sub-domains of life satisfaction, meaning and purpose, and positive affect (Tables 1 and 2). Negative affect comprises three principal negative emotions: anger, fear, and sadness (Pilkonis et al., 2013; Salsman et al., 2013). It was composed by the average of anger (anger-affect, hostility), sadness, fear-affect, and perceived stress (Table 1 and 2). All affective domains were obtained using the NIH toolbox with a written self-report (Pilkonis et al., 2013; Salsman et al., 2014, 2013).

As the positive and negative affect scores used in this study showed high intercorrelations (R = -0.6, see Fig. 1C and Supplementary Fig. 1), we created a composite score of mean affect by reversing the negative affect score and averaging it with the positive affect score. This enabled us to investigate positive and negative affect as separate entities, on the one hand, as well as a general estimate of mean affect that integrates both negative and positive emotions, on the other hand.

2.5. Structural imaging processing

MRI protocols of HCP were previously described in detail (Glasser et al., 2013; Van Essen et al., 2013). In short, MRI data used in the study was acquired on the HCP's custom 3T Siemens Skyra scanner equipped with a 32-channel head coil. Two T1-weighted (T1w) images with identical parameters were acquired using a 3D-MPRAGE sequence (0.7 mm isotropic voxels, matrix = 320×320 , 256 sagittal slices, TR = 2,400 ms, TE = 2.14 ms, TI = 1,000 ms, flip angle = 8°, iPAT = 2). Two T2w images were acquired using a 3D T2-SPACE sequence with

identical geometry (TR = 3,200 ms, TE = 565 ms, variable flip angle, iPAT = 2). T1w and T2w scans were acquired on the same day. The pipeline used to obtain the FreeSurfer segmentation is described in detail in a previous article (Glasser et al., 2013) and is recommended for the HCP-data. The pre-processing steps included co-registration of T1w and T2w scans, B1 (bias field) correction, and segmentation and surface reconstruction using FreeSurfer version 5.3-HCP to estimate brain volumes, cortical thickness and surface area. We also derived eight bilateral subcortical volumes (thalamus, caudate, putamen, pallidum, hippocampus, amygdala, accumbens area, ventral diencephalon) from FreeSurfer's automatic subcortical segmentation (Fischl et al., 2002) to evaluate their phenotypic and genetic correlation with behavioral traits.

2.6. Cortical morphological measures

For analyses including local cortical structure, we summarized surface-based morphological measures (i.e. cortical thickness and surface area) as parcels covering the entire cortical mantle to study their compressed features on a local topological scale (Betzel and Bassett, 2017). We applied a parcellation scheme on the cortical surface mesh, which is based on the combination of local gradient and global similarity approaches using a gradient-weighted Markov Random Field model (Schaefer et al., 2018). Using compressed features of structural MRI has been suggested to both improve signal-to-noise of brain measures (cf. Eickhoff et al., 2018; Genon et al., 2018) and optimize analysis scalability. The Schaefer parcellation has been extensively evaluated with regards to stability and convergence with histological mapping and alternative parcellations (Schaefer et al., 2018). In the context of the current study, we focused on the granularity of 200 parcels from the 7network solution. In order to improve signal-to-noise ratio and analysis speed, we opted to average unsmoothed structural data within each parcel. Thus, cortical thickness of each parcel was estimated as the trimmed mean (10 % trim) of vertex-wise cortical thickness and parcel-wise surface area was computed as the sum of vertex-wise area per parcel. The parcel-wise measures were used in all subsequent cortical analyses.

2.7. Phenotypic correlation analyses

Phenotypic correlations between cognitive and affective traits were assessed by cross-correlating the normalized behavioral measures, controlling for effects of age, sex and their interaction, using multiple linear regression models.

Phenotypic analyses between behavioral traits and local brain structure were carried out per parcel of cortical thickness and surface area, as well as per volume of subcortical structures. Each brain modality was predicted by cognition and affect, respectively, using multiple linear regression models while controlling for age, sex, age × sex interaction, age², age² × sex interaction, as well as global thickness (mean

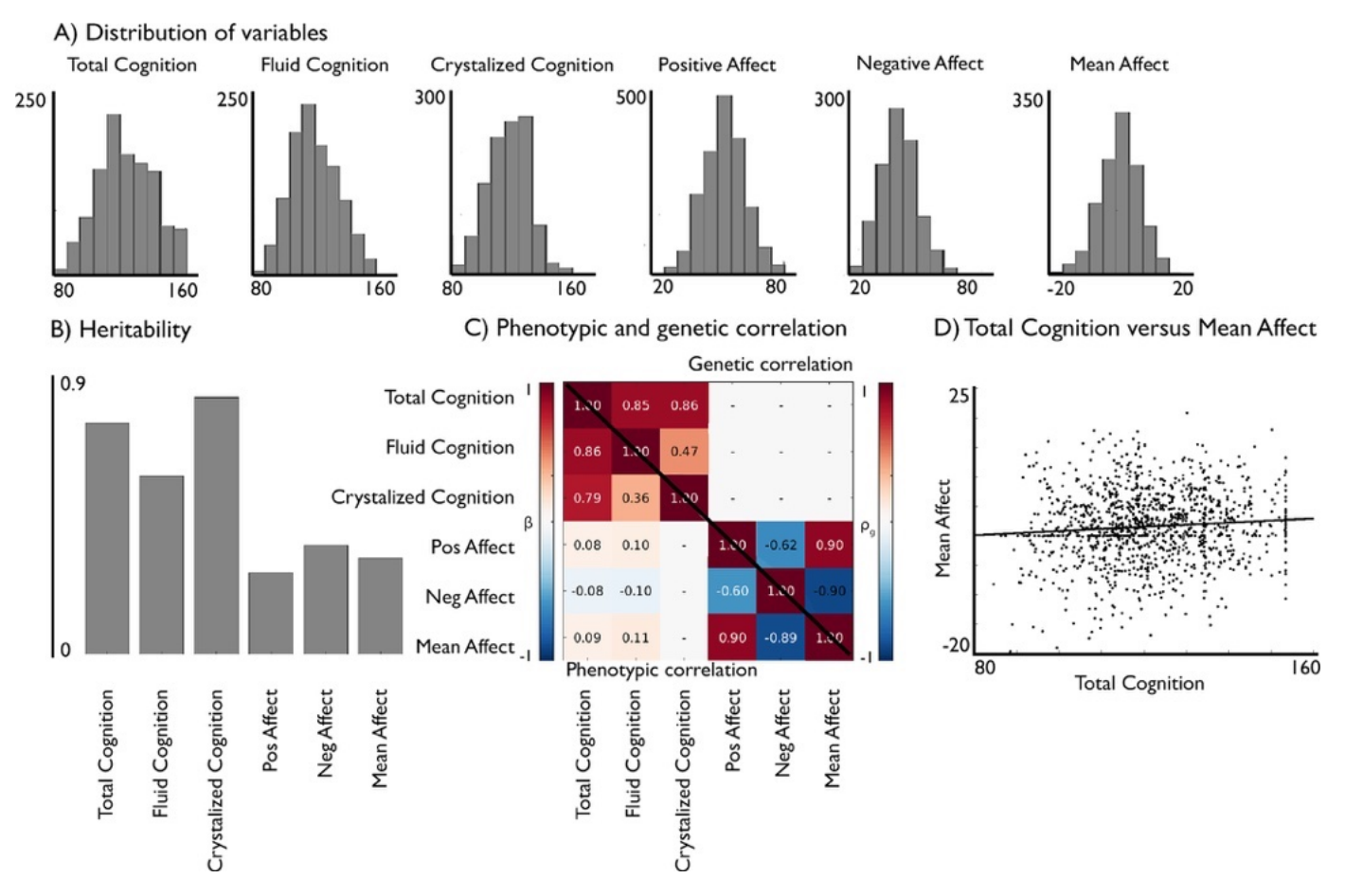


Fig. 1. Phenotypic and genetic relation of cognition and affect. (A) Distribution of cognitive and affective variables; (B) Their heritability (h²); (C) bottom triangle: phenotypic correlation (standardized beta values, FDRq<0.05) and upper triangle: genetic correlation (rho values, FDRq<0.05) of the cognitive and affective scores; (D) Scatter plot showing the phenotypic correlation between mean affect and total cognition.

cortical thickness) effects when investigating cortical thickness and intracranial volume (ICV) when assessing surface area and subcortical volumes. As in previous work (Bernhardt et al., 2014; Valk et al., 2016a, 2016b), we used SurfStat for Matlab [R2020a, The Mathworks, Natick, MA] (Worsley et al., 2009) to conduct the statistical comparisons.

Results of all phenotypic correlations were corrected for multiple comparisons using Benjamini-Hochberg false discovery rate (FDRq<0.05) (Benjamini and Hochberg, 1995). We displayed significant brain associations on the cortical surface.

2.8. Heritability and genetic correlation analyses

Using the pedigree-based design of HCP, we conducted analyses to estimate heritability and genetic correlation of cognitive and affective trait scores and brain structure. All genetic analyses were performed using the software package Sequential Oligogenic Linkage Analysis Routines (SOLAR, http://www.solar-eclipse-genetics.org), which employs a maximum likelihood variance-decomposition approach optimized to perform genetic analyses in pedigrees of arbitrary size and complexity (Almasy and Blangero, 1998; Kochunov et al., 2019). SOLAR models genetic proximity by covariance between family members (Almasy and Blangero, 1998; Kochunov et al., 2019).

Heritability (i.e. narrow-sense heritability h^2) is defined as the proportion of the phenotypic variance (σ_p^2) in a trait that is attributable to the additive effects of genes (σ_g^2) , i.e. $h^2 = \sigma_g^2/\sigma_p^2$. SOLAR estimates heritability by comparing the observed phenotypic covariance matrix with the covariance matrix predicted by kinship (Almasy and Blangero, 1998; Kochunov et al., 2019). Significance of the heritability estimate was

tested using a likelihood ratio test where the likelihood of a restricted model (with σ_g^2 constrained to zero) is compared with the likelihood of the estimated model. Twice the difference between the log likelihoods of these models yields a test statistic, which is asymptotically distributed as a 50:50 mixture of a X^2 variable with 1 degree-of-freedom and a point mass at zero (Almasy and Blangero, 1998; Kochunov et al., 2019).

To determine if variations in cognition or affect and brain structure were influenced by the same genetic factors, genetic correlation analyses were conducted. Genetic correlations indicate the proportion of variance that determines the extent to which genetic influences on one trait are shared with genetic influences on another trait (e.g. pleiotropy). In SOLAR, the phenotypic correlation (ρ_p) was decomposed through bivariate polygenic analyses to estimate genetic (ρ_g) and environmental (ρ_e) correlations using the following formula: $\rho_p = \rho_g \sqrt(h_1^2 h_2^2) + \rho_e \sqrt{[(1-h_1^2)(1-h_2^2)]},$ where ${h^2}_1$ and ${h^2}_2$ are the heritability estimates of the behavioral trait and the respective brain structural measure (Almasy et al., 1997; Glahn et al., 2010). To test for the significance of shared genetic effects, likelihood ratio tests were conducted (similar to heritability analyses) comparing models in which ρg was estimated with models in which ρ_g was constrained to zero (no shared genetic effect) and constrained to 1 (complete pleiotropy) (Almasy et al., 1997).

Significance of both the heritability and genetic correlation estimates was corrected for multiple comparisons by Benjamini-Hochberg FDRq<0.05 (Benjamini and Hochberg, 1995).

Heritability and genetic correlation analyses were conducted with simultaneous estimation for the effects of potential covariates. We thus included the same covariates as in our phenotypic analyses including age, sex, age \times sex interaction, age², age² \times sex interaction, as well as global thickness when investigating cortical thickness and ICV when assessing surface area and subcortical volumes. To ensure that our traits conform to the assumptions of normality, an inverse normal transformation was applied to all behavioral as well as brain structural traits prior to genetic analyses (Glahn et al., 2010).

2.9. Functional decoding

Parcels that were significantly correlated with both cognition and affect and shared genetic variance, were functionally characterized using the Behavioral Domain meta-data from the BrainMap metaanalysis database (http://www.brainmap.org, Laird et al., 2011, 2009). The BrainMap database enables the decoding of functions associated with specific brain regions. To investigate potential functional processes associated with parcels linked to both affect and cognition, we used the volumetric counterparts of the surface-based parcels as defined by Schaefer et al and available online (Schaefer et al., 2018, https://github.com/ThomasYeoLab/CBIG/tree/master/stable_projects/ brain_parcellation/Schaefer2018_LocalGlobal/Parcellations). although our empirical analysis focused on surface-based cortical data, functional decoding could be performed in volume space. In particular, we identified those meta-data labels (describing the computed contrast [behavioral domain as well as paradigm]) that were significantly more likely than chance to result in activation of a given parcel (Fox et al., 2014; Genon et al., 2018; Nostro et al., 2017). That is, functions were attributed to the parcels by quantitatively determining which types of experiments were associated with activation in the respective parcel region. Of note, we assessed associations of the parcels of interest with functional activations and included only tasks involving healthy adults. Significance was established using a binomial test (q<0.05, corrected for multiple comparisons using FDR) and we report results of both forward and reverse inference analyses.

3. Results

3.1. Heritability, phenotypic and genetic correlation of cognition and affect (Fig. 1)

First, we evaluated the phenotypic associations between cognitive test scores and affective self-report scores (Fig. 1, Supplementary Fig. 1). Both composite scores (total cognition and mean affect), as well as their sub-domains (fluid cognition, crystallized cognition, positive affect, and negative affect), were normally distributed (Fig. 1A). We observed high phenotypic interrelationships between the respective sub-tests of both cognitive and affective domains (Supplementary Fig. 1), supporting the use of the composite scores total cognition and mean affect as proxies for the constructs of cognition and affect, respectively. As expected, cognitive scores were all positively associated among each other, while positive affect correlated positively, and negative affect correlated negatively to mean affect. We observed that mean affect had a positive phenotypic relationship with total cognition ($\beta = 0.09$, FDRq < 0.05). Similarly, positive affect was positively associated with total ($\beta = 0.08$) and fluid ($\beta = 0.10$) cognitive abilities, whereas negative affect was negatively associated with total ($\beta = -0.08$) and fluid ($\beta = -0.10$) cognitive abilities (all FDRq < 0.05; Fig. 1C, lower triangle).

The heritability analysis revealed that all observed construct scores were heritable: total cognition (h^2 = 0.75, p < 0.001), which is a combination of fluid (h^2 = 0.58, p < 0.001) and crystallized (h^2 = 0.83, p < 0.001) cognition, as well as mean affect (h^2 = 0.31, p < 0.001), which is the signed average of positive (h^2 = 0.27, p < 0.001) and negative (h^2 = 0.36, p < 0.001) affect (Fig. 1B).

Next, we evaluated the genetic correlation between cognitive and affective scores. A strong positive genetic correlation between fluid and crystallized cognition ($\rho_g=0.47$, FDRq<0.05) and a negative genetic correlation between positive and negative affect ($\rho_g=-0.62$,

FDRq<0.05) was found (Fig. 1C, upper triangle), suggesting that both sub-domain-sets reflect partly overlapping genetic mechanisms. We did not observe a significant genetic correlation between total cognition and mean affect (FDRq > 0.05). At trend level, we observed genetic correlations between fluid cognition and mean affect ($\rho_g = 0.23, p < 0.03$), and between fluid cognition and positive affect ($\rho_g = 0.28, p < 0.02$). In the following, we focus on reporting the results for the composite scores of total cognition and mean affect which sufficiently capture phenotypic and genetic variance of the constructs of cognition and affect. To additionally allow for more detailed assessment, we report associations with the sub-domain measures in the supplementary materials.

3.2. Phenotypic association between cognition and local brain anatomy (Fig. 2)

To evaluate the phenotypic association of cognition and affect with brain anatomy, we first evaluated the correlation between cognition and local cortical thickness, while controlling for global thickness. We observed positive associations between thickness and total cognition in bilateral insula, bilateral cuneus, bilateral sensorimotor regions, left middle temporal gyrus, and right middle cingulate; whereas bilateral frontal regions and left parietal showed a negative relation with total cognitive score (Fig. 2A). Conversely, surface area showed only positive, but not negative, associations with cognitive scores. Total cognition was associated with local surface area in bilateral occipital areas, temporal poles, sensorimotor cortices, and lateral and orbital frontal cortices, as well as left anterior cingulate and right posterior-mid cingulate cortex (Fig. 2B). With regards to subcortical volumes, we observed a significant positive effect between total cognition and left hippocampal volume (Fig. 2C). Fluid and crystallized cognition sub-scores showed similar associations with local brain structure and volume (Supplementary Tables 1-3, 7-12).

3.3. Phenotypic association between affect and local brain anatomy (Fig. 2)

Next, we evaluated the association between affect and local brain structure. We found that affect measures showed significant associations with local cortical thickness and subcortical volumes, but not with local surface area. Mean affect was associated with cortical thickness negatively in left superior frontal cortex and positively in left occipital cortex, as well as right parietal cortex (Fig. 2A, Supplementary Table 4). In addition, bilateral caudate volume was significantly associated with mean affect (Fig. 2C, Supplementary Table 13).

3.4. Genetic correlation of cognition and affect with local brain structure (Fig. 3)

To assess if the phenotypic correlation between cognitive and affective traits on the one hand and local brain structure on the other is accounted for by shared genetic effects, we performed genetic correlation analyses through bivariate polygenic analyses. Both local thickness and surface area were heritable in our sample (cortical thickness h^2 =mean±sd: 0.35±0.11 and surface area: h^2 =0.42±0.13), as were subcortical volumes (h^2 =0.68±0.10, Supplementary Figure 4, Supplementary Tables 21-23).

There was a strong overlap between phenotypic correlations and genetic correlations. 34 out of 37 phenotypic correlations between total cognition and local cortical thickness could be attributed to shared genetic effects (FDRq<0.05, Fig. 3A, Supplementary Table 16) and genetic correlation patterns largely mirrored phenotypic associations between cognitive scores and local cortical thickness (see also Supplementary Fig. 5 and Supplementary Table 18). Similarly, the phenotypic associations between cognitive scores and subcortical volumes were mainly attributable to genetic correlations (Supplementary Table 20). Furthermore, the associations between local surface area and cognitive scores

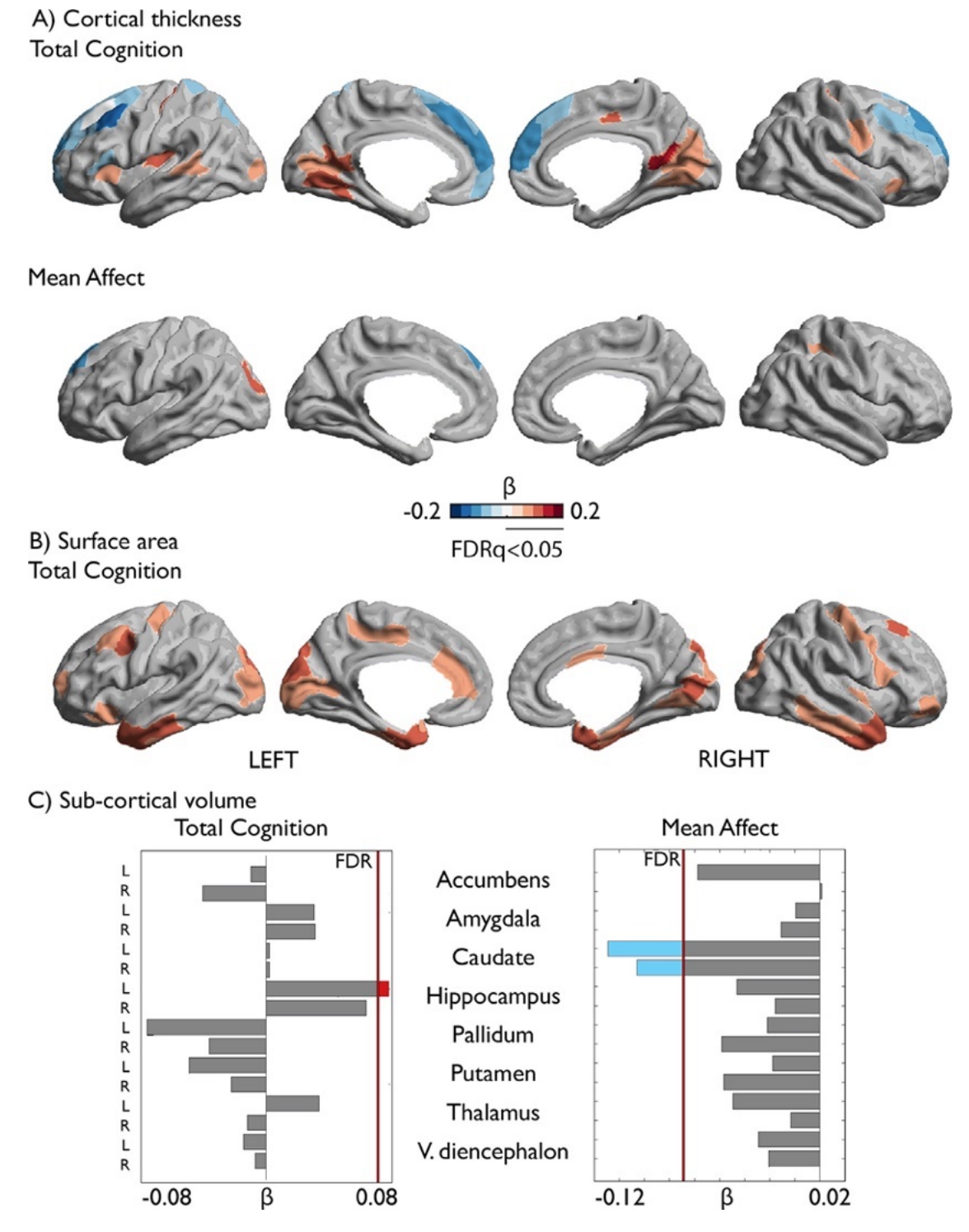


Fig. 2. Associations between cognition, affect and local brain structure. (A) Correlation between total cognition and local cortical thickness; Second row: Correlation between mean affect and local cortical thickness. (B) Correlation between total cognition and local surface area. Associations between surface area and affect were not significant. (C) Correlations between cognition / affect and sub-cortical regions volumes. Red indicates a positive association, and blue a negative association between cognition / affect and local brain structure. Only FDRq<0.05 corrected findings are depicted (For interpretation of the references to color in this figure legend, the reader is referred to the web version of this article.).

were largely associated with shared genetic factors. Here, 29 out of 42 phenotypic associations between total cognition and local surface area were accounted for by shared genetic factors (Fig. 3B, Supplementary Table 17; Supplementary Figure 6 and Supplementary Table 19 for subscore results). Among the associations with mean affect, thickness of left superior frontal cortex ($\rho_{\rm g}=$ -0.480, p=0.000, Fig. 3A, Supplementary Table 16) and bilateral caudate volumes (left: $\rho_{\rm g}=$ -0.28, p=0.001,

right: $\rho_{\rm g}$ = -0.28, p =0.001, Supplementary Table 20) were also related to shared genetic effects.

3.5. Shared brain basis between cognitive and affective tendencies (Fig. 4)

Last, we evaluated whether cognitive and affective traits also showed an overlapping relationship to local brain structure. Both cognition and

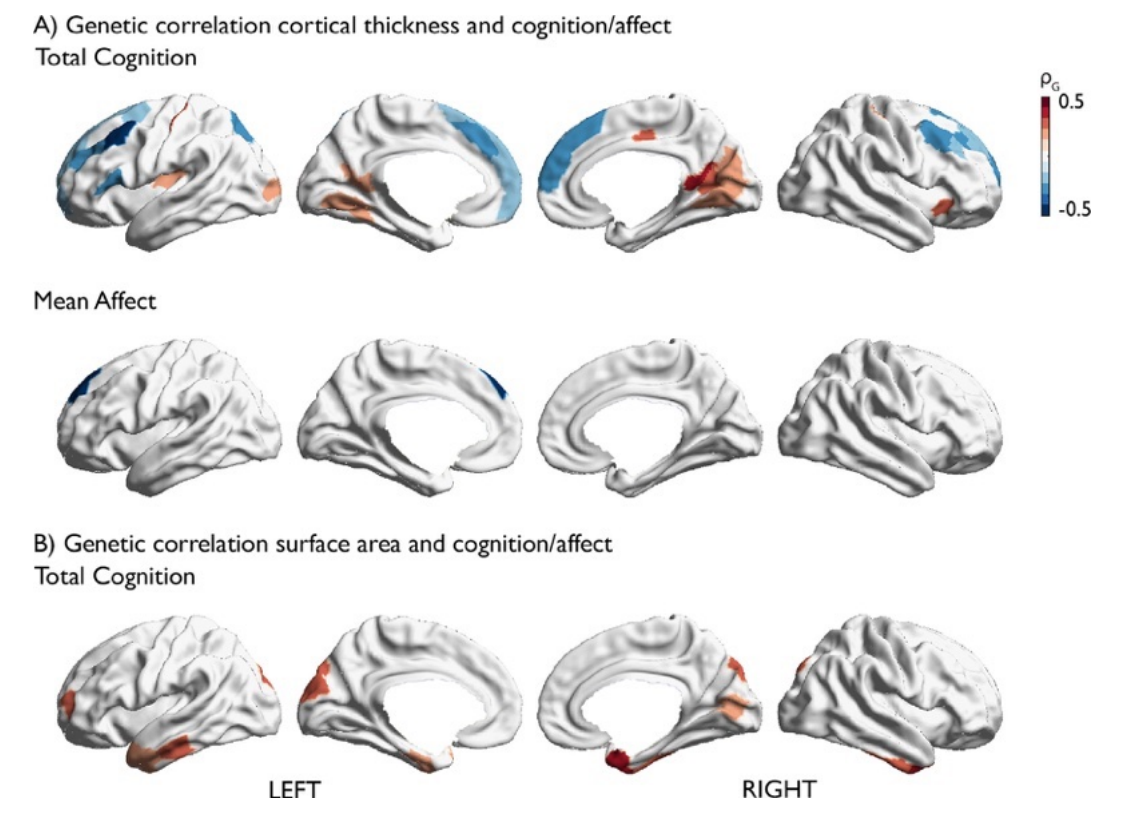


Fig. 3. Whole-brain genetic correlation between local cortical structure and cognition or affect. (A) Results for cortical thickness. (B) Results for surface area. Positive correlation is depicted in red, negative in blue. Only FDRq<0.05 corrected findings are depicted (For interpretation of the references to color in this figure legend, the reader is referred to the web version of this article.).

affect scores had an association (FDRq < 0.05) with thickness in the left superior frontal cortex. In both measures, these effects were accounted for by genetic correlations (Supplementary Tables 16 and 17). We performed functional decoding to further quantify the functional processes associated with this region and found this region to be involved in cognitive and socio-cognitive processes, as well as emotional processes (valence and negative emotions) and action inhibition (Fig. 4, for uncorrected results see Supplementary Figure 7). These behavioral domains were mirrored by activation related to Theory of Mind, Emotional Induction, Semantic monitor, and Go/No-go tasks (reverse inference only, Fig. 4).

4. Discussion

We evaluated shared behavioral, heritable and brain structural factors of cognitive and affective traits. We found that both cognitive and affective traits were heritable and observed significant genetic correlation between fluid cognition (but not total cognition) and trait affect. Following, we assessed the phenotypic correlation between cognitive and affective traits on the one hand, and macroscale brain anatomy on the other. Whereas cognition had widespread associations with local cortical thickness and surface area, trait affect showed only sparse associations. We found that most phenotypic behavior-brain associations were attributable to shared genetic effects, as indicated by significant genetic correlations. Finally, we evaluated whether total cognition and mean affect were embedded in a common brain structural correlate and found that both measures showed a shared phenotypic and genetic association with cortical thickness of left superior frontal cortex. Quantitative functional decoding further indicated that this region is involved in both cognitive and emotional functioning.

4.1. Heritability and genetic correlations of cognition, affect and brain structure

Complementing previous studies on affect, cognition, and macroscale brain anatomy, we interrogated the shared genetic basis of cognition and affect using pedigree-based approaches. We observed a moderate to strong heritability of cognitive scores ($h^2 = 0.6$ -0.8), which is in line with previous work: In childhood and adolescence-depending on measurement and cohort - 70 to 80 % of the variance in cognitive ability is estimated to be accounted for by genetic factors (Bartels et al., 2002; van Soelen et al., 2011; Wainwright et al., 2005). Using GWAS of adult samples, Davies et al. (2011) observed that 40% of the variation in crystallized-type intelligence and 51% of the variation in fluid-type intelligence between individuals is accounted for by genetic variants. Notably, crystallized cognition was observed to be more heritable than fluid cognition in the current sample. These findings are in line with a large meta-analysis assessing the heritability of cognitive traits based on their cultural load, where traits with higher cultural load were shown to be more heritable (Kan et al., 2013). Traits that we summarized as crystallized cognition were attributed a higher cultural load in Kan et al.'s study. This indicates that the known cultural and educational homogeneity of the HCP sample may have led to a high estimated heritability of crystallized cognition.

However, our findings on the heritability of affective self-reports were less strong. Previous work in a twin sample by Baker et al. revealed a strong heritability for negative affect, but none for positive affect (Baker et al., 1992), which was conceptually replicated by Zheng et al. (2016). In addition, angry temperament has been associated with genetic processes involved in memory and learning (Mick et al., 2014). Another twin study by Lykken and Tellegen (1996) found the heritability for subjective well-being to be 44–52%, which appears to

Left superior frontal cortex Cortical thickness - cognition and affect

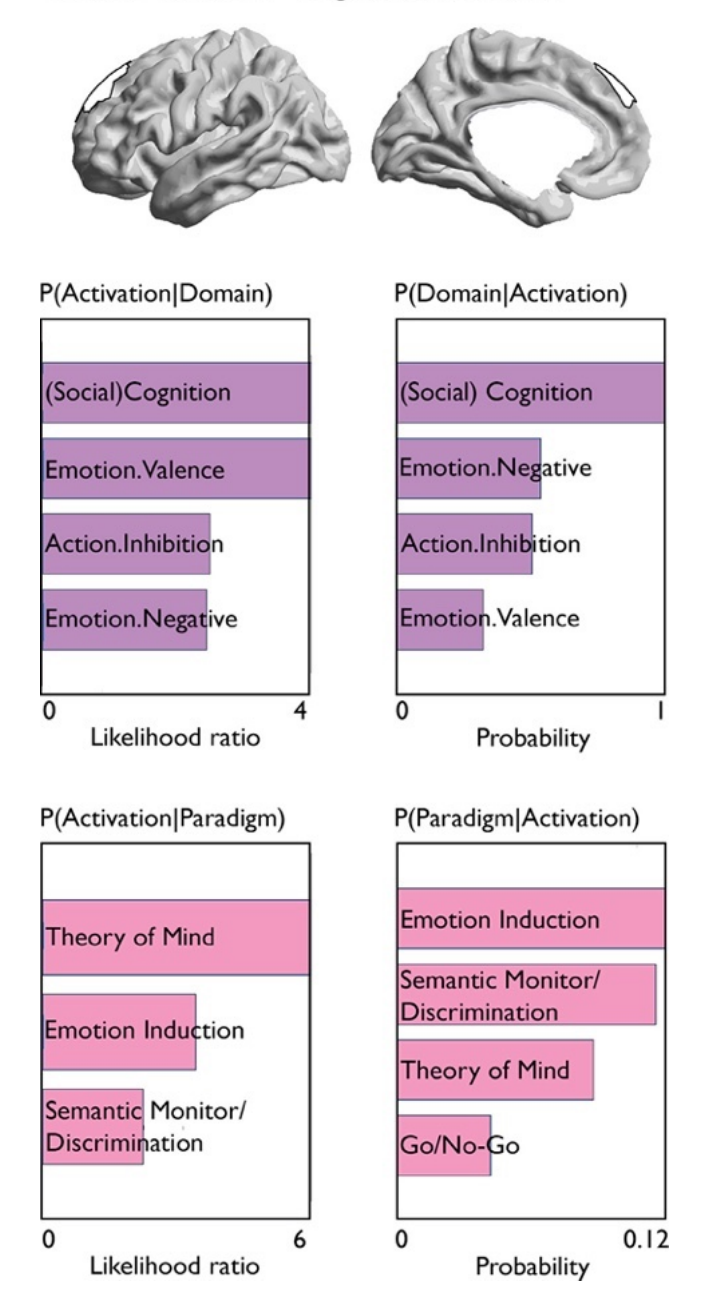


Fig. 4. Quantitative functional decoding of region showing association with both cognition and affect. Both forward inference and reverse inference of activation-domain and paradigm-domain contrasts are reported for the left superior frontal cortex which showed evidence of shared phenotypic and genetic association for cognition and affect.

be higher than the heritability scores we observed for affect measures. However, few studies to date have assessed the heritability of both cognitive and affective traits in the same cohort. Our observations suggest that inter-individual variance in cognition is more robustly explained by heritable factors, than in affect. This could be related to the challenge to quantify individual difference of affective traits in self-reports, which show weaker convergent validity, as opposed to tests for cognitive assessments (Heaton et al., 2014; Salsman et al., 2013).

Moreover, we replicated previous results that showed heritability of surface area and cortical thickness, which further indicated that phenotypic variance in cortical thickness and surface area is partly driven by additive genetic effects (Brouwer et al., 2014; Grasby et al., 2020; Panizzon et al., 2009; Winkler et al., 2010).

Extending previous work, we also observed strong genetic correlations between total cognition and local cortical structure which indicates that the majority of phenotypic associations between total cognition and cortical thickness and surface area, respectively, could be associated with shared genetic factors (Brouwer et al., 2014; Grasby et al., 2020; Toga and Thompson, 2005).

Affect was phenotypically correlated with superior frontal thickness and genetic correlation analyses yielded that this association was attributable to shared genetic effects. These results are in line with recent work implicating various genetic loci with well-being which showed significant enrichment for GABAergic interneurons sampled from hippocampus and prefrontal cortex (Baselmans et al., 2019; Okbay et al., 2016). However, we did not observe genetic associations between affect and hippocampal volumes in this sample. Moreover, affect was genetically correlated with bilateral caudate volume, a region which has been shown to share a genetic basis with neuropsychiatric health traits (Satizabal et al., 2019; Zhao et al., 2019).

4.2. Shared basis of cognition and affect in behavior, genetics and superior frontal cortex thickness

We combined behavioral and brain imaging approaches to study the association between cognition and trait affect. Scores for mean total cognition and affect showed a positive association at the behavioral level, highlighting the synergy of cognitive and affective traits. Previous work has suggested positive affect might have a motivating role in enhancing cognitive flexibility (Ashby et al., 1999; Fredrickson, 2001; Liu and Wang, 2014). In turn, cognitive control is a core feature of successful emotion regulation (Engen and Anderson, 2018; Ochsner and Gross, 2005) and contributes to psychological well-being over the lifespan (Mather and Carstensen, 2005).

Recent work indicated a shared genetic basis between local brain structure and complex behavioral traits (Grasby et al., 2020; Zhao et al., 2019). In line with this work, our study demonstrated that cognition and trait affect have a shared phenotypic and genetic relationship with cortical thickness in left superior frontal cortex. The superior frontal gyrus - which includes the dorsolateral prefrontal cortex — has been classically considered a core region for higher cognitive functions, including attention, working memory and cognitive control (Boisgueheneuc et al., 2006; Corbetta and Shulman, 2002). Yet, a growing body of research has highlighted its involvement in socioemotional processes, such as motivated behavior and emotion regulation (Engen and Anderson, 2018; Frank et al., 2014; Okon-Singer et al., 2015). Left superior frontal gyrus has also been implicated in selfawareness and introspection (Goldberg et al., 2006), as well as in psychiatric disorders of self-awareness, such as schizophrenia (Lee et al., 2016). Indeed, left superior frontal thickness has been shown to be modulated by schizophrenia-associated genetic variants, suggesting a shared genetic basis of schizophrenia-associated brain regions and the neurocognitive symptoms characterizing the disease (Lee et al., 2016). On a network level, the superior frontal cortex is situated at the intersection of the default mode network, the dorsal attention network and the frontoparietal control network (Li et al., 2013; Schaefer et al., 2018; Yeo et al., 2011). This particular network embedding suggests an integrating role of superior frontal cortex connectivity to broader associative, self-reflective processes, as well as controlling operations across the cortex (Andrews-Hanna et al., 2014; Li et al., 2013; Spreng et al., 2013). Our observation of an inter-relationship of cognition and affect in superior frontal cortex is further in line with a meta-analysis showing that interactions between emotion and cognition were associated with this region, next to medial prefrontal cortex and basal ganglia (Cromheeke and Mueller, 2014). In addition, the results we obtained from our functional decoding analysis are in line with the variety of cognitive and emotional

functions that previous studies have allocated to this region, such as activation related to social cognition, emotional valence and action inhibition (Bzdok et al., 2012; Cromheeke and Mueller, 2014; Hung et al., 2018). Interestingly, functional decoding only included a selection of cognitive and emotional labels. Labels involving positive emotion, implicit and working memory, attention, language processes, and spatial cognition, amongst others, did not load to this region. This may indicate that the overlap observed between the association of cognition and affect with cortical thickness of superior frontal cortex could be related to a rather specific set of functional processes relevant for both trait affect and cognition, possibly associated with emotional and cognitive control (Li et al., 2013; Song et al., 2017). Our results thus extend previous evidence of cognitive and affective behavior integration in superior frontal cortex by showing a macrostructural overlap of cognition and affect in superior frontal cortex that is based on shared genetic effects.

4.3. Dissociations of affect and cognition in brain structure

Both individual differences in cognitive and affective traits could be linked to local brain structure. Total cognition was associated with lower thickness in frontal regions which is in line with some studies (Goh et al., 2011; Salat et al., 2002; Sowell et al., 2001; Van Petten et al., 2004), but contradicting others (Fjell et al., 2006; Karama et al., 2009; Narr et al., 2006). At the same time, there is some congruency with previous studies involving the location of regions critical for cognition, including mostly frontal and parietal regions (Jung and Haier, 2007), but also anterior and posterior temporal, and occipital regions (Goh et al., 2011; Menary et al., 2013). Notably, we also observed associations between cognition and various regions within the insular cortices, functionally implicated in both cognitive, but also emotional processes (Kelly et al., 2012; Lindquist et al., 2012). In addition, we found wide-spread associations in temporal, frontal and occipital lobes between local surface area and cognitive ability, but not with affective traits. Mean affect was, however, phenotypically correlated with cortical thickness in left superior frontal cortex, left lateral occipital cortex and bilateral caudate volume. It is noteworthy that affective traits showed less strong and wide-spread associations to local thickness relative to cognitive scores. This observation is in line with reports suggesting inter-regional interactions, rather than local anatomy, may encode emotional experience (Kragel and LaBar, 2016; Langner et al., 2018; Pessoa, 2008). In fact, meta-analyses of functional neuroimaging studies did not find evidence for independent brain systems that specifically relate to positive and negative valence (Lindquist et al., 2016, 2012). This suggests that the neural representation of affect is characterized by dynamic interactions between brain regions and networks rather than functional specializations of distinct locations in the brain (Kragel and LaBar, 2016; Langner et al., 2018; Pessoa, 2008). Moreover, dissociable patterns of cortical thickness and surface area in relation to behavior might also underlie genetic influences. As such, individual variation in surface area has been associated with genes expressed pre-birth, whereas cortical thickness has been related to adult-specific gene expression and emerging genetic associations with cognitive abilities throughout development (Brouwer et al., 2014; Grasby et al., 2020; Panizzon et al., 2009).

5. Limitations and conclusions

We observed converging evidence for a heritable basis of interindividual differences in cognition and affect combining multi-level analysis within the HCP dataset and ad-hoc meta-analytical functional decoding. At the same time, we observed that correlations within each domain were generally stronger than between cognition and affect. Further research might benefit from studying task-based, as well as physiological measures of cognitive and affective inter-individual variation to further evaluate the dynamic relation between cognitive aptitude and habitual and transient affective experience. The singular nature of the twin-based HCP sample warrants the acquisition of comparable highresolution neuroimaging datasets including deeply phenotyped twins and families to test replication of results. Greater insight into the association between affect and cognition may be garnered by inspecting different samples, integrating more fine-grained genetic approaches with various indices of cortical anatomy. However, associations observed here were weak, and it is of note that the combination of behavioral assessments and its association with brain structure has been recently challenged: For example, Kharabian Masouleh et al. showed in an extensive study that the association of psychological traits and brain structure is rarely statistically significant or even reproducible in independent samples (Kharabian Masouleh et al., 2019). Additionally, Hedge and colleagues pointed out, that commonly used measurements of behavior may not be optimal to determine underlying neural correlates, due to low between-participant variability within established paradigms (Hedge et al., 2018). Here we utilized different levels of analysis to capture the association between affect and cognition. Follow-up work on the biological basis of complex behaviors may take a similar approach and integrate behavioral assessments with neuroimaging, behavioral and molecular genetics, and functional decoding. To conclude, the current work provides evidence at three levels of enquiry that cognitive abilities and affective traits are linked to partially overlapping neurobiological processes. We anticipate that the increased availability of open datasets with rich pheno- and genotyping will enable to outline more specific biological mechanisms that help describe the relationship between thoughts and feelings.

Data/code availability statement

To ensure reproducibility of this study using unrestricted and restricted data of the publicly available HCP dataset (www.humanconnectome.org), the code that has been used in our analyses can be found here: https://github.com/CNG-LAB/affect_cognition. As specified in the HCP Restricted Data Use Terms, investigator-assigned IDs of included participants will be shared upon publication of the study.

Declaration of Competing Interest

The authors declare no competing interests.

Credit authorship contribution statement

Nevena Kraljević: Conceptualization, Formal analysis, Writing – original draft, Writing – review & editing. H. Lina Schaare: Conceptualization, Formal analysis, Writing – original draft, Writing – review & editing. Simon B. Eickhoff: Conceptualization, Resources, Writing – review & editing, Funding acquisition. Peter Kochunov: Software, Resources, Writing – review & editing. B.T. Thomas Yeo: Resources, Writing – review & editing. Shahrzad Kharabian Masouleh: Conceptualization, Writing – original draft, Supervision. Sofie L. Valk: Conceptualization, Formal analysis, Writing – original draft, Writing – review & editing, Supervision.

Acknowledgements

We would like to sincerely thank all participants and contributors to the data provided by the Human Connectome Project, WU-Minn Consortium (Principal Investigators: David Van Essen and Kamil Ugurbil; 1U54MH091657) funded by the 16 NIH Institutes and Centers that support the NIH Blueprint for Neuroscience Research; and by the McDonnell Center for Systems Neuroscience at Washington University.

This study was supported by the European Union's Horizon 2020 Research and Innovation Programme under Grant Agreement no. 945539 (HBP SGA3). B.T.T.Y. is funded by the Singapore National

Research Foundation (NRF) Fellowship (Class of 2017) and the National University of Singapore Yong Loo Lin School of Medicine (NUH-SRO/2020/124/TMR/LOA). S.L.V. was supported by the Max Planck Gesellschaft (Otto Hahn award).

Supplementary materials

Supplementary material associated with this article can be found, in the online version, at doi:10.1016/j.neuroimage.2021.118561.

References

- Akshoomoff, N., Beaumont, J.L., Bauer, P.J., Dikmen, S.S., Gershon, R.C., Mungas, D., Slotkin, J., Tulsky, D., Weintraub, S., Zelazo, P.D., Heaton, R.K., 2013. NIH toolbox cognition function battery (CFB): composite scores of crystallized, fluid, and overall cognition. Monogr. Soc. Res. Child Dev. 78, 119–132. doi:10.1111/mono.12038.
- Almasy, L., Blangero, J., 1998. Multipoint quantitative-trait linkage analysis in general pedigrees. Am. J. Hum. Genet. 62, 1198–1211. doi:10.1086/301844.
- Almasy, L., Dyer, T.D., Blangero, J., 1997. Bivariate quantitative trait linkage analysis: pleiotropy versus co-incident linkages. Genet. Epidemiol. 14, 953–958 10.1002/(SICI)1098-2272(1997)14:6<953::AID-GEPI65>3.0.CO;2-K.
- Andrews-Hanna, J.R., Smallwood, J., Spreng, R.N., 2014. The default network and self-generated thought: component processes, dynamic control, and clinical relevance. Ann. NY Acad. Sci. 1316, 29–52. doi:10.1111/nyas.12360.
- Ashby, F.G., Isen, A.M., Turken, A.U., 1999. A neuropsychological theory of positive affect and its influence on cognition. Psychol. Rev. 106, 529–550. doi:10.1037/0033-295X.106.3.529.
- Atkinson, A.P., Heberlein, A.S., Adolphs, R., 2007. Spared ability to recognise fear from static and moving whole-body cues following bilateral amygdala damage. Neuropsychologia 45, 2772–2782. doi:10.1016/j.neuropsychologia.2007.04.019.
- Bajaj, S., Raikes, A., Smith, R., Dailey, N.S., Alkozei, A., Vanuk, J.R., Kilgore, W.D.S., 2018. The Relationship Between General Intelligence and Cortical Structure in Healthy Individuals. Neuroscience 388, 36–44. doi:10.1016/j.neuroscience.2018.07.008.
- Baker, L.A., Cesa, I.L., Gatz, M., Mellins, C., 1992. Genetic and environmental influences on positive and negative affect: support for a two-factor theory. Psychol. Aging 7, 158–163. doi:10.1037/0882-7974.7.1.158.
- Barrett, L.F., 2016. The theory of constructed emotion: an active inference account of interoception and categorization. Soc. Cogn. Affect. Neurosci. 12, nsw154. doi:10.1093/scan/nsw154.
- Bartels, M., Rietveld, M.J.H., Van Baal, G.C.M., Boomsma, D.I., 2002. Genetic and environmental influences on the development of intelligence. Behav. Genet. 32, 237–249. doi:10.1023/a:1019772628912.
- Baselmans, B.M.L., Jansen, R., Ip, H.F., van Dongen, J., Abdellaoui, A., van de Weijer, M.P., Bao, Y., Smart, M., Kumari, M., Willemsen, G., Hottenga, J.J., Boomsma, D.I., de Geus, E.J.C., Nivard, M.G., Bartels, M., 2019. Multivariate genome-wide analyses of the well-being spectrum. Nat. Genet. 51, 445–451. doi:10.1038/s41588-018-0320-8.
- Benjamini, Y., Hochberg, Y., 1995. Controlling the false discovery rate: a practical and powerful approach to multiple testing. J. R. Stat. Soc. Ser. B 57, 289–300. http://www.jstor.org/stable/2346101.
- Bernhardt, B.C., Valk, S.L., Silani, G., Bird, G., Frith, U., Singer, T., 2014. Selective disruption of sociocognitive structural brain networks in autism and alexithymia. Cereb. Cortex 24, 3258–3267. doi:10.1093/cercor/bht182.
- Betzel, R.F., Bassett, D.S., 2017. Multi-scale brain networks. Neuroimage 160, 73–83. doi:10.1016/j.neuroimage.2016.11.006.
- Boisgueheneuc, F.D., Levy, R., Volle, E., Seassau, M., Duffau, H., Kinkingnehun, S., Samson, Y., Zhang, S., Dubois, B., 2006. Functions of the left superior frontal gyrus in humans: a lesion study. Brain 129, 3315–3328. doi:10.1093/brain/awl244.
- Brans, R.G.H., Kahn, R.S., Schnack, H.G., van Baal, G.C.M., Posthuma, D., van Haren, N.E.M., Lepage, C., Lerch, J.P., Collins, D.L., Evans, A.C., Boomsma, D.I., Hulshoff Pol, H.E., 2010. Brain plasticity and intellectual ability are influenced by shared genes. J. Neurosci. 30, 5519–5524. doi:10.1523/JNEUROSCI.5841-09.2010.
- Brierley, B., Medford, N., Shaw, P., David, A.S., 2004. Emotional memory and perception in temporal lobectomy patients with amygdala damage. J. Neurol. Neurosurg. Psychiatry 75, 593–599. doi:10.1136/jnnp.2002.006403.
- Brouwer, R.M., van Soelen, I.L.C., Swagerman, S.C., Schnack, H.G., Ehli, E.A., Kahn, R.S., Hulshoff Pol, H.E., Boomsma, D.I., 2014. Genetic associations between intelligence and cortical thickness emerge at the start of puberty. Hum. Brain Mapp. 35, 3760– 3773. doi:10.1002/hbm.22435.
- Bzdok, D., Schilbach, L., Vogeley, K., Schneider, K., Laird, A.R., Langner, R., Eickhoff, S.B., 2012. Parsing the neural correlates of moral cognition: ALE meta-analysis on morality, theory of mind, and empathy. Brain Struct. Funct. 217, 783–796. doi:10.1007/s00429-012-0380-y.
- Corbetta, M., Shulman, G.L., 2002. Control of goal-directed and stimulus-driven attention in the brain. Nat. Rev. Neurosci. 3, 201–215. doi:10.1038/nrn755.
- Cromheeke, S., Mueller, S.C., 2014. Probing emotional influences on cognitive control: an ALE meta-analysis of cognition emotion interactions. Brain Struct. Funct. 219, 995–1008. doi:10.1007/s00429-013-0549-z.
- Davies, G., Tenesa, A., Payton, A., Yang, J., Harris, S.E., Liewald, D., Ke, X., Le Hellard, S., Christoforou, A., Luciano, M., McGhee, K., Lopez, L., Gow, A.J., Corley, J., Redmond, P., Fox, H.C., Haggarty, P., Whalley, L.J., McNeill, G., Goddard, M.E., Espeseth, T., Lundervold, A.J., Reinvang, I., Pickles, A., Steen, V.M., Ollier, W., Porteous, D.J., Horan, M., Starr, J.M., Pendleton, N., Visscher, P.M., Deary, I.J., 2011. Genome-wide association studies establish that human intelligence is highly heritable and polygenic. Mol. Psychiatry 16, 996–1005. doi:10.1038/mp.2011.85.

- Desrivières, S., Lourdusamy, A., Tao, C., Toro, R., Jia, T., Loth, E., Medina, L.M., Kepa, A., Fernandes, A., Ruggeri, B., Carvalho, F.M., Cocks, G., Banaschewski, T., Barker, G.J., Bokde, A.L.W., Büchel, C., Conrod, P.J., Flor, H., Heinz, A., Gallinat, J., Garavan, H., Gowland, P., Brühl, R., Lawrence, C., Mann, K., Martinot, M.L.P., Nees, F., Lathrop, M., Poline, J.-B., Rietschel, M., Thompson, P., Fauth-Bühler, M., Smolka, M.N., Pausova, Z., Paus, T., Feng, J., Schumann, G.IMAGEN Consortium, 2015. Single nucleotide polymorphism in the neuroplastin locus associates with cortical thickness and intellectual ability in adolescents. Mol. Psychiatry 20, 263–274. doi:10.1038/mp.2013.197.
- Diener, E., Emmons, R.A., 1984. The independence of positive and negative affect. J. Personal. Soc. Psychol. 47, 1105–1117. doi:10.1037/0022-3514.47.5.1105.
- Dolcos, F., Denkova, E., 2014. Current emotion research in cognitive neuroscience: linking enhancing and impairing effects of emotion on cognition. Emot. Rev. 6, 362–375. doi:10.1177/1754073914536449.
- Eickhoff, S.B., Constable, R.T., Yeo, B.T.T.T., 2018. Topographic organization of the cerebral cortex and brain cartography. Neuroimage 170, 332–347. doi:10.1016/j.neuroimage.2017.02.018.
- Engen, H.G., Anderson, M.C., 2018. Memory control: a fundamental mechanism of emotion regulation. Trends Cogn. Sci. 22, 982–995. doi:10.1016/j.tics.2018.07.015.
- Fischl, B., Salat, D.H., Busa, E., Albert, M., Dieterich, M., Haselgrove, C., van der Kouwe, A., Killiany, R., Kennedy, D., Klaveness, S., Montillo, A., Makris, N., Rosen, B., Dale, A.M., 2002. Whole brain segmentation. Neuron 33, 341–355. doi:10.1016/s0896-6273(02)00569-x.
- Fjell, A.M., Walhovd, K.B., Reinvang, I., Lundervold, A., Salat, D., Quinn, B.T., Fischl, B., Dale, A.M., 2006. Selective increase of cortical thickness in high-performing elderly-structural indices of optimal cognitive aging. Neuroimage 29, 984–994. doi:10.1016/J.NEUROIMAGE.2005.08.007.
- Fox, P.T., Lancaster, J.L., Laird, A.R., Eickhoff, S.B., 2014. Meta-analysis in human neuroimaging: computational modeling of large-scale databases. Annu. Rev. Neurosci. 37, 409–434. doi:10.1146/annurev-neuro-062012-170320.
- Frank, D.W., Dewitt, M., Hudgens-Haney, M., Schaeffer, D.J., Ball, B.H., Schwartz, N., Hussein, A.A., Smart, L.M., Sabatinelli, D., 2014. Emotion regulation: Quantitative meta-analysis of functional activation and deactivation. Neurosci. Biobehav. Rev. 45, 202–211. doi:10.1016/j.neubiorev.2014.06.010.
- Fredrickson, B.L., 2001. The role of positive emotions in positive psychology: the broaden-and-build theory of positive emotions. Am. Psychol. 56, 218–226. doi:10.1037/0003-066X.56.3.218.
- Genon, S., Reid, A., Langner, R., Amunts, K., Eickhoff, S.B., 2018. How to characterize the function of a brain region. Trends Cogn. Sci. doi:10.1016/j.tics.2018.01.010.
- Gershon, R.C., Slotkin, J., Manly, J.J., Blitz, D.L., Beaumont, J.L., Schnipke, D., Wallner-Allen, K., Golinkoff, R.M., Gleason, J.B., Hirsh-Pasek, K., Adams, M.J., Weintraub, S., 2013. NIH toolbox cognition battery (CB): Measuring language (vocabulary comprehension and reading decoding). Monogr. Soc. Res. Child Dev. 78, 49–69. doi:10.1111/mono.12034.
- Glahn, D.C., Winkler, A.M., Kochunov, P., Almasy, L., Duggirala, R., Carless, M.A., Curran, J.C., Olvera, R.L., Laird, A.R., Smith, S.M., Beckmann, C.F., Fox, P.T., Blangero, J., 2010. Genetic control over the resting brain. Proc. Natl. Acad. Sci. 107, 1223–1228. doi:10.1073/pnas.0909969107.
- Glasser, M.F., Sotiropoulos, S.N., Wilson, J.A., Coalson, T.S., Fischl, B., Andersson, J.L., Xu, J., Jbabdi, S., Webster, M., Polimeni, J.R., Van Essen, D.C., Jenkinson, M., 2013. The minimal preprocessing pipelines for the human connectome project. Neuroimage 80, 105–124. doi:10.1016/j.neuroimage.2013.04.127.
- Goh, S., Bansal, R., Xu, D., Hao, X., Liu, J., Peterson, B.S., 2011. Neuroanatomical correlates of intellectual ability across the life span. Dev. Cogn. Neurosci. 1, 305–312. doi:10.1016/j.dcn.2011.03.001.
- Goldberg, I.I., Harel, M., Malach, R., 2006. When the brain loses its self: prefrontal inactivation during sensorimotor processing. Neuron 50, 329–339. doi:10.1016/j.neuron.2006.03.015.
- Grasby, K.L., Jahanshad, N., Painter, J.N., Colodro-Conde, L., Bralten, J., Hibar, D.P., Lind, P.A., Pizzagalli, F., Ching, C.R.K., McMahon, M.A.B., Shatokhina, N., Zsembik, L.C.P., Thomopoulos, S.I., Zhu, A.H., Strike, L.T., Agartz, I., Alhusaini, S., Almeida, M.A.A., Alnæs, D., Amlien, I.K., Andersson, M., Ard, T., Armstrong, N.J., Ashley-Koch, A., Atkins, J.R., Bernard, M., Brouwer, R.M., Buimer, E.E.L., Bülow, R., Bürger, C., Cannon, D.M., Chakravarty, M., Chen, Q., Cheung, J.W., Couvy-Duchesne, B., Dale, A.M., Dalvie, S., de Araujo, T.K., de Zubicaray, G.I., de Zwarte, S.M.C., den Braber, A., Doan, N.T., Dohm, K., Ehrlich, S., Engelbrecht, H.R., Erk, S., Fan, C.C., Fedko, I.O., Foley, S.F., Ford, J.M., Fukunaga, M., Garrett, M.E., Ge, T., Giddaluru, S., Goldman, A.L., Green, M.J., Groenewold, N.A., Grotegerd, D., Gurholt, T.P., Gutman, B.A., Hansell, N.K., Harris, M.A., Harrison, M.B., Haswell, C.C., Hauser, M., Herms, S., Heslenfeld, D.J., Ho, N.F., Hoehn, D., Hoffmann, P., Holleran, L., Hoogman, M., Hottenga, J.J., Ikeda, M., Janowitz, D., Jansen, I.E., Jia, T., Jockwitz, C., Kanai, R., Karama, S., Kasperaviciute, D., Kaufmann, T., Kelly, S., Kikuchi, M., Klein, M., Knapp, M., Knodt, A.R., Krämer, B., Lam, M., Lancaster, T.M., Lee, P.H., Lett, T.A., Lewis, L.B., Lopes-Cendes, I., Luciano, M., Macciardi, F., Marquand, A.F., Mathias, S.R., Melzer, T.R., Milaneschi, Y., Mirza-Schreiber, N., Moreira, J.C.V., Mühleisen, T.W., Müller-Myhsok, B., Najt, P., Nakahara, S., Nho, K., Olde Loohuis, L.M., Orfanos, D.P., Pearson, J.F., Pitcher, T.L., Pütz, B., Quidé, Y., Ragothaman, A., Rashid, F.M., Reay, W.R., Redlich, R., Reinbold, C.S., Repple, J., Richard, G., Riedel, B.C., Risacher, S.L., Rocha, C.S., Mota, N.R., Salminen, L., Saremi, A., Saykin, A.J., Schlag, F., Schmaal, L., Schofield, P.R., Secolin, R., Shapland, C.Y., Shen, L., Shin, J., Shumskaya, E., Sønderby, I.E., Sprooten, E., Tansey, K.E., Teumer, A., Thalamuthu, A., Tordesillas-Gutiérrez, D., Turner, J.A., Uhlmann, A., Vallerga, C.L., van der Meer, D., van Donkelaar, M.M.J., van Eijk, L., van Erp, T.G.M., van Haren, N.E.M., van Rooij, D., van Tol, M.J., Veldink, J.H., Verhoef, E., Walton, E., Wang, M., Wang, Y., Wardlaw, J.M., Wen, W., Westlye, L.T., Whelan, C.D., Witt, S.H., Wittfeld, K., Wolf, C., Wolfers, T., Wu, J.Q., Yasuda, C.L., Zaremba, D.,

- Zhang, Z., Zwiers, M.P., Artiges, E., Assareh, A.A., Avesa-Arriola, R., Belger, A., Brandt, C.L., Brown, G.G., Cichon, S., Curran, J.E., Davies, G.E., Degenhardt, F., Dennis, M.F., Dietsche, B., Djurovic, S., Doherty, C.P., Espiritu, R., Garijo, D., Gil, Y., Gowland, P.A., Green, R.C., Häusler, A.N., Heindel, W., Ho, B.C., Hoffmann, W.U., Holsboer, F., Homuth, G., Hosten, N., Jack, C.R., Jang, M.H., Jansen, A., Kimbrel, N.A., Kolskår, K., Koops, S., Krug, A., Lim, K.O., Luykx, J.J., Mathalon, D.H., Mather, K.A., Mattay, V.S., Matthews, S., Mayoral Van Son, J., McEwen, S.C., Melle, I., Morris, D.W., Mueller, B.A., Nauck, M., Nordvik, J.E., Nöthen, M.M., O'Leary, D.S., Opel, N., Martinot, M.L.P., Pike, G.B., Preda, A., Quinlan, E.B., Rasser, P.E., Ratnakar, V., Reppermund, S., Steen, V.M., Tooney, P.A., Torres, F.R., Veltman, D.J., Voyvodic, J.T., Whelan, R., White, T., Yamamori, H., Adams, H.H.H., Bis, J.C., Debette, S., Decarli, C., Fornage, M., Gudnason, V., Hofer, E., Ikram, M.A., Launer, L., Longstreth, W.T., Lopez, O.L., Mazoyer, B., Mosley, T.H., Roshchupkin, G.V, Satizabal, C.L., Schmidt, R., Seshadri, S., Yang, Q., Alvim, M.K.M., Ames, D., Anderson, T.J., Andreassen, O.A., Arias-Vasquez, A., Bastin, M.E., Baune, B.T., Beckham, J.C., Blangero, J., Boomsma, D.I., Brodaty, H., Brunner, H.G., Buckner, R.L., Buitelaar, J.K., Bustillo, J.R., Cahn, W., Cairns, M.J., Calhoun, V., Carr, V.J., Caseras, X., Caspers, S., Cavalleri, G.L., Cendes, F., Corvin, A., Crespo-Facorro, B., Dalrymple-Alford, J.C., Dannlowski, U., de Geus, E.J.C., Deary, I.J., Delanty, N., Depondt, C., Desrivières, S., Donohoe, G., Espeseth, T., Fernández, G., Fisher, S.E., Flor, H., Forstner, A.J., Francks, C., Franke, B., Glahn, D.C., Gollub, R.L., Grabe, H.J., Gruber, O., Håberg, A.K., Hariri, A.R., Hartman, C.A., Hashimoto, R., Heinz, A., Henskens, F.A., Hillegers, M.H.J., Hoekstra, P.J., Holmes, A.J., Hong, L.E., Hopkins, W.D., et al., 2020. The genetic architecture of the human cerebral cortex. Science 367. doi:10.1126/science.aay6690.
- Hanford, L.C., Pinnock, F., Hall, G.B., Heinrichs, R.W., 2019. Cortical thickness correlates of cognitive performance in cognitively-matched individuals with and without schizophrenia. Brain and Cognition 132, 129–137. doi:10.1016/j.bandc.2019.04.003.
- Heaton, R.K., Akshoomoff, N., Tulsky, D., Mungas, D., Weintraub, S., Dikmen, S., Beaumont, J., Casaletto, K.B., Conway, K., Slotkin, J., Gershon, R., 2014. Reliability and validity of composite scores from the NIH toolbox cognition battery in adults. J. Int. Neuropsychol. Soc. 20, 588–598. doi:10.1017/S1355617714000241.
- Hedge, C., Powell, G., Sumner, P., 2018. The reliability paradox: Why robust cognitive tasks do not produce reliable individual differences. Behav. Res. Methods 50, 1166– 1186. doi:10.3758/s13428-017-0935-1.
- Hung, Y., Gaillard, S.L., Yarmak, P., Arsalidou, M., 2018. Dissociations of cognitive inhibition, response inhibition, and emotional interference: voxelwise ALE meta-analyses of fMRI studies. Hum. Brain Mapp. 39, 4065–4082. doi:10.1002/hbm.24232.
- Joshi, A.A., Leporé, N., Joshi, S.H., Lee, A.D., Barysheva, M., Stein, J.L., McMahon, K.L., Johnson, K., de Zubicaray, G.I., Martin, N.G., Wright, M.J., Toga, A.W., Thompson, P.M., 2011. The contribution of genes to cortical thickness and volume. Neuroreport 22, 101–105. doi:10.1097/WNR.0b013e3283424c84.
- Jung, R.E., Haier, R.J., 2007. The Parieto-frontal integration theory (P-FIT) of intelligence: converging neuroimaging evidence. Behav. Brain Sci. 30, 135–154. doi:10.1017/S0140525X07001185.
- Kan, K.J., Wicherts, J.M., Dolan, C.V, van der Maas, H.L.J., 2013. On the nature and nurture of intelligence and specific cognitive abilities: the more heritable, the more culture dependent. Psychol. Sci. 24, 2420–2428. doi:10.1177/0956797613493292.
- Karama, S., Ad-Dab'bagh, Y., Haier, R.J., Deary, I.J., Lyttelton, O.C., Lepage, C., Evans, A.C., 2009. Positive association between cognitive ability and cortical thickness in a representative US sample of healthy 6 to 18 year-olds. Intelligence 37, 145– 155. doi:10.1016/j.intell.2008.09.006.
- Kelly, C., Toro, R., Di Martino, A., Cox, C.L., Bellec, P., Castellanos, F.X., Milham, M.P., 2012. A convergent functional architecture of the insula emerges across imaging modalities. Neuroimage 61, 1129–1142. doi:10.1016/j.neuroimage.2012.03.021.
- Khalsa, S.S., Adolphs, R., Cameron, O.G., Critchley, H.D., Davenport, P.W., Feinstein, J.S., Feusner, J.D., Garfinkel, S.N., Lane, R.D., Mehling, W.E., Meuret, A.E., Nemeroff, C.B., Oppenheimer, S., Petzschner, F.H., Pollatos, O., Rhudy, J.L., Schramm, L.P., Simmons, W.K., Stein, M.B., Stephan, K.E., Van den Bergh, O., Van Diest, I., von Leupoldt, A., Paulus, M.P., Ainley, V., et al., 2018. Interoception and mental health: a roadmap. Biol. Psychiatry Cogn. Neurosci. Neuroimaging 3, 501–513. doi:10.1016/j.bpsc.2017.12.004.
- Kharabian Masouleh, S., Eickhoff, S.B., Hoffstaedter, F., Genon, S., 2019. Empirical examination of the replicability of associations between brain structure and psychological variables. elife 8, e43464. doi:10.7554/eLife.43464.001.
- Kochunov, P., Patel, B., Ganjgahi, H., Donohue, B., Ryan, M., Hong, E.L., Chen, X., Adhikari, B., Jahanshad, N., Thompson, P.M., Van't Ent, D., den Braber, A., de Geus, E.J.C., Brouwer, R.M., Boomsma, D.I., Hulshoff Pol, H.E., de Zubicaray, G.I., McMahon, K.L., Martin, N.G., Wright, M.J., Nichols, T.E., 2019. Homogenizing estimates of heritability among SOLAR-Eclipse, OpenMx, APACE, and FPHI software packages in neuroimaging data. Front. Neuroinform. 13, 16. doi:10.3389/fn-inf.2019.00016.
- Kragel, P.A., LaBar, K.S., 2016. Decoding the nature of emotion in the brain. Trends Cogn. Sci. 20, 444–455. doi:10.1016/J.TICS.2016.03.011.
- LaBar, K.S., LeDoux, J.E., Spencer, D.D., Phelps, E.A., 1995. Impaired fear conditioning following unilateral temporal lobectomy in humans. J. Neurosci. 15, 6846–6855.
- Laird, A.R., Eickhoff, S.B., Fox, P.M., Uecker, A.M., Ray, K.L., Saenz, J.J., McKay, D.R., Bzdok, D., Laird, R.W., Robinson, J.L., Turner, J.A., Turkeltaub, P.E., Lancaster, J.L., Fox, P.T., 2011. The BrainMap strategy for standardization, sharing, and meta-analysis of neuroimaging data. BMC Res. Notes 4, 349. doi:10.1186/1756-0500-4-349.
- Laird, A.R., Eickhoff, S.B., Kurth, F., Fox, P.M., Uecker, A.M., Turner, J.A., Robinson, J.L., Lancaster, J.L., Fox, P.T., 2009. ALE meta-analysis workfl ows via the BrainMap database: progress towards a probabilistic functional brain atlas. Front. Neuroinform. 3, 23. doi:10.3389/neuro.11.023.2009.
- Langner, R., Leiberg, S., Hoffstaedter, F., Eickhoff, S.B., 2018. Towards a human self-regulation system: common and distinct neural signatures of emo-

- tional and behavioural control. Neurosci. Biobehav. Rev. 90, 400–410. doi:10.1016/j.neubjorev.2018.04.022.
- Lee, P.H., Baker, J.T., Holmes, A.J., Jahanshad, N., Ge, T., Jung, J.Y., Cruz, Y., Manoach, D.S., Hibar, D.P., Faskowitz, J., McMahon, K.L., De Zubicaray, G.I., Martin, N.H., Wright, M.J., Ongür, D., Buckner, R., Roffman, J., Thompson, P.M., Smoller, J.W., 2016. Partitioning heritability analysis reveals a shared genetic basis of brain anatomy and schizophrenia. Mol. Psychiatry 21, 1680–1689. doi:10.1038/mp.2016.164.
- Li, W., Qin, W., Liu, H., Fan, L., Wang, J., Jiang, T., Yu, C., 2013. Subregions of the human superior frontal gyrus and their connections. Neuroimage 78, 46–58. doi:10.1016/j.neuroimage.2013.04.011.
- Lindquist, K.A., Satpute, A.B., Wager, T.D., Weber, J., Barrett, L.F., 2016. The brain basis of positive and negative affect: evidence from a meta-analysis of the human neuroimaging literature. Cereb. Cortex 26, 1910–1922. doi:10.1093/cercor/bhv001.
- Lindquist, K.A., Wager, T.D., Kober, H., Bliss-Moreau, E., Barrett, L.F., 2012. The brain basis of emotion: a meta-analytic review. Behav. Brain Sci. 35, 121–143. doi:10.1017/S0140525X11000446.
- Liu, Y., Wang, Z., 2014. Positive affect and cognitive control: approach-motivation intensity influences the balance between cognitive flexibility and stability. Psychol. Sci. 25, 1116–1123. doi:10.1177/0956797614525213.
- Lykken, D., Tellegen, A., 1996. Happiness is a stochastic phenomenon. Psychol. Sci. 7, 186–189. doi:10.1111/j.1467-9280.1996.tb00355.x.
- Mather, M., Carstensen, L.L., 2005. Aging and motivated cognition: the positivity effect in attention and memory. Trends Cogn. Sci. 9, 496–502. doi:10.1016/j.tics.2005.08.005.
- Menary, K., Collins, P.F., Porter, J.N., Muetzel, R., Olson, E.A., Kumar, V., Steinbach, M., Lim, K.O., Luciana, M., 2013. Associations between cortical thickness and general intelligence in children, adolescents and young adults. Intelligence 41, 597–606. doi:10.1016/J.INTELL.2013.07.010.
- Mick, E., McGough, J., Deutsch, C.K., Frazier, J.A., Kennedy, D., Goldberg, R.J., 2014. Genome-wide association study of proneness to anger. PLoS One 9, e87257. doi:10.1371/journal.pone.0087257.
- Narr, K.L., Woods, R.P., Thompson, P.M., Szeszko, P., Robinson, D., Dimtcheva, T., Gurbani, M., Toga, A.W., Bilder, R.M., 2006. Relationships between IQ and regional cortical gray matter thickness in healthy adults. Cereb. Cortex 17, 2163–2171. doi:10.1093/cercor/bh1125.
- Nostro, A.D., Müller, V.I., Reid, A.T., Eickhoff, S.B., 2017. Correlations between personality and brain structure: a crucial role of gender. Cereb. Cortex 27, 3698–3712. doi:10.1093/cercor/bhw191.
- Ochsner, K.N., Gross, J.J., 2005. The cognitive control of emotion. Trends Cogn. Sci. 9, 242–249. doi:10.1016/j.tics.2005.03.010.
- Okbay, A., Baselmans, B.M.L., De Neve, J.-E., Turley, P., Nivard, M.G., Fontana, M.A., Meddens, S.F.W., Linnér, R.K., Rietveld, C.A., Derringer, J., Gratten, J., Lee, J.J., Liu, J.Z., de Vlaming, R., Ahluwalia, T.S., Buchwald, J., Cavadino, A., Frazier-Wood, A.C., Furlotte, N.A., Garfield, V., Geisel, M.H., Gonzalez, J.R., Haitjema, S., Karlsson, R., van der Laan, S.W., Ladwig, K.-H., Lahti, J., van der Lee, S.J., Lind, P.A., Liu, T., Matteson, L., Mihailov, E., Miller, M.B., Minica, C.C., Nolte, I.M., Mook-Kanamori, D., van der Most, P.J., Oldmeadow, C., Qian, Y., Raitakari, O., Rawal, R., Realo, A., Rueedi, R., Schmidt, B., Smith, A.V, Stergiakouli, E., Tanaka, T., Taylor, K., Thorleifsson, G., Wedenoja, J., Wellmann, J., Westra, H.-J., Willems, S.M., Zhao, W., Amin, N., Bakshi, A., Bergmann, S., Bjornsdottir, G., Boyle, P.A., Cherney, S., Cox, S.R., Davies, G., Davis, O.S.P., Ding, J., Direk, N., Eibich, P., Emeny, R.T., Fatemifar, G., Faul, J.D., Ferrucci, L., Forstner, A.J., Gieger, C., Gupta, R., Harris, T.B., Harris, J.M., Holliday, E.G., Hottenga, J.J., De Jager, P.L., Kaakinen, M.A., Kajantie, E., Karhunen, V., Kolcic, I., Kumari, M., Launer, L.J., Franke, L., Li-Gao, R., Liewald, D.C., Koini, M., Loukola, A., Marques-Vidal, P., Montgomery, G.W., Mosing, M.A., Paternoster, L., Pattie, A., Petrovic, K.E., Pulkki-Råback, L., Quaye, L., Räikkönen, K., Rudan, I., Scott, R.J., Smith, J.A., Sutin, A.R., Trzaskowski, M., Vinkhuyzen, A.E., Yu, L., Zabaneh, D., Attia, J.R., Bennett, D.A., Berger, K., Bertram, L., Boomsma, D.I., Snieder, H., Chang, S.C., Cucca, F., Deary, I.J., van Duijn, C.M., Eriksson, J.G., Bültmann, U., de Geus, E.J.C., Groenen, P.J.F., Gudnason, V., Hansen, T., Hartman, C.A., Haworth, C.M.A., Hayward, C., Heath, A.C., Hinds, D.A., Hyppönen, E., Iacono, W.G., Järvelin, M.R., Jöckel, K.H., Kaprio, J., Kardia, S.L.R., Keltikangas-Järvinen, L., Kraft, P., Kubzansky, L.D., Lehtimäki, T., Magnusson, P.K.E., Martin, N.G., McGue, M., Metspalu, A., Mills, M., de Mutsert, R., Oldehinkel, A.J., Pasterkamp, G., Pedersen, N.L., Plomin, R., Polasek, O., Power, C., Rich, S.S., Rosendaal, F.R., et al., 2016. Genetic variants associated with subjective well-being, depressive symptoms, and neuroticism identified through genome-wide analyses. Nat. Genet. 48, 624-633. doi:10.1038/ng.3552.
- Okon-Singer, H., Hendler, T., Pessoa, L., Shackman, A.J., 2015. The neurobiology of emotion-cognition interactions: Fundamental questions and strategies for future research. Front. Hum. Neurosci. 9, 1–14. doi:10.3389/fnhum.2015.00058.
- Oschwald, J., Guye, S., Liem, F., Rast, P., Willis, S., Röcke, C., Jäncke, L., Martin, M., Mérillat, S., 2019. Brain structure and cognitive ability in healthy aging: a review on longitudinal correlated change. Rev. Neurosci. 31, 1–57. doi:10.1515/revneuro.2018-0096
- Panizzon, M.S., Fennema-Notestine, C., Eyler, L.T., Jernigan, T.L., Prom-Wormley, E., Neale, M., Jacobson, K., Lyons, M.J., Grant, M.D., Franz, C.E., Xian, H., Tsuang, M., Fischl, B., Seidman, L., Dale, A., Kremen, W.S., 2009. Distinct genetic influences on cortical surface area and cortical thickness. Cereb. Cortex 19, 2728–2735. doi:10.1093/cercor/bln026.
- Pessoa, L., 2008. On the relationship between emotion and cognition. Nat. Rev. Neurosci. 9, 148–158. doi:10.1038/nrn2317.
- Pilkonis, P.A., Choi, S.W., Salsman, J.M., Butt, Z., Moore, T.L., Lawrence, S.M., Zill, N., Cyranowski, J.M., Kelly, M.A.R., Knox, S.S., Cella, D., 2013. Assessment of self-reported negative affect in the NIH Toolbox. Psychiatry Res. 206, 88–97. doi:10.1016/j.psychres.2012.09.034.

- Rohr, C.S., Dreyer, F.R., Aderka, I.M., Margulies, D.S., Frisch, S., Villringer, A., Okon-Singer, H., 2015. Individual differences in common factors of emotional traits and executive functions predict functional connectivity of the amygdala. Neuroimage 120, 154–163. doi:10.1016/j.neuroimage.2015.06.049.
- Russell, J.A., Carroll, J.M., 1999. On the bipolarity of positive and negative affect. Psychol. Bull. 125, 3–30. doi:10.1037//0033-2909.125.1.3.
- Salat, D.H., Kaye, J.A., Janowsky, J.S., 2002. Greater orbital prefrontal volume selectively predicts worse working memory performance in older adults. Cereb. Cortex 12, 494– 505. doi:10.1093/cercor/12.5.494.
- Salsman, J.M., Butt, Z., Pilkonis, P.A., Cyranowski, J.M., Zill, N., Hendrie, H.C., Kupst, M.J., Kelly, M.A.R., Bode, R.K., Choi, S.W., Lai, J.S., Griffith, J.W., Stoney, C.M., Brouwers, P., Knox, S.S., Cella, D., 2013. Emotion assessment using the NIH Toolbox. Neurology 80, S76–S86. doi:10.1212/WNL.0b013e3182872e11.
- Salsman, J.M., Lai, J.-S., Hendrie, H.C., Butt, Z., Zill, N., Pilkonis, P.A., Peterson, C., Stoney, C.M., Brouwers, P., Cella, D., 2014. Assessing psychological well-being: self-report instruments for the NIH Toolbox. Qual. Life Res. 23, 205–215. doi:10.1007/s11136-013-0452-3.
- Satizabal, C.L., Adams, H.H.H., Hibar, D.P., White, C.C., Knol, M.J., Stein, J.L., Scholz, M., Sargurupremraj, M., Jahanshad, N., Roshchupkin, G.V., Smith, A.V., Bis, J.C., Jian, X., Luciano, M., Hofer, E., Teumer, A., van der Lee, S.J., Yang, J., Yanek, L.R., Lee, T.V., Li, S., Hu, Y., Koh, J.Y., Eicher, J.D., Desrivères, S., Arias-Vasquez, A., Chauhan, G., Athanasiu, L., Rentería, M.E., Kim, S., Hoehn, D., Armstrong, N.J., Chen, Q., Holmes, A.J., et al., 2019. Genetic architecture of subcortical brain structures in 38,851 individuals. Nat. Genet. 51, 1624–1636. doi:10.1038/s41588-019-0511-v.
- Schaefer, A., Kong, R., Gordon, E.M., Laumann, T.O., Zuo, X.-N., Holmes, A.J., Eickhoff, S.B., Yeo, B.T.T., 2018. Local-global parcellation of the human cerebral cortex from intrinsic functional connectivity MRI. Cereb. Cortex 28, 3095–3114. doi:10.1093/cercor/bhx179.
- Shaw, P., Greenstein, D., Lerch, J., Clasen, L., Lenroot, R., Gogtay, N., Evans, A., Rapoport, J., Giedd, J., 2006. Intellectual ability and cortical development in children and adolescents. Nature 440, 676. doi:10.1038/nature04513.
- Song, S., Zilverstand, A., Song, H., D'Oleire Uquillas, F., Wang, Y., Xie, C., Cheng, L., Zou, Z., 2017. The influence of emotional interference on cognitive control: a metaanalysis of neuroimaging studies using the emotional Stroop task. Sci. Rep. 7, 1–9. doi:10.1038/s41598-017-02266-2.
- Sowell, E.R., Delis, D., Stiles, J., Jernigan, T.L., 2001. Improved memory functioning and frontal lobe maturation between childhood and adolescence: a structural MRI study. J. Int. Neuropsychol. Soc. 7, 312–322. doi:10.1017/S135561770173305X.
- Spreng, R.N., Sepulcre, J., Turner, G.R., Stevens, W.D., Schacter, D.L., 2013. Intrinsic architecture underlying the relations among the default, dorsal attention, and frontoparietal control networks of the human brain. J. Cogn. Neurosci. 25, 74–86. doi:10.1162/jocn_a_00281.
- Thompson, P.M., Jahanshad, N., Ching, C.R.K., Salminen, L.E., Thomopoulos, S.I., Bright, J., Baune, B.T., Bertolín, S., Bralten, J., Bruin, W.B., Bülow, R., Chen, J., Chye, Y., Dannlowski, U., de Kovel, C.G.F., Donohoe, G., Eyler, L.T., Faraone, S.V., Favre, P., Filippi, C.A., Frodl, T., Garijo, D., Gil, Y., Grabe, H.J., Grasby, K.L., Hajek, T., Han, L.K.M., Hatton, S.N., Hilbert, K., Ho, T.C., Holleran, L., Homuth, G., Hosten, N., Houenou, J., Ivanov, I., Jia, T., Kelly, S., Klein, M., Kwon, J.S., Laansma, M.A., Leerssen, J., Lueken, U., Nunes, A., Neill, J.O., Opel, N., et al., 2020. ENIGMA and global neuroscience: a decade of large-scale studies of the brain in health and disease across more than 40 countries. Transl. Psychiatry 10, 1–28. doi:10.1038/s41398-020-0705-1.
- Toga, A.W., Thompson, P.M., 2005. Genetics of brain structure and intelligence. Annu. Rev. Neurosci. 28, 1–23. doi:10.1146/annurev.neuro.28.061604.135655.

- Tsuchiya, N., Moradi, F., Felsen, C., Yamazaki, M., Adolphs, R., 2009. Intact rapid detection of fearful faces in the absence of the amygdala. Nat. Neurosci. 12, 1224–1225. doi:10.1038/nn.2380.
- Valk, S.L., Bernhardt, B.C., Böckler, A., Kanske, P., Singer, T., 2016a. Substrates of metacognition on perception and metacognition on higher-order cognition relate to different subsystems of the mentalizing network. Hum. Brain Mapp. 37, 3388–3399. doi:10.1002/bbm.23247.
- Valk, S.L., Bernhardt, B.C., Böckler, A., Trautwein, F.M., Kanske, P., Singer, T., 2016b.
 Socio-cognitive phenotypes differentially modulate large-scale structural covariance networks. Cereb. Cortex 27. bhv319. doi:10.1093/cercor/bhv319.
- Valk, S.L., Hoffstaedter, F., Camilleri, J.A., Kochunov, P., Yeo, B.T.T., Eickhoff, S.B., 2020. Personality and local brain structure: their shared genetic basis and reproducibility. Neuroimage 220, 117067. doi:10.1016/j.neuroimage.2020.117067.
- Van Essen, D.C., Smith, S.M., Barch, D.M., Behrens, T.E.J., Yacoub, E., Ugurbil, K., 2013. The WU-Minn human connectome project: an overview. Neuroimage 80, 62–79. doi:10.1016/j.neuroimage.2013.05.041.
- Van Petten, C., Plante, E., Davidson, P.S.., Kuo, T.Y., Bajuscak, L., Glisky, E.L., 2004. Memory and executive function in older adults: relationships with temporal and prefrontal gray matter volumes and white matter hyperintensities. Neuropsychologia 42, 1313–1335. doi:10.1016/J.NEUROPSYCHOLOGIA.2004.02.009.
- van Soelen, I.L.C., Brouwer, R.M., Leeuwen, M.van, Kahn, R.S., Hulshoff Pol, H.E., Boomsma, D.I., 2011. Heritability of verbal and performance intelligence in a pediatric longitudinal sample. Twin Res. Hum. Genet. 14, 119–128. doi:10.1375/twin.14.2.119.
- Wainwright, M.A., Wright, M.J., Geffen, G.M., Luciano, M., Martin, N.G., 2005. The genetic basis of academic achievement on the queensland core skills test and its shared genetic variance with IQ. Behav. Genet. 35, 133–145. doi:10.1007/s10519-004-1014-9.
- Watson, D., Tellegen, A., 1985. Toward a consensual structure of mood. Psychol. Bull. 98, 219–235. doi:10.1037/0033-2909.98.2.219.
- Winkler, A.M., Kochunov, P., Blangero, J., Almasy, L., Zilles, K., Fox, P.T., Duggirala, R., Glahn, D.C., 2010. Cortical thickness or grey matter volume? The importance of selecting the phenotype for imaging genetics studies. Neuroimage 53, 1135–1146. doi:10.1016/j.neuroimage.2009.12.028.
- Worsley, K.J., Taylor, J., Carbonell, F., Chung, M.K., Duerden, E., Bernhardt, B., Lyttelton, O., Boucher, M., Evans, A.C., 2009. A Matlab toolbox for the statistical analysis of univariate and multivariate surface and volumetric data using linear mixed effects models and random field theory. NeuroImage S102 Organisation for Human Brain Mapping 2009 Annual Meeting.
- Yeo, B.T.T., Krienen, F.M., Sepulcre, J., Sabuncu, M.R., Lashkari, D., Hollinshead, M., Roffman, J.L., Smoller, J.W., Zöllei, L., Polimeni, J.R., Fisch, B., Liu, H., Buckner, R.L., 2011. The organization of the human cerebral cortex estimated by intrinsic functional connectivity. J. Neurophysiol. 106, 1125–1165. doi:10.1152/jn.00338.2011.
- Zhao, B., Luo, T., Li, T., Li, Y., Zhang, J., Shan, Y., Wang, X., Yang, L., Zhou, F., Zhu, Z., Zhu, H., 2019. Genome-wide association analysis of 19,629 individuals identifies variants influencing regional brain volumes and refines their genetic coarchitecture with cognitive and mental health traits. Nat. Genet. 51, 1637–1644. doi:10.1038/s41588-019-0516-6.
- Zheng, Y., Plomin, R., von Stumm, S., 2016. Heritability of intraindividual mean and variability of positive and negative affect: genetic analysis of daily affect ratings over a month. Psychol. Sci. 27, 1611–1619. doi:10.1177/0956797616669994.

BEHAVIORAL, ANATOMICAL AND HERITABLE CONVERGENCE OF AFFECT AND COGNITION IN SUPERIOR FRONTAL CORTEX

-SUPPLEMENT-

Nevena Kraljevic*^{1,2}, H. Lina Schaare*^{1,7}, Simon B. Eickhoff^{1,2}, Peter Kochunov³, B. T. Thomas Yeo^{4,5,6}, Shahrzad Kharabian Masouleh^{1,2}, Sofie L. Valk^{1,2,7}

Corresponding authors:

schaare[at]cbs.mpg.de; s.valk[at]fz-juelich.de

¹⁾ Institute of Neuroscience and Medicine (INM-7: Brain and Behaviour), Research Centre Jülich, Jülich, Germany
²⁾ Institute of Systems Neuroscience, Heinrich Heine University Düsseldorf, Düsseldorf, Germany
³⁾ Maryland Psychiatric Research Center, University of Maryland School of Medicine, Baltimore, Maryland, USA
⁴⁾ Department of Electrical and Computer Engineering, Centre for Sleep and Cognition, Centre for Translational
MR Research, N.1 Institute for Health and Institute for Digital Medicine, National University of Singapore,
Singapore, Singapore
⁵⁾ Athinoula A. Martinos Center for Biomedical Imaging, Massachusetts General Hospital, Charlestown, MA, USA
⁶⁾ NUS Graduate School for Integrative Sciences and Engineering, National University of Singapore, Singapore,
Singapore
⁷⁾ Otto Hahn group Cognitive Neurogenetics, Max Planck Institute for Human Cognitive and Brain Sciences,
Leipzig, Germany

* authors contributed equally

SUPPLEMENTARY RESULTS

Phenotypic association of sub-scores of cognition and affect with local brain anatomy

We evaluated the phenotypic correlation between cognition and local cortical thickness, while controlling for global thickness. We observed that cognitive sub-scores for fluid and crystallized cognition showed similar patterns of positive and negative relations to total cognition with cortical thickness (Supplementary Figure 2, Supplementary Tables 2-3). Fluid cognition was negatively associated with primarily frontal regions and positively associated with medial occipital cortex. Crystallized cognition was related to wide-spread effects in cortical thickness of frontal and parietal regions (negative associations), as well as temporal, sensorimotor and insular thickness (positive associations).

Fluid cognition was positively related to surface area primarily in bilateral occipital and temporal pole regions (Supplementary Figure 3) and crystallized cognition was positively related to surface area in bilateral inferior temporal areas, lateral frontal and parietal areas, as well as left anterior cingulate cortex (Supplementary Figure 3). See further Supplementary Tables 8-9.

With regards to subcortical volumes, we found that crystallized cognition was positively associated with bilateral hippocampal and right amygdalar volume and fluid cognition was negatively associated with left pallidum volume (Supplementary Tables 11-12).

Sub-score analyses of affect yielded that positive affect was negatively associated with cortical thickness in left superior frontal cortex, whereas negative affect was negatively associated with occipital cortical thickness (Supplementary Figure 2, Supplementary Tables 5-6). Furthermore, there were significant phenotypic associations for both positive and negative affect with bilateral caudate volumes (Supplementary Tables 14-15). Effects with surface area were not significant.

Genetic correlation of sub-scores of cognition and affect with local brain anatomy

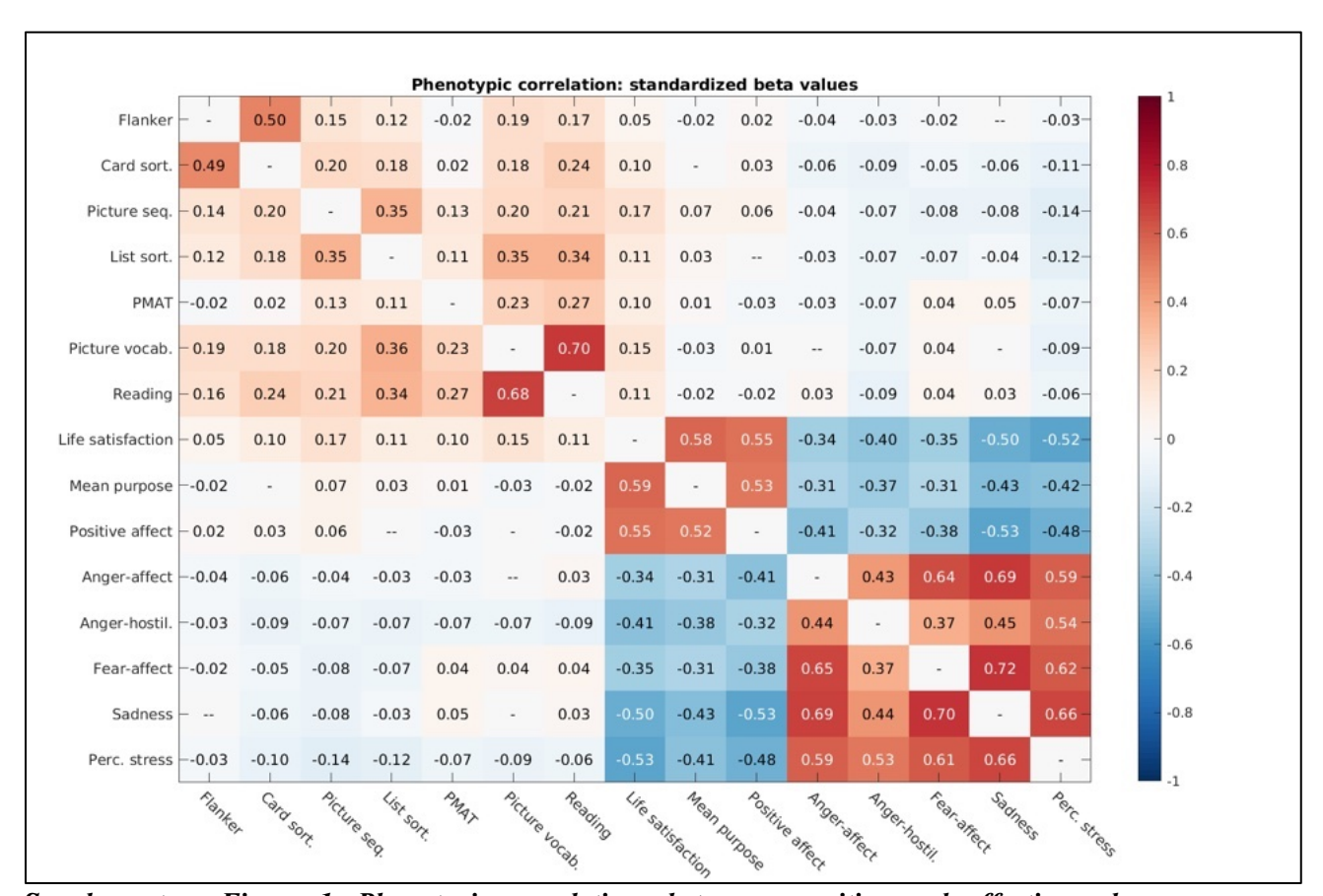
To assess if the correlation between cognitive and affective traits on the one hand and local brain structure on the other is driven by shared genetic effects, genetic correlation analyses were performed through a bivariate polygenetic analysis. In general, there was a strong overlap between phenotypic correlations and genetic correlations (Supplementary Figure 5, Supplementary Figure 6). 18 out of 21 phenotypic correlations between fluid cognition, and 36 out of 42 phenotypic correlations for crystallized cognition and local cortical thickness could be attributed to genetic effects (Supplementary Table 18).

Regarding associations with surface area, we found 11 out of 14 related to fluid cognition and 36 out of 56 related to crystallized cognition to be attributable to shared genetic effects (Supplementary Table 19).

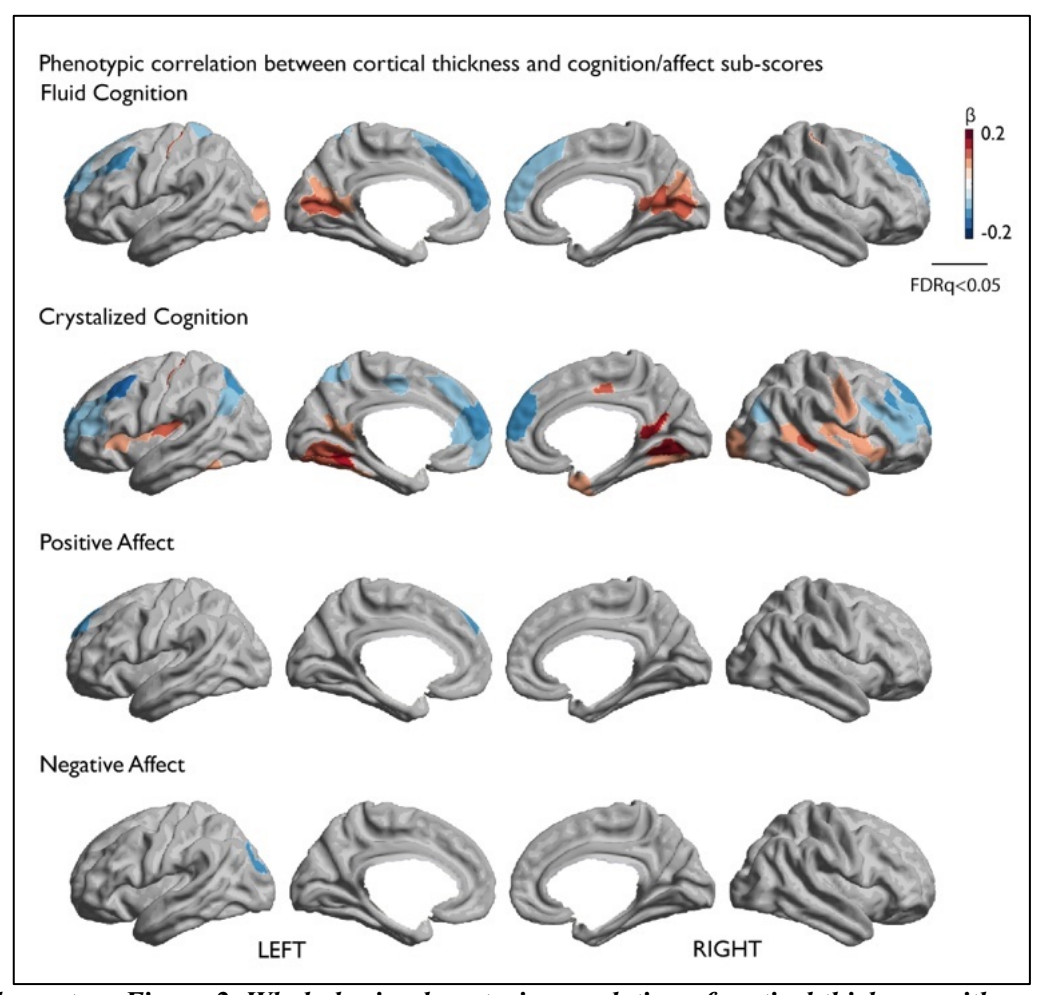
Fluid cognition was also genetically correlated with volume in the left pallidum (ρ_g =-0.230, p=0.003) and there was a genetic correlation between crystallized cognition and bilateral hippocampal volume (left: ρ_g =0.159, p=0.004; right: ρ_g =0.098, p=0.026; Supplementary Table 20).

Genetic correlations with affective sub-scores yielded that only the phenotypic association of positive affect with superior frontal cortex was driven by shared genetic effects (Supplementary Figure 5, Supplementary Table 18). We also found that the associations of positive, as well as negative affect with bilateral caudate volumes were driven by genetic correlations (Supplementary Tables 20).

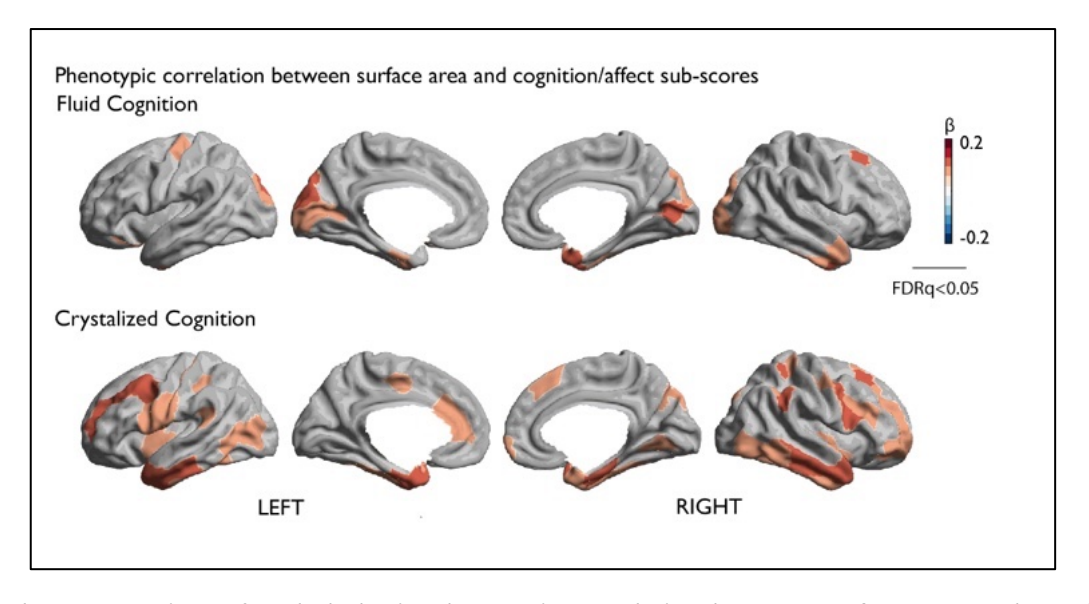
SUPPLEMENTARY FIGURES



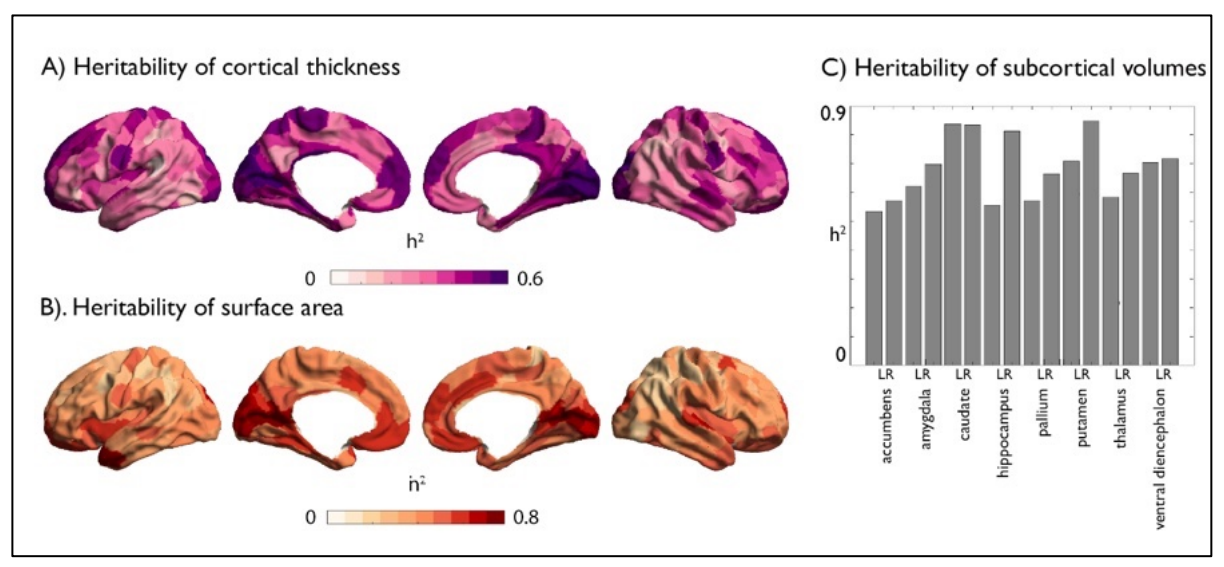
Supplementary Figure 1. Phenotypic correlations between cognitive and affective sub-scores. Abbreviations: Card sort.: Dimensional Change Card Sorting, Picture seq.: Picture Sequence Memory, List sort.: List Sorting, PMAT: Penn Matrix Test pattern comparison test, Picture vocab.: Picture Vocabulary, Anger-hostil.: Anger sub-scale Hostility, Perc. stress: Perceived stress.



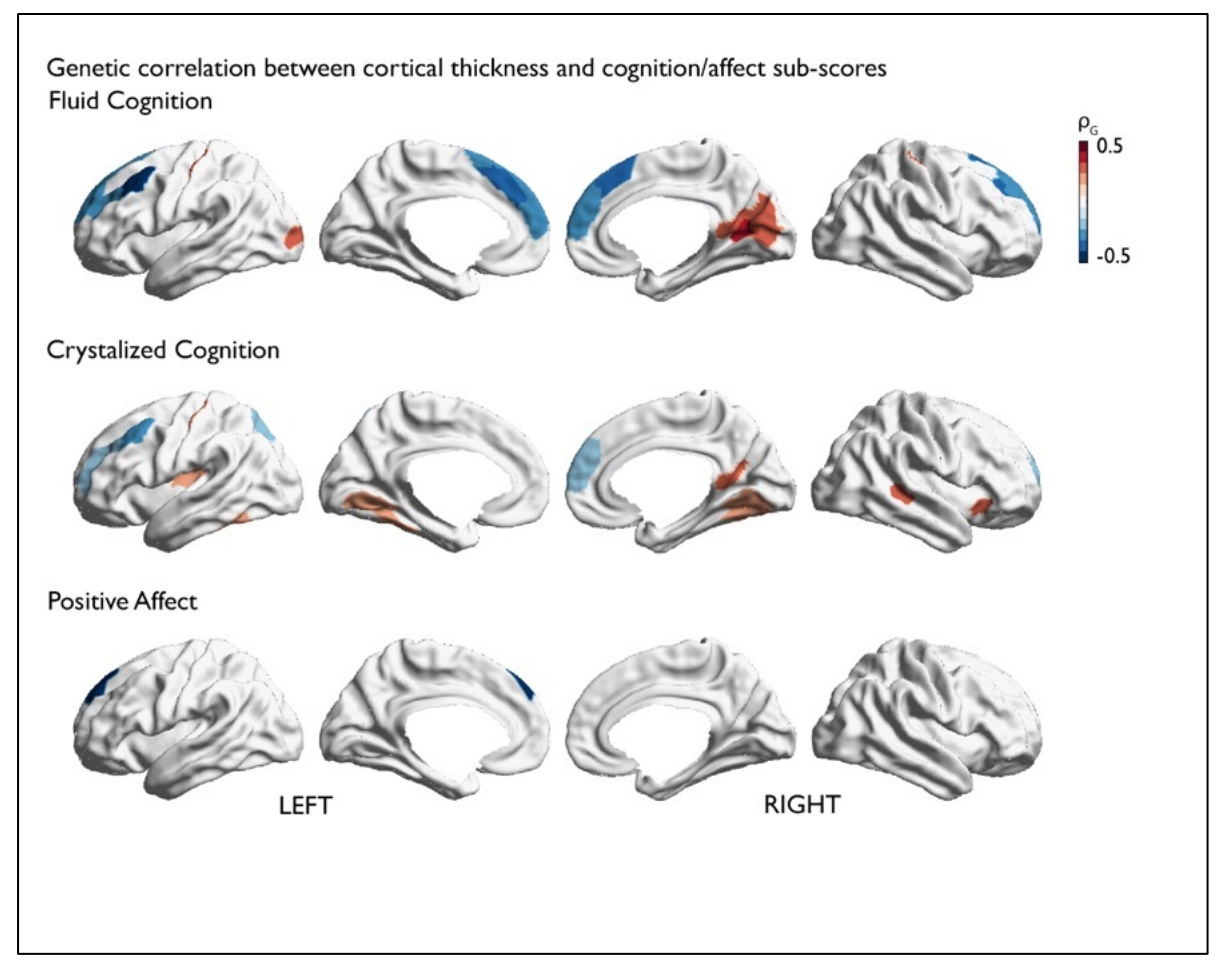
Supplementary Figure 2. Whole-brain phenotypic correlation of cortical thickness with cognitive and affective sub-scores. Positive correlation is depicted in red, negative in blue. Only correlations at FDRq<0.05 are depicted



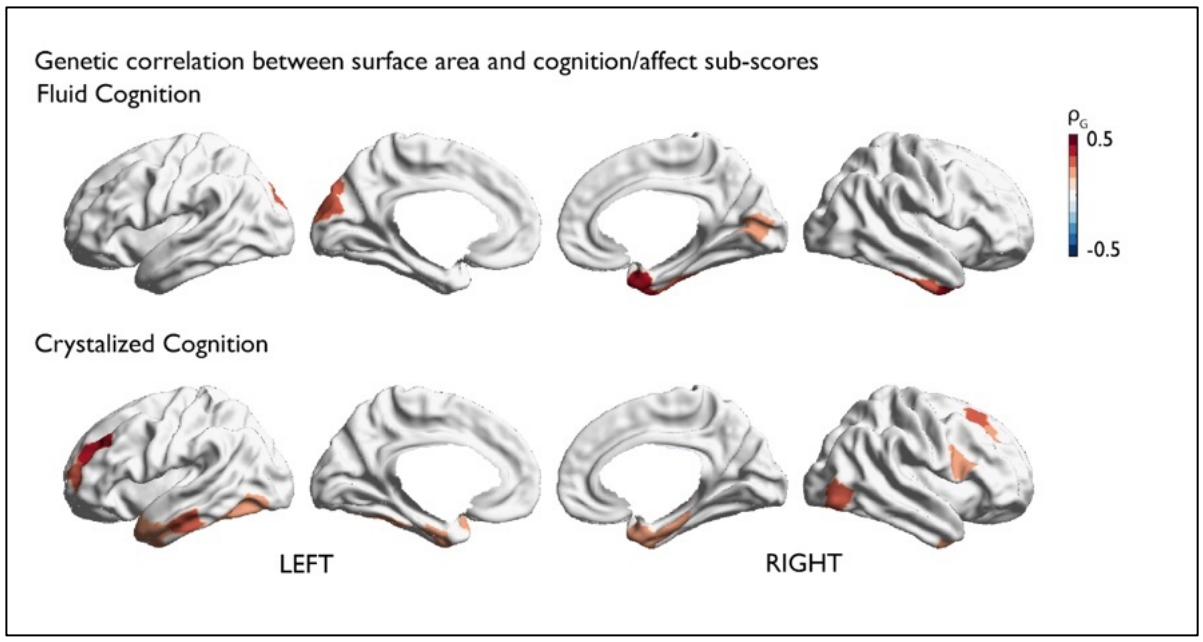
Supplementary Figure 3. Whole-brain phenotypic correlation between surface area and cognitive sub-scores. Positive correlation is depicted in red, negative in blue. Only correlations at FDRq<0.05 are depicted. Associations with affective sub-scores were not significant.



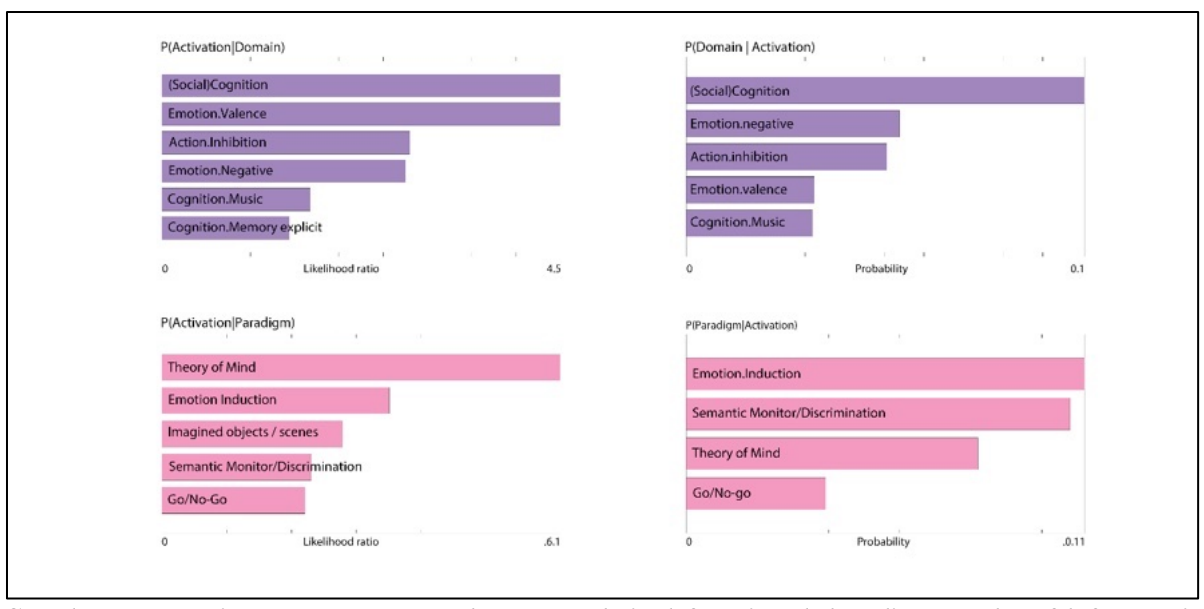
Supplementary Figure 4. Heritability of local cortical thickness, surface area and subcortical volumes. Heritability of local cortical thickness, surface area and subcortical volumes. A) Heritability of local cortical thickness per parcel (200 parcel solution Schaefer, 2018); B) Heritability of local surface area per parcel. C) Heritability of subcortical volumes per FreeSurfer-segmented region.



Supplementary Figure 5. Whole-brain genetic correlation of cortical thickness with cognitive and affective sub-scores. Positive correlation is depicted in red, negative in blue. Only correlations at FDRq<0.05 are depicted.



Supplementary Figure 6. Whole-brain genetic correlation between surface area and cognitive sub-scores. Positive correlation is depicted in red, negative in blue. Only correlations at FDRq<0.05 are depicted. Associations with affective sub-scores were not significant.



Supplementary Figure 7. Uncorrected meta-analytical functional decoding results of left superior frontal cortex cluster using Brainmap (p<0.05).

SUPPLEMENTARY TABLESSupplementary Table 1. Total cognition and local cortical thickness.

	Tota	al Cognit	tion		Fluid		Cı	rystallize	ed	Pos	sitive Aff	ect	Neg	ative Af	fect	M	ean Affe	ct
	β	SD	р	β	SD	р	β	SD	p	β	SD	р	β	SD	р	β	SD	p
7Networks_LH_Vis_1	0.095	0.026	0.000	0.043	0.027	0.051	0.132	0.026	0.000	-0.005	0.026	0.424	0.035	0.026	0.089	-0.022	0.026	0.200
7Networks_LH_Vis_4	0.110	0.029	0.000	0.072	0.029	0.006	0.121	0.029	0.000	0.010	0.029	0.367	-0.019	0.029	0.258	0.016	0.029	0.292
7Networks_LH_Vis_9	0.074	0.025	0.002	0.081	0.026	0.001	0.046	0.026	0.036	0.062	0.025	0.007	-0.049	0.025	0.027	0.062	0.025	0.007
7Networks_LH_Vis_10	0.087	0.027	0.001	0.096	0.027	0.000	0.048	0.027	0.039	0.005	0.027	0.423	-0.023	0.027	0.196	0.015	0.027	0.282
7Networks_LH_SomMot_3	0.094	0.024	0.000	0.061	0.024	0.006	0.103	0.024	0.000	0.010	0.024	0.336	-0.030	0.024	0.106	0.022	0.024	0.179
7Networks_LH_SomMot_10	0.139	0.025	0.000	0.110	0.025	0.000	0.135	0.025	0.000	0.052	0.025	0.019	-0.048	0.025	0.028	0.056	0.025	0.013
7Networks_LH_DorsAttn_Post_7	-0.073	0.025	0.002	-0.038	0.025	0.060	-0.096	0.025	0.000	-0.049	0.024	0.022	0.019	0.025	0.218	-0.039	0.024	0.057
7Networks_LH_DorsAttn_Post_10	-0.076	0.025	0.001	-0.077	0.025	0.001	-0.057	0.025	0.011	-0.016	0.025	0.263	-0.006	0.025	0.399	-0.006	0.024	0.411
7Networks_LH_DorsAttn_FEF_2	-0.071	0.024	0.001	-0.062	0.024	0.005	-0.063	0.024	0.004	-0.065	0.023	0.003	0.052	0.024	0.013	-0.066	0.023	0.003
7Networks_LH_SalVentAttn_FrOperIns_2	0.084	0.023	0.000	0.067	0.024	0.002	0.081	0.024	0.000	0.014	0.023	0.282	0.016	0.023	0.244	-0.001	0.023	0.483
7Networks_LH_SalVentAttn_PFCl_1	-0.088	0.023	0.000	-0.070	0.023	0.001	-0.086	0.023	0.000	-0.010	0.023	0.333	0.001	0.023	0.475	-0.006	0.023	0.389
7Networks_LH_Default_Temp_5	0.069	0.023	0.001	0.055	0.023	0.009	0.056	0.023	0.008	0.013	0.023	0.286	-0.025	0.023	0.136	0.021	0.023	0.179
7Networks_LH_Default_PFC_4	-0.083	0.025	0.000	-0.073	0.025	0.002	-0.070	0.025	0.002	-0.053	0.025	0.016	0.052	0.025	0.017	-0.058	0.025	0.009
7Networks_LH_Default_PFC_5	-0.070	0.024	0.002	-0.053	0.024	0.015	-0.066	0.024	0.003	-0.057	0.024	0.009	0.057	0.024	0.009	-0.063	0.024	0.004
7Networks_LH_Default_PFC_7	-0.114	0.025	0.000	-0.098	0.025	0.000	-0.103	0.025	0.000	-0.046	0.025	0.031	0.036	0.025	0.072	-0.046	0.025	0.031
7Networks_LH_Default_PFC_9	-0.078	0.024	0.001	-0.077	0.024	0.001	-0.054	0.024	0.013	-0.094	0.024	0.000	0.078	0.024	0.001	-0.096	0.024	0.000
7Networks_LH_Default_PFC_10	-0.103	0.023	0.000	-0.100	0.024	0.000	-0.081	0.024	0.000	-0.041	0.023	0.042	0.029	0.024	0.113	-0.039	0.023	0.050
7Networks_LH_Default_PFC_11	-0.157	0.023	0.000	-0.127	0.024	0.000	-0.146	0.024	0.000	-0.055	0.024	0.010	0.031	0.024	0.096	-0.049	0.024	0.020
7Networks_LH_Default_PFC_13	-0.086	0.024	0.000	-0.089	0.025	0.000	-0.064	0.025	0.005	-0.073	0.024	0.001	0.070	0.024	0.002	-0.079	0.024	0.001
7Networks_LH_Default_pCunPCC_1	0.098	0.026	0.000	0.079	0.026	0.001	0.091	0.026	0.000	0.012	0.026	0.315	0.002	0.026	0.461	0.006	0.026	0.411
7Networks_RH_Vis_4	0.086	0.028	0.001	0.017	0.029	0.275	0.143	0.028	0.000	0.022	0.028	0.221	0.007	0.028	0.401	0.009	0.028	0.379
7Networks_RH_Vis_9	0.083	0.028	0.002	0.100	0.028	0.000	0.038	0.028	0.089	-0.023	0.028	0.207	0.017	0.028	0.270	-0.023	0.028	0.211
7Networks_RH_Vis_10			0.093	0.027	0.000	0.049	0.027	0.035	0.043	0.027	0.054	-0.050	0.027	0.031	0.052	0.027	0.026	
7Networks_RH_Vis_13	0.088 0.027 0. 0.088 0.025 0.			0.083	0.025	0.000	0.067	0.025	0.004	-0.006	0.025	0.404	-0.016	0.025	0.253	0.005	0.025	0.413

7Networks_RH_SomMot_1	0.079	0.023	0.000	0.052	0.024	0.015	0.087	0.024	0.000	0.011	0.023	0.316	-0.010	0.023	0.334	0.012	0.023	0.305
7Networks_RH_SomMot_7	0.073	0.023	0.001	0.052	0.024	0.015	0.071	0.024	0.001	-0.003	0.023	0.448	0.006	0.023	0.397	-0.005	0.023	0.415
7Networks_RH_SomMot_8	0.092	0.027	0.000	0.055	0.027	0.021	0.100	0.027	0.000	0.066	0.027	0.007	-0.050	0.027	0.030	0.065	0.027	0.007
7Networks_RH_SomMot_12	0.096	0.026	0.000	0.095	0.027	0.000	0.066	0.027	0.007	0.057	0.026	0.015	-0.036	0.026	0.089	0.052	0.026	0.024
7Networks_RH_Cont_PFCv_1	0.085	0.027	0.001	0.061	0.027	0.014	0.084	0.027	0.001	0.063	0.027	0.010	-0.002	0.027	0.464	0.038	0.027	0.082
7Networks_RH_Cont_PFCl_5	-0.072	0.023	0.001	-0.049	0.023	0.018	-0.077	0.023	0.000	-0.025	0.023	0.138	0.030	0.023	0.093	-0.031	0.023	0.090
7Networks_RH_Cont_PFCl_6	-0.081	0.024	0.000	-0.048	0.024	0.022	-0.101	0.024	0.000	-0.051	0.024	0.016	0.035	0.024	0.073	-0.048	0.024	0.021
7Networks_RH_Cont_PFCl_7	-0.063	0.022	0.002	-0.051	0.022	0.010	-0.053	0.022	0.008	-0.044	0.021	0.021	0.038	0.022	0.040	-0.045	0.021	0.017
7Networks_RH_Cont_PFCmp_2	-0.075	0.022	0.000	-0.069	0.023	0.001	-0.062	0.023	0.003	-0.020	0.022	0.183	0.048	0.022	0.015	-0.038	0.022	0.045
7Networks_RH_Default_PFCdPFCm_4	-0.105	0.024	0.000	-0.076	0.024	0.001	-0.112	0.024	0.000	-0.050	0.024	0.019	0.043	0.024	0.035	-0.052	0.024	0.015
7Networks_RH_Default_PFCdPFCm_5	-0.123	0.023	0.000	-0.115	0.023	0.000	-0.094	0.023	0.000	-0.059	0.023	0.005	0.083	0.023	0.000	-0.079	0.023	0.000
7Networks_RH_Default_PFCdPFCm_6	-0.084	0.023	0.000	-0.080	0.024	0.000	-0.065	0.024	0.003	-0.049	0.023	0.017	0.037	0.023	0.056	-0.049	0.023	0.019
7Networks RH Default pCunPCC 1	0.153	0.026	0.000	0.115	0.026	0.000	0.152	0.026	0.000	0.033	0.026	0.103	-0.041	0.026	0.058	0.041	0.026	0.057

Supplementary Table 2. Fluid cognition and local cortical thickness.

	Tota	al Cogni	tion		Fluid		C	rystallize	ed	Pos	sitive Aff	ect	Neg	ative Af	fect	M	ean Affe	ct
	β	SD	р	β	SD	р	β	SD	р	β	SD	р	β	SD	р	β	SD	р
7Networks_LH_Vis_9	0.074	0.025	0.002	0.081	0.026	0.001	0.046	0.026	0.036	0.062	0.025	0.007	-0.049	0.025	0.027	0.062	0.025	0.007
7Networks_LH_Vis_10	0.087	0.027	0.001	0.096	0.027	0.000	0.048	0.027	0.039	0.005	0.027	0.423	-0.023	0.027	0.196	0.015	0.027	0.282
7Networks_LH_Vis_12	0.060	0.026	0.011	0.085	0.026	0.001	0.009	0.027	0.363	-0.002	0.026	0.474	-0.060	0.026	0.012	0.031	0.026	0.116
7Networks_LH_SomMot_10	0.139	0.025	0.000	0.110	0.025	0.000	0.135	0.025	0.000	0.052	0.025	0.019	-0.048	0.025	0.028	0.056	0.025	0.013
7Networks_LH_DorsAttn_Post_10	-0.076	0.025	0.001	-0.077	0.025	0.001	-0.057	0.025	0.011	-0.016	0.025	0.263	-0.006	0.025	0.399	-0.006	0.024	0.411
7Networks_LH_SalVentAttn_PFCl_1	-0.088	0.023	0.000	-0.070	0.023	0.001	-0.086	0.023	0.000	-0.010	0.023	0.333	0.001	0.023	0.475	-0.006	0.023	0.389
7Networks_LH_Default_PFC_7	-0.114	0.025	0.000	-0.098	0.025	0.000	-0.103	0.025	0.000	-0.046	0.025	0.031	0.036	0.025	0.072	-0.046	0.025	0.031
7Networks_LH_Default_PFC_9	-0.078	0.024	0.001	-0.077	0.024	0.001	-0.054	0.024	0.013	-0.094	0.024	0.000	0.078	0.024	0.001	-0.096	0.024	0.000
7Networks_LH_Default_PFC_10	-0.103	0.023	0.000	-0.100	0.024	0.000	-0.081	0.024	0.000	-0.041	0.023	0.042	0.029	0.024	0.113	-0.039	0.023	0.050
7Networks_LH_Default_PFC_11	-0.157	0.023	0.000	-0.127	0.024	0.000	-0.146	0.024	0.000	-0.055	0.024	0.010	0.031	0.024	0.096	-0.049	0.024	0.020
7Networks_LH_Default_PFC_13	-0.086	0.024	0.000	-0.089	0.025	0.000	-0.064	0.025	0.005	-0.073	0.024	0.001	0.070	0.024	0.002	-0.079	0.024	0.001
7Networks_LH_Default_pCunPCC_1	0.098	0.026	0.000	0.079	0.026	0.001	0.091	0.026	0.000	0.012	0.026	0.315	0.002	0.026	0.461	0.006	0.026	0.411

7Networks_RH_Vis_9	0.083	0.028	0.002	0.100	0.028	0.000	0.038	0.028	0.089	-0.023	0.028	0.207	0.017	0.028	0.270	-0.023	0.028	0.211
7Networks_RH_Vis_10	0.088	0.027	0.001	0.093	0.027	0.000	0.049	0.027	0.035	0.043	0.027	0.054	-0.050	0.027	0.031	0.052	0.027	0.026
7Networks_RH_Vis_13	0.088	0.025	0.000	0.083	0.025	0.000	0.067	0.025	0.004	-0.006	0.025	0.404	-0.016	0.025	0.253	0.005	0.025	0.413
7Networks_RH_SomMot_12	0.096	0.026	0.000	0.095	0.027	0.000	0.066	0.027	0.007	0.057	0.026	0.015	-0.036	0.026	0.089	0.052	0.026	0.024
7Networks_RH_Cont_PFCmp_2	-0.075	0.022	0.000	-0.069	0.023	0.001	-0.062	0.023	0.003	-0.020	0.022	0.183	0.048	0.022	0.015	-0.038	0.022	0.045
7Networks_RH_Default_PFCdPFCm_4	-0.105	0.024	0.000	-0.076	0.024	0.001	-0.112	0.024	0.000	-0.050	0.024	0.019	0.043	0.024	0.035	-0.052	0.024	0.015
7Networks_RH_Default_PFCdPFCm_5	-0.123	0.023	0.000	-0.115	0.023	0.000	-0.094	0.023	0.000	-0.059	0.023	0.005	0.083	0.023	0.000	-0.079	0.023	0.000
7Networks_RH_Default_PFCdPFCm_6	-0.084	0.023	0.000	-0.080	0.024	0.000	-0.065	0.024	0.003	-0.049	0.023	0.017	0.037	0.023	0.056	-0.049	0.023	0.019
7Networks RH Default pCunPCC 1	0.153	0.026	0.000	0.115	0.026	0.000	0.152	0.026	0.000	0.033	0.026	0.103	-0.041	0.026	0.058	0.041	0.026	0.057

${\it Supplementary\ Table\ 3.}\ Crystallized\ cognition\ and\ local\ cortical\ thickness.$

	Tot	al Cogni	tion		Fluid		C	rystalliz	ed	Pos	sitive Af	ect	Neg	gative Af	fect	M	ean Affe	ect
	β	SD	р	β	SD	р	β	SD	р	β	SD	р	β	SD	р	β	SD	р
7Networks_LH_Vis_1	0.095	0.026	0.000	0.043	0.027	0.051	0.132	0.026	0.000	-0.005	0.026	0.424	0.035	0.026	0.089	-0.022	0.026	0.200
7Networks_LH_Vis_2	0.060	0.024	0.006	0.017	0.024	0.245	0.096	0.024	0.000	0.002	0.024	0.474	0.014	0.024	0.276	-0.007	0.024	0.388
7Networks_LH_Vis_4	0.110	0.029	0.000	0.072	0.029	0.006	0.121	0.029	0.000	0.010	0.029	0.367	-0.019	0.029	0.258	0.016	0.029	0.292
7Networks_LH_SomMot_3	0.094	0.024	0.000	0.061	0.024	0.006	0.103	0.024	0.000	0.010	0.024	0.336	-0.030	0.024	0.106	0.022	0.024	0.179
7Networks_LH_SomMot_8	-0.050	0.024	0.020	-0.022	0.024	0.182	-0.072	0.024	0.001	0.013	0.024	0.287	-0.009	0.024	0.361	0.012	0.024	0.303
7Networks_LH_SomMot_10	0.139	0.025	0.000	0.110	0.025	0.000	0.135	0.025	0.000	0.052	0.025	0.019	-0.048	0.025	0.028	0.056	0.025	0.013
7Networks_LH_DorsAttn_Post_1	0.055	0.025	0.013	0.027	0.025	0.139	0.074	0.025	0.001	0.015	0.025	0.266	-0.031	0.025	0.103	0.026	0.024	0.148
7Networks_LH_DorsAttn_Post_7	-0.073	0.025	0.002	-0.038	0.025	0.060	-0.096	0.025	0.000	-0.049	0.024	0.022	0.019	0.025	0.218	-0.039	0.024	0.057
7Networks_LH_DorsAttn_Post_9	-0.067	0.026	0.005	-0.042	0.026	0.054	-0.075	0.026	0.002	0.029	0.026	0.134	-0.023	0.026	0.188	0.029	0.026	0.132
7Networks_LH_SalVentAttn_FrOperIns_2	0.084	0.023	0.000	0.067	0.024	0.002	0.081	0.024	0.000	0.014	0.023	0.282	0.016	0.023	0.244	-0.001	0.023	0.483
7Networks_LH_SalVentAttn_FrOperIns_3	0.044	0.026	0.042	0.008	0.026	0.372	0.078	0.026	0.001	0.006	0.025	0.404	0.005	0.025	0.416	0.001	0.025	0.490
7Networks_LH_SalVentAttn_PFCl_1	-0.088	0.023	0.000	-0.070	0.023	0.001	-0.086	0.023	0.000	-0.010	0.023	0.333	0.001	0.023	0.475	-0.006	0.023	0.389
7Networks_LH_Cont_PFCl_2	-0.060	0.024	0.006	-0.032	0.024	0.091	-0.068	0.024	0.002	-0.032	0.024	0.087	0.004	0.024	0.432	-0.021	0.024	0.191
7Networks_LH_Cont_PFCl_3	-0.052	0.022	0.008	-0.024	0.022	0.138	-0.072	0.022	0.001	-0.037	0.022	0.043	0.059	0.022	0.003	-0.053	0.022	0.007
7Networks_LH_Default_Par_4	-0.033	0.022	0.069	0.000	0.023	0.493	-0.069	0.023	0.001	0.056	0.022	0.006	-0.030	0.022	0.090	0.048	0.022	0.015
7Networks_LH_Default_PFC_4	-0.083	0.025	0.000	-0.073	0.025	0.002	-0.070	0.025	0.002	-0.053	0.025	0.016	0.052	0.025	0.017	-0.058	0.025	0.009

7Networks_LH_Default_PFC_6	-0.068	0.026	0.005	-0.045	0.026	0.043	-0.076	0.026	0.002	-0.045	0.026	0.040	0.000	0.026	0.499	-0.026	0.026	0.158
7Networks_LH_Default_PFC_7	-0.114	0.025	0.000	-0.098	0.025	0.000	-0.103	0.025	0.000	-0.046	0.025	0.031	0.036	0.025	0.072	-0.046	0.025	0.031
7Networks_LH_Default_PFC_10	-0.103	0.023	0.000	-0.100	0.024	0.000	-0.081	0.024	0.000	-0.041	0.023	0.042	0.029	0.024	0.113	-0.039	0.023	0.050
7Networks_LH_Default_PFC_11	-0.157	0.023	0.000	-0.127	0.024	0.000	-0.146	0.024	0.000	-0.055	0.024	0.010	0.031	0.024	0.096	-0.049	0.024	0.020
7Networks_LH_Default_pCunPCC_1	0.098	0.026	0.000	0.079	0.026	0.001	0.091	0.026	0.000	0.012	0.026	0.315	0.002	0.026	0.461	0.006	0.026	0.411
7Networks_RH_Vis_3	0.024	0.024	0.153	-0.027	0.024	0.131	0.084	0.024	0.000	0.029	0.023	0.106	0.015	0.024	0.261	0.009	0.023	0.356
7Networks_RH_Vis_4	0.086	0.028	0.001	0.017	0.029	0.275	0.143	0.028	0.000	0.022	0.028	0.221	0.007	0.028	0.401	0.009	0.028	0.379
7Networks_RH_Vis_8	0.055	0.023	0.009	0.023	0.023	0.166	0.078	0.023	0.000	0.053	0.023	0.011	-0.024	0.023	0.151	0.043	0.023	0.030
7Networks_RH_SomMot_1	0.079	0.023	0.000	0.052	0.024	0.015	0.087	0.024	0.000	0.011	0.023	0.316	-0.010	0.023	0.334	0.012	0.023	0.305
7Networks_RH_SomMot_3	0.051	0.024	0.018	0.027	0.024	0.132	0.073	0.024	0.001	0.040	0.024	0.047	-0.036	0.024	0.069	0.043	0.024	0.039
7Networks_RH_SomMot_7	0.073	0.023	0.001	0.052	0.024	0.015	0.071	0.024	0.001	-0.003	0.023	0.448	0.006	0.023	0.397	-0.005	0.023	0.415
7Networks_RH_SomMot_8	0.092	0.027	0.000	0.055	0.027	0.021	0.100	0.027	0.000	0.066	0.027	0.007	-0.050	0.027	0.030	0.065	0.027	0.007
7Networks_RH_SomMot_10	0.056	0.022	0.006	0.040	0.022	0.036	0.062	0.022	0.003	-0.007	0.022	0.381	-0.013	0.022	0.274	0.003	0.022	0.440
7Networks_RH_SalVentAttn_TempOccPar_1	0.067	0.025	0.004	0.037	0.025	0.071	0.079	0.025	0.001	0.021	0.025	0.193	-0.028	0.025	0.134	0.027	0.025	0.136
7Networks_RH_SalVentAttn_FrOperIns_4	0.045	0.024	0.032	0.012	0.025	0.319	0.079	0.024	0.001	0.022	0.024	0.177	-0.005	0.024	0.414	0.016	0.024	0.258
7Networks_RH_Limbic_TempPole_1	0.064	0.027	0.010	0.024	0.028	0.188	0.090	0.027	0.001	0.008	0.027	0.377	-0.001	0.027	0.487	0.005	0.027	0.422
7Networks_RH_Cont_PFCv_1	0.085	0.027	0.001	0.061	0.027	0.014	0.084	0.027	0.001	0.063	0.027	0.010	-0.002	0.027	0.464	0.038	0.027	0.082
7Networks_RH_Cont_PFCl_3	-0.060	0.022	0.003	-0.037	0.022	0.049	-0.068	0.022	0.001	0.010	0.022	0.317	0.012	0.022	0.287	-0.001	0.022	0.488
7Networks_RH_Cont_PFCl_4	-0.050	0.021	0.009	-0.022	0.021	0.144	-0.064	0.021	0.001	-0.026	0.021	0.105	0.021	0.021	0.152	-0.027	0.021	0.101
7Networks_RH_Cont_PFCl_5	-0.072	0.023	0.001	-0.049	0.023	0.018	-0.077	0.023	0.000	-0.025	0.023	0.138	0.030	0.023	0.093	-0.031	0.023	0.090
7Networks_RH_Cont_PFCl_6	-0.081	0.024	0.000	-0.048	0.024	0.022	-0.101	0.024	0.000	-0.051	0.024	0.016	0.035	0.024	0.073	-0.048	0.024	0.021
7Networks_RH_Default_Par_1	-0.040	0.024	0.048	-0.005	0.024	0.412	-0.069	0.024	0.002	-0.001	0.024	0.491	0.010	0.024	0.336	-0.006	0.024	0.404
7Networks_RH_Default_Temp_5	0.069	0.025	0.003	0.022	0.025	0.186	0.098	0.025	0.000	0.016	0.025	0.258	-0.015	0.025	0.271	0.017	0.025	0.240
7Networks_RH_Default_PFCdPFCm_4	-0.105	0.024	0.000	-0.076	0.024	0.001	-0.112	0.024	0.000	-0.050	0.024	0.019	0.043	0.024	0.035	-0.052	0.024	0.015
7Networks_RH_Default_PFCdPFCm_5	-0.123	0.023	0.000	-0.115	0.023	0.000	-0.094	0.023	0.000	-0.059	0.023	0.005	0.083	0.023	0.000	-0.079	0.023	0.000
7Networks_RH_Default_pCunPCC_1	0.153	0.026	0.000	0.115	0.026	0.000	0.152	0.026	0.000	0.033	0.026	0.103	-0.041	0.026	0.058	0.041	0.026	0.057

Supplementary Table 4. Mean affect and local cortical thickness.

	Tot	al Cogni	tion		Fluid		C	rystallize	ed	Pos	sitive Aff	ect	Neg	ative Af	fect	M	ean Affe	ct
	β	SD	р	β	SD	р	β	SD	р	β	SD	р	β	SD	р	β	SD	р
7Networks_LH_Vis_14	-0.007	0.023	0.382	-0.002	0.024	0.461	-0.012	0.023	0.312	0.068	0.023	0.002	-0.098	0.023	0.000	0.092	0.023	0.000
7Networks_LH_Default_PFC_9	-0.078	0.024	0.001	-0.077	0.024	0.001	-0.054	0.024	0.013	-0.094	0.024	0.000	0.078	0.024	0.001	-0.096	0.024	0.000
7Networks_RH_DorsAttn_Post_5	0.012	0.022	0.295	0.023	0.022	0.146	-0.012	0.022	0.296	0.071	0.022	0.001	-0.065	0.022	0.002	0.076	0.022	0.000

Supplementary Table 5. Positive affect and local cortical thickness.

	Tota	al Cognit	ion		Fluid		C	rystallize	ed	Pos	itive Aff	ect	Neg	gative Af	fect	M	ean Affe	ct
	β	SD	р	β SD p			β	SD	р	β	SD	р	β	SD	р	β	SD	p
7Networks_LH_Default_PFC_9	-0.078	0.024	0.001	-0.077	0.024	0.001	-0.054	0.024	0.013	-0.094	0.024	0.000	0.078	0.024	0.001	-0.096	0.024	0.000

Supplementary Table 6. Negative affect and local cortical thickness.

	Tota	al Cogni	tion		Fluid		C	rystallize	ed	Po	sitive Af	fect	Neg	ative Af	fect	M	Iean Affe	ect	
	β	SD	p	β	SD	p	β	SD	р	β	SD	p	β	SD	р	β	SD	p	
7Networks LH Vis 14	-0.007	0.023	0.382	-0.002	0.024	0.461	-0.012	0.023	0.312	0.068	0.023	0.002	-0.098	0.023	0.000	0.092	0.023	0.000	

Supplementary Table 7. Total cognition and local surface area.

	Tot	al Cogni	tion		Fluid		C	rystalliz	ed	Pos	sitive Aff	ect	Neg	ative Af	fect	M	ean Affe	ct
	β	SD	р	β	SD	р	β	SD	р	β	SD	р	β	SD	р	β	SD	p
7Networks_LH_Vis_7	0.076	0.073 0.028 0.005 0		0.085	0.027	0.001	0.030	0.028	0.138	0.003	0.027	0.459	-0.040	0.027	0.068	0.023	0.027	0.192
7Networks_LH_Vis_9	0.073	0.028	0.005	0.073	0.028	0.005	0.028	0.029	0.165	0.008	0.028	0.392	-0.039	0.027	0.080	0.025	0.027	0.179
7Networks_LH_Vis_10	0.073 0.028 0.005			0.082	0.028	0.002	0.034	0.028	0.118	0.023	0.027	0.198	-0.036	0.027	0.095	0.033	0.027	0.115
7Networks_LH_Vis_11	0.072	0.026	0.003	0.052	0.026	0.023	0.067	0.026	0.005	0.015	0.025	0.271	-0.048	0.025	0.030	0.035	0.025	0.085
7Networks_LH_Vis_13	0.112	0.026	0.000	0.113	0.026	0.000	0.061	0.026	0.010	0.050	0.025	0.024	-0.044	0.025	0.042	0.053	0.025	0.019
7Networks_LH_Vis_14	0.078	0.027	0.002	0.081	0.027	0.001	0.042	0.027	0.064	0.052	0.026	0.024	-0.015	0.026	0.286	0.038	0.026	0.075
7Networks_LH_SomMot_8	0.079	0.026	0.001	0.057	0.026	0.013	0.076	0.026	0.002	0.044	0.025	0.040	-0.040	0.025	0.054	0.047	0.025	0.030
7Networks_LH_SomMot_10	0.082	0.027	0.001	0.060	0.027	0.012	0.081	0.027	0.001	-0.021	0.026	0.210	0.012	0.026	0.322	-0.018	0.026	0.238

Previors Incline Inc	7Networks_LH_SomMot_12	0.083	0.027	0.001	0.077	0.027	0.002	0.061	0.027	0.012	-0.008	0.026	0.375	-0.009	0.026	0.360	0.000	0.026	0.495
Reversis_H_limbic_TempPote_1 0.25 0.02 <	7Networks_LH_SalVentAttn_Med_2	0.075	0.026	0.002	0.076	0.026	0.002	0.047	0.027	0.039	0.027	0.026	0.145	-0.015	0.026	0.273	0.024	0.026	0.175
Retworks_IH_Limbic_TempPole_2 0.087 0.027 0.01 0.05 0.027 0.019 0.089 0.027 0.001 0.029 0.020	7Networks_LH_Limbic_OFC_1	0.076	0.025	0.001	0.089	0.024	0.000	0.035	0.025	0.078	0.036	0.024	0.065	-0.026	0.024	0.141	0.035	0.024	0.073
Retworks_H_Limbic_TempPole3 0.113 0.027 0.004 0.019 0.027 0.004 0.027 0.004 0.027 0.004 0.027 0.004 0.027 0.004 0.024 0.004 0.023 0.004 0.023 0.004 0.023 0.004 0.023 0.004 0.024 0.004 0.024 0.004 0.024 0.004 0.024 0.004 0.024 0.004 0.024 0.004 0.024 0.004 0.024 0.004 0.024 0.004 0.024 0.004 0.024 0.004 0.024 0.004 0.024 0.004	7Networks_LH_Limbic_TempPole_1	0.126	0.025	0.000	0.085	0.025	0.000	0.126	0.026	0.000	0.032	0.025	0.096	-0.040	0.025	0.052	0.041	0.025	0.051
Retworks_IH_Limbic_TempPote_4 0.78 0.22 0.00 0.01 0.02	7Networks_LH_Limbic_TempPole_2	0.087	0.027	0.001	0.056	0.027	0.019	0.089	0.027	0.001	0.049	0.026	0.031	-0.040	0.026	0.061	0.050	0.026	0.028
Retworks_LII_Cont_PFC12 0.000 0.020 0.0	7Networks_LH_Limbic_TempPole_3	0.113	0.027	0.000	0.075	0.027	0.002	0.119	0.027	0.000	0.027	0.026	0.149	-0.016	0.026	0.273	0.024	0.026	0.178
Retworks_LH_Cont_PFC1_5 0.095 0.028 0.005 0.025 0.005 0.02	7Networks_LH_Limbic_TempPole_4	0.078	0.023	0.000	0.049	0.023	0.017	0.091	0.023	0.000	0.014	0.023	0.268	-0.005	0.023	0.417	0.011	0.022	0.319
7Networks_LH_Default_Temp_1 0.098 0.025 0.009 0.025 0.020 0.012 0.025 0.020 0.013 0.025 0.009 0.013 0.025 0.009 0.013 0.025 0.009 0.014 0.026 0.009 0.014 0.025 0.009 0.014 0.025 0.009 0.009 0.009 0.014 0.025 0.024 0.009 0.009 0.031 0.025 0.014 0.025 0.026 0.009 <th< th=""><th>7Networks_LH_Cont_PFCl_2</th><th>0.090</th><th>0.026</th><th>0.000</th><th>0.047</th><th>0.026</th><th>0.033</th><th>0.108</th><th>0.026</th><th>0.000</th><th>0.023</th><th>0.025</th><th>0.180</th><th>-0.021</th><th>0.025</th><th>0.205</th><th>0.024</th><th>0.025</th><th>0.165</th></th<>	7Networks_LH_Cont_PFCl_2	0.090	0.026	0.000	0.047	0.026	0.033	0.108	0.026	0.000	0.023	0.025	0.180	-0.021	0.025	0.205	0.024	0.025	0.165
7Networks_LH_Default_Temp_2 0.116 0.026 0.004 0.026 0.004 0.026 0.004 0.026 0.004 0.026 0.004 0.026 0.004 0.026 0.004 0.026 0.004 0.026 0.004 0.026 0.004 0.026 0.004 0.026 0.004 0.026 0.004 0.026 0.004 0.026 0.004 0.026 0.004 0.004 0.022 0.048 0.024 0.034 0.026 0.026 0.026 0.004 0.004 0.022 0.048 0.024 0.024 0.026 0.026 0.004 0.004 0.022 0.048 0.014 0.022 0.026 0.027 <th< th=""><th>7Networks_LH_Cont_PFCl_5</th><th>0.095</th><th>0.028</th><th>0.000</th><th>0.046</th><th>0.028</th><th>0.051</th><th>0.115</th><th>0.028</th><th>0.000</th><th>0.006</th><th>0.027</th><th>0.411</th><th>0.043</th><th>0.027</th><th>0.056</th><th>-0.020</th><th>0.027</th><th>0.232</th></th<>	7Networks_LH_Cont_PFCl_5	0.095	0.028	0.000	0.046	0.028	0.051	0.115	0.028	0.000	0.006	0.027	0.411	0.043	0.027	0.056	-0.020	0.027	0.232
Networks_LH_Default_PFC_1	7Networks_LH_Default_Temp_1	0.098	0.025	0.000	0.052	0.025	0.020	0.113	0.025	0.000	0.036	0.025	0.071	-0.025	0.025	0.155	0.034	0.025	0.082
Networks_LH_Default_PFC_6 0.078 0.023 0.000 0.032 0.000 0.032 0.000 0.022 0.048 0.014 0.022 0.014 0.022 0.036 0.033 0.000 0.032 0.000 0.022 0.048 0.024 0.026 0.035 0.000 0.026 0.000 0.025 0.049 0.016 0.025 0.026 0.000 0.026 0.000 0.025 0.049 0.016 0.027 0.016 0.027 0.016 0.027 0.016 0.027 0.016 0.027 0.016 0.027 0.016 0.027 0.010 0.026 0.027 0.010 0.028 0.000 0.016 0.027 0.010 0.028 0.027 0.026 0.027 0.020 0.027 0.020 0.027 0.020 0.027 0.020 0.027 0.020 0.027 0.020 0.027 0.020 0.027 0.020 0.021 0.020 0.020 0.020 0.020 0.020 0.020 0.020 0.	7Networks_LH_Default_Temp_2	0.116	0.026	0.000	0.070	0.026	0.004	0.121	0.026	0.000	0.034	0.026	0.091	-0.031	0.026	0.114	0.036	0.026	0.078
Networks_LH_Default_PFC_8 0.068 0.026 0.044 0.047 0.026 0.035 0.070 0.026 0.004 0.002 0.423 0.016 0.025 0.423 0.016 0.025 0.266 0.009 0.025 0.436 7Networks_LH_Default_PFC_11 0.078 0.028 0.020 0.031 0.027 0.113 0.100 0.026 0.026 0.027 0.021 0.002 0.026 0.027 0.026 0.027 0.026 0.027 0.027 0.027 0.027 0.027 0.027 0.027 0.027 0.028 0.027 0.027 0.027 0.028 0.029 0.027 0.027<	7Networks_LH_Default_PFC_1	0.075	0.024	0.001	0.066	0.024	0.003	0.056	0.025	0.011	0.043	0.024	0.034	-0.043	0.024	0.034	0.048	0.024	0.020
Networks_LH_Default_PFC_11 0.078 0.028 0.020 0.033 0.027 0.113 0.100 0.028 0.000 0.016 0.027 0.272 0.021 0.021 0.020 0.023 0.027 0.040 Networks_RH_Vis_4 0.085 0.027 0.000 0.016 0.027 0.012 0.022 0.026 0.323 0.021 0.026 0.226 Networks_RH_Vis_9 0.010 0.027 0.001 0.027 0.010 0.027 0.001 0.025 0.026 0.029 0.026 0.033 0.026 0.024 0.026 0.023 0.021 0.026 0.023 0.021 0.026 0.023 0.024 0.026 0.023 0.024 0.024 0.024 0.026 0.023 0.024 0.024 0.025 0.024 0.025 0.024 0.024 0.025 0.024 0.024 0.025 0.024 0.024 0.025 0.024 0.024 0.025 0.021 0.024 0.025 0.021 0.024 <th>7Networks_LH_Default_PFC_6</th> <th>0.078</th> <th>0.023</th> <th>0.000</th> <th>0.054</th> <th>0.023</th> <th>0.009</th> <th>0.080</th> <th>0.023</th> <th>0.000</th> <th>0.000</th> <th>0.022</th> <th>0.498</th> <th>-0.014</th> <th>0.022</th> <th>0.261</th> <th>0.008</th> <th>0.022</th> <th>0.363</th>	7Networks_LH_Default_PFC_6	0.078	0.023	0.000	0.054	0.023	0.009	0.080	0.023	0.000	0.000	0.022	0.498	-0.014	0.022	0.261	0.008	0.022	0.363
Networks_RH_Vis_4 0.085 0.027 0.001 0.063 0.027 0.009 0.075 0.027 0.003 0.026 0.026 0.101 0.026 0.223 0.021 0.026 0.026 0.103 0.026 0.026 0.021 0.026 0.026 0.027 0.002 0.026 0.027 0.002 0.026 0.027 0.002 0.026 0.027 0.002 0.026 0.027 0.002 0.026 0.027 0.002 0.026 0.027 0.002 0.026 0.027 0.002 0.027 0.002 0.027 0.002 0.027 0.002 0.026 0.001 0.026 0.027 0.003 0.026 0.001 0.026 0.027 0.003 0.026 0.027 0.026 0.027 0.026 0.027 0.026 0.027 0.026 0.027 0.023 0.026 0.027 0.023 0.026 0.027 0.023 0.026 0.027 0.023 0.026 0.027 0.023 0.026 0.027	7Networks_LH_Default_PFC_8	0.068	0.026	0.004	0.047	0.026	0.035	0.070	0.026	0.004	0.000	0.025	0.493	-0.016	0.025	0.266	0.009	0.025	0.363
Networks_RH_Vis_9 0.108 0.027 0.000 0.108 0.027 0.000 0.010 0.027 0.000 0.021 0.022 0.022 0.026 0.129 0.026 0.328 0.019 0.026 0.328 0.019 0.026 0.328 0.019 0.026 0.028 0.024 0.024 0.024 0.025 0.026 0.024 0.026 0.024 0.026 0.024 0.026 0.024 0.026 0.023 0.026 0.023 0.026 0.023 0.024 0.025 0.026 0.029 0.026 0.020 0.027 0.026 0.020 0.027 0.026 0.020 0.027 0.026 0.027 0.027 0.026 0.027 0.027 0.027 0.027 0.027 0.027 0.027 0.027 0.028 0.027 0.028 0.027 0.038 0.027 0.026 0.027 0.028 0.027 0.028 0.027 0.028 0.027 0.028 0.027 0.028 0.027 0.028	7Networks_LH_Default_PFC_11	0.078	0.028	0.002	0.033	0.027	0.113	0.100	0.028	0.000	0.016	0.027	0.272	0.021	0.027	0.211	-0.002	0.027	0.466
Networks_RH_Vis_12 0.079 0.027 0.002 0.081 0.027 0.001 0.038 0.027 0.081 0.035 0.026 0.094 -0.054 0.026 0.019 0.026 0.030 7Networks_RH_Vis_14 0.095 0.026 0.004 0.027 0.026 0.001 0.080 0.026 0.001 0.080 0.026 0.001 0.067 0.025 0.004 -0.055 0.025 0.014 0.068 0.025 0.003 7Networks_RH_SomMot_12 0.075 0.028 0.004 0.025 0.024 0.025 0.024 0.025 0.024 0.027 0.028 0.024 0.068 0.028 0.028 0.028 0.024 0.028 0.028 0.028 0.028 0.029 0.028 0.028 0.029 0.028 0.029 0.028 0.029 0.028 0.029 0.028 0.029 0.028 0.029 0.028 0.029 0.028 0.029 0.028 0.029 0.028 0.029 0.029 </th <th>7Networks_RH_Vis_4</th> <th>0.085</th> <th>0.027</th> <th>0.001</th> <th>0.063</th> <th>0.027</th> <th>0.009</th> <th>0.075</th> <th>0.027</th> <th>0.003</th> <th>0.026</th> <th>0.026</th> <th>0.161</th> <th>-0.012</th> <th>0.026</th> <th>0.323</th> <th>0.021</th> <th>0.026</th> <th>0.206</th>	7Networks_RH_Vis_4	0.085	0.027	0.001	0.063	0.027	0.009	0.075	0.027	0.003	0.026	0.026	0.161	-0.012	0.026	0.323	0.021	0.026	0.206
Networks_RH_Vis_14 0.095 0.026 0.000 0.077 0.026 0.001 0.080 0.026 0.001 0.080 0.026 0.001 0.080 0.026 0.001 0.067 0.025 0.004 -0.055 0.025 0.014 0.068 0.025 0.003 7Networks_RH_SomMot_12 0.075 0.028 0.004 0.056 0.028 0.024 0.068 0.028 0.028 0.024 0.028 0.024 0.028 0.024 0.028 0.024 0.028 0.024 0.068 0.028 0.008 -0.020 0.027 0.038 0.027 0.038 0.026 0.150 0.028 0.024 0.068 0.028 0.008 -0.020 0.027 0.238 0.027 0.016 0.027 0.018 0.027 0.028 0.027 0.016 0.027 0.008 0.027 0.028 0.028 0.028 0.027 0.028 0.027 0.028 0.029 0.028 0.027 0.008 0.027 0.028	7Networks_RH_Vis_9	0.108	0.027	0.000	0.108	0.027	0.000	0.061	0.027	0.012	0.022	0.026	0.199	-0.012	0.026	0.328	0.019	0.026	0.234
7Networks_RH_SomMot_10 0.072 0.027 0.004 0.027 0.039 0.076 0.027 0.003 -0.038 0.026 0.072 0.026 0.358 -0.027 0.026 0.150 7Networks_RH_SomMot_12 0.075 0.028 0.004 0.028 0.024 0.068 0.028 0.008 -0.020 0.027 0.238 0.009 0.026 0.358 -0.027 0.228 0.150 7Networks_RH_SomMot_14 0.076 0.027 0.003 0.066 0.027 0.008 0.027 0.030 0.026 0.027 0.012 0.066 0.027 0.008 -0.030 0.026 0.124 0.023 0.026 0.128 7Networks_RH_DorsAttn_PrCv_1 0.088 0.027 0.008 0.027 0.038 0.029 0.094 0.023 0.009 0.024 0.024 0.027 0.000 0.024 0.028 0.028 0.029 0.024 0.023 0.020 0.023 0.029 0.003 0.029 0.028 0	7Networks_RH_Vis_12	0.079	0.027	0.002	0.081	0.027	0.001	0.038	0.027	0.081	0.035	0.026	0.094	-0.054	0.026	0.019	0.049	0.026	0.030
7Networks_RH_SomMot_12 0.075 0.028 0.004 0.028 0.024 0.068 0.028 0.008 -0.020 0.027 0.238 0.009 0.027 0.371 -0.016 0.027 0.278 7Networks_RH_SomMot_14 0.076 0.027 0.003 0.060 0.027 0.038 0.029 0.001 0.027 0.012 0.066 0.027 0.008 -0.030 0.026 0.124 0.025 0.026 0.128 7Networks_RH_DorsAttn_PrCv_1 0.088 0.027 0.001 0.048 0.027 0.038 0.029 0.038 0.029 0.094 0.103 0.029 0.000 0.024 0.025 0.048 0.010 0.027 0.226 7Networks_RH_SalVentAttn_FrC_1 0.082 0.029 0.002 0.094 0.023 0.004 0.023 0.004 0.023 0.004 0.023 0.004 0.023 0.004 0.023 0.004 0.023 0.004 0.023 0.004 0.023 0.023 0.024	7Networks_RH_Vis_14	0.095	0.026	0.000	0.077	0.026	0.001	0.080	0.026	0.001	0.067	0.025	0.004	-0.055	0.025	0.014	0.068	0.025	0.003
7Networks_RH_SomMot_14 0.076 0.027 0.003 0.027 0.012 0.026 0.027 0.012 0.066 0.027 0.008 -0.030 0.026 0.124 0.023 0.026 0.192 -0.030 0.026 0.128 7Networks_RH_DorsAttn_PrCv_1 0.088 0.027 0.001 0.048 0.027 0.038 0.100 0.024 0.000 0.044 0.027 0.048 0.027 0.226 7Networks_RH_SalVentAttn_PrC_1 0.082 0.029 0.002 0.038 0.029 0.094 0.103 0.029 0.002 0.094 0.103 0.029 0.003 0.026 0.124 0.023 0.026 0.128 0.226 7Networks_RH_SalVentAttn_FrOperIns_2 0.081 0.023 0.001 0.023 0.004 0.023 0.004 0.023 0.003 0.026 0.123 0.026 0.023 0.026 0.023 0.018 0.027 0.018 0.026 0.248 -0.048 0.026 0.033 0.036 0.02	7Networks_RH_SomMot_10	0.072	0.027	0.004	0.047	0.027	0.039	0.076	0.027	0.003	-0.038	0.026	0.072	0.009	0.026	0.358	-0.027	0.026	0.150
7Networks_RH_DorsAttn_PrCv_1 0.088 0.027 0.001 0.048 0.027 0.038 0.100 0.027 0.000 0.044 0.027 0.048 0.010 0.027 0.355 0.020 0.027 0.226 7Networks_RH_SalVentAttn_PrC_1 0.082 0.029 0.002 0.038 0.029 0.094 0.103 0.029 0.000 0.025 0.028 0.190 -0.003 0.028 0.464 0.015 0.028 0.290 7Networks_RH_SalVentAttn_FrOperIns_2 0.081 0.023 0.001 0.023 0.001 0.023 0.001 0.023 0.026 0.023 0.020 0.023 0.004 0.082 0.023 0.000 0.082 0.023 0.000 0.082 0.023 0.001 0.023 0.018 0.027 0.018 0.026 0.248 -0.048 0.026 0.033 0.036 0.026 0.082 7Networks_RH_Limbic_TempPole_1 0.121 0.027 0.000 0.028 0.027 0.001 0.018 <	7Networks_RH_SomMot_12	0.075	0.028	0.004	0.056	0.028	0.024	0.068	0.028	0.008	-0.020	0.027	0.238	0.009	0.027	0.371	-0.016	0.027	0.278
7Networks_RH_SalVentAttn_FrOperIns_2 0.081 0.029 0.002 0.038 0.029 0.002 0.038 0.029 0.004 0.103 0.029 0.000 0.025 0.028 0.190 -0.003 0.028 0.464 0.015 0.028 0.290 0.004 0.005 0.004 0.005 0.000 0.005 0.000 0.00	7Networks_RH_SomMot_14	0.076	0.027	0.003	0.060	0.027	0.012	0.066	0.027	0.008	-0.030	0.026	0.124	0.023	0.026	0.192	-0.030	0.026	0.128
7Networks_RH_SalVentAttn_FrOperIns_2 0.081 0.023 0.000 0.061 0.023 0.004 0.082 0.023 0.000 0.023 0.023 0.023 0.158 -0.019 0.023 0.206 0.023 0.158 7Networks_RH_Limbic_TempPole_1 0.121 0.027 0.000 0.102 0.027 0.000 0.088 0.027 0.001 0.018 0.026 0.248 -0.048 0.026 0.033 0.036 0.026 0.082	7Networks_RH_DorsAttn_PrCv_1	0.088	0.027	0.001	0.048	0.027	0.038	0.100	0.027	0.000	0.044	0.027	0.048	0.010	0.027	0.355	0.020	0.027	0.226
7Networks_RH_Limbic_TempPole_1	7Networks_RH_SalVentAttn_PrC_1	0.082	0.029	0.002	0.038	0.029	0.094	0.103	0.029	0.000	0.025	0.028	0.190	-0.003	0.028	0.464	0.015	0.028	0.290
	7Networks_RH_SalVentAttn_FrOperIns_2	0.081	0.023	0.000	0.061	0.023	0.004	0.082	0.023	0.000	0.023	0.023	0.158	-0.019	0.023	0.206	0.023	0.023	0.153
7Networks RH Limbic TempPole 2 0.093 0.026 0.000 0.078 0.026 0.001 0.070 0.026 0.004 0.043 0.026 0.048 -0.023 0.026 0.184 0.037 0.025 0.074	7Networks_RH_Limbic_TempPole_1	0.121	0.027	0.000	0.102	0.027	0.000	0.088	0.027	0.001	0.018	0.026	0.248	-0.048	0.026	0.033	0.036	0.026	0.082
**************************************	7Networks_RH_Limbic_TempPole_2	0.093	0.026	0.000	0.078	0.026	0.001	0.070	0.026	0.004	0.043	0.026	0.048	-0.023	0.026	0.184	0.037	0.025	0.074
7Networks_RH_Limbic_TempPole_3 0.088 0.027 0.001 0.041 0.027 0.067 0.105 0.027 0.000 0.010 0.027 0.349 -0.012 0.026 0.324 0.012 0.026 0.319	7Networks_RH_Limbic_TempPole_3	0.088	0.027	0.001	0.041	0.027	0.067	0.105	0.027	0.000	0.010	0.027	0.349	-0.012	0.026	0.324	0.012	0.026	0.319
7Networks_RH_Cont_Temp_1 0.069 0.026 0.004 0.035 0.026 0.092 0.084 0.026 0.001 0.028 0.025 0.137 -0.009 0.025 0.363 0.021 0.025 0.207	7Networks_RH_Cont_Temp_1	0.069	0.026	0.004	0.035	0.026	0.092	0.084	0.026	0.001	0.028	0.025	0.137	-0.009	0.025	0.363	0.021	0.025	0.207
7Networks_RH_Cont_PFCl_1 0.074 0.024 0.001 0.053 0.024 0.015 0.072 0.024 0.002 0.022 0.024 0.176 -0.010 0.024 0.340 0.018 0.024 0.224	7Networks_RH_Cont_PFCl_1	0.074	0.024	0.001	0.053	0.024	0.015	0.072	0.024	0.002	0.022	0.024	0.176	-0.010	0.024	0.340	0.018	0.024	0.224

7Networks_RH_Cont_Cing_2	0.073	0.028	0.004	0.072	0.027	0.004	0.045	0.028	0.051	0.025	0.027	0.172	-0.003	0.027	0.455	0.016	0.027	0.272	
7Networks_RH_Default_Temp_1	0.111	0.026	0.000	0.083	0.026	0.001	0.110	0.026	0.000	0.055	0.025	0.016	-0.049	0.025	0.028	0.058	0.025	0.011	
7Networks_RH_Default_Temp_2	0.082	0.025	0.001	0.037	0.025	0.070	0.108	0.025	0.000	0.062	0.025	0.006	-0.019	0.025	0.217	0.046	0.025	0.031	
7Networks RH Default PFCdPFCm 7	0.125	0.029	0.000	0.098	0.029	0.000	0.101	0.029	0.000	0.015	0.028	0.295	-0.009	0.028	0.377	0.013	0.028	0.316	

Supplementary Table 8. Fluid cognition and local surface area.

	Tot	al Cogni	tion		Fluid		C	rystalliz	ed	Pos	itive Aff	ect	Neg	gative Af	fect	M	lean Affe	ect
	β	SD	р	β	SD	р	β	SD	р	β	SD	р	β	SD	р	β	SD	р
7Networks_LH_Vis_7	0.076	0.028	0.003	0.085	0.027	0.001	0.030	0.028	0.138	0.003	0.027	0.459	-0.040	0.027	0.068	0.023	0.027	0.192
7Networks_LH_Vis_10	0.075	0.028	0.004	0.082	0.028	0.002	0.034	0.028	0.118	0.023	0.027	0.198	-0.036	0.027	0.095	0.033	0.027	0.115
7Networks_LH_Vis_13	0.112	0.026	0.000	0.113	0.026	0.000	0.061	0.026	0.010	0.050	0.025	0.024	-0.044	0.025	0.042	0.053	0.025	0.019
7Networks_LH_Vis_14	0.078	0.027	0.002	0.081	0.027	0.001	0.042	0.027	0.064	0.052	0.026	0.024	-0.015	0.026	0.286	0.038	0.026	0.075
7Networks_LH_SomMot_12	0.083	0.027	0.001	0.077	0.027	0.002	0.061	0.027	0.012	-0.008	0.026	0.375	-0.009	0.026	0.360	0.000	0.026	0.495
7Networks_LH_Limbic_OFC_1	0.076	0.025	0.001	0.089	0.024	0.000	0.035	0.025	0.078	0.036	0.024	0.065	-0.026	0.024	0.141	0.035	0.024	0.073
7Networks_LH_Limbic_TempPole_1	0.126	0.025	0.000	0.085	0.025	0.000	0.126	0.026	0.000	0.032	0.025	0.096	-0.040	0.025	0.052	0.041	0.025	0.051
7Networks_RH_Vis_8	0.070	0.028	0.006	0.080	0.027	0.002	0.035	0.028	0.108	0.011	0.027	0.335	-0.025	0.027	0.172	0.020	0.027	0.224
7Networks_RH_Vis_9	0.108	0.027	0.000	0.108	0.027	0.000	0.061	0.027	0.012	0.022	0.026	0.199	-0.012	0.026	0.328	0.019	0.026	0.234
7Networks_RH_Vis_12	0.079	0.027	0.002	0.081	0.027	0.001	0.038	0.027	0.081	0.035	0.026	0.094	-0.054	0.026	0.019	0.049	0.026	0.030
7Networks_RH_Vis_14	0.095	0.026	0.000	0.077	0.026	0.001	0.080	0.026	0.001	0.067	0.025	0.004	-0.055	0.025	0.014	0.068	0.025	0.003
7Networks_RH_Limbic_TempPole_1	0.121	0.027	0.000	0.102	0.027	0.000	0.088	0.027	0.001	0.018	0.026	0.248	-0.048	0.026	0.033	0.036	0.026	0.082
7Networks_RH_Limbic_TempPole_2	0.093	0.026	0.000	0.078	0.026	0.001	0.070	0.026	0.004	0.043	0.026	0.048	-0.023	0.026	0.184	0.037	0.025	0.074
7Networks_RH_Default_Temp_1	0.111	0.026	0.000	0.083	0.026	0.001	0.110	0.026	0.000	0.055	0.025	0.016	-0.049	0.025	0.028	0.058	0.025	0.011
7Networks_RH_Default_PFCdPFCm_7	0.125	0.029	0.000	0.098	0.029	0.000	0.101	0.029	0.000	0.015	0.028	0.295	-0.009	0.028	0.377	0.013	0.028	0.316

Supplementary Table 9. Crystallized cognition and local surface area.

	Tot	tal Cogni	tion		Fluid		C	rystalliz	ed	Pos	sitive Aff	ect	Neg	ative Af	fect	M	ean Affe	ct
	β	SD	р	β	SD	р	β	SD	р	β	SD	р	β	SD	р	β	SD	p
7Networks_LH_Vis_8	0.057	0.029	0.024	0.015	0.029	0.299	0.089	0.029	0.001	-0.004	0.028	0.445	-0.009	0.028	0.379	0.002	0.028	0.465
7Networks_LH_Vis_11	0.072	0.026	0.003	0.052	0.026	0.023	0.067	0.026	0.005	0.015	0.025	0.271	-0.048	0.025	0.030	0.035	0.025	0.085

7Networks_LH_SomMot_4	0.037	0.026	0.080	0.002	0.026	0.474	0.067	0.026	0.005	-0.003	0.025	0.451	0.022	0.025	0.195	-0.014	0.025	0.296
7Networks_LH_SomMot_6	0.045	0.026	0.044	0.009	0.026	0.365	0.073	0.026	0.003	-0.004	0.025	0.438	-0.006	0.025	0.403	0.001	0.025	0.483
7Networks_LH_SomMot_8	0.079	0.026	0.001	0.057	0.026	0.013	0.076	0.026	0.002	0.044	0.025	0.040	-0.040	0.025	0.054	0.047	0.025	0.030
7Networks_LH_SomMot_10	0.082	0.027	0.001	0.060	0.027	0.012	0.081	0.027	0.001	-0.021	0.026	0.210	0.012	0.026	0.322	-0.018	0.026	0.238
7Networks_LH_DorsAttn_Post_1	0.048	0.024	0.022	0.025	0.024	0.141	0.062	0.024	0.005	-0.003	0.023	0.455	0.036	0.023	0.057	-0.021	0.023	0.178
7Networks_LH_DorsAttn_Post_2	0.031	0.028	0.134	-0.007	0.028	0.408	0.073	0.028	0.005	-0.012	0.027	0.334	0.026	0.027	0.174	-0.021	0.027	0.225
7Networks_LH_DorsAttn_Post_5	0.034	0.028	0.108	-0.017	0.027	0.261	0.086	0.027	0.001	0.016	0.027	0.276	0.002	0.027	0.469	0.008	0.027	0.382
7Networks_LH_DorsAttn_PrCv_1	0.060	0.028	0.016	0.024	0.028	0.194	0.081	0.028	0.002	0.040	0.027	0.068	-0.010	0.027	0.353	0.029	0.027	0.144
7Networks_LH_SalVentAttn_ParOper_1	0.058	0.028	0.020	0.024	0.028	0.194	0.071	0.028	0.006	0.033	0.027	0.113	-0.002	0.027	0.472	0.020	0.027	0.232
7Networks_LH_SalVentAttn_FrOperIns_1	0.053	0.023	0.011	0.030	0.023	0.095	0.064	0.023	0.003	0.020	0.022	0.190	-0.008	0.022	0.354	0.016	0.022	0.240
7Networks_LH_SalVentAttn_FrOperIns_3	0.041	0.025	0.049	0.012	0.025	0.314	0.067	0.025	0.004	-0.004	0.024	0.442	0.004	0.024	0.431	-0.004	0.024	0.429
7Networks_LH_SalVentAttn_FrOperIns_4	0.067	0.027	0.007	0.027	0.027	0.160	0.085	0.027	0.001	0.038	0.026	0.074	-0.004	0.026	0.445	0.024	0.026	0.183
7Networks_LH_SalVentAttn_PFCl_1	0.066	0.027	0.007	0.015	0.027	0.293	0.103	0.027	0.000	-0.035	0.026	0.089	0.028	0.026	0.142	-0.035	0.026	0.088
7Networks_LH_Limbic_TempPole_1	0.126	0.025	0.000	0.085	0.025	0.000	0.126	0.026	0.000	0.032	0.025	0.096	-0.040	0.025	0.052	0.041	0.025	0.051
7Networks_LH_Limbic_TempPole_2	0.087	0.027	0.001	0.056	0.027	0.019	0.089	0.027	0.001	0.049	0.026	0.031	-0.040	0.026	0.061	0.050	0.026	0.028
7Networks_LH_Limbic_TempPole_3	0.113	0.027	0.000	0.075	0.027	0.002	0.119	0.027	0.000	0.027	0.026	0.149	-0.016	0.026	0.273	0.024	0.026	0.178
7Networks_LH_Limbic_TempPole_4	0.078	0.023	0.000	0.049	0.023	0.017	0.091	0.023	0.000	0.014	0.023	0.268	-0.005	0.023	0.417	0.011	0.022	0.319
7Networks_LH_Cont_PFCl_2	0.090	0.026	0.000	0.047	0.026	0.033	0.108	0.026	0.000	0.023	0.025	0.180	-0.021	0.025	0.205	0.024	0.025	0.165
7Networks_LH_Cont_PFCl_5	0.095	0.028	0.000	0.046	0.028	0.051	0.115	0.028	0.000	0.006	0.027	0.411	0.043	0.027	0.056	-0.020	0.027	0.232
7Networks_LH_Default_Temp_1	0.098	0.025	0.000	0.052	0.025	0.020	0.113	0.025	0.000	0.036	0.025	0.071	-0.025	0.025	0.155	0.034	0.025	0.082
7Networks_LH_Default_Temp_2	0.116	0.026	0.000	0.070	0.026	0.004	0.121	0.026	0.000	0.034	0.026	0.091	-0.031	0.026	0.114	0.036	0.026	0.078
7Networks_LH_Default_PFC_6	0.078	0.023	0.000	0.054	0.023	0.009	0.080	0.023	0.000	0.000	0.022	0.498	-0.014	0.022	0.261	0.008	0.022	0.363
7Networks_LH_Default_PFC_8	0.068	0.026	0.004	0.047	0.026	0.035	0.070	0.026	0.004	0.000	0.025	0.493	-0.016	0.025	0.266	0.009	0.025	0.363
7Networks_LH_Default_PFC_11	0.078	0.028	0.002	0.033	0.027	0.113	0.100	0.028	0.000	0.016	0.027	0.272	0.021	0.027	0.211	-0.002	0.027	0.466
7Networks_RH_Vis_1	0.058	0.025	0.009	0.028	0.025	0.128	0.069	0.025	0.003	0.050	0.024	0.019	-0.023	0.024	0.167	0.041	0.024	0.043
7Networks_RH_Vis_4	0.085	0.027	0.001	0.063	0.027	0.009	0.075	0.027	0.003	0.026	0.026	0.161	-0.012	0.026	0.323	0.021	0.026	0.206
7Networks_RH_Vis_5	0.067	0.028	0.008	0.036	0.028	0.100	0.085	0.028	0.001	0.011	0.027	0.345	0.003	0.027	0.460	0.005	0.027	0.431
7Networks_RH_Vis_14	0.095	0.026	0.000	0.077	0.026	0.001	0.080	0.026	0.001	0.067	0.025	0.004	-0.055	0.025	0.014	0.068	0.025	0.003
7Networks_RH_SomMot_10	0.072	0.027	0.004	0.047	0.027	0.039	0.076	0.027	0.003	-0.038	0.026	0.072	0.009	0.026	0.358	-0.027	0.026	0.150
7Networks_RH_SomMot_13	0.068	0.029	0.009	0.023	0.029	0.214	0.091	0.029	0.001	0.035	0.028	0.105	-0.041	0.028	0.071	0.042	0.028	0.064

7Networks_RH_SomMot_15	0.056	0.030	0.031	0.014	0.030	0.322	0.079	0.030	0.004	0.046	0.029	0.056	-0.033	0.029	0.125	0.044	0.029	0.062
7Networks_RH_DorsAttn_Post_1	0.030	0.025	0.110	-0.004	0.025	0.428	0.063	0.025	0.005	0.025	0.024	0.150	0.002	0.024	0.463	0.013	0.024	0.293
7Networks_RH_DorsAttn_PrCv_1	0.088	0.027	0.001	0.048	0.027	0.038	0.100	0.027	0.000	0.044	0.027	0.048	0.010	0.027	0.355	0.020	0.027	0.226
7Networks_RH_SalVentAttn_PrC_1	0.082	0.029	0.002	0.038	0.029	0.094	0.103	0.029	0.000	0.025	0.028	0.190	-0.003	0.028	0.464	0.015	0.028	0.290
7Networks_RH_SalVentAttn_FrOperIns_1	0.057	0.025	0.012	0.028	0.025	0.134	0.080	0.025	0.001	-0.010	0.024	0.341	0.018	0.024	0.226	-0.016	0.024	0.260
7Networks_RH_SalVentAttn_FrOperIns_2	0.081	0.023	0.000	0.061	0.023	0.004	0.082	0.023	0.000	0.023	0.023	0.158	-0.019	0.023	0.206	0.023	0.023	0.153
7Networks_RH_Limbic_OFC_3	0.059	0.025	0.009	0.028	0.025	0.126	0.072	0.025	0.002	0.046	0.024	0.029	-0.029	0.024	0.110	0.042	0.024	0.040
7Networks_RH_Limbic_TempPole_1	0.121	0.027	0.000	0.102	0.027	0.000	0.088	0.027	0.001	0.018	0.026	0.248	-0.048	0.026	0.033	0.036	0.026	0.082
7Networks_RH_Limbic_TempPole_2	0.093	0.026	0.000	0.078	0.026	0.001	0.070	0.026	0.004	0.043	0.026	0.048	-0.023	0.026	0.184	0.037	0.025	0.074
7Networks_RH_Limbic_TempPole_3	0.088	0.027	0.001	0.041	0.027	0.067	0.105	0.027	0.000	0.010	0.027	0.349	-0.012	0.026	0.324	0.012	0.026	0.319
7Networks_RH_Cont_Par_1	0.051	0.029	0.039	0.006	0.029	0.414	0.093	0.029	0.001	0.023	0.028	0.201	-0.022	0.028	0.215	0.025	0.028	0.181
7Networks_RH_Cont_Par_2	0.031	0.029	0.138	-0.021	0.028	0.230	0.088	0.029	0.001	-0.021	0.028	0.229	-0.012	0.028	0.337	-0.005	0.028	0.422
7Networks_RH_Cont_Temp_1	0.069	0.026	0.004	0.035	0.026	0.092	0.084	0.026	0.001	0.028	0.025	0.137	-0.009	0.025	0.363	0.021	0.025	0.207
7Networks_RH_Cont_PFCl_1	0.074	0.024	0.001	0.053	0.024	0.015	0.072	0.024	0.002	0.022	0.024	0.176	-0.010	0.024	0.340	0.018	0.024	0.224
7Networks_RH_Cont_PFCl_2	0.032	0.027	0.112	-0.007	0.026	0.397	0.074	0.027	0.003	0.033	0.026	0.098	-0.025	0.026	0.161	0.033	0.026	0.100
7Networks_RH_Cont_PFCl_4	0.053	0.026	0.022	0.032	0.026	0.111	0.068	0.027	0.005	-0.031	0.026	0.116	0.044	0.026	0.044	-0.041	0.026	0.053
7Networks_RH_Cont_PFCl_5	0.022	0.026	0.208	-0.020	0.026	0.224	0.068	0.026	0.005	0.017	0.026	0.257	-0.005	0.026	0.427	0.012	0.026	0.317
7Networks_RH_Cont_pCun_1	0.056	0.027	0.019	0.035	0.027	0.100	0.068	0.027	0.006	0.000	0.026	0.497	0.015	0.026	0.288	-0.008	0.026	0.379
7Networks_RH_Cont_PFCmp_2	0.055	0.025	0.015	0.024	0.025	0.172	0.063	0.025	0.006	0.061	0.024	0.006	-0.037	0.024	0.063	0.055	0.024	0.012
7Networks_RH_Default_Temp_1	0.111	0.026	0.000	0.083	0.026	0.001	0.110	0.026	0.000	0.055	0.025	0.016	-0.049	0.025	0.028	0.058	0.025	0.011
7Networks_RH_Default_Temp_2	0.082	0.025	0.001	0.037	0.025	0.070	0.108	0.025	0.000	0.062	0.025	0.006	-0.019	0.025	0.217	0.046	0.025	0.031
7Networks_RH_Default_Temp_4	0.026	0.027	0.164	-0.025	0.026	0.173	0.093	0.027	0.000	0.032	0.026	0.105	0.008	0.026	0.377	0.014	0.026	0.292
7Networks_RH_Default_PFCdPFCm_6	0.068	0.027	0.007	0.033	0.027	0.113	0.088	0.027	0.001	0.020	0.026	0.231	-0.010	0.026	0.346	0.017	0.026	0.262
7Networks_RH_Default_PFCdPFCm_7	0.125	0.029	0.000	0.098	0.029	0.000	0.101	0.029	0.000	0.015	0.028	0.295	-0.009	0.028	0.377	0.013	0.028	0.316

Supplementary Table 10. Total cognition and subcortical volumes.

	Tot	al Cogni	tion		Fluid		C	rystalliz	ed	Pos	sitive Aff	fect	Neg	gative Af	fect	M	ean Affe	ct
	β	SD	p	β	SD	p	β	SD	p	β	SD	p	β	SD	p	β	SD	p
hipp 1	0.078	0.025	0.001	0.027	0.025	0.141	0.056	0.012	0.000	-0.023	0.024	0.173	0.050	0.024	0.020	-0.040	0.024	0.049

Supplementary Table 11. Fluid cognition and subcortical volumes.

	Tota	al Cognit	ion		Fluid		Cı	rystallize	ed	Pos	itive Aff	ect	Neg	gative Af	fect	M	ean Affe	ct
	β	SD	p	β	SD	р	β	SD	p	β	SD	p	β	SD	p	β	SD	p
pall_l	-0.076	0.028	0.004	-0.088	0.028	0.001	-0.006	0.007	0.178	-0.013	0.027	0.321	0.039	0.027	0.076	-0.029	0.027	0.148

Supplementary Table 12. Crystallized cognition and subcortical volumes.

	Tot	al Cogni	tion		Fluid		C	rystalliz	ed	Pos	sitive Aff	ect	Neg	gative Af	fect	M	ean Affe	ct
	β	SD	p	β	SD	р	β	SD	р	β	SD	р	β	SD	р	β	SD	р
amy_r	0.031	0.023	0.092	-0.001	0.023	0.482	0.014	0.005	0.003	-0.001	0.023	0.491	0.032	0.023	0.081	-0.018	0.023	0.219
hipp_l	0.078	0.025	0.001	0.027	0.025	0.141	0.056	0.012	0.000	-0.023	0.024	0.173	0.050	0.024	0.020	-0.040	0.024	0.049
hipp_r	0.063	0.024	0.004	0.020	0.023	0.192	0.044	0.011	0.000	-0.001	0.023	0.477	0.036	0.023	0.056	-0.020	0.023	0.186

Supplementary Table 13. Mean affect and subcortical volumes.

	Tot	al Cogni	tion		Fluid		C	rystalliz	ed	Pos	itive Aff	ect	Neg	gative Af	fect	M	ean Affe	ct
	β	SD	р	β	SD	р	β	SD	р	β	SD	р	β	SD	р	β	SD	p
caud_l	0.002	0.026	0.467	-0.027	0.025	0.147	0.020	0.012	0.056	-0.099	0.025	0.000	0.086	0.025	0.000	-0.104	0.025	0.000
caud_r	0.002	0.025	0.467	-0.025	0.025	0.161	0.018	0.012	0.067	-0.081	0.024	0.000	0.077	0.024	0.001	-0.088	0.024	0.000

Supplementary Table 14. Positive affect and subcortical volumes.

	Tot	al Cogni	tion		Fluid		C	rystalliz	ed	Pos	itive Aff	ect	Neg	gative Af	fect	M	ean Affe	ct
	β	SD	р	β	SD	р	β	SD	р	β	SD	р	β	SD	р	β	SD	р
caud_l	0.002	0.026	0.467	-0.027	0.025	0.147	0.020	0.012	0.056	-0.099	0.025	0.000	0.086	0.025	0.000	-0.104	0.025	0.000
caud_r	0.002	0.025	0.467	-0.025	0.025	0.161	0.018	0.012	0.067	-0.081	0.024	0.000	0.077	0.024	0.001	-0.088	0.024	0.000

Supplementary Table 15. Negative affect and subcortical volumes.

	Tot	al Cogni	tion		Fluid		C	rystalliz	ed	Pos	itive Aff	ect	Neg	gative Af	fect	M	ean Affe	ct
NA	β	SD	р	β	SD	р	β	SD	р	β	SD	р	β	SD	р	β	SD	р
caud_l	0.002	0.026	0.467	-0.027	0.025	0.147	0.020	0.012	0.056	-0.099	0.025	0.000	0.086	0.025	0.000	-0.104	0.025	0.000
caud_r	0.002	0.025	0.467	-0.025	0.025	0.161	0.018	0.012	0.067	-0.081	0.024	0.000	0.077	0.024	0.001	-0.088	0.024	0.000

Supplementary Table 16. Genetic correlation of cognition and affect with local cortical thickness. Environmental correlation (ρ_e) and genetic correlation (ρ_g) per parcel associated with total cognition score and mean affect score, respectively (see Figure 3A).

Total Cognition	$ ho_e$	p	$ ho_g$	p
7Networks LH Vis 1	-0.027	0.697	0.211	0.003
7Networks LH Vis 4	0.000	0.998	0.182	0.004
7Networks LH Vis 9	-0.057	0.412	0.189	0.003
7Networks_LH_Vis_10	0.029	0.688	0.134	0.020
7Networks LH SomMot 3	0.009	0.905	0.201	0.004
7Networks LH SomMot 10	-0.078	0.265	0.327	0.000
7Networks_LH_DorsAttn_Post_7	0.144	0.052	-0.235	0.001
7Networks_LH_DorsAttn_FEF_2	0.043	0.559	-0.214	0.009
7Networks LH SalVentAttn PFCl 1	0.113	0.096	-0.274	0.000
7Networks LH Default Temp 5	-0.046	0.528	0.245	0.014
7Networks LH Default PFC 4	0.018	0.806	-0.177	0.007
7Networks_LH_Default_PFC_5	0.124	0.084	-0.281	0.001
7Networks_LH_Default_PFC_7	-0.018	0.802	-0.212	0.001
7Networks LH Default PFC 9	0.017	0.814	-0.171	0.007
7Networks LH Default PFC 10	-0.044	0.530	-0.235	0.002
7Networks_LH_Default_PFC_11	0.124	0.075	-0.432	0.000
7Networks LH Default PFC 13	0.042	0.567	-0.212	0.003
7Networks LH Default pCunPCC 1	0.014	0.852	0.187	0.008
7Networks RH Vis 4	-0.119	0.104	0.176	0.004
7Networks RH Vis 9	-0.075	0.310	0.158	0.009
7Networks_RH_Vis_10	-0.173	0.018	0.256	0.000
7Networks_RH_Vis_13	-0.091	0.209	0.215	0.001
7Networks RH SomMot 7	-0.023	0.754	0.137	0.035
7Networks_RH_SomMot_8	-0.053	0.464	0.256	0.003
7Networks_RH_SomMot_12	-0.060	0.403	0.226	0.001
7Networks RH Cont PFCv 1	-0.106	0.127	0.313	0.001
7Networks RH Cont PFCl 5	-0.011	0.875	-0.179	0.015
7Networks RH Cont PFCl 6	-0.008	0.909	-0.210	0.007
7Networks_RH_Cont_PFCl_7	0.140	0.049	-0.287	0.001
7Networks_RH_Cont_PFCmp_2	0.179	0.016	-0.283	0.000
7Networks RH Default PFCdPFCm 4	0.051	0.482	-0.247	0.000
7Networks RH Default PFCdPFCm 5	-0.078	0.283	-0.217	0.001
7Networks_RH_Default_PFCdPFCm_6	0.150	0.036	-0.299	0.000
7Networks_RH_Default_pCunPCC_1	-0.043	0.563	0.329	0.000
Mean affect	$ ho_e$	p	$ ho_{\!g}$	р
7Networks LH Default PFC 9	0.120	0.071	-0.480	0.000

Supplementary Table 17. Genetic correlation between cognition and local surface area. Environmental correlation (ρ_e) and genetic correlation (ρ_g) per parcel associated with total cognition score (see Figure 3B).

Total Cognition	$ ho_e$	р	$ ho_g$	p
7Networks LH Vis 7	0.025	0.742	0.118	0.042
7Networks LH Vis 10	-0.063	0.411	0.101	0.039
7Networks LH Vis 13	-0.128	0.085	0.239	0.000
7Networks_LH_Vis_14	0.022	0.770	0.150	0.034
7Networks LH SomMot 8	0.000	0.997	0.151	0.024
7Networks LH SomMot 10	0.039	0.564	0.172	0.024
7Networks_LH_SomMot_12	0.003	0.966	0.182	0.006
7Networks_LH_SalVentAttn_Med_2	-0.074	0.303	0.206	0.004
7Networks LH Limbic TempPole 1	0.008	0.911	0.213	0.001
7Networks LH Limbic TempPole 3	0.050	0.474	0.174	0.015
7Networks LH Limbic TempPole 4	-0.030	0.682	0.167	0.006
7Networks_LH_Cont_PFCl_2	-0.064	0.387	0.242	0.001
7Networks_LH_Cont_PFCl_5	0.055	0.421	0.205	0.037
7Networks LH Default Temp 1	-0.111	0.141	0.199	0.001
7Networks LH Default Temp 2	-0.044	0.536	0.293	0.000
7Networks_LH_Default_PFC_6	-0.017	0.823	0.154	0.011
7Networks LH Default PFC 8	-0.068	0.350	0.179	0.012
7Networks RH Vis 4	0.009	0.904	0.135	0.037
7Networks RH Vis 9	-0.068	0.390	0.176	0.001
7Networks RH Vis 12	-0.004	0.954	0.147	0.017
7Networks_RH_Vis_14	-0.070	0.323	0.257	0.001
7Networks_RH_Limbic_TempPole_1	-0.204	0.004	0.322	0.000
7Networks RH Limbic TempPole 2	-0.119	0.094	0.231	0.001
7Networks_RH_Limbic_TempPole_3	-0.076	0.290	0.202	0.004
7Networks_RH_Cont_PFCl_1	-0.017	0.805	0.163	0.009
7Networks RH Cont Cing 2	-0.103	0.153	0.210	0.006
7Networks RH Default Temp 1	0.073	0.291	0.173	0.008
7Networks RH Default Temp 2	-0.042	0.549	0.193	0.009
7Networks_RH_Default_PFCdPFCm_7	0.030	0.666	0.228	0.008

Supplementary Table 18. Genetic correlation of cognitive and affective sub-scores and local cortical thickness.

Fluid Cognition	$ ho_e$	p	$ ho_{g}$	p
7Networks LH_Vis_9	-0.058	0.388	0.240	0.002
7Networks LH Vis 10	0.048	0.498	0.146	0.039
7Networks LH SomMot 10	-0.069	0.300	0.319	0.000
7Networks LH SalVentAttn PFCl 1	0.131	0.043	-0.315	0.000
7Networks LH Default PFC 7	0.043	0.525	-0.258	0.002
7Networks LH Default PFC 9	0.066	0.343	-0.240	0.002
7Networks LH Default PFC 10	0.056	0.401	-0.355	0.000

			1	
7Networks LH Default PFC 11	0.145	0.026	-0.479	0.000
7Networks LH Default PFC 13	0.049	0.471	-0.271	0.002
7Networks_RH_Vis_9	-0.133	0.060	0.270	0.000
7Networks RH Vis 10	-0.177	0.011	0.333	0.000
7Networks RH Vis 13	-0.127	0.066	0.287	0.000
7Networks RH SomMot 12	-0.089	0.191	0.298	0.001
7Networks RH Cont PFCmp 2	0.195	0.005	-0.362	0.000
7Networks_RH_Default_PFCdPFCm_4	0.060	0.389	-0.231	0.005
7Networks RH Default PFCdPFCm 5	-0.022	0.751	-0.260	0.001
7Networks RH Default PFCdPFCm 6	0.166	0.015	-0.380	0.000
7Networks_RH_Default_pCunPCC_1	-0.044	0.531	0.308	0.001
Crystallized Cognition	$ ho_e$	p	$ ho_{\!g}$	p
7Networks_LH_Vis_1	0.038	0.609	0.220	0.001
7Networks_LH_Vis_2	0.053	0.471	0.178	0.007
7Networks_LH_Vis_4	-0.009	0.896	0.184	0.001
7Networks_LH_SomMot_3	-0.001	0.987	0.205	0.001
7Networks_LH_SomMot_10	-0.097	0.185	0.287	0.000
7Networks_LH_DorsAttn_Post_1	-0.084	0.291	0.204	0.004
7Networks_LH_DorsAttn_Post_7	0.087	0.270	-0.213	0.001
7Networks_LH_DorsAttn_Post_9	0.015	0.839	-0.135	0.021
7Networks_LH_SalVentAttn_FrOperIns_2	0.050	0.509	0.131	0.045
7Networks_LH_SalVentAttn_FrOperIns_3	-0.044	0.566	0.173	0.010
7Networks_LH_SalVentAttn_PFCl_1	0.096	0.177	-0.219	0.000
7Networks_LH_Cont_PFCl_2	0.082	0.274	-0.189	0.003
7Networks_LH_Cont_PFCl_3	-0.011	0.885	-0.194	0.013
7Networks_LH_Default_PFC_4	0.018	0.816	-0.137	0.020
7Networks_LH_Default_PFC_7	-0.048	0.523	-0.160	0.007
7Networks_LH_Default_PFC_11	0.069	0.353	-0.312	0.000
7Networks_LH_Default_pCunPCC_1	-0.039	0.607	0.177	0.006
7Networks_RH_Vis_3	-0.084	0.273	0.204	0.001
7Networks_RH_Vis_4	-0.067	0.380	0.220	0.000
7Networks_RH_Vis_8	-0.007	0.926	0.162	0.006
7Networks_RH_SomMot_1	0.053	0.492	0.144	0.020
7Networks_RH_SomMot_3	-0.049	0.535	0.188	0.007
7Networks_RH_SomMot_8	0.011	0.884	0.214	0.006
7Networks_RH_SomMot_10	-0.027	0.724	0.205	0.029
7Networks_RH_SalVentAttn_TempOccPar_1	-0.018	0.814	0.188	0.016
7Networks_RH_SalVentAttn_FrOperIns_4	0.008	0.917	0.193	0.024
7Networks_RH_Limbic_TempPole_1	-0.011	0.883	0.210	0.011
7Networks_RH_Cont_PFCv_1	-0.085	0.250	0.249	0.003
7Networks_RH_Cont_PFCl_3	-0.035	0.646	-0.149	0.025
7Networks_RH_Cont_PFCl_5	0.030	0.681	-0.186	0.005
7Networks_RH_Cont_PFCl_6	-0.112	0.117	-0.167	0.016
7Networks RH Default Par 1	0.040	0.610	-0.251	0.009

7Networks_RH_Default_Temp_5	-0.035	0.643	0.299	0.001
7Networks_RH_Default_PFCdPFCm_4	0.017	0.830	-0.208	0.001
7Networks_RH_Default_PFCdPFCm_5	-0.094	0.213	-0.135	0.020
7Networks_RH_Default_pCunPCC_1	-0.030	0.706	0.280	0.000
Positive affect	$ ho_e$	p	$ ho_{g}$	p
Positive affect 7Networks LH Default PFC 9	<i>ρ</i> _e 0.129	p 0.044	ρ_g -0.540	p
	,			-
	,			

Supplementary Table 19. Genetic correlation of cognitive sub-scores and local surface area.

Fluid Cognition	$ ho_e$	p	$ ho_g$	p
7Networks LH Vis 7	0.006	0.937	0.158	0.028
7Networks LH Vis 10	-0.085	0.268	0.158	0.009
7Networks_LH_Vis_13	-0.109	0.132	0.290	0.000
7Networks LH SomMot 12	0.032	0.631	0.165	0.042
7Networks LH Limbic TempPole 1	-0.018	0.796	0.182	0.023
7Networks_RH_Vis_9	-0.082	0.296	0.222	0.000
7Networks_RH_Vis_12	-0.005	0.944	0.182	0.018
7Networks RH Vis 14	-0.083	0.215	0.284	0.002
7Networks RH Limbic TempPole 1	-0.179	0.008	0.361	0.000
7Networks RH Limbic TempPole 2	-0.156	0.020	0.311	0.000
7Networks_RH_Default_Temp_1	0.001	0.985	0.179	0.028
Crystallized Cognition	$ ho_e$	p	$ ho_{\!g}$	p
7Networks_LH_SomMot_4	-0.058	0.433	0.168	0.022
7Networks_LH_SomMot_6	-0.041	0.577	0.147	0.011
7Networks_LH_DorsAttn_Post_1	-0.121	0.124	0.197	0.003
7Networks_LH_DorsAttn_Post_2	-0.068	0.378	0.175	0.008
7Networks_LH_DorsAttn_Post_5	-0.014	0.852	0.221	0.010
7Networks_LH_DorsAttn_PrCv_1	0.003	0.972	0.176	0.016
7Networks_LH_SalVentAttn_PFCl_1	-0.172	0.035	0.324	0.000
7Networks_LH_Limbic_TempPole_1	0.024	0.757	0.203	0.000
7Networks_LH_Limbic_TempPole_2	0.019	0.797	0.136	0.026
7Networks_LH_Limbic_TempPole_3	0.060	0.409	0.180	0.005
7Networks_LH_Limbic_TempPole_4	-0.058	0.451	0.190	0.000
7Networks_LH_Cont_PFCl_2	-0.069	0.379	0.255	0.000
7Networks_LH_Cont_PFCl_5	0.089	0.220	0.223	0.010
7Networks_LH_Default_Temp_1	0.016	0.837	0.155	0.002
7Networks_LH_Default_Temp_2	-0.052	0.493	0.282	0.000
7Networks_LH_Default_PFC_6	0.066	0.394	0.108	0.043
7Networks_RH_Vis_1	-0.083	0.258	0.145	0.010
7Networks_RH_Vis_5	-0.136	0.066	0.298	0.001

7Networks RH Vis 14	-0.002	0.977	0.161	0.015
7Networks_RH_SomMot_13	-0.048	0.538	0.200	0.005
7Networks_RH_DorsAttn_Post_1	-0.034	0.657	0.117	0.045
7Networks_RH_DorsAttn_PrCv_1	0.011	0.882	0.221	0.002
7Networks_RH_SalVentAttn_PrC_1	0.054	0.472	0.202	0.008
7Networks_RH_Limbic_OFC_3	0.000	0.996	0.137	0.032
7Networks_RH_Limbic_TempPole_1	-0.118	0.106	0.183	0.001
7Networks_RH_Limbic_TempPole_3	-0.069	0.358	0.204	0.001
7Networks_RH_Cont_Par_2	0.006	0.938	0.200	0.026
7Networks_RH_Cont_Temp_1	-0.025	0.756	0.180	0.012
7Networks_RH_Cont_PFCl_1	0.042	0.568	0.117	0.035
7Networks_RH_Cont_PFCl_2	-0.056	0.473	0.174	0.019
7Networks_RH_Cont_PFCmp_2	-0.108	0.146	0.180	0.004
7Networks_RH_Default_Temp_1	0.135	0.059	0.153	0.008
7Networks_RH_Default_Temp_2	0.115	0.112	0.150	0.019
7Networks_RH_Default_Temp_4	0.023	0.749	0.167	0.013
7Networks_RH_Default_PFCdPFCm_6	-0.092	0.213	0.195	0.003
7Networks_RH_Default_PFCdPFCm_7	-0.134	0.072	0.269	0.000

Supplementary Table 20. Genetic correlation of cognitive and affective scores and subcortical volumes.

Total Cognition	$ ho_e$	p	$ ho_g$	p
hipp l	0.175	0.015	0.057	0.349
Fluid Cognition	$ ho_e$	p	$ ho_g$	p
pall_l	0.089	0.212	-0.230	0.003
Crystallized Cognition	$ ho_e$	p	$ ho_g$	p
amy r	0.042	0.621	0.075	0.138
hipp l	0.124	0.093	0.159	0.004
hipp r	0.214	0.008	0.098	0.026
Mean affect		р	0	р
1,1cuii uiicet	$ ho_e$	Р	$ ho_g$	Р
caud l	ρ_e 0.041	0.603	-0.280	0.001
	_	_		
caud l	0.041	0.603	-0.280	0.001
caud l	0.041	0.603	-0.280	0.001
caud l	0.041	0.603	-0.280 -0.283	0.001
caud 1 caud r Positive affect	0.041 0.084 ρ_e	0.603 0.297 p	-0.280 -0.283	0.001 0.001 p
caud l caud r Positive affect caud l	0.041 0.084 Pe 0.018	0.603 0.297 p 0.820	-0.280 -0.283 -0.275	0.001 0.001 p 0.002
caud l caud r Positive affect caud l	0.041 0.084 Pe 0.018	0.603 0.297 p 0.820	-0.280 -0.283 -0.275	0.001 0.001 p 0.002
caud l caud r Positive affect caud l caud r	0.041 0.084 Pe 0.018 0.083	0.603 0.297 p 0.820 0.284	-0.280 -0.283 -0.275 -0.275	0.001 0.001 p 0.002 0.001

Supplementary Table 21. Heritability of local cortical thickness.

Parcel	h ²	р
7Networks_LH_Vis_1	0.411	0.000
7Networks_LH_Vis_2	0.387	0.000
7Networks_LH_Vis_3	0.168	0.002
7Networks_LH_Vis_4	0.476	0.000
7Networks_LH_Vis_5	0.512	0.000
7Networks_LH_Vis_6	0.437	0.000
7Networks_LH_Vis_7	0.509	0.000
7Networks_LH_Vis_8	0.237	0.000
7Networks_LH_Vis_9	0.472	0.000
7Networks_LH_Vis_10	0.600	0.000
7Networks_LH_Vis_11	0.400	0.000
7Networks_LH_Vis_12	0.464	0.000
7Networks_LH_Vis_13	0.557	0.000
7Networks_LH_Vis_14	0.454	0.000
7Networks_LH_SomMot_1	0.445	0.000
7Networks_LH_SomMot_2	0.260	0.000
7Networks_LH_SomMot_3	0.439	0.000
7Networks_LH_SomMot_4	0.416	0.000
7Networks_LH_SomMot_5	0.274	0.000
7Networks_LH_SomMot_6	0.511	0.000
7Networks_LH_SomMot_7	0.330	0.000
7Networks_LH_SomMot_8	0.269	0.000
7Networks_LH_SomMot_9	0.305	0.000
7Networks_LH_SomMot_10	0.460	0.000
7Networks_LH_SomMot_11	0.199	0.000
7Networks_LH_SomMot_12	0.423	0.000
7Networks_LH_SomMot_13	0.367	0.000
7Networks_LH_SomMot_14	0.332	0.000
7Networks_LH_SomMot_15	0.531	0.000
7Networks_LH_SomMot_16	0.348	0.000
7Networks_LH_DorsAttn_Post_1	0.364	0.000
7Networks_LH_DorsAttn_Post_2	0.240	0.000
7Networks_LH_DorsAttn_Post_3	0.349	0.000
7Networks_LH_DorsAttn_Post_4	0.298	0.000
7Networks_LH_DorsAttn_Post_5	0.142	0.004
7Networks_LH_DorsAttn_Post_6	0.225	0.000
7Networks_LH_DorsAttn_Post_7	0.460	0.000
7Networks_LH_DorsAttn_Post_8	0.278	0.000
7Networks_LH_DorsAttn_Post_9	0.486	0.000
7Networks_LH_DorsAttn_Post_10	0.479	0.000
7Networks_LH_DorsAttn_FEF_1	0.307	0.000
7Networks_LH_DorsAttn_FEF_2	0.337	0.000

7Networks_LH_DorsAttn_PrCv_1	0.272	0.000
7Networks_LH_SalVentAttn_ParOper 1	0.102	0.043
7Networks_LH_SalVentAttn_ParOper 2	0.311	0.000
7Networks_LH_SalVentAttn_ParOper 3	0.255	0.000
7Networks_LH_SalVentAttn_FrOperI ns 1	0.309	0.000
7Networks_LH_SalVentAttn_FrOperI ns 2	0.404	0.000
7Networks_LH_SalVentAttn_FrOperI ns 3	0.392	0.000
7Networks_LH_SalVentAttn_FrOperI ns 4	0.225	0.000
7Networks_LH_SalVentAttn_PFCl_1	0.434	0.000
7Networks_LH_SalVentAttn_Med_1	0.343	0.000
7Networks_LH_SalVentAttn_Med_2	0.351	0.000
7Networks_LH_SalVentAttn_Med_3	0.288	0.000
7Networks_LH_Limbic_OFC_1	0.306	0.000
7Networks_LH_Limbic_OFC_2	0.423	0.000
7Networks_LH_Limbic_TempPole_1	0.479	0.000
7Networks_LH_Limbic_TempPole_2	0.356	0.000
7Networks_LH_Limbic_TempPole_3	0.241	0.000
7Networks_LH_Limbic_TempPole_4	0.430	0.000
7Networks_LH_Cont_Par_1	0.257	0.000
7Networks_LH_Cont_Par_2	0.288	0.000
7Networks_LH_Cont_Par_3	0.113	0.022
7Networks_LH_Cont_Temp_1	0.203	0.000
7Networks_LH_Cont_OFC_1	0.348	0.000
7Networks_LH_Cont_PFCl_1	0.280	0.000
7Networks_LH_Cont_PFCl_2	0.404	0.000
7Networks_LH_Cont_PFCl_3	0.274	0.000
7Networks_LH_Cont_PFCl_4	0.373	0.000
7Networks_LH_Cont_PFCl_5	0.234	0.000
7Networks_LH_Cont_pCun_1	0.387	0.000
7Networks_LH_Cont_Cing_1	0.558	0.000
7Networks_LH_Cont_Cing_2	0.427	0.000
7Networks_LH_Default_Temp_1	0.250	0.000
7Networks_LH_Default_Temp_2	0.290	0.000
7Networks_LH_Default_Temp_3	0.350	0.000
7Networks_LH_Default_Temp_4	0.226	0.000
7Networks_LH_Default_Temp_5	0.238	0.000
7Networks_LH_Default_Par_1	0.330	0.000
7Networks_LH_Default_Par_2	0.328	0.000
7Networks_LH_Default_Par_3	0.240	0.000
7Networks_LH_Default_Par_4	0.255	0.000
7Networks_LH_Default_PFC_1	0.355	0.000
7Networks_LH_Default_PFC_2	0.323	0.000

7Networks LH Default PFC 3	0.168	0.001	7Networks RH SomMot 15	0.378	0.000
7Networks LH Default PFC 4	0.488	0.000	7Networks RH SomMot 16	0.233	0.000
7Networks LH Default PFC 5	0.322	0.000	7Networks RH SomMot 17	0.481	0.000
7Networks LH Default PFC 6	0.322	0.000	7Networks RH SomMot 18	0.400	0.000
7Networks LH Default PFC 7	0.483	0.000	7Networks RH SomMot 19	0.369	0.000
7Networks LH Default PFC 8	0.463	0.000	7Networks RH DorsAttn Post 1	0.273	0.000
7Networks LH Default PFC 9	0.540	0.000	7Networks RH DorsAttn Post 2	0.273	0.000
7Networks LH Default PFC 10		0.000			0.000
7Networks LH Default PFC 11	0.359	0.000	7Networks_RH_DorsAttn_Post_3 7Networks_RH_DorsAttn_Post_4	0.274	0.000
7Networks_LH_Default_PFC_12	0.471	0.000	7Networks_RH_DorsAttn_Post_5	0.226	0.000
7Networks_LH_Default_PFC_13	0.429	0.000	7Networks_RH_DorsAttn_Post_6	0.395	0.000
7Networks_LH_Default_pCunPCC_1	0.434	0.000	7Networks_RH_DorsAttn_Post_7	0.208	0.000
7Networks_LH_Default_pCunPCC_2	0.240	0.000	7Networks_RH_DorsAttn_Post_8	0.397	0.000
7Networks_LH_Default_pCunPCC_3	0.458	0.000	7Networks_RH_DorsAttn_Post_9	0.359	0.000
7Networks_LH_Default_pCunPCC_4	0.362	0.000	7Networks_RH_DorsAttn_Post_10	0.378	0.000
7Networks_LH_Default_PHC_1	0.484	0.000	7Networks_RH_DorsAttn_FEF_1	0.306	0.000
7Networks_RH_Vis_1	0.379	0.000	7Networks_RH_DorsAttn_FEF_2	0.269	0.000
7Networks_RH_Vis_2	0.437	0.000	7Networks_RH_DorsAttn_PrCv_1	0.283	0.000
7Networks_RH_Vis_3	0.436	0.000	7Networks_RH_SalVentAttn_TempOc	0.299	0.000
7Networks_RH_Vis_4	0.580	0.000	cPar_1 7Networks RH SalVentAttn TempOc	0.240	0.000
7Networks_RH_Vis_5	0.336	0.000	cPar_2	0.2.0	0.000
7Networks_RH_Vis_6	0.544	0.000	7Networks_RH_SalVentAttn_TempOc	0.303	0.000
7Networks_RH_Vis_7	0.523	0.000	cPar_3 7Networks RH SalVentAttn PrC 1	0.168	0.003
7Networks_RH_Vis_8	0.505	0.000	7Networks_RH_SalVentAttn_FrOperI	0.381	0.000
7Networks_RH_Vis_9	0.585	0.000	ns 1	0.501	0.000
7Networks_RH_Vis_10	0.514	0.000	7Networks_RH_SalVentAttn_FrOperI	0.459	0.000
7Networks_RH_Vis_11	0.277	0.000	ns_2 7Networks_RH_SalVentAttn_FrOperI	0.308	0.000
7Networks_RH_Vis_12	0.544	0.000	ns 3	0.308	0.000
7Networks_RH_Vis_13	0.520	0.000	7Networks_RH_SalVentAttn_FrOperI	0.238	0.000
7Networks_RH_Vis_14	0.345	0.000	7Naturalis DII SalVant Atta Mad 1	0.211	0.000
7Networks_RH_Vis_15	0.342	0.000	7Networks_RH_SalVentAttn_Med_1		
7Networks_RH_SomMot_1	0.452	0.000	7Networks_RH_SalVentAttn_Med_2	0.487	0.000
7Networks_RH_SomMot_2	0.286	0.000	7Networks_RH_SalVentAttn_Med_3 7Networks_RH_Limbic_OFC_1	0.381	0.000
7Networks_RH_SomMot_3	0.374	0.000	7Networks RH Limbic OFC 2		0.000
7Networks_RH_SomMot_4	0.316	0.000		0.335	
7Networks_RH_SomMot_5	0.224	0.000	7Networks_RH_Limbic_OFC_3	0.423	0.000
7Networks_RH_SomMot_6	0.319	0.000	7Networks_RH_Limbic_TempPole_1	0.263	0.000
7Networks_RH_SomMot_7	0.517	0.000	7Networks_RH_Limbic_TempPole_2	0.353	0.000
7Networks_RH_SomMot_8	0.287	0.000	7Networks_RH_Limbic_TempPole_3	0.462	0.000
7Networks_RH_SomMot_9	0.348	0.000	7Networks_RH_Cont_Par_1	0.196	0.000
7Networks_RH_SomMot_10	0.202	0.000	7Networks_RH_Cont_Par_2	0.159	0.002
7Networks_RH_SomMot_11	0.316	0.000	7Networks_RH_Cont_Par_3	0.198	0.000
7Networks_RH_SomMot_12	0.440	0.000	7Networks_RH_Cont_Temp_1	0.246	0.000
7Networks_RH_SomMot_13	0.279	0.000	7Networks_RH_Cont_PFCv_1	0.259	0.000
7Networks_RH_SomMot_14	0.480	0.000	7Networks_RH_Cont_PFCl_1	0.276	0.000
	1		7Networks_RH_Cont_PFCl_2	0.324	0.000

7Networks_RH_Cont_PFCl_3	0.385	0.000
7Networks_RH_Cont_PFCl_4	0.427	0.000
7Networks_RH_Cont_PFCl_5	0.382	0.000
7Networks_RH_Cont_PFCl_6	0.336	0.000
7Networks_RH_Cont_PFCl_7	0.318	0.000
7Networks_RH_Cont_pCun_1	0.279	0.000
7Networks_RH_Cont_Cing_1	0.525	0.000
7Networks_RH_Cont_Cing_2	0.394	0.000
7Networks_RH_Cont_PFCmp_1	0.289	0.000
7Networks_RH_Cont_PFCmp_2	0.460	0.000
7Networks_RH_Default_Par_1	0.196	0.001
7Networks_RH_Default_Par_2	0.201	0.000
7Networks_RH_Default_Par_3	0.173	0.001
7Networks_RH_Default_Temp_1	0.331	0.000
7Networks_RH_Default_Temp_2	0.377	0.000
7Networks_RH_Default_Temp_3	0.463	0.000
7Networks_RH_Default_Temp_4	0.275	0.000

7Networks_RH_Default_Temp_5	0.214	0.000
7Networks_RH_Default_PFCv_1	0.403	0.000
7Networks_RH_Default_PFCdPFCm_ 1	0.349	0.000
7Networks_RH_Default_PFCdPFCm_ 2	0.331	0.000
7Networks_RH_Default_PFCdPFCm_ 3	0.361	0.000
7Networks_RH_Default_PFCdPFCm_ 4	0.481	0.000
7Networks_RH_Default_PFCdPFCm_ 5	0.498	0.000
7Networks_RH_Default_PFCdPFCm_ 6	0.402	0.000
7Networks_RH_Default_PFCdPFCm_ 7	0.280	0.000
7Networks_RH_Default_pCunPCC_1	0.432	0.000
7Networks_RH_Default_pCunPCC_2	0.435	0.000
7Networks_RH_Default_pCunPCC_3	0.254	0.000

Supplementary Table 22. Heritability of local surface area.

Parcel	h ²	р
7Networks_LH_Vis_1	0.610	0.000
7Networks_LH_Vis_2	0.554	0.000
7Networks_LH_Vis_3	0.399	0.000
7Networks_LH_Vis_4	0.406	0.000
7Networks_LH_Vis_5	0.331	0.000
7Networks_LH_Vis_6	0.619	0.000
7Networks_LH_Vis_7	0.645	0.000
7Networks_LH_Vis_8	0.398	0.000
7Networks_LH_Vis_9	0.472	0.000
7Networks_LH_Vis_10	0.795	0.000
7Networks_LH_Vis_11	0.447	0.000
7Networks_LH_Vis_12	0.591	0.000
7Networks_LH_Vis_13	0.644	0.000
7Networks_LH_Vis_14	0.462	0.000
7Networks_LH_SomMot_1	0.463	0.000
7Networks_LH_SomMot_2	0.509	0.000
7Networks_LH_SomMot_3	0.416	0.000
7Networks_LH_SomMot_4	0.345	0.000
7Networks_LH_SomMot_5	0.434	0.000
7Networks_LH_SomMot_6	0.498	0.000
7Networks_LH_SomMot_7	0.288	0.000
7Networks_LH_SomMot_8	0.477	0.000
7Networks_LH_SomMot_9	0.222	0.000

7Networks_LH_SomMot_10	0.363	0.000
7Networks_LH_SomMot_11	0.416	0.000
7Networks_LH_SomMot_12	0.479	0.000
7Networks_LH_SomMot_13	0.440	0.000
7Networks_LH_SomMot_14	0.291	0.000
7Networks_LH_SomMot_15	0.475	0.000
7Networks_LH_SomMot_16	0.380	0.000
7Networks_LH_DorsAttn_Post_1	0.407	0.000
7Networks_LH_DorsAttn_Post_2	0.405	0.000
7Networks_LH_DorsAttn_Post_3	0.483	0.000
7Networks_LH_DorsAttn_Post_4	0.390	0.000
7Networks_LH_DorsAttn_Post_5	0.246	0.000
7Networks_LH_DorsAttn_Post_6	0.213	0.000
7Networks_LH_DorsAttn_Post_7	0.354	0.000
7Networks_LH_DorsAttn_Post_8	0.322	0.000
7Networks_LH_DorsAttn_Post_9	0.417	0.000
7Networks_LH_DorsAttn_Post_10	0.364	0.000
7Networks_LH_DorsAttn_FEF_1	0.279	0.000
7Networks_LH_DorsAttn_FEF_2	0.244	0.000
7Networks_LH_DorsAttn_PrCv_1	0.330	0.000
7Networks_LH_SalVentAttn_ParOper_1	0.408	0.000
7Networks_LH_SalVentAttn_ParOper 2	0.470	0.000
7Networks_LH_SalVentAttn_ParOper_3	0.327	0.000
7Networks_LH_SalVentAttn_FrOperIns_1	0.619	0.000
7Networks_LH_SalVentAttn_FrOperIns_2	0.570	0.000

7Networks_LH_SalVentAttn_FrOperI	0.528	0.000	7Networks_LH_Default_PFC_11	0.352	0.000
ns 3	0.270	0.000	7Networks_LH_Default_PFC_12	0.333	0.000
7Networks_LH_SalVentAttn_FrOperI ns 4	0.370	0.000	7Networks_LH_Default_PFC_13	0.324	0.000
7Networks_LH_SalVentAttn_PFCl_1	0.314	0.000	7Networks_LH_Default_pCunPCC_1	0.700	0.000
7Networks_LH_SalVentAttn_Med_1	0.587	0.000	7Networks_LH_Default_pCunPCC_2	0.494	0.000
7Networks_LH_SalVentAttn_Med_2	0.435	0.000	7Networks_LH_Default_pCunPCC_3	0.372	0.000
7Networks_LH_SalVentAttn_Med_3	0.353	0.000	7Networks_LH_Default_pCunPCC_4	0.435	0.000
7Networks_LH_Limbic_OFC_1	0.586	0.000	7Networks_LH_Default_PHC_1	0.602	0.000
7Networks_LH_Limbic_OFC_2	0.590	0.000	7Networks_RH_Vis_1	0.523	0.000
7Networks_LH_Limbic_TempPole_1	0.548	0.000	7Networks_RH_Vis_2	0.492	0.000
7Networks_LH_Limbic_TempPole_2	0.459	0.000	7Networks_RH_Vis_3	0.459	0.000
7Networks_LH_Limbic_TempPole_3	0.423	0.000	7Networks_RH_Vis_4	0.519	0.000
7Networks_LH_Limbic_TempPole_4	0.603	0.000	7Networks_RH_Vis_5	0.238	0.000
7Networks_LH_Cont_Par_1	0.236	0.000	7Networks_RH_Vis_6	0.646	0.000
7Networks_LH_Cont_Par_2	0.246	0.000	7Networks_RH_Vis_7	0.631	0.000
7Networks_LH_Cont_Par_3	0.208	0.000	7Networks_RH_Vis_8	0.369	0.000
7Networks_LH_Cont_Temp_1	0.341	0.000	7Networks_RH_Vis_9	0.774	0.000
7Networks_LH_Cont_OFC_1	0.449	0.000	7Networks_RH_Vis_10	0.760	0.000
7Networks_LH_Cont_PFCl_1	0.446	0.000	7Networks_RH_Vis_11	0.267	0.000
7Networks_LH_Cont_PFCl_2	0.408	0.000	7Networks_RH_Vis_12	0.578	0.000
7Networks_LH_Cont_PFCl_3	0.386	0.000	7Networks_RH_Vis_13	0.553	0.000
7Networks_LH_Cont_PFCl_4	0.330	0.000	7Networks_RH_Vis_14	0.401	0.000
7Networks_LH_Cont_PFCl_5	0.226	0.000	7Networks_RH_Vis_15	0.308	0.000
7Networks_LH_Cont_pCun_1	0.506	0.000	7Networks_RH_SomMot_1	0.652	0.000
7Networks_LH_Cont_Cing_1	0.516	0.000	7Networks_RH_SomMot_2	0.568	0.000
7Networks_LH_Cont_Cing_2	0.303	0.000	7Networks_RH_SomMot_3	0.510	0.000
7Networks_LH_Default_Temp_1	0.659	0.000	7Networks_RH_SomMot_4	0.513	0.000
7Networks_LH_Default_Temp_2	0.363	0.000	7Networks_RH_SomMot_5	0.317	0.000
7Networks_LH_Default_Temp_3	0.392	0.000	7Networks_RH_SomMot_6	0.508	0.000
7Networks_LH_Default_Temp_4	0.503	0.000	7Networks_RH_SomMot_7	0.428	0.000
7Networks_LH_Default_Temp_5	0.354	0.000	7Networks_RH_SomMot_8	0.314	0.000
7Networks_LH_Default_Par_1	0.336	0.000	7Networks_RH_SomMot_9	0.213	0.000
7Networks_LH_Default_Par_2	0.278	0.000	7Networks_RH_SomMot_10	0.315	0.000
7Networks_LH_Default_Par_3	0.160	0.002	7Networks_RH_SomMot_11	0.520	0.000
7Networks_LH_Default_Par_4	0.353	0.000	7Networks_RH_SomMot_12	0.380	0.000
7Networks_LH_Default_PFC_1	0.478	0.000	7Networks_RH_SomMot_13	0.368	0.000
7Networks_LH_Default_PFC_2	0.591	0.000	7Networks_RH_SomMot_14	0.460	0.000
7Networks_LH_Default_PFC_3	0.449	0.000	7Networks_RH_SomMot_15	0.204	0.000
7Networks_LH_Default_PFC_4	0.562	0.000	7Networks_RH_SomMot_16	0.302	0.000
7Networks_LH_Default_PFC_5	0.414	0.000	7Networks_RH_SomMot_17	0.160	0.003
7Networks_LH_Default_PFC_6	0.597	0.000	7Networks_RH_SomMot_18	0.475	0.000
7Networks_LH_Default_PFC_7	0.402	0.000	7Networks_RH_SomMot_19	0.444	0.000
7Networks_LH_Default_PFC_8	0.446	0.000	7Networks_RH_DorsAttn_Post_1	0.510	0.000
7Networks_LH_Default_PFC_9	0.393	0.000	7Networks_RH_DorsAttn_Post_2	0.339	0.000
7Networks_LH_Default_PFC_10	0.447	0.000	7Networks_RH_DorsAttn_Post_3	0.402	0.000

7Ni-true also DII Danis Attis Danis A	0.232	0.000	7N-transler DII Cout DECL 1	0.527	0.000
7Networks_RH_DorsAttn_Post_4			7Networks_RH_Cont_PFCl_1		
7Networks_RH_DorsAttn_Post_5	0.267	0.000	7Networks_RH_Cont_PFCl_2	0.346	0.000
7Networks_RH_DorsAttn_Post_6	0.247	0.000	7Networks_RH_Cont_PFCl_3	0.396	0.000
7Networks_RH_DorsAttn_Post_7	0.192	0.001	7Networks_RH_Cont_PFCl_4	0.415	0.000
7Networks_RH_DorsAttn_Post_8	0.227	0.000	7Networks_RH_Cont_PFCl_5	0.327	0.000
7Networks_RH_DorsAttn_Post_9	0.451	0.000	7Networks_RH_Cont_PFCl_6	0.272	0.000
7Networks_RH_DorsAttn_Post_10	0.393	0.000	7Networks_RH_Cont_PFCl_7	0.418	0.000
7Networks_RH_DorsAttn_FEF_1	0.216	0.000	7Networks_RH_Cont_pCun_1	0.416	0.000
7Networks_RH_DorsAttn_FEF_2	0.586	0.000	7Networks_RH_Cont_Cing_1	0.469	0.000
7Networks_RH_DorsAttn_PrCv_1	0.337	0.000	7Networks_RH_Cont_Cing_2	0.379	0.000
7Networks_RH_SalVentAttn_TempOc	0.335	0.000	7Networks_RH_Cont_PFCmp_1	0.569	0.000
cPar_1 7Networks RH SalVentAttn TempOc	0.222	0.000	7Networks_RH_Cont_PFCmp_2	0.425	0.000
cPar 2	0.222	0.000	7Networks_RH_Default_Par_1	0.314	0.000
7Networks_RH_SalVentAttn_TempOc	0.419	0.000	7Networks_RH_Default_Par_2	0.206	0.000
cPar 3	0.215	0.000	7Networks_RH_Default_Par_3	0.198	0.000
7Networks_RH_SalVentAttn_PrC_1	0.315	0.000	7Networks_RH_Default_Temp_1	0.490	0.000
7Networks_RH_SalVentAttn_FrOperI ns 1	0.584	0.000	7Networks_RH_Default_Temp_2	0.416	0.000
7Networks_RH_SalVentAttn_FrOperI	0.547	0.000	7Networks_RH_Default_Temp_3	0.408	0.000
ns_2	0.425	0.000	7Networks_RH_Default_Temp_4	0.374	0.000
7Networks_RH_SalVentAttn_FrOperI ns 3	0.435	0.000	7Networks_RH_Default_Temp_5	0.453	0.000
7Networks RH SalVentAttn FrOperI	0.488	0.000	7Networks_RH_Default_PFCv_1	0.367	0.000
ns_4			7Networks_RH_Default_PFCdPFCm_	0.574	0.000
7Networks_RH_SalVentAttn_Med_1	0.577	0.000	1	0.402	0.000
7Networks_RH_SalVentAttn_Med_2	0.527	0.000	7Networks_RH_Default_PFCdPFCm_ 2	0.493	0.000
7Networks_RH_SalVentAttn_Med_3	0.488	0.000	7Networks RH Default PFCdPFCm	0.188	0.001
7Networks_RH_Limbic_OFC_1	0.532	0.000	3		
7Networks_RH_Limbic_OFC_2	0.516	0.000	7Networks_RH_Default_PFCdPFCm_	0.592	0.000
7Networks_RH_Limbic_OFC_3	0.461	0.000	4 7Networks RH Default PFCdPFCm	0.381	0.000
7Networks_RH_Limbic_TempPole_1	0.509	0.000	5	0.501	0.000
7Networks_RH_Limbic_TempPole_2	0.493	0.000	7Networks_RH_Default_PFCdPFCm_	0.400	0.000
7Networks_RH_Limbic_TempPole_3	0.455	0.000	7 Networks BH Default DECADECTS	0.207	0.000
7Networks_RH_Cont_Par_1	0.283	0.000	7Networks_RH_Default_PFCdPFCm_	0.307	0.000
7Networks_RH_Cont_Par_2	0.228	0.000	7Networks_RH_Default_pCunPCC_1	0.666	0.000
7Networks_RH_Cont_Par_3	0.225	0.000	7Networks_RH_Default_pCunPCC_2	0.401	0.000
7Networks_RH_Cont_Temp_1	0.370	0.000	7Networks_RH_Default_pCunPCC_3	0.319	0.000
7Networks_RH_Cont_PFCv_1	0.358	0.000	-		

Supplementary Table 23. Heritability of subcortical volumes.

Volume	h ²	p
accumb_1	0.535	0.000
accumb_r	0.571	0.000
amy_l	0.621	0.000
amy_r	0.698	0.000
caud_l	0.837	0.000

caud_r	0.835	0.000
hipp_l	0.556	0.000
hipp_r	0.812	0.000
spall_l	0.571	0.000
pall_r	0.666	0.000
put_l	0.709	0.000
put_r	0.848	0.000
thal_l	0.584	0.000
thal_r	0.667	0.000
ventDC_1	0.704	0.000
ventDC_r	0.718	0.000

5 Study 2

Network and State Specificity in Connectivity-Based Predictions of Individual Behavior

Nevena Kraljević^{1, 2}, Robert Langner^{1, 2}, Vincent Küppers^{2, 3}, Federico Raimondo^{1, 2}, Kaustubh R. Patil^{1, 2}, Simon B. Eickhoff^{1, 2}, Veronika I. Müller^{2, 1}

- 1) Institute of Systems Neuroscience, Medical Faculty and University Hospital Düsseldorf, Heinrich Heine University Düsseldorf
- 2) Institute of Neuroscience and Medicine (INM-7: Brain and Behaviour), Research Centre Jülich, Jülich, Germany
- 3) Department of Nuclear Medicine, Faculty of Medicine and University Hospital Cologne, University of Cologne, Cologne, Germany

Human Brain Mapping (2024)

DOI: 10.1002/hbm.26753

Impact Factor (2023): 3.5

Own contributions

Conception and design of study

Implementation, reviewing and adapting analysis code

Statistical data analysis

Interpretation of results

Preparing figures

Writing paper

Total contribution 85 %

RESEARCH ARTICLE



WILEY

Network and state specificity in connectivity-based predictions of individual behavior

Nevena Kraljević^{1,2} | Robert Langner^{1,2} | Vincent Küppers^{2,3} | Federico Raimondo 1,2 | Kaustubh R. Patil 1,2 | Simon B. Eickhoff 1,2 Veronika I. Müller 1,2

Correspondence

Nevena Kraljević and Veronika I. Müller, Institute of Systems Neuroscience, Medical Faculty and University Hospital Düsseldorf. Heinrich Heine University Düsseldorf, Düsseldorf, Germany.

Email: nevena.kraljevic@hhu.de and v. mueller@fz-juelich.de

Funding information

Horizon 2020 Framework Programme. Grant/Award Number: 945539 (HBP SGA3); Helmholtz Portfolio Theme "Supercomputing and Modeling for the Human Brain"

Abstract

Predicting individual behavior from brain functional connectivity (FC) patterns can contribute to our understanding of human brain functioning. This may apply in particular if predictions are based on features derived from circumscribed, a priori defined functional networks, which improves interpretability. Furthermore, some evidence suggests that task-based FC data may yield more successful predictions of behavior than resting-state FC data. Here, we comprehensively examined to what extent the correspondence of functional network priors and task states with behavioral target domains influences the predictability of individual performance in cognitive, social, and affective tasks. To this end, we used data from the Human Connectome Project for large-scale out-of-sample predictions of individual abilities in working memory (WM), theory-of-mind cognition (SOCIAL), and emotion processing (EMO) from FC of corresponding and non-corresponding states (WM/SOCIAL/EMO/resting-state) and networks (WM/SOCIAL/EMO/whole-brain connectome). Using root mean squared error and coefficient of determination to evaluate model fit revealed that predictive performance was rather poor overall. Predictions from whole-brain FC were slightly better than those from FC in task-specific networks, and a slight benefit of predictions based on FC from task versus resting state was observed for performance in the WM domain. Beyond that, we did not find any significant effects of a correspondence of network, task state, and performance domains. Together, these results suggest that multivariate FC patterns during both task and resting states contain rather little information on individual performance levels, calling for a reconsideration of how the brain mediates individual differences in mental abilities.

brain-based prediction, brain-behavior relationships, fMRI, functional connectivity, interindividual differences, machine learning

This is an open access article under the terms of the Creative Commons Attribution License, which permits use, distribution and reproduction in any medium, provided the original work is properly cited.

© 2024 The Author(s). Human Brain Mapping published by Wiley Periodicals LLC.

¹Institute of Systems Neuroscience, Medical Faculty and University Hospital Düsseldorf, Heinrich Heine University Düsseldorf, Düsseldorf, Germany

²Institute of Neuroscience and Medicine (INM-7: Brain and Behaviour), Research Centre Jülich, Jülich, Germany

³Department of Nuclear Medicine, Faculty of Medicine and University Hospital Cologne, University of Cologne, Cologne, Germany

and-conditions) on Wiley Online Library for rules of use; OA articles are governed by the applicable Creative Commons

Practitioner Points

- Better prediction of behavior from task versus resting-state functional connectivity (FC) only
 in a cognitive domain.
- Little evidence for specificity of state, network, or task similarity.
- Predicting complex behavior based on FC remains a significant challenge.
- We extend research on brain-based behavior prediction beyond the cognitive domain.

1 | INTRODUCTION

No two individuals are alike in perception, affect, thought, and behavior, but also brain structure and function. A major goal of neuroscience is uncovering the relationships between these dimensions by investigating individual differences. An approach that has recently become popular is predicting individual behavior, affective characteristics or cognitive abilities from brain data (Gao et al., 2019; Greene et al., 2018; Kong et al., 2019; Larabi et al., 2021; Nostro et al., 2018; Ooi et al., 2022; Rosenberg et al., 2020; Sasse et al., 2023; Shen et al., 2017). Such predictive modeling is thought to yield important insights about generalizable brain-behavior relationships and is considered a crucial step toward personalized medicine (Mueller et al., 2013; D. Wang et al., 2015).

A number of studies in this area have shown that, for example, regional gray-matter volume and structural connectivity significantly predict age (Cole et al., 2017; Franke et al., 2012; More et al., 2023), reading comprehension (Cui et al., 2018), inhibitory control (N. He et al., 2020), or fear of pain (X. Wang et al., 2019). Similarly, functional neuroimaging data has also been reported to predict different behaviors or traits, ranging from personality (Dubois, Galdi, Han, et al., 2018; Nostro et al., 2018) or life satisfaction (Itahashi et al., 2021) to cognitive abilities such as creative thinking (Zhuang et al., 2021), cognitive flexibility (Chén et al., 2019), or working memory (WM) capacity (Stark et al., 2021).

While a variety of different brain characteristics have been employed as features to predict behavior, one of the most widely used measures (Yeung et al., 2022) is resting-state (in the following also "rest" or "REST") functional connectivity (FC) obtained from functional magnetic resonance imaging (fMRI). Some recent studies, however, suggest that behavior prediction may benefit from the use of task-based FC, as compared to resting-state data (Avery et al., 2020; Greene et al., 2018; Jiang et al., 2020; Rosenberg et al., 2016, 2016; Stark et al., 2021). For example, Sripada and colleagues found that the correlation between predicted and observed scores of a general cognitive ability factor improved when using FC from the 2-back WM-task state (r = .50), as compared to using resting-state FC (r = .26; Sripada et al., 2019, 2020). A similar pattern has been reported for the prediction of different measures of attention (Yoo et al., 2018) as well as for the prediction of intelligence based on FC from tasks taxing executive functioning (L. He et al., 2021) or attention (Rosenberg et al., 2016).

Importantly, all the studies mentioned above showed an improvement in prediction performance for task-fMRI data derived from the same domain as the predicted measure (i.e., prediction of stop-signal task performance based on FC derived from stop-signal task-fMRI data). However, there is not only resting versus task states but rather different task states depending on which task is performed during fMRI data acquisition. That is, every task performed in the scanner can be thought of as eliciting a specific state. Interestingly, it has been shown that in predicting intelligence, using almost any other task state (i.e., fMRI acquired during a WM task as well as an emotion task) or task-rest combinations outperforms using resting-state FC only (Gao et al., 2019; Greene et al., 2018, 2020; Sripada et al., 2020).

Based on the concept of convergent and discriminant validity (Campbell & Fiske, 1959; Schumann et al., 2022), it would be expected, however, that connectivity patterns observed during the same or a similar task, hence coming from the same domain as the predicted target behavior (i.e., representing the same state; convergent validity), lead to better prediction performance than do patterns observed during a task state from an unrelated domain (discriminant validity). In line with this idea, recent studies reported better accuracies for predicting general cognitive ability (Sripada et al., 2020) and fluid intelligence (Gao et al., 2019) from FC during task states involving executive functions ("same-domain"), as compared to prediction from unrelated task or resting states ("other-domain"). This improvement was particularly pronounced when FC data of the cognitively demanding WM task was used, as compared to task states from other domains (although the authors did not test for the statistical significance of the observed numerical differences between prediction accuracies). These examples suggest the possibility of state specificity when predicting behavior from corresponding FC patterns.

While most studies predicted task performance from states of the same domain (i.e., prediction of intelligence from FC of a WM task state), others predicted task performance from FC observed during the exact same task. Avery et al. (2020), for example, predicted individual performance accuracy in an n-back WM task based on FC derived from fMRI data obtained while the n-back task was performed, which showed an increase in accuracy when using this task's fMRI data, as compared to rest data (Avery et al., 2020). Building on this, Stark and colleagues investigated the difference in prediction accuracy between predictions of performance in different working and episodic memory tasks from FC obtained while performing an n-back WM task. Importantly, the highest prediction accuracy (r = .36) was achieved when n-back task performance was predicted using FC during the very same task (i.e., n-back performance measured in the MR scanner), followed by the prediction of performance in a different WM task (list sorting; r = .24), followed by predictions

of episodic memory performance scores (r = .05-.11) (Stark et al., 2021). These results suggest a specificity benefit of the state used for calculating FC, which goes beyond the prediction of ability in a given broadly defined cognitive domain (i.e., WM) and narrows it down to specific tasks (i.e., n-back versus list sorting). That is, beyond the effect of state specificity (i.e., domain congruence benefits for prediction accuracy), a state-target similarity effect (i.e., task congruence benefits for prediction accuracy) should manifest in even better prediction accuracies for the performance in tasks during which FC data were acquired, as compared to the performance in other tasks of the same domain.

The literature to date is inconclusive regarding the effects of state specificity and state–target similarity on FC-based predictions of mental abilities and psychological traits. In particular, the majority of studies investigating such prediction models have focused on cognitive targets such as intelligence or attention (Yeung et al., 2022). Thus, clear evidence for state specificity and state–target similarity is still lacking, especially in domains like emotion processing and social cognition.

The studies above mainly used whole-brain FC for behavior prediction. Sometimes, post hoc examination of the most predictive features from the whole-brain feature space are used for better interpretability (e.g., Chén et al., 2019; Dubois, Galdi, Paul, & Adolphs, 2018; Itahashi et al., 2021; Jiang et al., 2020; Pläschke et al., 2020). However, such post hoc analyses come with their own limitations, as feature weights are context-dependent, their reliability is rather low, and the results can be highly specific to the given dataset (Tian & Zalesky, 2021). Besides predicting behavior from whole-brain FC, several studies reported on predictions using particular functional networks as priors (J. Chen et al., 2021: Heckner et al., 2023; Nostro et al., 2018). That is, prediction models in these investigations exclusively rely on FC between regions that show activation during a given task. It is argued that this aides and constrains the functional interpretability of any observed associations (e.g., most predictive features), since such models are based on brain regions for which the association between brain and mental function has already been established independently.

Therefore, network-based prediction has the advantage of better interpretability of the results due to the a priori knowledge about the mental function a given network subserves (Nostro et al., 2018; Pläschke et al., 2017). Similar to state specificity, FC within networks associated with functions that are more closely related to the target behavior (e.g., predicting WM performance from WM network features) should also be more informative than networks that are associated with very different functions (e.g., predicting WM performance from pain network features). Few studies have investigated this network specificity, with some suggesting some network specificity with regard to personality (Nostro et al., 2018), but others showing a lack of specificity (Heckner et al., 2023; Pläschke et al., 2020).

The current project, therefore, aimed to investigate the influence of brain state (same- vs. other-domain), similarity of target behavior to the features within one domain (same vs. similar task from same domain), and functional network priors (same- vs. other-domain

network) on the predictability of individual behavior. This included the specific question of whether FC from same-domain states and in same-domain networks can predict individual behavior better than FC from other-domain states or networks. Hence, we tested the following three hypotheses: (1) State specificity: behavior should be better predicted based on FC patterns observed in the same domain, hence during the state corresponding to the behavior to be predicted, as compared to FC patterns observed in other (non-corresponding) domains. (2) State-target similarity: task performance should be better predicted based on FC patterns observed during the exact same task, as compared to another similar task from the same domain. (3) Network specificity: behavior should be better predicted based on FC patterns observed in the networks corresponding to the predicted behavior, as compared to FC patterns in other (non-corresponding) networks.

2 | METHODS

To investigate whether there is state specificity, state–target similarity and/or network specificity in brain–behavior prediction, we used the Human Connectome Project (HCP) Young Adult dataset. We divided it into two samples: in the first sample, we defined networks, and in the second sample, we computed FC in predefined networks from the first sample during different task states. Using FC within each network as features, we predicted six different target variables, matching the selected states and networks. We included the following three phenotypic domains: WM, theory of mind/social cognition (SOCIAL), and emotion processing (EMO).

2.1 | Samples

Data were obtained from the Young Adult S1200 release of the publicly available database provided by the HCP (Van Essen et al., 2013), which comprised data from 1206 healthy individuals. We only included participants for whom all the data required for our analyses were available. That is, (a) all four resting-state fMRI scans; (b) fMRI data of the WM, SOCIAL, and EMO tasks; and (c) the performance measures (accuracy and reaction time) of these three tasks performed in the scanner, as well as (d) all the performance measures we aimed to predict for tasks that were performed outside the scanner for each domain. Hence, every subject was required to have both (in-scanner and out-of-scanner) tasks per domain (three domains, six tasks in total). Of the 1206 individuals, 180 participants were excluded due to missing imaging data and 71 due to data quality issues. We further excluded subjects with accuracy below 50% in the six tasks of interest (n = 77). Performance accuracy was measured as the percentage of correct trials. We chose to include only subjects producing more than 50% correct trials, to ensure that only participants were included who were attentive during the task and hence present the given states we aimed to investigate. From the remaining sample of 878 subjects,

10970193, 2024, 8, Downloaded from https://onlinelibrary.wiley.com/doi/10.1002/hbm.26753, Wiley Online Library on [13/03/2025]. See the Terms and Conditions (https://onlinelibrary.wiley.com/terms-and-conditions) on Wiley Online Library for rules of use; OA articles are governed by the applicable Creative Commons Licenses

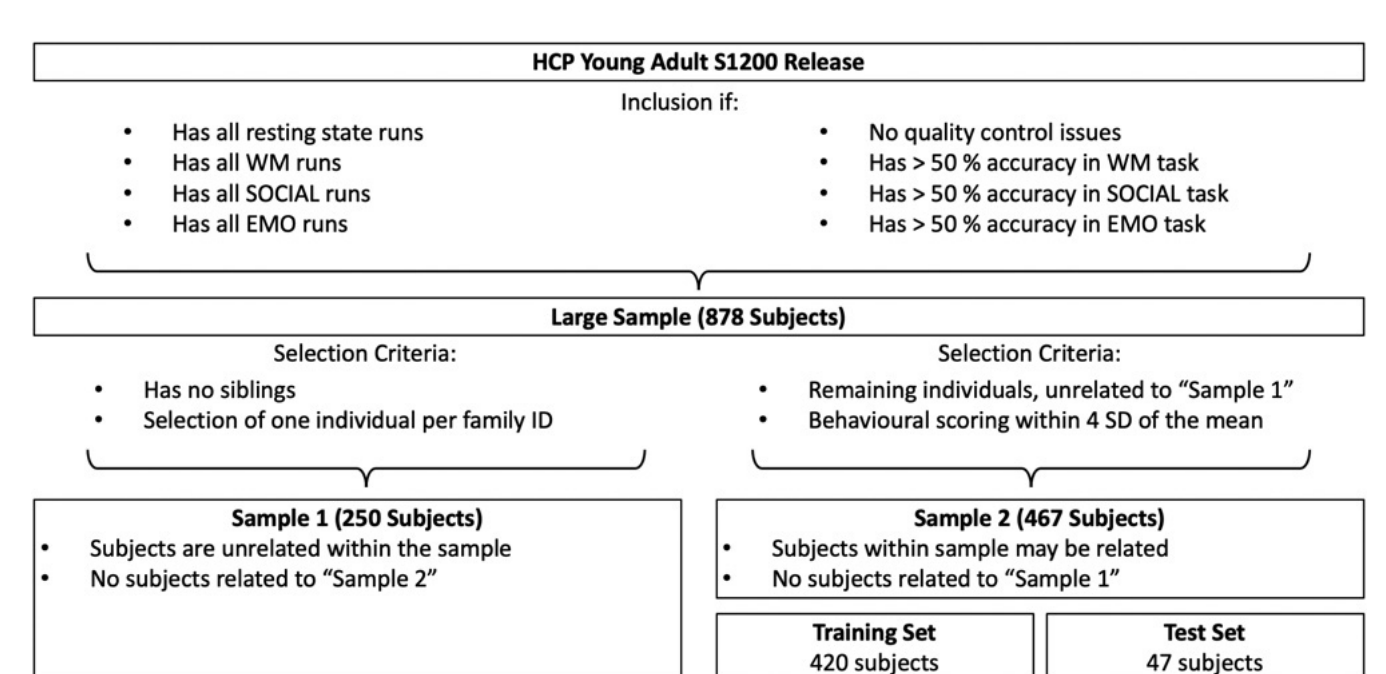


FIGURE 1 Overview of the sampling procedure.

two nonoverlapping subsamples were randomly generated: one for independently delineating task-based networks via general linear modeling (GLM; sample 1) and one for brain-behavior prediction within those (and other) networks (sample 2). Thus, the first sample can be thought of as the sample for "network extraction" and the second sample for "feature extraction and prediction." We carefully accounted for the family structure and resulting dependencies in this dataset by ensuring that (i) sample 1 contained only one individual per family, (ii) there was no kinship between the two samples, and (iii) a leave-n-family-out cross-validation (CV) scheme for prediction analyses within sample 2 was used (Poldrack et al., 2020). For an overview of the sample selection, see Figure 1.

Sample 1, used for delineating task networks, consisted of 250 unrelated subjects (138 females; age mean = 28.6 years, standard deviation [SD] = 3.8, range = 22–36 years). Sample 2, used for prediction, consisted of all the remaining individuals with no siblings in the first sample. Further, we removed individuals that scored higher/lower than 4 SDs from the mean in any of the six target scores of interest, leaving us with 467 participants (252 females, mean age = 28.8 years, SD = 3.7, range = 22–36 years) for sample 2. Note that this sample contains siblings, which was accounted for in the prediction pipeline through family subsampling in the CV (Poldrack et al., 2020). From sample 2 we further randomly selected a holdout sample (47 subjects), which was not used in any of the CVs. Therefore, sample 2 consisted of 420 individuals that were used for CV and final training, while n = 47 participants were held back for subsequently testing generalizability.

The analyses of the HCP data were approved by the ethics committee of the Medical Faculty at the Heinrich Heine University Düsseldorf.

2.2 | Network delineation

Two different approaches were employed for delineating task-specific networks: (i) networks reflecting brain activation in a large sample of participants during the tasks of interest using the task fMRI data of sample 1, and (ii) activation likelihood estimation (ALE) meta-analyses across previously published neuroimaging results of the same tasks. For brevity, we here only report the methods and results of the first approach to network delineation. Further details on the results of the second, meta-analytic, approach can be found in the supplementary material.

2.2.1 | Delineation of task-networks in sample 1

Ultimately, our network extraction approach aimed to delineate networks that were as closely as possible related to the states we aimed to predict in the second sample. For this, we included strictly only the task of interest for network delineation in both approaches—the single study and the meta-analyses. To cover a variety of domains, we chose three very different tasks performed in the scanner: n-back for the WM domain, emotion recognition/face processing for the EMO domain, and social cognition/theory of mind for the SOCIAL domain. For details on the tasks, see Barch et al. (2013). Briefly, an n-back task was used for WM, presenting a sequence of different stimuli with the instruction to either decide whether the current stimulus is the same as the one used two trials ago (2-back) or to recognize a specific target (0-back). EMO was a face-matching task in which angry or fearful faces had to be matched (EMO condition), in contrast to matching shapes (neutral condition). In the SOCIAL task, animated moving

shapes were shown in either interacting or random manner and had to be labeled subsequently as interacting or randomly moving.

For the delineation of the task-specific networks revealing nodes that are activated in our task of interest, we used the minimally preprocessed volumetric task fMRI data of participants of sample 1. The preprocessing included artifact removal, motion correction, and registration to the MNI standard volume space. More details regarding the preprocessing pipeline can be found in Glasser et al., 2013. The minimally preprocessed data were input for the GLM, performed using FSL (Version 5.0.9) (Jenkinson et al., 2012; Smith et al., 2004; Woolrich et al., 2009). For the subject-level GLM we modified the scripts provided by the HCP (Barch et al., 2013; https://github.com/Washington-University/HCPpipelines), which are based on the FSL FEAT module (Woolrich et al., 2001, 2004), for use of volumetric data.

The subject-level GLM included for either run (two different phase encoding directions) temporal high-pass filtering (200 s cutoff), spatial smoothing (8 mm FWHM Gaussian kernel), and the GLM fitting. The respective stimuli in each task were modeled as blocked predictors, temporal derivatives of each predictor, 6 movement parameters and their derivatives as regressors of no interest. For each task, linear contrasts between conditions were computed: 2-back > 0-back for WM; interaction > random for SOCIAL; and faces > shapes for EMO, respectively. Data across both phase encoding directions were then combined with a fixed-effects GLM analysis.

For the group-level GLM, we modified an FSL workflow developed by (Esteban et al., 2019), which estimated the group effects using FSL FMRIB's Local Analysis of Mixed Effects by performing a one-sample t test across subjects. Group-level activation maps were thresholded at cluster-level p < .05 (FWE-corrected for multiple comparisons) with a cluster-forming threshold of p < .001. The resulting activation maps can be seen in the Supplemental Figures \$1-\$3. From these clusters, we extracted only the peak coordinates from gray matter with a minimum distance of 15 mm. This resulted in three networks: WM-NW, SOCIAL-NW, and EMO-NW. For an overview of the workflow, please see Figure 2. For comparison with the taskspecific networks, we used FC between the Power nodes (Power et al., 2011) as a functionally defined, spatially distributed, wholebrain representation of the connectome. The Power nodes represent a combination of resting-state FC ROIs and task-based meta-analytic ROIs, yielding 264 nonoverlapping independent ROIs.

2.3 | Prediction in sample 2

2.3.1 | Targets: Behavioral measures

To assess state specificity and state–target similarity, we selected behavioral performance during different tasks: First, we used performance collected in the scanner for our three domains of interest (WM, SOCIAL, EMO \rightarrow "same task"/in-scanner task). Second, we selected scores of tasks/questionnaires that measured behavior not exactly in the same state but still in the same behavioral domains

("similar task"/out-of-scanner task). The two levels of tasks ("same" and "similar") from the same domain enable us to advance insights beyond state specificity, into state-target similarity.

For "same task" scores (in-scanner task), reaction time and accuracy of task performance were used. These two scores were combined by calculating the Inverse Efficiency Score (IES; Townsend & Ashby, 1983), which is defined as the mean response time across correct trials of the condition of interest divided by its accuracy. This was employed to address the issue of ceiling effects in the accuracy scores. Hence, for WM (subsequently called "n-back"), IES was calculated using mean response time and accuracy of the 2-back blocks. For EMO, we used response time and accuracy in the face-block of the emotional face-matching task (subsequently called "matching" or "EMO matching"). For SOCIAL, since the accuracy in both interaction and random trials involved theory-of-mind cognition (Castelli et al., 2000), we averaged response time and accuracy of both interaction and random trials before creating the IES (subsequently called "Social Cognition").

For "similar task" scores (out-of-scanner task or questionnaire scores) in the WM domain, we selected the unadjusted list sorting score from the NIH Toolbox List Sorting Working Memory Test (subsequently called "List Sorting"). For SOCIAL, we computed a social satisfaction compound score (Babakhanyan et al., 2018) across five different scales (friendship, loneliness, emotional support, instrumental support, and perceived rejection) of the self-report Emotion Battery of the NIH Toolbox (Salsman et al., 2013) (subsequently called "Social Satisfaction" or "Satisfaction"). For EMO, we computed the IES using reaction time and accuracy of the Penn Emotion Recognition Test (Gur et al., 2001, 2010) (subsequently called "Emotion Recognition" or "Recognition"). See supplementary Table S1 for an overview of all targets included.

2.3.2 | Features: FC

Resting-state fMRI and the three sets of task fMRI data (WM, SOCIAL, EMO) from sample 2 were used for calculating FC within each network of interest (WM, SOCIAL, EMO, and Power). The network extraction is explained in detail in the section "Delineation of task-networks in Sample 1"; for an illustration of the methods applied, please see Figure 2. For all four states we used all runs available (four runs for REST and two runs each for the tasks) and their full duration per run. MRI protocols of HCP were previously described in detail (Glasser et al., 2013; Van Essen et al., 2013). For the task-fMRI data, we used the minimally preprocessed version provided by the HCP, which includes removal of spatial distortions, volume realignment, registration to the anatomical image, bias field reduction, normalization to the global mean, and masking the data with the final brain mask (Glasser et al., 2013). The approach to treat task fMRI comparable to resting state fMRI data has been suggested by (Greene et al., 2020). For the resting-state fMRI data, we used the ICA-FIX denoised data provided by the HCP, which uses the minimally preprocessed fMRI data (processed in the same way as task fMRI data) as input and

FIGURE 2 Overview of the applied methods. Yellow blocks depict the network extraction from sample 1. Violet blocks depict the network-based prediction in sample 2, together with the feature extraction (functional connectivities) from the networks delineated in the first step and sample. The upper heatmap under "FC-Features" shows the FC from the different states in the WM-network. GLM: General linear modeling, PE: Phase encoding; FC: Functional connectivity; Soc. Cog., Social cognition task (in-scanner task); Soc. Satisf., Social Satisfaction Questionnaire (out-of-scanner score); Emo. Match., Emotional Face-Matching task (in-scanner task); Emo. Recog., Emotional Face Recognition task (out-of-scanner score).

denoises it through classification of ICA components. This classifier identifies "good" and "bad" components and automatically removes artifactual or "bad" components. For further details, see Griffanti et al. (2014), Salimi-Khorshidi et al. (2014), and Smith et al. (2013).

Additional processing as well as the FC analysis for both restingstate and task-fMRI data were performed using SPM12 (www.fil.ion. ucl.ac.uk/spm/software/spm12/) and MATLAB 2020a (The Math-Works, Natick, MA). Nuisance regression was done to control for mean white matter and cerebrospinal-fluid signals, mean global signal, within-scanner motion using the 6 movement parameters and their derivatives stored in the Movement_Regressors_dt.txt file provided by the HCP. Further, we applied band-pass filtering [0.01–0.1 Hz] and detrended the time series. We opted for the band-pass filter, as this has been shown to be successful in filtering out movement and physiological artifacts, without leading to information loss (Ciric et al., 2017; Satterthwaite et al., 2013). Using the network coordinates obtained from sample 1 (depicted in Figure 2 and in the supplemental material in Figures S7–S13 and Tables S2–S7), for each network, we

PLS models trained on FC matrices as features for each target task

and Conditions (https://onlinelibrary.wiley.com/term:

and-conditions) on Wiley Online Library for rules of use; OA articles are governed by the applicable Creative Commons License

1.0970193, 2024, 8, Downloaded from https://onlinelibrary.wiley.com/doi/10.1002/hbm.26753, Wiley Online Library on [13/03/2025]. See the Terms

modeled a 5-mm sphere around each node's coordinate. The sphere size was the same for all coordinates to ensure the same number of voxels within each node. However, as we extracted multiple peak coordinates from larger clusters of task-activation in sample 1, larger activated regions are represented by multiple spheres. From each sphere, we extracted the mean time series. We then calculated the Pearson's correlations between all pairs of nodes of each respective network, before applying Fisher's Z-transformation. These steps were done for each run separately (four runs for REST and two runs each for the tasks) and for each state (REST, WM, SOCIAL, and EMO). The z-scored FC values were finally averaged across all runs of each state. This was done for all four networks as well as for each of the four states. Connectivity matrices for the WM network can be seen in Figure 2, all other networks averaged across all subjects can be found in the supplemental material (Figures S14–S20).

To ensure that any effects were not due to the different lengths of the tasks performed in the scanner, we trimmed all time series to the length of the shortest scan duration (EMO: 2:16 min) for a control analysis. These results are reported in the supplemental material (Figure S22).

2.3.3 | Network-based prediction of individual behavior

We predicted the task performance/characteristics for each domain from resting- and task-state FC (four states: REST, WM, EMO, SOCIAL; to investigate state specificity) and task of interest (same and similar tasks in WM, EMO, SOCIAL; to further investigate state-target similarity) of the delineated networks (four networks: whole-brain Power nodes and three task networks [WM, SOCIAL, EMO from sample 1; to investigate network specificity]).

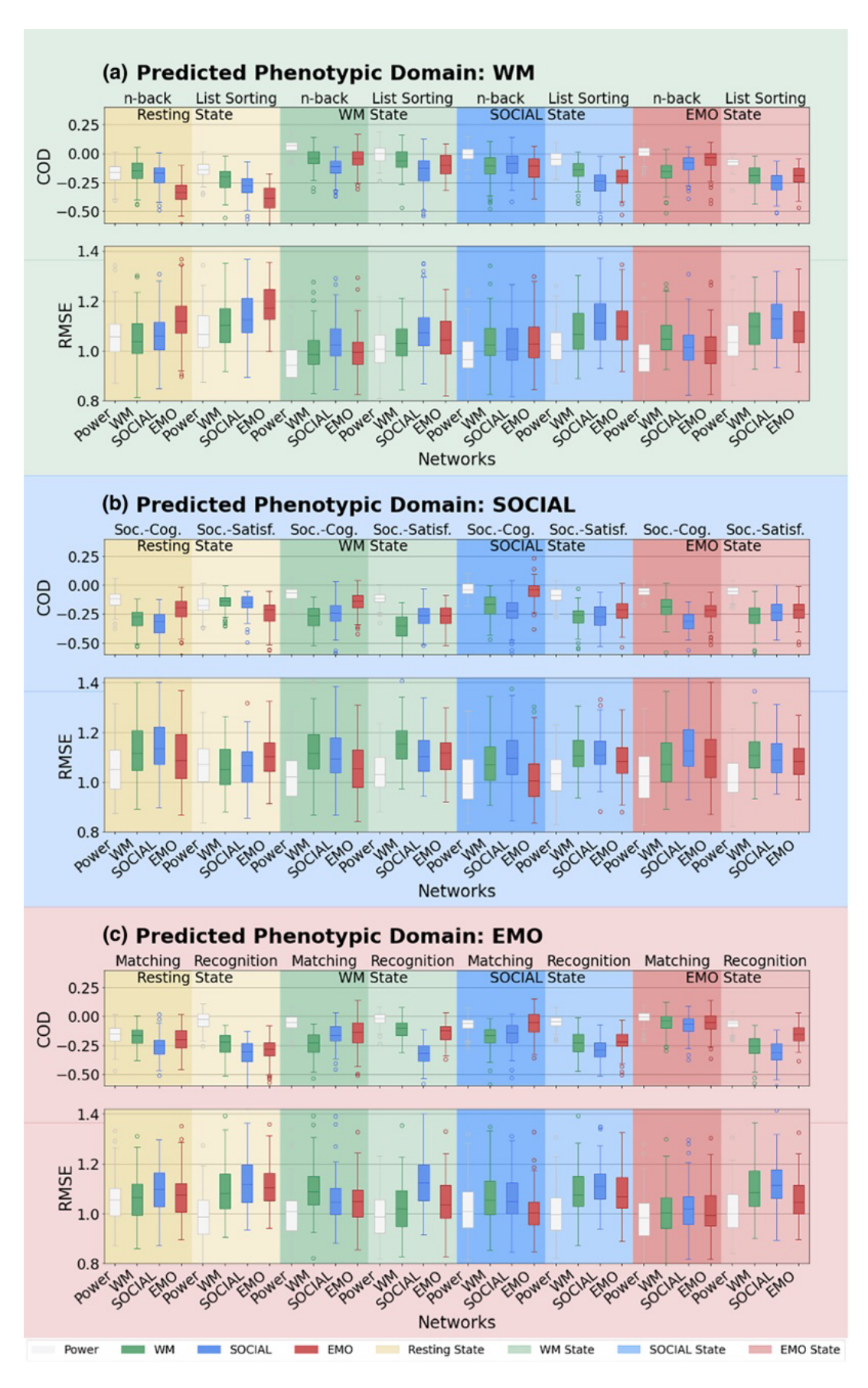
For the main analysis, we used partial least squares (PLS) as the prediction model. PLS is a form of supervised learning which uses linear regression fitting, but it can handle violation of the assumption of no multicollinearity by reducing the dimensionality of correlated variables. However, to confirm our results and to cover models that have been used in the past for behavioral prediction, we additionally performed analyses using other algorithms: Kernel ridge regression, which, like PLS, is a linear parametric model. As well as support vector regression (with both linear and nonlinear RBF kernel) and random forest as nonparametric models, where both can capture nonlinear relationships. Finally, we used PLS and kernel ridge also with connectivity-based prediction modeling (CBPM; Finn et al., 2015; Shen et al., 2017) as a popular feature reduction. CBPM correlates the features to the target variable, retaining only the features showing a significant relation to the target for the model to learn. Note that all models were trained using the same set of FC features and target variables. All results from the additional analyses are presented in the supplemental material (Figures \$21-\$28).

Separate prediction analyses were conducted for each combination of network, state, and behavioral score, resulting in a total of 4 states \times 4 networks \times 6 targets = 96 predictions. The FC pattern

of the respective network and state constituted the given feature space, and the respective behavioral scores were the targets. All algorithms were used as implemented in JuLearn (Hamdan et al., 2023), which is a toolbox based on scikit-learn (Pedregosa et al., 2011). It includes hyperparameter tuning, nested-CV, and feature reduction methods making sure that data leakage is avoided. For PLS, we tuned the hyperparameters in an inner fivefold CV, with the number of latent components increasing in steps from 1 to 10. As having a sibling in the training set could lead to a better prediction of the related participant's score in the validation set, we applied a 100× leave-30%-families-out CV scheme on 420 subjects from sample 2 to account for the family structure of the sample (i.e., individuals from the same family were not split into training or validation sample but kept in either one of them). This is done to counter potential nonindependence induced by the family structure in the HCP dataset (Poldrack et al., 2020). We deconfounded the features by regressing out age and sex as well as normalizing them by z-transformation. For comparability of prediction performance between the different behavioral scores, we additionally normalized the targets. To avoid data leakage, confound regression and normalization were done within the CV. That is, the confound regression models and parameters for z-transformation were computed in the CV on the training set only (70% of the families) and then applied to the test set (30% of the families) (Poldrack et al., 2020). Prediction performance was evaluated by the root mean squared error (RMSE) as well as the coefficient of determination (COD), as a measure of goodness of model fit, averaged across all CV runs. Additionally, the mean Pearson correlation across all CV runs between predicted and observed scores was calculated. After hyperparameter tuning and CV, we finally applied the model, that has been trained on all the data provided and with the hyperparameter tuning performed on it, to the randomly drawn holdout sample (47 subjects from sample 2) to evaluate the model's generalizability.

The RMSE was used for testing for significant differences of prediction performance between states, networks and, tasks using machine-learning (ML)-adjusted t tests (Nadeau & Bengio, 1999). These modified t tests are evaluated and adjusted for comparing ML algorithms (Bouckaert & Frank, 2004) to account for violating the independence assumption in a paired Student's t test. This is done by correcting the variance estimate through considering the training and sample size. In our case, due to the leave-30%-families-out CV scheme, the number of data points changed in each fold. Therefore, we used the mean training sample size across the 100 folds for the adjustment.

Within each phenotypic domain, we first tested effects of state and network by averaging prediction performance of the respective other factors (i.e., averaging across networks and task when testing for state effects, and across state and task when testing for network effects). As state–target similarity is an extension of state specificity, we here only averaged across networks for same and similar tasks, respectively. Significant effects (Bonferroni corrected for multiple comparisons) were then further assessed by comparing the respective individual prediction scores between each other.



3 | RESULTS

In a first step (upper/yellow part of Figure 2), we compared the resulting task-networks from both sample 1 and the meta-analyses to ensure they covered and showed overlap with frequently observed regions in previously reported large-scale analyses (WM: Daamen et al., 2015; Fuentes-Claramonte et al., 2019; Kennedy et al., 2017; Rottschy et al., 2012; Snoek et al., 2021; https://identifiers.org/ neurovault.collection:7103; SOCIAL: T. Chen et al., 2023; Hennion et al., 2016; Mossad et al., 2022; Patil et al., 2017; EMO: Chaudhary et al., 2023; Herrmann et al., 2020; Nord et al., 2017; Snoek et al., 2021; https://identifiers.org/neurovault.collection:7103). The resulting WM-NW had 49 nodes, the SOCIAL-NW had 66 nodes, and EMO-NW had 84 nodes. For an overview of the networks, please see Figure 2. Please refer to the supplemental material for a comprehensive depiction of the original activation maps resulting from the group-level (Figures S1-S3) and the activation likelihood maps of meta-analyses (Figures S4-S6). extracted networks (Figures \$7-\$13) and further details on the exact coordinates, including the anatomical labels (supplemental Tables \$2-\$7).

Following this, we examined the FC of sample 2 within the networks derived from sample 1 for each individual state. Averaged across all subjects, the pattern of FC of all networks looks similar between different states. However, we see a tighter network coupling within the WM-NW in the WM state, compared to the other states (i.e., SOCIAL, EMO, and resting state; see Supplemental Figures \$14 and \$15). A tendency of higher FC within the congruent network was also visible in the EMO domain (Supplemental Figures \$18 and \$19). However, the picture was more fuzzy within the SOCIAL domain (Supplemental Figures \$16 and \$17), where no apparent pattern was discernable. This further motivated the next step—the application of ML and its assessment—to investigate whether the algorithms would be able to pick up complex and subtle signal that we were unable to observe within the averaged FC matrices.

The main focus of this study, therefore, lies on the prediction analyses (bottom/violet part of Figure 2). We mainly report on the outcomes of the prediction analyses using PLS. Predictions using different algorithms and approaches showed highly similar patterns and their details can be found in the supplementary material. Furthermore, regarding outcome measures, we here focus on the RMSE from the CV as well as the COD as a measure of goodness of fit. In the supplementary material, additional results of Pearson's r of the predicted and observed score from the CV can be found.

Averaged across all CV-folds per prediction, the COD and RMSE (Figure 3) revealed that the models show a poor fit and prediction accuracies are rather low. Note, that COD values below zero indicate that

prediction of individual scores were worse than predicting the mean of the target. The mean COD showed a positive mean value only for 2 out of 96 predictions, while all others showed a mean COD of zero or a negative value. Other models (e.g., kernel ridge regression or SVR) yielded some more COD values above zero, but no model achieved a mean COD higher than 0.07. Similarly, the RMSE was quite high for all predictions. Because these scores indicated a generally poor fit to the data, we refrained from applying the best model to the holdout sample. The correlations (for details, see the supplementary material) between predicted and observed values ranged from -0.11 to 0.32 with a mean prediction accuracy of 0.08 (SD: 0.09) and only one mean correlation from the 96 predictions reaching a medium effect size.

3.1 | State specificity in network-based prediction

To answer the question if the correspondence between state and target (e.g., WM score predicted using FC during WM state) improves predictions, and whether there even is state specificity (e.g., WM scores predicted significantly better from FC during WM state than from FC during other states: REST, SOCIAL, or EMO), we examined the differences in prediction accuracy between states.

No significant differences were found for the SOCIAL and EMO domain (Figure 4b,c). For the WM domain, the ML-adjusted t test (Bonferroni corrected for multiple comparisons) showed a significant benefit for all task states compared to the resting state (see Figure 4a; see Table 1 for mean RMSE and significant t test statistics). However, non-WM domain states (i.e., SOCIAL and EMO) only showed a significant difference to the WM state at an uncorrected threshold (not shown in Table 1). This difference was also significant when using other algorithms and feature selection approaches (PLS with CBPM, random forest, and SVR with the RBF kernel). At an uncorrected threshold, the difference was also significant for all other models (kernel ridge regression, SVR with linear kernel, and CBPM with ridge regression), as well as when using only the trimmed time-series.

To asses which effect was driving the significant differences, we compared prediction performance between states using *post hoc* ML-adjusted *t* tests, while keeping network and task constant. That is, we only compared predictions between same-domain networks and tasks (e.g., comparing the prediction performance of "same" WM task score based on FC between Power nodes in *resting state* to the prediction performance of "same" WM task score based on FC between Power nodes in *WM state*). Comparing prediction performance between rest and different states for each network and WM score revealed that the difference between REST and WM state was driven by the difference in prediction performance of the n-back task using the Power

FIGURE 4 State and network specificity: State (a–c) and network (d–e) specificity for each phenotypic domain (a and d–prediction of WM scores, b and e–prediction of SOCIAL scores, c and f–prediction of EMO scores). For state specificity, (a–c) RMSE of all networks (POWER, WM, SOCIAL, EMO) and the two tasks of the respective domain in a given state (REST, WM, SOCIAL, EMO) are averaged. For network specificity, all states (REST, WM, SOCIAL, EMO) and the two task of the respective domain are averaged in a given network (Power nodes, WM, SOCIAL, EMO). Green: WM, blue: SOCIAL, red: EMOTION, yellow: resting state. Horizontal bars indicate significance p_{corr} <.05.

nodes and the EMO network (for mean RMSE and significant t test statistics, see Table 1). The EMO network additionally showed a difference between WM and REST state when predicting list sorting. The difference between REST and EMO state was also driven by Power nodes and the EMO network when predicting n-back performance, and by the EMO network when predicting list sorting. The significant difference in REST versus SOCIAL was driven by the Power nodes in predicting n-back performance.

Overall, state had a significant influence on predicting WM scores, with better predictions when using task compared to resting state. This state-specific improvement was, however, not uniformly observed and mainly driven by predictions based on FC within the Power nodes and the EMO network.

3.2 | State-target similarity in network-based prediction

In a next step, we examined differences in predictability between the "same" and "similar" tasks in a given domain. We were interested in whether the behavior would be predicted better in the state where

the predicted behavior was measured ("same task"), and whether the FC-based predictivity could translate to a related task ("similar task"). An example would be the comparison between the predictability of n-back task performance (WM task performed during scanning) and the list sorting task (WM task performed outside of the scanner) based on FC patterns observed during the WM n-back task.

For this comparison of "same task" with "similar task," we found a slight (numerical) benefit in the performance of the "same task." However, a direct statistical comparison of RMSE values using ML-adjusted t tests did not show any significant effects after Bonferroni correction for multiple comparisons (see Figure 5).

3.3 | Network specificity in network-based prediction

Finally, we set out to answer the question if predicting task performance does benefit from being based on FC within a network known to be engaged in performing that same task (e.g., n-back task performance predicted from FC within the WM-network), as compared to other task-related networks (e.g., n-back task performance predicted

TABLE 1 Comparison of prediction accuracies between states.

Domain of predicted performance	State A	RMSE mean (SD)	State B	RMSE mean (SD)	t	p- Value
Significant main effect of state						
WM	REST	1.10 (0.06)	WM	1.02 (0.05)	5.10	<.001
	REST	1.10 (0.06)	SOCIAL	1.05 (0.06)	3.49	.013
	REST	1.10 (0.06)	EMOTION	1.05 (0.06)	3.68	.007
Significant post hoc tests for sp	ecific state—task—network coml	oinations				
WM	REST (n-back, Power nodes)	1.06 (0.09)	WM (n-back, Power nodes)	0.95 (0.09)	4.83	<.001
	REST (n-back, EMO network)	1.13 (0.10)	WM (n-back, EMO network)	1.00 (0.10)	3.51	.016
	REST (List Sorting, EMO network)	1.19 (0.09)	WM (List Sorting, EMO network)	1.05 (0.09)	4.10	.002
	REST (n-back task, Power nodes)	1.06 (0.09)	SOCIAL (n-back task, Power nodes)	0.98 (0.09)	3.21	.043
	REST (n-back task, Power nodes)	1.06 (0.09)	EMOTION (n-back task, Power nodes)	0.97 (0.09)	3.72	.008
	REST (n-back, EMO network)	1.13 (0.10)	EMOTION (n-back, EMO network)	1.00 (0.10)	3.40	.023
	REST (List Sorting, EMO network)	1.19 (0.09)	EMOTION (List Sorting, EMO network)	1.10 (0.09)	3.32	.030

Note: Machine-learning-adjusted t test to assess state specificity using the averaged 100 RMSE values obtained from 100-fold cross-validation within the state listed in column "State A" versus the state listed in column "State B." p-Values are Bonferroni corrected for multiple comparisons. Post hoc t tests between individual predictions of the task in the network (both noted in brackets) and the state listed in column "State A" versus the state listed in column "State B"

State-Target Similarity

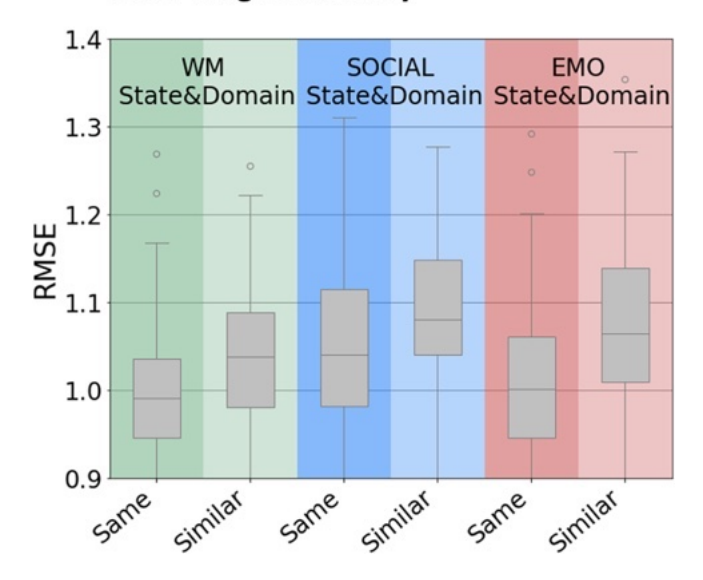


FIGURE 5 State-target similarity: Boxplots of the distribution of RMSE from the $100\times$ CV averaged across all networks (Power nodes, WM, SOCIAL, EMO network) within a given state (WM, SOCIAL, and EMO) and task (SAME or SIMILAR). Green: WM, blue: SOCIAL, red: EMOTION, gray: averaged across networks. Darker background: target is the "same" task performed in the scanner, lighter background: target is the "similar" task performed outside the scanner.

from FC within a SOCIAL task-based network or the whole-brain connectome). ML-adjusted t tests showed, for all three domains, a benefit for the whole-brain Power nodes over the task-specific networks (see Figure 4d–f). In the WM domain, FC between the Power nodes predicted WM-related targets better than did FC within the n-back WM-specific network, the SOCIAL-specific network, or the EMO-specific network (see Figure 4d and Table 2 for mean RMSE and t test statistics). In the SOCIAL domain, the Power nodes predicted SOCIAL-related targets better than did the WM-specific, SOCIAL-specific, or EMO-specific networks (see Figure 4e). Finally, in the EMO domain, the Power nodes again predicted EMO-related targets better than all three domain-specific networks including the EMO-specific network derived from an emotional face-matching task (see Figure 4f).

Post hoc tests (see Table 2) indicated that the difference between the Power and WM networks was driven by the EMO and WM state when predicting social satisfaction, while there was no specific state or task driving the effects for the EMO and WM domain. The priority of Power over the SOCIAL-specific network was in particular evident when predicting social cognition and social satisfaction in the EMO state and when predicting emotion recognition in the REST, SOCIAL, and EMO states. No specific state or task was driving the effect for the WM domain. The effect of Power versus the EMO-specific network was driven by the predictions of list sorting and emotion recognition in the REST state. No specific state or task was driving the effect in the SOCIAL domain.

TABLE 2 Comparison of prediction accuracies between networks.

TABLE 2 Comparison of prediction accuracies between networks.						
Domain of predicted performance	Network A	RMSE mean (SD)	Network B	RMSE mean (SD)	t	p- Value
Significant main effect of ne	twork					
WM	Power nodes	1.02 (0.06)	WM	1.06 (0.06)	-3.30	.025
			SOCIAL	1.08 (0.06)	-4.65	<.001
			EMO	1.08 (0.06)	-6.03	<.001
SOCIAL	Power nodes	1.04 (0.07)	WM	1.11 (0.06)	-6.37	<.001
			SOCIAL	1.11 (0.06)	-5.72	<.001
			EMO	1.08 (0.07)	-4.43	<.001
EMO	Power nodes	1.01 (0.06)	WM	1.07 (0.07)	-5.05	<.001
			SOCIAL	1.09 (0.06)	-7.10	<.001
			EMO	1.05 (0.06)	-3.93	.003
Significant post hoc tests for	specific network—task—state combi	inations				
WM	Power (List Sorting, REST state)	1.07 (0.09)	EMO (List Sorting, REST state)	1.19 (0.09)	-4.41	.002
SOCIAL	Power (Soc. Cog., EMO state)	1.02 (0.11)	SOCIAL (Soc. Cog., EMO state)	1.14 (0.11)	-4.80	<.001
	Power (Soc. Satisf., EMO state)	1.01 (0.08)	WM (Soc. Satisf., EMO state)	1.11 (0.08)	-3.82	.017
	Power (Soc. Satisf., WM state)	1.04 (0.08)	WM (Soc. Satisf., WM state)	1.15 (0.08)	-3.68	.027
EMO	Power (Emo. Recog., REST state)	1.00 (0.09)	SOCIAL (Emo. Recog., REST state)	1.13 (0.10)	-4.05	.008
			EMO (Emo. Recog., REST state)	1.11 (0.09)	-4.39	.002
	Power (Emo. Recog., WM state)	0.99 (0.09)	SOCIAL (Emo. Recog., WM state)	1.13 (0.10)	-5.18	<.001
	Power (Emo. Recog., SOCIAL state)	1.00 (0.09)	SOCIAL (Emo. Recog., SOCIAL state)	1.11 (0.09)	-4.47	.002
	Power (Emo. Recog., EMO state)	1.01 (0.09)	SOCIAL (Emo. Recog., EMO state)	1.12 (0.09)	-4.47	.002

Note: Machine-learning-adjusted *t* tests to assess network specificity using the averaged 100 RMSE values obtained from 100-fold cross-validation within the network listed in column "Network A" versus the network listed in column "Network B." *p*-Values are Bonferroni corrected for multiple comparisons. *Post hoc t* tests between individual predictions of the task in the state (both noted in brackets) and the network listed in column "Network A" versus the state listed in column "Network B."

Abbreviations: Emo. Recog., Emotional Face Recognition task (out-of-scanner score).; Soc. Cog., Social cognition task (in-scanner task); Soc. Satisf., Social Satisfaction Questionnaire (out-of-scanner score).

This superiority of the Power nodes over functional network definitions in all three domains was not present in other ML algorithms. However, we still saw a similar trend when trimming the time series to the shortest task (EMO: 2:16 min), as the Power nodes performed better in all domains and networks, except for the EMO domain where the EMO network did not perform significantly worse.

4 | DISCUSSION

Using state-of-the-art fMRI preprocessing and ML approaches, this study investigated brain-behavior relationships. Specifically, how brain features from specific states and networks, or the task similarity within the behavioral domain, affects this relationship. Based on

previous studies, we hypothesized that brain features obtained from networks and/or states that are corresponding to the target task are more informative about individual behavior than those obtained from other (non-corresponding) states or networks. Additionally, we expected that behavior in the task performed during fMRI data acquisition will be predicted better than similar tasks of the same phenotypic domain. Contrary to expectations, we found no significant differences in predictability (when correcting for multiple comparisons) that would indicate specific benefits of state, task, or network correspondence. Rather, our results show a general benefit of predicting WM scores using (any) task state, relative to rest, and for predicting performance in any domain from whole-brain FC (Power nodes), relative to predefined functional networks. Importantly, however, prediction accuracies were overall quite low, raising the question to what extent the observed differences (or their absence) in prediction

and-conditions) on Wiley Online Library for rules of use; OA articles are governed by the applicable Creative Commons License

WILEY 13 of 19

performance between state and network conditions, and task similarity can be meaningfully interpreted.

4.1 | Is there state specificity for brain-behavior prediction?

We expected not only an improvement in predicting behavior based on FC during task states compared to FC at rest as demonstrated by (Greene et al., 2018), but especially in predicting behavior based on FC within corresponding states. However, apart from the overall low prediction performance, our results, show only weak evidence for the former, that is, an advantage of task states compared to resting state, but only for predicting WM scores (see Figure 4a). Previous studies have already reported that predictions of cognitive scores such as intelligence or attention improve when using task fMRI data (vs. resting state) to derive FC patterns (Avery et al., 2020; Greene et al., 2018; Jiang et al., 2020). But also when combining task and rest (Jiang et al., 2020), and specifically when using FC within a WM task state (Avery et al., 2020; Jiang et al., 2020; Sripada et al., 2020; Stark et al., 2021). Our results extend this work to different states and additionally show that this benefit of using task-fMRI data cannot be assumed for behaviors other than WM. Task-fMRI data may lead to better predictions compared to resting-state data, particularly for WM performance, possibly because task-based fMRI has a more constrained setup which potentially enhances reliability. Resting-state fMRI has been shown to be less reliable than stimulating (such as movies or task) fMRI (Noble et al., 2019). Task-based modulations of brain states may therefore contain more information about individual differences in brain functioning and behavior (Greene et al., 2018). This is consistent with a recent emphasis on shifting from solely focusing on resting-state FC (Finn, 2021; Greene et al., 2018) to accelerate progress in human neuroscience. Possibly, predictive performance can be improved by using naturalistic stimuli (Finn & Bandettini, 2021), as such settings are still more constrained than rest but less constrained than certain laboratory tasks. However, using movie data would not readily allow testing of state specificity effects, and therefore would not be a ready-made solution to the current research question.

4.2 | Is there state-target similarity?

Surprisingly, prediction accuracy was low even when FC was derived from the exact same task state in which the behavioral data were collected, with no improvement when predicting the same score, as compared to a similar score (see Figure 5). Also using the HCP dataset and WM task data, Stark et al. (2021) reported similar though slightly higher accuracies than ours for n-back ("same task") and list-sorting ("similar task") scores, with higher correlations for the former (but not tested for significance). We here extend these insights by also testing effects of task similarity for SOCIAL and EMO scores and by showing that although n-back WM performance seems to be predicted better,

the difference between "same task" and "similar task" score prediction is not significant.

A possible reason for the lack of support of our hypothesis might lie in the nature of the task used in the scanner. That is, a lot of paradigms were developed in experimental contexts (Hedge et al., 2018) and therefore optimized for inducing a robust effect across participants instead of assessing interindividual differences. This might especially be the case for experimental tasks used in the scanner. For example, the emotional face-matching task (Hariri et al., 2002) used for EMO assessment was developed to induce robust amygdala activation, rather than capturing individual emotion processing abilities. Additionally, the tasks used here were rather short and may have lacked enough difficult items for a clearer differentiation between participants. The n-back task, for example, most strongly differentiates between individuals when using high-load conditions (>3-back), both in terms of behavior and brain activity (Lamichhane et al., 2020). Therefore, using behavioral measurements from tasks optimized for obtaining stable group-average effects might have counteracted the successful prediction of interindividual differences.

4.3 | Is there network specificity for brain-behavior predictions?

We based the network specificity hypothesis on the assumption that if networks are reliably engaged during a task, then these networks should play an important role in the task outcome (i.e., specific performance). Importantly, our aim to demonstrate network specificity was based on the idea that a priori task-defined networks improve interpretability (Bzdok et al., 2012; Langner et al., 2018; Müller et al., 2018; Rottschy et al., 2012) as they reflect interactions between regions that are jointly engaged during a specific task and should therefore be biologically meaningful (J. Chen et al., 2021; Nostro et al., 2018; Pläschke et al., 2017). Further, visual inspection of FC within task networks and states averaged across subjects (see supplemental Figures \$14-\$20) revealed the expected stronger FC within the congruent networks and states, respectively. This was most strongly expressed in WM and EMO, whereas in SOCIAL no clear pattern was visible. Yet, this apparently tighter coupling of congruent networks did not provide enough information for the prediction of individual behavior to translate into a significant improvement.

Nonetheless, our results showed that prediction performance was weak regardless of the networks used (see Figure 3—COD). Comparison of the differences between networks showed that prediction from the whole-brain representation (Power et al., 2011) significantly improved prediction compared to the task specific networks (see Figure 4d-f). The reason for an advantage of the whole-brain connectome remains to be revealed. We assume that some subtle pieces of information in the whole-brain connectome, which are not captured by the task networks, reflect individual processing differences in some parts of the tasks at hand and thus contribute to some extent to behavior prediction. Additionally, the whole-brain connectome has considerably more nodes than the task networks studied here, giving

the model much more features to learn from. These nodes can potentially capture interactions and integration of multiple brain regions, including regions, that are not consistently involved in the investigated mental processes and do not translate into group-level average task networks. However, despite the whole-brain Power nodes performing, on average, significantly better than the task networks, they were not consistently superior (see Supplemental Figure \$29 showing the prediction performance sorted by network size).

Nevertheless, our results suggest that there is no network specificity, which is in line with the findings of Heckner et al., 2023 and Pläschke et al., 2017, 2020. Using networks based on group analyses may therefore not be a suitable avenue for assessing individual differences (Finn et al., 2017; O'Connor et al., 2017; Shah et al., 2016). Brain mapping results from group analyses typically reveal regions with low inter-subject variability (Hedge et al., 2018), and groupaveraged patterns of brain activation often look quite different from patterns observed on the individual subject level (Miller et al., 2002). In addition, it has been shown that brain regions, for which activation has been found to be associated with behavioral outcomes, are not necessarily those that show up in standard group-average analyses (Ganis et al., 2005). Our results now indicate that this might also apply to networks derived from large samples that also reflect small average effects (HCP-derived networks) or from large-scale meta-analyses. However, improvement may be gained through an individualization of the networks prior to prediction. For example, Kong and colleagues employed a multi-session hierarchical Bayesian model to estimate individual-specific cortical network parcellations, significantly improving prediction performance relative to other parcellations (Kong et al., 2019). Similarly, using a different approach (Li et al., 2019) demonstrated an improvement in prediction accuracy using an iterative search based on a population-based functional atlas in combination with a map of inter-individual variability (D. Wang et al., 2015).

4.4 Methodological considerations

In this study, we aimed to predict complex behavior based on FC. Generally, our prediction accuracies were rather low. Nevertheless, they are comparable to the accuracies (correlation between predicted and observed score) reported in the literature (Dubois, Galdi, Han, et al., 2018; Greene et al., 2018; Heckner et al., 2023; Kandaleft et al., 2022; Ooi et al., 2022; Tomasi & Volkow, 2020). However, using correlation alone as a measure for prediction accuracy can skew the picture. All measures individually (correlation, COD, RMSE) have been shown to have their drawbacks and therefore it has been suggested that they should be considered together as a whole (Poldrack et al., 2020). Our results emphasize the importance of using more than one measure and especially using more than Pearson's r as a measure for prediction performance, as this metric, when used in isolation, may draw an overly optimistic picture. As illustrated in our plots (see supplementary material), Pearson's r invites the observer to interpret some apparent patterns. Yet, when looking at the model fit given by COD values, it can be easily seen that most models barely fit the data

(see e.g. Figure 3). Surprisingly, only few prediction studies in the neuroimaging literature have reported metrics other than r. However, if they did, results were rather similar to ours, with finding only small amounts of variance explained (COD) and reporting high prediction errors on average (Dubois, Galdi, Han, et al., 2018; Kandaleft et al., 2022; Ooi et al., 2022).

There may be several reasons why we did not successfully predict behavioral performance. One is predicting behavioral scores of single tasks or questionnaires, like WM, as opposed to compound scores across many tests, like overall cognition (Akshoomoff et al., 2013; Dubois, Galdi, Paul, & Adolphs, 2018). Studies using compound scores generally report better accuracies (McCormick et al., 2022; Ooi et al., 2022), as they may capture individual abilities better and show higher reliabilities compared to individual test scores (Hedge et al., 2018). However, the interpretation and biological foundation of compound scores is debatable (Dubois, Galdi, Paul, & Adolphs, 2018; McFarland, 2012; Van Der Maas et al., 2006). In this study, we aimed to investigate specificity, and hence we focused on individual tasks or questionnaires at the cost of a potential decrease in prediction performance.

Another reason for the low prediction performance, related to the first explanation, might be the reliability of the predicted measures but also the features, setting an upper bound for detecting relationships (Cohen et al., 2013; Vul et al., 2009; Yarkoni & Braver, 2010). Using the HCP test-retest sample calculation of the correlations between measurement time points 1 and 2 (test-retest reliability) of the scores we used revealed reliabilities between 0.5 and 0.8, with highest reliabilities for the WM domain. In our and other studies, WM or intelligence scores were generally predicted better than other cognitive measures (Avery et al., 2020; Kandaleft et al., 2022; Ooi et al., 2022; Sripada et al., 2020; Takeuchi et al., 2021), which could be because these constructs are measured more accurately than others.

Finally, for ML applications in CV schemes, sample size is an important factor for achieving good prediction performance. The more data is available, the better a model can learn. In our case, our sample size decreased due to our carving out a subsample for a priori network delineation, leaving us with 420 subjects in the training set. This step was essential to assess network specificity using networks as close as possible to the investigated tasks. Other studies using the HCP dataset and similar algorithms have in part achieved slightly better predictions, possibly through larger training sets (Jiang et al., 2020; Ooi et al., 2022). The effects we sought to detect are presumably very small; hence, a substantially larger dataset and/or more reliable behavioral assessments could be required to detect them (Marek et al., 2022).

4.5 Limitations and outlook

We are aware that there is a plethora of preprocessing pipelines and feature selection models that may improve prediction. We used a well-established preprocessing pipeline (Glasser et al., 2016) and widely used ML models that previously yielded the highest predictions (Greene et al., 2018; Jiang et al., 2020; Yeung et al., 2022). Given that we saw a similar pattern of prediction accuracies irrespective of the model used, we would not expect a substantial change of the result pattern if other models were used.

Further, we aimed to cover a broad range of task network representations by (i) extracting networks from a high-powered single study using task fMRI data, (ii) using ALE meta-analyses based on previously published neuroimaging results (see supplemental material), as well as (iii) including a whole-brain representation (Power et al., 2011) for comparison with the task networks. We acknowledge that different whole-brain representations, such as the parcellation by Schaefer et al. (2018) could yield different and possibly even better prediction accuracies. Also, the inclusion of data-driven approaches to network definition, like principle component analysis or group independent component analysis, could lead to different results. Testing the influence of such methodological choices is an important research topic and should be addressed more systematically in future studies. Until then, our results should only be generalized to settings that employ the same or similar methods as were used here. We here, hence, limited our analyses to one whole-brain representation, as our focus was on task networks and their interpretability. This also entails using the task-specific networks in their most accurate representation, encompassing their unique spatial distributions as well as their different sizes. We believe that both aspects constitute fundamental inherent characteristics of networks.

Finally, the HCP dataset comprises young and healthy adults, with an above-population average intelligence. As the majority of subjects in the HCP dataset were highly educated, performed generally well on the tests, and as tests are optimized for group effects, the between-subject variability in this dataset is relatively limited, that is, suboptimal for approaches relying on individual differences. Nevertheless, the HCP currently offers the only dataset that allows for the investigation of such complex research questions as state specificity, state-target similarity, and network specificity in brain-based prediction settings, because it covers a vast array of phenotypic domains, both in and outside the scanner, while providing high-quality fMRI data in task and resting states in a large number of participants.

4.6 | Conclusions

Here, using state-of-the-art ML algorithms for out-of-sample prediction analyses, we aimed to investigate the specific influence of the factors state, task, and network on behavior prediction from FC patterns. Based on previous research on brain-behavior relationships, we hypothesized that FC features from corresponding state, tasks, and networks would be more informative than non-corresponding features and hence improve prediction. We only found improvement for using task over resting state fMRI, as well as better predictions for whole brain compared to task specific networks. However, across three behavioral domains, predictive performance was generally poor,

and there were no significant patterns indicating specificity of state, networks, or task similarity, when looking at RMSE and COD. A significant improvement of prediction performance based on task-fMRI (vs. resting-state fMRI) was only observed for the WM domain. Of note, an isolated consideration of Pearson's correlation coefficient as the sole index of model fit would have led us to different and apparently overly optimistic conclusions. Hence, even with maximum state–network–behavior compatibility, the relationship between FC and behavior remains low. This study therefore emphasizes the need for a critical assessment of prediction accuracies and suggests that individual behavior cannot be successfully predicted based solely on

AUTHOR CONTRIBUTIONS

FC in task-specific networks.

Nevena Kraljević: Conceptualization, methodology, software, formal analysis, writing—original draft, writing—review and editing, visualization. Robert Langner: Conceptualization, methodology, supervision, writing—review and editing. Vincent Küppers, Writing—review and editing: methodology. Federico Raimondo: Methodology, software, writing—review and editing. Kaustubh R. Patil: Methodology, software, writing—review and editing. Simon B. Eickhoff: Funding acquisition, resources, supervision, writing—review and editing. Veronika I. Müller: Conceptualization, methodology, supervision, writing—review and editing.

ACKNOWLEDGMENTS

The authors would like to sincerely thank all participants and contributors to the data provided by the Human Connectome Project, WU-Minn Consortium (Principal Investigators: David Van Essen and Kamil Ugurbil; 1U54MH091657) funded by the 16 NIH Institutes and Centers that support the NIH Blueprint for Neuroscience Research; and by the McDonnell Center for Systems Neuroscience at Washington University. The work was supported by: Helmholtz Portfolio Theme "Supercomputing and Modeling for the Human Brain"; European Union's Horizon 2020 Research and Innovation Programme under grant agreement No. 945539 (HBP SGA3). Open Access funding enabled and organized by Projekt DEAL.

CONFLICT OF INTEREST STATEMENT

The authors declare no competing interest.

DATA AVAILABILITY STATEMENT

The data used in this study were obtained from the Human Connectome Project (HCP) database, which is publicly accessible at https://www.humanconnectome.org/. However, some parameters needed application for restricted access, which all authors handling the data had granted by the HCP. The three meta-analytically defined networks will be openly available via the ANIMA-database (Reid et al., 2016; https://anima.fz-juelich.de/).

ORCID

Nevena Kraljević https://orcid.org/0000-0003-0869-648X



REFERENCES

- Akshoomoff, N., Beaumont, J. L., Bauer, P. J., Dikmen, S. S., Gershon, R. C., Mungas, D., Slotkin, J., Tulsky, D., Weintraub, S., Zelazo, P. D., & Heaton, R. K. (2013). NIH toolbox cognition function battery (CFB): Composite scores of crystallized, fluid, and overall cognition. Monographs of the Society for Research in Child Development, 78(4), 119–132. https://doi.org/10.1111/mono.12038
- Avery, E. W., Yoo, K., Rosenberg, M. D., Greene, A. S., Gao, S., Na, D. L., Scheinost, D., Constable, T. R., & Chun, M. M. (2020). Distributed patterns of functional connectivity predict working memory performance in novel healthy and memory-impaired individuals. *Journal of Cognitive Neuroscience*, 32(2), 241–255. https://doi.org/10.1162/jocn_a_01487
- Babakhanyan, I., McKenna, B. S., Casaletto, K. B., Nowinski, C. J., & Heaton, R. K. (2018). National Institutes of Health toolbox emotion battery for English- and Spanish-speaking adults: Normative data and factor-based summary scores. *Patient Related Outcome Measures*, 9, 115–127, https://doi.org/10.2147/PROM.S151658
- Barch, D. M., Burgess, G. C., Harms, M. P., Petersen, S. E., Schlaggar, B. L.,
 Corbetta, M., Glasser, M. F., Curtiss, S., Dixit, S., Feldt, C., Nolan, D.,
 Bryant, E., Hartley, T., Footer, O., Bjork, J. M., Poldrack, R., Smith, S.,
 Johansen-Berg, H., Snyder, A. Z., ... WU-Minn HCP Consortium.
 (2013). Function in the human connectome: Task-fMRI and individual
 differences in behavior. *NeuroImage*, 80, 169–189. https://doi.org/10.
 1016/j.neuroimage.2013.05.033
- Bouckaert, R. R., & Frank, E. (2004). Evaluating the replicability of significance tests for comparing learning algorithms. In H. Dai, R. Srikant, & C. Zhang (Eds.), Advances in knowledge discovery and data mining (Vol. 3056, pp. 3-12). Springer. https://doi.org/10.1007/978-3-540-24775-3 3
- Bzdok, D., Schilbach, L., Vogeley, K., Schneider, K., Laird, A. R., Langner, R., & Eickhoff, S. B. (2012). Parsing the neural correlates of moral cognition: ALE meta-analysis on morality, theory of mind, and empathy. *Brain Structure and Function*, 217(4), 783–796. https://doi. org/10.1007/s00429-012-0380-y
- Campbell, D. T., & Fiske, D. W. (1959). Convergent and discriminant validation by the multitrait-multimethod matrix. *Psychological Bulletin*, 56(2), 81–105. https://doi.org/10.1037/h0046016
- Castelli, F., Happé, F., Frith, U., & Frith, C. (2000). Movement and mind: A functional imaging study of perception and interpretation of complex intentional movement patterns. *NeuroImage*, 12(3), 314–325. https:// doi.org/10.1006/nimg.2000.0612
- Chaudhary, S., Zhang, S., Zhornitsky, S., Chen, Y., Chao, H. H., & Li, C.-S. R. (2023). Age-related reduction in trait anxiety: Behavioral and neural evidence of automaticity in negative facial emotion processing. *Neuro-Image*, 276, 120207. https://doi.org/10.1016/j.neuroimage.2023. 120207
- Chen, J., Müller, V. I., Dukart, J., Hoffstaedter, F., Baker, J. T., Holmes, A. J., Vatansever, D., Nickl-Jockschat, T., Liu, X., Derntl, B., Kogler, L., Jardri, R., Gruber, O., Aleman, A., Sommer, I. E., Eickhoff, S. B., & Patil, K. R. (2021). Intrinsic connectivity patterns of task-defined brain networks allow individual prediction of cognitive symptom dimension of schizophrenia and are linked to molecular architecture. *Biological Psychiatry*, 89(3), 308–319. https://doi.org/10.1016/j.biopsych.2020.09.024
- Chén, O. Y., Cao, H., Reinen, J. M., Qian, T., Gou, J., Phan, H., De Vos, M., & Cannon, T. D. (2019). Resting-state brain information flow predicts cognitive flexibility in humans. *Scientific Reports*, 9(1), 3879. https://doi.org/10.1038/s41598-019-40345-8
- Chen, T., Gau, S. S.-F., Wu, Y.-Y., & Chou, T.-L. (2023). Neural substrates of theory of mind in adults with autism spectrum disorder: An fMRI study of the social animation task. *Journal of the Formosan Medical Association*, 122(7), 621–628. https://doi.org/10.1016/j.jfma.2022. 10.009
- Ciric, R., Wolf, D. H., Power, J. D., Roalf, D. R., Baum, G. L., Ruparel, K., Shinohara, R. T., Elliott, M. A., Eickhoff, S. B., Davatzikos, C., Gur, R. C.,

- Gur, R. E., Bassett, D. S., & Satterthwaite, T. D. (2017). Benchmarking of participant-level confound regression strategies for the control of motion artifact in studies of functional connectivity. *NeuroImage*, 154, 174–187. https://doi.org/10.1016/j.neuroimage.2017.03.020
- Cohen, J., Cohen, P., West, S. G., & Aiken, L. S. (2013). Applied multiple regression/correlation analysis for the behavioral sciences. Taylor & Francis. Retrieved from https://books.google.de/books?id=fAnSOgbdFXIC
- Cole, J. H., Poudel, R. P. K., Tsagkrasoulis, D., Caan, M. W. A., Steves, C., Spector, T. D., & Montana, G. (2017). Predicting brain age with deep learning from raw imaging data results in a reliable and heritable biomarker. *NeuroImage*, 163, 115–124. https://doi.org/10.1016/j. neuroimage.2017.07.059
- Cui, Z., Su, M., Li, L., Shu, H., & Gong, G. (2018). Individualized prediction of reading comprehension ability using gray matter volume. *Cerebral Cortex*, 28(5), 1656–1672. https://doi.org/10.1093/cercor/bhx061
- Daamen, M., Bäuml, J. G., Scheef, L., Sorg, C., Busch, B., Baumann, N., Bartmann, P., Wolke, D., Wohlschläger, A., & Boecker, H. (2015). Working memory in preterm-born adults: Load-dependent compensatory activity of the posterior default mode network. *Human Brain Mapping*, 36(3), 1121–1137. https://doi.org/10.1002/hbm.22691
- Dubois, J., Galdi, P., Han, Y., Paul, L. K., & Adolphs, R. (2018). Resting-state functional brain connectivity best predicts the personality dimension of openness to experience. *Personality Neuroscience*, 1, e6. https://doi. org/10.1017/pen.2018.8
- Dubois, J., Galdi, P., Paul, L. K., & Adolphs, R. (2018). A distributed brain network predicts general intelligence from resting-state human neuroimaging data. *Philosophical Transactions of the Royal Society B: Biologi*cal Sciences, 373(1756), 20170284. https://doi.org/10.1098/rstb. 2017.0284
- Esteban, O., Ciric, R., Finc, K., Durnez, J., Ghosh, S., & Poldrack, R. A. (2019). Task fMRI analysis using FSL and data preprocessed with fMRI-Prep [computer software]. Zenodo. https://doi.org/10.5281/zenodo. 2635848
- Finn, E. S. (2021). Is it time to put rest to rest? *Trends in Cognitive Sciences*, 25(12), 1021–1032. https://doi.org/10.1016/j.tics.2021.09.005
- Finn, E. S., & Bandettini, P. A. (2021). Movie-watching outperforms rest for functional connectivity-based prediction of behavior. *NeuroImage*, 235, 117963. https://doi.org/10.1016/j.neuroimage.2021.117963
- Finn, E. S., Scheinost, D., Finn, D. M., Shen, X., Papademetris, X., & Constable, R. T. (2017). Can brain state be manipulated to emphasize individual differences in functional connectivity? *NeuroImage*, 160, 140–151. https://doi.org/10.1016/j.neuroimage.2017.03.064
- Finn, E. S., Shen, X., Scheinost, D., Rosenberg, M. D., Huang, J., Chun, M. M., Papademetris, X., & Constable, R. T. (2015). Functional connectome fingerprinting: Identifying individuals using patterns of brain connectivity. *Nature Neuroscience*, 18(11), 1664–1671. https:// doi.org/10.1038/nn.4135
- Franke, K., Luders, E., May, A., Wilke, M., & Gaser, C. (2012). Brain maturation: Predicting individual BrainAGE in children and adolescents using structural MRI. *NeuroImage*, 63(3), 1305–1312. https://doi.org/10.1016/j.neuroimage.2012.08.001
- Fuentes-Claramonte, P., Martín-Subero, M., Salgado-Pineda, P., Alonso-Lana, S., Moreno-Alcázar, A., Argila-Plaza, I., Santo-Angles, A., Albajes-Eizagirre, A., Anguera-Camós, M., Capdevila, A., Sarró, S., McKenna, P. J., Pomarol-Clotet, E., & Salvador, R. (2019). Shared and differential default-mode related patterns of activity in an autobiographical, a self-referential and an attentional task. *PLoS One*, 14(1), e0209376. https://doi.org/10.1371/journal.pone.0209376
- Ganis, G., Thompson, W. L., & Kosslyn, S. M. (2005). Understanding the effects of task-specific practice in the brain: Insights from individual-differences analyses. Cognitive, Affective, & Behavioral Neuroscience, 5(2), 235–245. https://doi.org/10.3758/CABN.5.2.235
- Gao, S., Greene, A. S., Constable, R. T., & Scheinost, D. (2019). Combining multiple connectomes improves predictive modeling of phenotypic

KRALJEVIĆ ET AL. WILEY 17 of 19

- measures. *Neurolmage*, 201, 116038. https://doi.org/10.1016/j.neuroimage.2019.116038
- Glasser, M. F., Smith, S. M., Marcus, D. S., Andersson, J. L. R., Auerbach, E. J., Behrens, T. E. J., Coalson, T. S., Harms, M. P., Jenkinson, M., Moeller, S., Robinson, E. C., Sotiropoulos, S. N., Xu, J., Yacoub, E., Ugurbil, K., & Van Essen, D. C. (2016). The Human Connectome Project's neuroimaging approach. *Nature Neuroscience*, 19(9), 1175–1187. https://doi.org/10.1038/nn.4361
- Glasser, M. F., Sotiropoulos, S. N., Wilson, J. A., Coalson, T. S., Fischl, B., Andersson, J. L., Xu, J., Jbabdi, S., Webster, M., Polimeni, J. R., Van Essen, D. C., & Jenkinson, M. (2013). The minimal preprocessing pipelines for the Human Connectome Project. *NeuroImage*, 80, 105–124. https://doi.org/10.1016/j.neuroimage.2013.04.127
- Greene, A. S., Gao, S., Noble, S., Scheinost, D., & Constable, R. T. (2020). How tasks change whole-brain functional organization to reveal brain-phenotype relationships. *Cell Reports*, 32(8), 108066. https://doi.org/10.1016/j.celrep.2020.108066
- Greene, A. S., Gao, S., Scheinost, D., & Constable, R. T. (2018). Task-induced brain state manipulation improves prediction of individual traits. *Nature Communications*, *9*(1), 1. https://doi.org/10.1038/s41467-018-04920-3
- Griffanti, L., Salimi-Khorshidi, G., Beckmann, C. F., Auerbach, E. J., Douaud, G., Sexton, C. E., Zsoldos, E., Ebmeier, K. P., Filippini, N., Mackay, C. E., Moeller, S., Xu, J., Yacoub, E., Baselli, G., Ugurbil, K., Miller, K. L., & Smith, S. M. (2014). ICA-based artefact removal and accelerated fMRI acquisition for improved resting state network imaging. *NeuroImage*, 95, 232–247. https://doi.org/10.1016/J. NEUROIMAGE.2014.03.034
- Gur, R. C., Ragland, J. D., Moberg, P. J., Turner, T. H., Bilker, W. B., Kohler, C., Siegel, S. J., & Gur, R. E. (2001). Computerized neurocognitive scanning: I. Methodology and validation in healthy people. *Neuropsychopharmacology*, 25(5), 766–776. https://doi.org/10.1016/ S0893-133X(01)00278-0
- Gur, R. C., Richard, J., Hughett, P., Calkins, M. E., Macy, L., Bilker, W. B., Brensinger, C., & Gur, R. E. (2010). A cognitive neuroscience-based computerized battery for efficient measurement of individual differences: Standardization and initial construct validation. *Journal of Neu*roscience Methods, 187(2), 254–262. https://doi.org/10.1016/j. ineumeth.2009.11.017
- Hamdan, S., More, S., Sasse, L., Komeyer, V., Patil, K. R., & Raimondo, F. (2023). Julearn: An easy-to-use library for leakage-free evaluation and inspection of ML models. https://doi.org/10.48550/ARXIV.2310. 12568
- Hariri, A. R., Tessitore, A., Mattay, V. S., Fera, F., & Weinberger, D. R. (2002). The amygdala response to emotional stimuli: A comparison of faces and scenes. *NeuroImage*, 17(1), 317–323. https://doi.org/10.1006/nimg.2002.1179
- He, L., Liu, W., Zhuang, K., Meng, J., & Qiu, J. (2021). Executive function-related functional connectomes predict intellectual abilities. *Intelligence*, 85, 101527. https://doi.org/10.1016/j.intell.2021.101527
- He, N., Rolls, E. T., Zhao, W., & Guo, S. (2020). Predicting human inhibitory control from brain structural MRI. Brain Imaging and Behavior, 14(6), 2148–2158. https://doi.org/10.1007/s11682-019-00166-9
- Heckner, M. K., Cieslik, E. C., Patil, K. R., Gell, M., Eickhoff, S. B., Hoffstädter, F., & Langner, R. (2023). Predicting executive functioning from functional brain connectivity: Network specificity and age effects. Cerebral Cortex, 33, 6495–6507. https://doi.org/10.1093/ cercor/bhac520
- Hedge, C., Powell, G., & Sumner, P. (2018). The reliability paradox: Why robust cognitive tasks do not produce reliable individual differences. Behavior Research Methods, 50(3), 1166–1186. https://doi.org/10.3758/s13428-017-0935-1
- Hennion, S., Delbeuck, X., Koelkebeck, K., Brion, M., Tyvaert, L., Plomhause, L., Derambure, P., Lopes, R., & Szurhaj, W. (2016). A functional magnetic resonance imaging investigation of theory of mind

- impairments in patients with temporal lobe epilepsy. *Neuropsychologia*, 93, 271–279. https://doi.org/10.1016/j.neuropsychologia.2016. 11.007
- Herrmann, L., Vicheva, P., Kasties, V., Danyeli, L. V., Szycik, G. R., Denzel, D., Fan, Y., Meer, J. V. D., Vester, J. C., Eskoetter, H., Schultz, M., & Walter, M. (2020). fMRI revealed reduced amygdala activation after Nx4 in mildly to moderately stressed healthy volunteers in a randomized, placebo-controlled, cross-over trial. *Scientific Reports*, 10(1), 3802. https://doi.org/10.1038/s41598-020-60392-w
- Itahashi, T., Kosibaty, N., Hashimoto, R.-I., & Aoki, Y. Y. (2021). Prediction of life satisfaction from resting-state functional connectome. *Brain and Behavior*, 11(9), e2331. https://doi.org/10.1002/brb3.2331
- Jenkinson, M., Beckmann, C. F., Behrens, T. E. J., Woolrich, M. W., & Smith, S. M. (2012). FSL. Neurolmage, 62(2), 782-790. https://doi.org/ 10.1016/j.neuroimage.2011.09.015
- Jiang, R., Zuo, N., Ford, J. M., Qi, S., Zhi, D., Zhuo, C., Xu, Y., Fu, Z., Bustillo, J., Turner, J. A., Calhoun, V. D., & Sui, J. (2020). Task-induced brain connectivity promotes the detection of individual differences in brain-behavior relationships. *NeuroImage*, 207, 116370. https://doi. org/10.1016/j.neuroimage.2019.116370
- Kandaleft, D., Murayama, K., Roesch, E., & Sakaki, M. (2022). Resting-state functional connectivity does not predict individual differences in the effects of emotion on memory. *Scientific Reports*, 12(1), 14481. https://doi.org/10.1038/s41598-022-18543-8
- Kennedy, K. M., Boylan, M. A., Rieck, J. R., Foster, C. M., & Rodrigue, K. M. (2017). Dynamic range in BOLD modulation: Lifespan aging trajectories and association with performance. *Neurobiology of Aging*, 60, 153–163. https://doi.org/10.1016/j.neurobiologing.2017.08.027
- Kong, R., Li, J., Orban, C., Sabuncu, M. R., Liu, H., Schaefer, A., Sun, N., Zuo, X.-N., Holmes, A. J., Eickhoff, S. B., & Yeo, B. T. T. (2019). Spatial topography of individual-specific cortical networks predicts human cognition, personality, and emotion. *Cerebral Cortex*, 29(6), 2533– 2551. https://doi.org/10.1093/cercor/bhy123
- Lamichhane, B., Westbrook, A., Cole, M. W., & Braver, T. S. (2020). Exploring brain-behavior relationships in the N-back task. *NeuroImage*, 212, 116683. https://doi.org/10.1016/j.neuroimage.2020.116683
- Langner, R., Leiberg, S., Hoffstaedter, F., & Eickhoff, S. B. (2018). Towards a human self-regulation system: Common and distinct neural signatures of emotional and behavioural control. *Neuroscience and Biobehavioral Reviews*, 90(May), 400–410. https://doi.org/10.1016/j. neubiorev.2018.04.022
- Larabi, D. I., Gell, M., Amico, E., Eickhoff, S. B., & Patil, K. R. (2021). Spatially localized fMRI metrics as predictive and highly distinct state-independent fingerprints. bioRxiv [Preprint]. https://doi.org/10.1101/2021.08.03.454862
- Li, M., Wang, D., Ren, J., Langs, G., Stoecklein, S., Brennan, B. P., Lu, J., Chen, H., & Liu, H. (2019). Performing group-level functional image analyses based on homologous functional regions mapped in individuals. PLOS Biology, 17(3), e2007032. https://doi.org/10.1371/journal. pbio.2007032
- Marek, S., Tervo-Clemmens, B., Calabro, F. J., Montez, D. F., Kay, B. P., Hatoum, A. S., Donohue, M. R., Foran, W., Miller, R. L., Hendrickson, T. J., Malone, S. M., Kandala, S., Feczko, E., Miranda-Dominguez, O., Graham, A. M., Earl, E. A., Perrone, A. J., Cordova, M., Doyle, O., ... Dosenbach, N. U. F. (2022). Reproducible brain-wide association studies require thousands of individuals. *Nature*, 603(7902), 654–660. https://doi.org/10.1038/s41586-022-04492-9
- McCormick, E. M., Arnemann, K. L., Ito, T., Hanson, S. J., & Cole, M. W. (2022). Latent functional connectivity underlying multiple brain states. Network Neuroscience, 1–21, 570–590. https://doi.org/10.1162/netn_a_00234
- McFarland, D. J. (2012). A single g factor is not necessary to simulate positive correlations between cognitive tests. *Journal of Clinical and Experimental Neuropsychology*, 34(4), 378–384. https://doi.org/10.1080/13803395.2011.645018



- Miller, M. B., Van Horn, J. D., Wolford, G. L., Handy, T. C., Valsangkar-Smyth, M., Inati, S., Grafton, S., & Gazzaniga, M. S. (2002). Extensive individual differences in brain activations associated with episodic retrieval are reliable over time. *Journal of Cognitive Neuroscience*, 14(8), 1200–1214. https://doi.org/10.1162/089892902760807203
- More, S., Antonopoulos, G., Hoffstaedter, F., Caspers, J., Eickhoff, S. B., & Patil, K. R. (2023). Brain-age prediction: A systematic comparison of machine learning workflows. *NeuroImage*, 270, 119947. https://doi.org/10.1016/j.neuroimage.2023.119947
- Mossad, S. I., Vandewouw, M. M., de Villa, K., Pang, E. W., & Taylor, M. J. (2022). Characterising the spatial and oscillatory unfolding of theory of mind in adults using fMRI and MEG. Frontiers in Human Neuroscience, 16, 921347. https://doi.org/10.3389/fnhum.2022.921347
- Mueller, S., Wang, D., Fox, M. D., Yeo, B. T. T., Sepulcre, J., Sabuncu, M. R., Shafee, R., Lu, J., & Liu, H. (2013). Individual variability in functional connectivity architecture of the human brain. *Neuron*, 77(3), 586–595. https://doi.org/10.1016/J.NEURON.2012.12.028
- Müller, V. I., Cieslik, E. C., Laird, A. R., Fox, P. T., Radua, J., Mataix-Cols, D., Tench, C. R., Yarkoni, T., Nichols, T. E., Turkeltaub, P. E., Wager, T. D., & Eickhoff, S. B. (2018). Ten simple rules for neuroimaging meta-analysis. *Neuroscience & Biobehavioral Reviews*, 84, 151–161. https://doi.org/10.1016/J.NEUBIOREV.2017.11.012
- Nadeau, C., & Bengio, Y. (1999). Inference for the generalization error. Advances in Neural Information Processing Systems, 12, 307–313.
- Noble, S., Scheinost, D., & Constable, R. T. (2019). A decade of test-retest reliability of functional connectivity: A systematic review and metaanalysis. *NeuroImage*, 203, 116157. https://doi.org/10.1016/j. neuroimage.2019.116157
- Nord, C. L., Gray, A., Charpentier, C. J., Robinson, O. J., & Roiser, J. P. (2017). Unreliability of putative fMRI biomarkers during emotional face processing. *NeuroImage*, 156, 119–127. https://doi.org/10.1016/j.neuroimage.2017.05.024
- Nostro, A. D., Müller, V. I., Varikuti, D. P., Pläschke, R. N., Hoffstaedter, F., Langner, R., Patil, K. R., & Eickhoff, S. B. (2018). Predicting personality from network-based resting-state functional connectivity. *Brain Structure and Function*, 223(6), 2699–2719. https://doi.org/10.1007/s00429-018-1651-z
- O'Connor, D., Potler, N. V., Kovacs, M., Xu, T., Ai, L., Pellman, J., Vanderwal, T., Parra, L. C., Cohen, S., Ghosh, S., Escalera, J., Grant-Villegas, N., Osman, Y., Bui, A., Craddock, R. C., & Milham, M. P. (2017). The healthy brain network serial scanning initiative: A resource for evaluating inter-individual differences and their reliabilities across scan conditions and sessions. *GigaScience*, *6*(2), giw011. https://doi.org/10.1093/gigascience/giw011
- Ooi, L. Q. R., Chen, J., Zhang, S., Kong, R., Tam, A., Li, J., Dhamala, E., Zhou, J. H., Holmes, A. J., & Yeo, B. T. T. (2022). Comparison of individualized behavioral predictions across anatomical, diffusion and functional connectivity MRI. *NeuroImage*, 263, 119636. https://doi.org/10.1016/j.neuroimage.2022.119636
- Patil, I., Calò, M., Fornasier, F., Young, L., & Silani, G. (2017). Neuroanatomical correlates of forgiving unintentional harms. *Scientific Reports*, 7(1), 45967. https://doi.org/10.1038/srep45967
- Pedregosa, F., Varoquaux, G., Gramfort, A., Michel, V., Thirion, B., Grisel, O., Blondel, M., Prettenhofer, P., Weiss, R., Dubourg, V., Vanderplas, J., Passos, A., & Cournapeau, D. (2011). Scikit-learn: Machine learning in python. *Journal of Machine Learning Research*, 12, 2825–2830.
- Pläschke, R. N., Cieslik, E. C., Müller, V. I., Hoffstaedter, F., Plachti, A., Varikuti, D. P., Goosses, M., Latz, A., Caspers, S., Jockwitz, C., Moebus, S., Gruber, O., Eickhoff, C. R., Reetz, K., Heller, J., Südmeyer, M., Mathys, C., Caspers, J., Grefkes, C., ... Eickhoff, S. B. (2017). On the integrity of functional brain networks in schizophrenia, Parkinson's disease, and advanced age: Evidence from connectivity-based single-subject classification. Human Brain Mapping, 38(12), 5845–5858. https://doi.org/10.1002/hbm.23763

- Pläschke, R. N., Patil, K. R., Cieslik, E. C., Nostro, A. D., Varikuti, D. P., Plachti, A., Lösche, P., Hoffstaedter, F., Kalenscher, T., Langner, R., & Eickhoff, S. B. (2020). Age differences in predicting working memory performance from network-based functional connectivity. *Cortex*, 132, 441–459. https://doi.org/10.1016/j.cortex.2020.08.012
- Poldrack, R. A., Huckins, G., & Varoquaux, G. (2020). Establishment of best practices for evidence for prediction: A review. *JAMA Psychiatry*, 77(5), 534–540. https://doi.org/10.1001/jamapsychiatry.2019.3671
- Power, J. D., Cohen, A. L., Nelson, S. M., Wig, G. S., Barnes, K. A., Church, J. A., Vogel, A. C., Laumann, T. O., Miezin, F. M., Schlaggar, B. L., & Petersen, S. E. (2011). Functional network organization of the human brain. *Neuron*, 72(4), 665–678. https://doi.org/10. 1016/j.neuron.2011.09.006
- Reid, A. T., Bzdok, D., Genon, S., Langner, R., Müller, V. I., Eickhoff, C. R., Hoffstaedter, F., Cieslik, E.-C., Fox, P. T., Laird, A. R., Amunts, K., Caspers, S., & Eickhoff, S. B. (2016). ANIMA: A data-sharing initiative for neuroimaging meta-analyses. *NeuroImage*, 124, 1245–1253. https://doi.org/10.1016/j.neuroimage.2015.07.060
- Rosenberg, M. D., Scheinost, D., Greene, A. S., Avery, E. W., Kwon, Y. H., Finn, E. S., Ramani, R., Qiu, M., Constable, R. T., & Chun, M. M. (2020). Functional connectivity predicts changes in attention observed across minutes, days, and months. *Proceedings of the National Academy of Sciences*, 117(7), 3797–3807. https://doi.org/10.1073/pnas. 1912226117
- Rosenberg, M. D., Zhang, S., Hsu, W.-T., Scheinost, D., Finn, E. S., Shen, X., Constable, R. T., Li, C.-S. R., & Chun, M. M. (2016). Methylphenidate modulates functional network connectivity to enhance attention. *Journal of Neuroscience*, 36(37), 9547–9557. https://doi.org/10.1523/ JNEUROSCI.1746-16.2016
- Rottschy, C., Langner, R., Dogan, I., Reetz, K., Laird, A. R., Schulz, J. B., Fox, P. T., & Eickhoff, S. B. (2012). Modelling neural correlates of working memory: A coordinate-based meta-analysis. *NeuroImage*, 60(1), 830–846. https://doi.org/10.1016/j.neuroimage.2011.11.050
- Salimi-Khorshidi, G., Douaud, G., Beckmann, C. F., Glasser, M. F., Griffanti, L., & Smith, S. M. (2014). Automatic denoising of functional MRI data: Combining independent component analysis and hierarchical fusion of classifiers. *NeuroImage*, 90, 449–468. https://doi.org/10. 1016/j.neuroimage.2013.11.046
- Salsman, J. M., Butt, Z., Pilkonis, P. A., Cyranowski, J. M., Zill, N., Hendrie, H. C., Kupst, M. J., Kelly, M. A. R., Bode, R. K., Choi, S. W., Lai, J.-S., Griffith, J. W., Stoney, C. M., Brouwers, P., Knox, S. S., & Cella, D. (2013). Emotion assessment using the NIH toolbox. *Neurology*, 80(11 Suppl 3), S76–S86. https://doi.org/10.1212/WNL. 0b013e3182872e11
- Sasse, L., Larabi, D. I., Omidvarnia, A., Jung, K., Hoffstaedter, F., Jocham, G., Eickhoff, S. B., & Patil, K. R. (2023). Intermediately synchronised brain states optimise trade-off between subject specificity and predictive capacity. *Communications Biology*, 6(1), 705. https://doi.org/10.1038/s42003-023-05073-w
- Satterthwaite, T. D., Elliott, M. A., Gerraty, R. T., Ruparel, K., Loughead, J., Calkins, M. E., Eickhoff, S. B., Hakonarson, H., Gur, R. C., Gur, R. E., & Wolf, D. H. (2013). An improved framework for confound regression and filtering for control of motion artifact in the preprocessing of resting-state functional connectivity data. *NeuroImage*, 64, 240–256. https://doi.org/10.1016/j.neuroimage.2012.08.052
- Schaefer, A., Kong, R., Gordon, E. M., Laumann, T. O., Zuo, X.-N., Holmes, A. J., Eickhoff, S. B., & Yeo, B. T. T. (2018). Local-global parcellation of the human cerebral cortex from intrinsic functional connectivity MRI. *Cerebral Cortex*, 28(9), 3095–3114. https://doi.org/10. 1093/cercor/bhx179
- Schumann, F., Steinborn, M. B., Flehmig, H. C., Kürten, J., Langner, R., & Huestegge, L. (2022). On doing multi-act arithmetic: A multitrait-multimethod approach of performance dimensions in integrated multitasking. Frontiers in Psychology, 13, 946626. https://doi.org/10.3389/fpsyg.2022.946626

KRALJEVIĆ ET AL. WILEY 19 of 19

- Shah, L. M., Cramer, J. A., Ferguson, M. A., Birn, R. M., & Anderson, J. S. (2016). Reliability and reproducibility of individual differences in functional connectivity acquired during task and resting state. *Brain and Behavior*, 6(5), e00456. https://doi.org/10.1002/brb3.456
- Shen, X., Finn, E. S., Scheinost, D., Rosenberg, M. D., Chun, M. M., Papademetris, X., & Constable, R. T. (2017). Using connectome-based predictive modeling to predict individual behavior from brain connectivity. *Nature Protocols*, 12(3), 506–518. https://doi.org/10.1038/nprot.2016.178
- Smith, S. M., Beckmann, C. F., Andersson, J., Auerbach, E. J., Bijsterbosch, J., Douaud, G., Duff, E., Feinberg, D. A., Griffanti, L., Harms, M. P., Kelly, M., Laumann, T., Miller, K. L., Moeller, S., Petersen, S., Power, J., Salimi-Khorshidi, G., Snyder, A. Z., Vu, A. T., ... Glasser, M. F. (2013). Resting-state fMRI in the Human Connectome Project. NeuroImage, 80, 144–168. https://doi.org/10.1016/J. NEUROIMAGE.2013.05.039
- Smith, S. M., Jenkinson, M., Woolrich, M. W., Beckmann, C. F., Behrens, T. E. J., Johansen-Berg, H., Bannister, P. R., De Luca, M., Drobnjak, I., Flitney, D. E., Niazy, R. K., Saunders, J., Vickers, J., Zhang, Y., De Stefano, N., Brady, J. M., & Matthews, P. M. (2004). Advances in functional and structural MR image analysis and implementation as FSL. NeuroImage, 23, S208–S219. https://doi.org/10. 1016/j.neuroimage.2004.07.051
- Snoek, L., Van Der Miesen, M. M., Beemsterboer, T., Van Der Leij, A., Eigenhuis, A., & Steven Scholte, H. (2021). The Amsterdam open MRI collection, a set of multimodal MRI datasets for individual difference analyses. *Scientific Data*, 8(1), 85. https://doi.org/10.1038/s41597-021-00870-6
- Sripada, C., Angstadt, M., Rutherford, S., Kessler, D., Kim, Y., Yee, M., & Levina, E. (2019). Basic units of inter-individual variation in resting state connectomes. *Scientific Reports*, 9(1), 1900. https://doi.org/10.1038/s41598-018-38406-5
- Sripada, C., Angstadt, M., Rutherford, S., Taxali, A., & Shedden, K. (2020). Toward a "treadmill test" for cognition: Improved prediction of general cognitive ability from the task activated brain. *Human Brain Mapping*, 41(12), 3186–3197. https://doi.org/10.1002/hbm.25007
- Stark, G. F., Avery, E. W., Rosenberg, M. D., Greene, A. S., Gao, S., Scheinost, D., Todd Constable, R., Chun, M. M., & Yoo, K. (2021). Using functional connectivity models to characterize relationships between working and episodic memory. *Brain and Behavior*, 11(8), e02105. https://doi.org/10.1002/brb3.2105
- Takeuchi, H., Taki, Y., Nouchi, R., Yokoyama, R., Kotozaki, Y., Nakagawa, S., Sekiguchi, A., Iizuka, K., Hanawa, S., Araki, T., Miyauchi, C. M., Sakaki, K., Sassa, Y., Nozawa, T., Ikeda, S., Yokota, S., Magistro, D., & Kawashima, R. (2021). General intelligence is associated with working memory-related functional connectivity change: Evidence from a large-sample study. *Brain Connectivity*, 11(2), 89–102. https://doi.org/10.1089/brain.2020.0769
- Tian, Y., & Zalesky, A. (2021). Machine learning prediction of cognition from functional connectivity: Are feature weights reliable? *Neuro-Image*, 245, 118648. https://doi.org/10.1016/j.neuroimage.2021. 118648
- Tomasi, D., & Volkow, N. D. (2020). Network connectivity predicts language processing in healthy adults. *Human Brain Mapping*, 41(13), 3696–3708. https://doi.org/10.1002/hbm.25042
- Townsend, J. T., & Ashby, F. G. (1983). The stochastic modeling of elementary psychological processes. Cambridge University Press.
- Van Der Maas, H. L. J., Dolan, C. V., Grasman, R. P. P. P., Wicherts, J. M., Huizenga, H. M., & Raijmakers, M. E. J. (2006). A dynamical model of general intelligence: The positive manifold of intelligence by mutualism. *Psychological Review*, 113, 842–861. https://doi.org/10.1037/ 0033-295X.113.4.842

- Van Essen, D. C., Smith, S. M., Barch, D. M., Behrens, T. E. J., Yacoub, E., Ugurbil, K., & WU-Minn HCP Consortium. (2013). The WU-Minn Human Connectome Project: An overview. *NeuroImage*, 80, 62–79. https://doi.org/10.1016/j.neuroimage.2013.05.041
- Vul, E., Harris, C., Winkielman, P., & Pashler, H. (2009). Puzzlingly high correlations in fMRI studies of emotion, personality, and social cognition. Perspectives on Psychological Science, 4(3), 274–290. https://doi.org/10.1111/j.1745-6924.2009.01125.x
- Wang, D., Buckner, R. L., Fox, M. D., Holt, D. J., Holmes, A. J., Stoecklein, S., Langs, G., Pan, R., Qian, T., Li, K., Baker, J. T., Stufflebeam, S. M., Wang, K., Wang, X., Hong, B., & Liu, H. (2015). Parcellating cortical functional networks in individuals. *Nature Neuroscience*, 18(12), 1853–1860. https://doi.org/10.1038/nn.4164
- Wang, X., Baeken, C., Fang, M., Qiu, J., Chen, H., & Wu, G.-R. (2019). Predicting trait-like individual differences in fear of pain in the healthy state using gray matter volume. *Brain Imaging and Behavior*, 13(5), 1468–1473. https://doi.org/10.1007/s11682-018-9960-7
- Woolrich, M. W., Behrens, T. E. J., Beckmann, C. F., Jenkinson, M., & Smith, S. M. (2004). Multilevel linear modelling for FMRI group analysis using Bayesian inference. *NeuroImage*, 21(4), 1732–1747. https://doi.org/10.1016/j.neuroimage.2003.12.023
- Woolrich, M. W., Jbabdi, S., Patenaude, B., Chappell, M., Makni, S., Behrens, T., Beckmann, C., Jenkinson, M., & Smith, S. M. (2009). Bayesian analysis of neuroimaging data in FSL. *NeuroImage*, 45(1), S173–S186. https://doi.org/10.1016/j.neuroimage.2008.10.055
- Woolrich, M. W., Ripley, B. D., Brady, M., & Smith, S. M. (2001). Temporal autocorrelation in univariate linear modeling of FMRI data. *Neuro-Image*, 14(6), 1370–1386. https://doi.org/10.1006/nimg.2001.0931
- Yarkoni, T., & Braver, T. S. (2010). Cognitive neuroscience approaches to individual differences in working memory and executive control: Conceptual and methodological issues. In A. Gruszka, G. Matthews, & B. Szymura (Eds.), Handbook of individual differences in cognition (pp. 87– 107). Springer. https://doi.org/10.1007/978-1-4419-1210-7 6
- Yeung, A. W. K., More, S., Wu, J., & Eickhoff, S. B. (2022). Reporting details of neuroimaging studies on individual traits prediction: A literature survey. NeuroImage, 256, 119275. https://doi.org/10.1016/j.neuroimage. 2022.119275
- Yoo, K., Rosenberg, M. D., Hsu, W.-T., Zhang, S., Li, C.-S. R., Scheinost, D., Constable, R. T., & Chun, M. M. (2018). Connectome-based predictive modeling of attention: Comparing different functional connectivity features and prediction methods across datasets. *NeuroImage*, 167, 11–22. https://doi.org/10.1016/j.neuroimage.2017.11.010
- Zhuang, K., Yang, W., Li, Y., Zhang, J., Chen, Q., Meng, J., Wei, D., Sun, J., He, L., Mao, Y., Wang, X., Vatansever, D., & Qiu, J. (2021). Connectome-based evidence for creative thinking as an emergent property of ordinary cognitive operations. *NeuroImage*, 227, 117632. https://doi.org/10.1016/j.neuroimage.2020.117632

SUPPORTING INFORMATION

Additional supporting information can be found online in the Supporting Information section at the end of this article.

How to cite this article: Kraljević, N., Langner, R., Küppers, V., Raimondo, F., Patil, K. R., Eickhoff, S. B., & Müller, V. I. (2024). Network and state specificity in connectivity-based predictions of individual behavior. *Human Brain Mapping*, 45(8), e26753. https://doi.org/10.1002/hbm.26753

Network and State Specificity in Connectivity-Based Predictions of Individual Behavior

Supplemental Material

Nevena Kraljević^{1, 2}, Robert Langner^{1, 2}, Vincent Küppers^{1, 3}, Federico Raimondo^{1, 2}, Kaustubh R. Patil^{1, 2}, Simon B. Eickhoff^{1, 2}, Veronika I. Müller^{2, 1}

Methods

Overview of references per task:

Table S1: Behavioral Scores used in the prediction

Domain	"Same" / In-scanner	"Similar" / Out-of-scanner
	task	task
Working Memory /	N-back (Barch et al., 2013)	List sorting (NIH Toolbox List
WM		Sorting Working Memory
		Test; (Cognition Measures,
		n.d.)
Theory of mind /	Labelling of interaction	Compound score "Social
SOCIAL	between animated shapes as	Satisfaction" (Babakhanyan et
	random or interaction (Castelli	al., 2018) composed of scores
	et al., 2000; Wheatley et al.,	for:
	2007)	Friendship, loneliness,
		emotional support,
		instrumental support, and
		perceived rejection all from

		NIH Toolbox Emotion battery
		(Emotion Measures, n.d.;
		Salsman et al., 2013).
Emotion Recognition /	Face-matching. Adapted by	Penn Emotion Recognition
EMO	(Hariri et al., 2002)	Test (Gur et al., 2002, 2010)

Network Delineation

Network Delineation via Meta-Analysis

As a second approach, to offer feature spaces that are entirely independent from the target, we performed three activation likelihood estimation (ALE) meta-analyses for each of the selected tasks: WM, SOCIAL, and EMO. WM and EMO were based on previous meta-analyses (WM: Rottschy et al., 2012; EMO: Müller, Höhner, et al., 2018), but were extended by including recent publications (findings up to March 2020) and reduced to those tasks that matched the three tasks used in the HCP (i.e. only 2-back vs. 0 back experiments for WM, matching faces > matching shapes for EMO). For SOCIAL we performed our own literature search and coding procedure, following the guidelines for neuroimaging meta-analyses (Müller, Cieslik, et al., 2018) and including experiments that used a theory of mind task using animated shapes and report results of the interaction > random contrast. For each specific task, a meta-analysis was calculated using the ALE algorithm (details about the method see Müller, Cieslik, et al., 2018 and Kogler et al., 2020. From these resulting ALE maps, illustrating spatial convergence across experiments, we extracted all peak coordinates with a minimum distance of 15 mm using FSL. This resulted in three networks from the meta-analyses: MetaWM, MetaSOCIAL, and MetaEMO. The three meta-analytically defined networks will be openly available via the ANIMA-database (Reid et al., 2016; https://anima.fz-juelich.de/).

Network-based prediction of individual behavior

In addition to PLS, we used Support Vector Regression (SVR), Random Forest, kernel ridge regression algorithms for prediction. Lastly, we performed connectivity-based prediction modelling (CBPM; Finn et al., 2015; Shen et al., 2017) as a popular feature reduction technique with both PLS and kernel ridge as algorithms.

For each algorithm we tuned the hyperparameters in an inner 5x-CV loop. For SVR we ran two different kernels: linear and RBF-kernel. For the linear kernel we tuned the regularization parameter C within [1e-6, 1e-5, 1e-4, 0.0005, 0.001, 0.005], with maximum 2000 iterations. For the RBF-kernel we used the same regularization parameter range, but extended it by [0.01, 0.1, 1, 5, 10]. For the random forest prediction, the number of trees was set to 2000, with mean squared error as the criterion. The number of features was tuned within [0.14, 0.22, 0.33, 0.5, 0.75], with a minimum number of 5 samples required to be at a leaf node. For kernel ridge regression we tuned the lambdas in a range from 0-1000000. In the CBPM feature reduction, feature selection was based on Pearson correlation, retaining features with correlations below the significance threshold of 0.01 and grouping and summing them by positive and negative correlated features. We used the same hyperparameter tuning outlined above with the respective algorithms.

For the significance tests, we used the Nadeau-Bengio machine learning adjusted t-test (Nadeau & Bengio, 1999): $t = \frac{\frac{1}{n} \sum_{j=1}^{n} x_j}{\sqrt{(\frac{1}{n} + \frac{n_{test}}{n_{train}})\hat{\sigma}^2}}$. Within each cognitive domain, we first tested effects of state

and network by averaging prediction performance of the respective other factors (i.e., averaging across networks and task when testing for state effects, and across state and task when testing for network effects). As domain specificity is an extension of state specificity, we here only averaged across networks for same and similar tasks, respectively. Significant effects (corrected for multiple comparisons) were then further assessed by comparing the respective individual prediction scores between each other. In particular, to assess i) state specificity we compared the prediction performance between states, while keeping network and task constant. That is, we only compared predictions between corresponding networks and tasks (e.g. comparing the prediction performance of "same" WM task score based on FC within Power nodes in resting state to the prediction performance of "same" WM task score based on FC within Power nodes in WM state). To assess ii) network specificity we compared the prediction performance between all networks, while keeping state and task constant (e.g. comparison of prediction performance of "same" WM score in resting state WM networks compared to "same" WM score in resting state in EMO networks). To assess iii) domain specificity we compared the prediction performance of "same" and "similar" task scores, while keeping state and network constant (e.g. comparison of prediction performance of "same" WM task score based on Power nodes in WM state to prediction performance of "similar" WM task score based on Power nodes in WM state).

Results

WM SOCIAL EMO

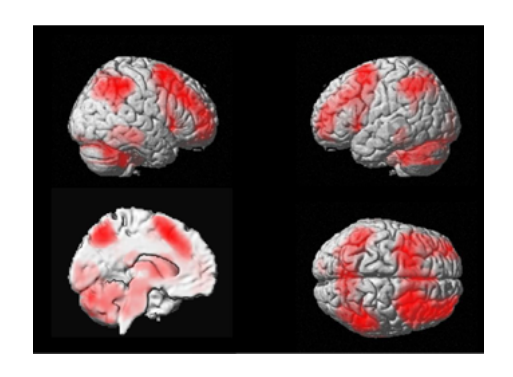


Figure S1. Group-level activation map of WM-task (p < 0.05 (cluster-level FWE-corrected threshold 0.05, cluster-forming threshold p < 0.001)

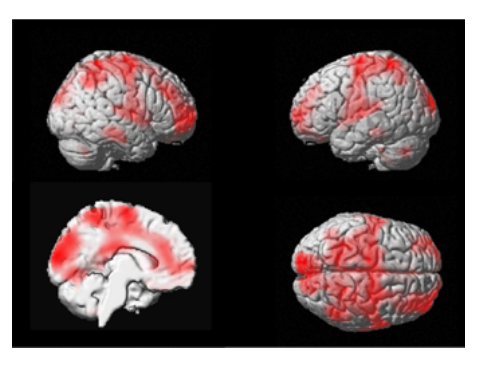


Figure S2. Group-level activation map of SOCIAL-task (cluster-level FWE-corrected threshold 0.05, cluster-forming threshold p < 0.001)

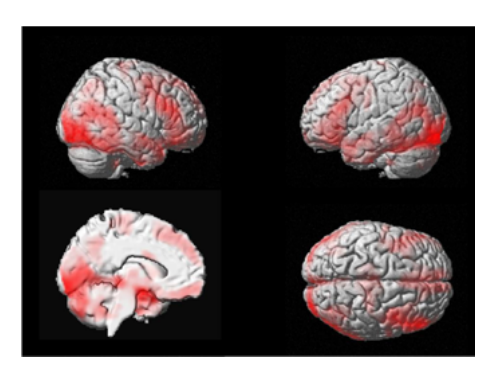


Figure S3. Group-level activation map of EMOtask (cluster-level FWE-corrected threshold 0.05, cluster-forming threshold p < 0.001)

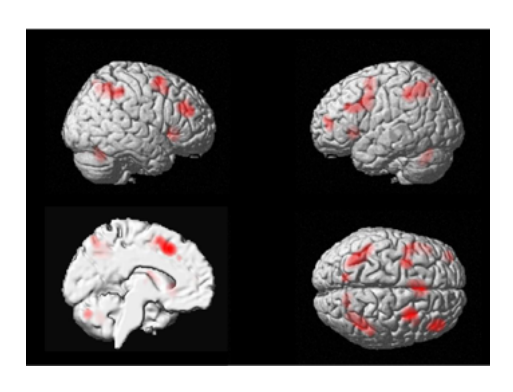


Figure S4. Activation likelihood estimation map of WM meta-analysis (cluster-level FWE-corrected threshold 0.05, cluster-forming threshold p < 0.001).

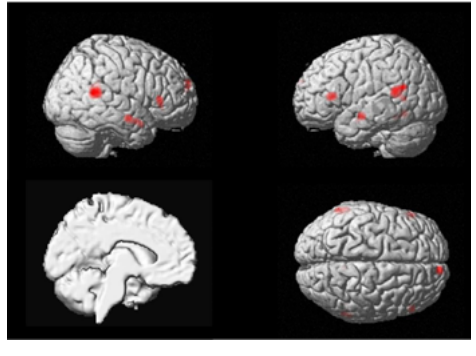


Figure S5. Activation likelihood estimation map of SOCIAL meta-analysis (cluster-level FWE-corrected threshold 0.05, cluster-forming threshold p < 0.001).

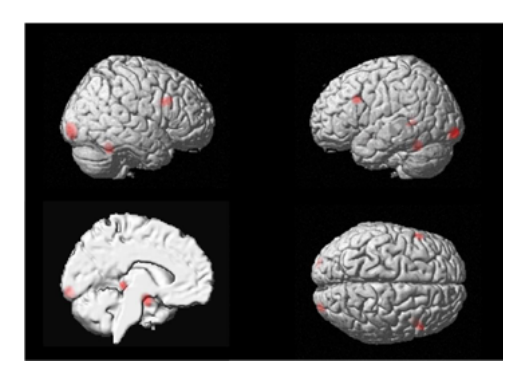


Figure S6. Activation likelihood estimation map of EMO meta-analysis (cluster-level FWE-corrected threshold 0.05, cluster-forming threshold p < 0.001).

Table S2. List of peak coordinates for WM-NW, extracted with a minimum distance of 15 mm (from Fig. S1)

Node	Х	Υ	Z	Brain Structure
1	34	-58	-32	R Cerebellum Crus I
2	46	-46	46	R Intraparietal Suclus
3	-30	-60	-32	L Cerebellum VI
4	-6	18	48	L Paracingulate Gyrus
5	32	6	58	R Middle Frontal Gyrus
6	-28	6	54	L Middle Frontal Gyrus

7	-44	-52	46	L Intraparietal Sulcus
8	40	34	28	R Middle Frontal Gyrus
9	-8	-64	50	L Superior Parietal Lobule
10	8	-68	54	R Precuneous Cortex
11	34	22	4	R anterior Insular Cortex
12	-32	50	16	L Frontal Pole
13	-32	20	0	L anterior Insular Cortex
14	-44	26	34	L Middle Frontal Gyrus
15	38	-60	-48	R Cerebellum Crus II
16	12	-76	-24	R Cerebellum Crus I
17	38	48	18	R Frontal Pole
18	-8	-80	-26	L Cerebellum Crus I
19	-16	8	12	L Caudate
20	18	10	16	R Caudate
21	58	-30	-14	R posterior Middle Temporal Gyrus
22	-8	-58	-54	L Cerebellum IX
23	52	10	16	R Inferior Frontal Gyrus
24	24	46	-14	R Frontal Pole
25	-12	-92	2	L Occipital Pole
26	10	2	6	R Thalamus
27	0	-50	-18	Cerebellum I-IV
28	0	-30	-4	L Thalamus
29	8	-58	-54	R Cerebellum IX
30	48	6	30	R Precentral Gyrus
31	-24	50	-12	L Frontal Pole
32	2	-12	16	R Thalamus
33	0	-62	-36	Cerebellum Vermis VIIIb
34	-56	-36	-14	L Middle Temporal Gyrus
35	2	12	24	Cingulate Gyrus
36	-2	-32	24	R Midcingulate Gyrus
37	-44	-50	20	L Angular Gyrus
38	28	-58	66	R Superior Lateral Occipital Cortex
39	-14	-26	-32	Brain Stem
40	20	-28	14	R Thalamus
41	20	-96	-14	R Occipital Pole
42	34	-90	-18	R Inferior Lateral Occipital Cortex
43	16	28	-22	R Frontal Orbital Cortex
44	24	-20	-6	R Hippocampus
45	-22	-58	0	L Lingual Gyrus

Table S3. List of peak coordinates for WM-Meta, extracted with a minimum distance of 15 mm (from Fig. S4)

Node	Х	Υ	Z	Z Brain Structure	
1	-46	6	36	L Middle Frontal Gyrus	
2	-28	2	54	L Middle Frontal Gyrus	

3	-46	26	28	L Middle Frontal Gyrus
4	-34	-54	48	L Intraparietal Suclus
5	42	-46	44	R Intraparietal Sulcus
6	10	-66	52	R Precuneous Cortex
7	-2	18	48	L Pre-supplementary motor area
8	-2	32	38	L Paracingulate Gyrus
9	30	8	56	R Middle Frontal Gyrus
10	32	24	-2	R anterior insular cortex
11	44	34	26	R Middle Frontal Gyrus
12	-32	-60	-34	L Cerebellum Crus I
13	30	-60	-30	R Cerebellum IV
14	-32	22	0	L anteior insular cortex
15	-38	50	8	L Frontal Pole
16	10	-76	-24	R Cerebellum IV
17	-8	-76	-28	L Cerebellum Crus I
18	-12	-68	60	L Superior Parietal Lobule
19	-16	-2	16	L Caudate

Table S4. List of peak coordinates for SOCIAL -NW, extracted with a minimum distance of 15 mm (from Fig. S2)

Node	Х	Υ	Z	Brain Structure
1	-12	-94	18	L Occipital Pole
2	-22	-52	64	L Superior Parietal Lobule
3	22	-50	68	R Superior Parietal Lobule
4	18	-86	24	R Superior Lateral Occipital Cortex
5	-10	-80	34	L Cuneal Cortex
6	-18	-12	70	L Precentral Gyrus
7	10	-80	-6	R Lingual Gyrus
8	12	-74	38	R Precuneous Cortex
9	16	-10	74	R Superior Frontal Gyrus
10	26	-44	10	R Precuneous Cortex
11	2	-24	30	R Posterior Cingulate Gyrus
12	28	66	2	R Frontal Pole
13	48	-56	46	R Inferior Parietal Lobules
14	40	54	-6	R Lateral Frontal Orbital Cortex
15	-26	68	4	L Frontal Pole
16	0	16	10	Septum
17	40	48	10	R Frontal Pole
18	50	-2	-2	R Planum Polare
19	-20	-26	76	L Precentral Gyrus
20	-2	-10	70	L Supplementary Motor Area
21	2	40	16	R Anterior Cingulate Gyrus
22	-46	-10	60	L Precentral Gyrus
23	-22	-76	4	L Intracalcarine Cortex

	24	42	38	32	R Middle Frontal Gyrus
	25	-12	26	6	L Caudate
	26	-48	-2	-4	L Planum Polare
	27	-8	-76	-4	L Lingual Gyrus
	28	38	14	8	R Frontal Operculum Cortex
	29	4	46	2	R Anterior Cingulate Gyrus
	30	-42	-26	62	L Postcentral Gyrus
	31	48	-8	52	R Precentral Gyrus
	32	20	-26	76	R Precentral Gyrus
	33	-62	2	20	R Precentral Gyrus
	34	-46	-36	16	L Inferior Parietal Lobule
	35	2	4	50	R Supplementary Motor Area
	36	14	26	8	R Caudate
	37	42	-22	62	R Postcentral Gyrus
	38	20	-30	24	R Thalamus
	39	2	-30	50	R Precentral Gyrus
	40	-42	-60	48	L Intraparietal Sulcus
	41	-8	-10	52	L Supplementary Motor Area
	42	-26	46	-12	L Medial Frontal Obital Cortex
	43	66	-20	8	R posterior Superior Temporal Gyrus
	44	-42	12	-8	R Anterior Insular Cortex
	45	14	-16	46	R Precentral Gyrus
	46	-38	-14	24	L Parietal Opercular Cotex
	47	60	-2	38	R Precentral Gyrus
	48	-36	12	10	L Anterior Insular Cortex
	49	-28	44	36	L Frontal Pole
	50	36	-10	20	R Parietal Opercular Cortex
	51	30	22	60	R Middle Frontal Gyrus
	52	-12	18	-16	L Medial Frontal Obital Cortex
	53	40	-66	8	R inferior Lateral Occipital Cortex
	54	12	48	-26	R medial frontal orbital cortex
	55	-14	32	-22	L Frontal Orbital Cortex
	56	2	-70	-20	Cerebellum Vermis VI
	57	44	-36	34	R Intraparietal Sulcus
	58	44	-32	18	R Inferior Parietal Lobule
	59	-32	-52	30	L Intraparietal Sulcus
	60	-46	32	38	L Middle Frontal Gyrus
	61	62	-26	-16	R posterior Middle Temporal Gyrus
	62	-46	-66	-38	L Cerebellum Crus I
	63	-64	-30	-14	L Posterior Middle Temporal Gyrus
	64	-26	-48	-50	L Cerebellum VIIIb
	65	-34	-34	-38	L Cerebellum VI
-	66	48	-62	-38	R Cerebellum Crus I

Table S5. List of peak coordinates for SOCIAL-Meta, extracted with a minimum distance of 15 mm (from Fig. S5)

Node	Х	Υ	Z	Brain Structure
1	58	-48	14	R Inferior Parietal Lobule
2	-58	-46	16	L Supramarginal Gyrus
3	62	-8	-16	R Middle Temporal Gyrus
4	54	6	-22	R Temporal Pole
5	10	62	22	R Frontal Pole
6	-44	-58	-10	L Mid Fusiform Gyrus
7	54	28	6	R Inferior Frontal Gyrus
8	-54	26	10	L Inferior Frontal Gyrus
9	8	-48	50	R Precuneous Cortex
10	8	-54	36	R Precuneous Cortex
11	-60	-8	-14	R Middle Temporal Gyrus

Table S6. List of peak coordinates for EMO-NW, extracted with a minimum distance of 15 mm (from Fig. S3)

No de				Due in Characteria
Node	X	Υ	<u>Z</u>	Brain Structure
1	24	-96	-4	R Occipital Pole
2	42	-48	-20	R Mid Fusiform Gyrus
3	-20	-94	-12	L Occipital Pole
4	38	-72	-14	R Posterior Fusiform Gyrus
5	18	-4	-16	R Amygdala
6	-18	-4	-18	L Amygdala
7	-34	-86	-12	L inferior lateral Occipital Cortex
8	-40	-54	-20	L Mid Fusiform Gyrus
9	44	18	24	R Inferior Frontal Gyrus
10	-4	-82	2	L Intracalcarine Cortex
11	14	-32	-2	R Thalamus
12	-8	-76	-38	L Cerebellum Crus II
13	34	34	-14	R Frontal Pole
14	32	-6	-38	R Parahippocampal Gyrus
15	-40	18	26	L Middle Frontal Gyrus
16	48	-64	18	R Superior Lateral Occipital Cortex
17	-10	-32	-2	L Thalamus
18	-34	-10	-32	L Parahippocampus
19	14	-70	10	R Intracalcarine Cortex
20	50	-42	14	R Posterior Superior Termporal Sulcus
21	-24	-24	-8	L Hippocampus
22	-36	30	-16	L Frontal Orbital Cortex
23	-2	-2	-16	L Hypothalamus
24	20	-38	-44	R Cerebellum X
25	0	-52	-36	Cerebellum Vermis IX

26	22	-52	4	R Lingual Gyrus
27	-20	-36	-44	L Cerebellum X
28	-50	-72	18	L Superior Lateral Occipital Cortex
29	50	-10	-12	R Superior Temporal Gyrus
30	62	-52	12	R Middle Temporal Gyrus
31	60	-42	-4	R Middle Temporal Gyrus
32	10	-78	-38	R Cerebellum Crus II
33	2	52	-14	R Frontal Medial Cortex
34	46	2	54	R Middle Frontal Gyrus
35	-52	-46	12	L Posterior Superior Termporal Sulcus
36	34	-56	44	R Intraparietal Sulcus
37	-44	40	-2	L Frontal Pole
38	-60	-40	-8	L Middle Temporal Gyrus
39	4	-60	40	R Precuneus
40	0	4	28	Midcingulate Cortex
41	36	-74	24	R superior lateral Occipital Cortex
42	4	58	32	R Frontal Pole
43	2	38	50	R medial superior Frontal Gyrus
44	52	28	-6	R Inferior Frontal Gyrus
45	-30	-68	-48	L Cerebellum VIIb
46	-52	-10	-12	L Superior Temporal Gyrus
47	22	-68	24	R Parieto-occipital sulcus
48	6	-12	6	R Thalamus
49	24	-32	-20	R Parahippocampal Gyrus
50	-40	2	54	L Middle Frontal Gyrus
51	28	-24	60	R Precentral Gyrus
52	-50	12	46	L Middle Frontal Gyrus
53	22	0	6	R Putamen
54	34	20	54	R Middle Frontal Gyrus
55	8	-96	26	R Occipital Pole
56	-4	-22	58	L Precentral Gyrus
57	16	-26	72	R Precentral Gyrus
58	2	4	-2	R Basal Forebrain
59	-18	-92	-28	L Cerebellum Crus I
60	8	6	12	R Caudate
61	0	-86	36	Cuneal Cortex
62	-14	-26	72	L Precentral Gyrus
63	6	-40	68	R Postcentral Gyrus
64	-64	-6	28	L Postcentral Gyrus
65	-12	10	4	L Caudate
66	66	-2	28	R Postcentral Gyrus
67	-50	-10	32	L Precentral Gyrus
68	-50	-28	-2	L Posterior Superior Temporal Gyrus
69	-38	18	58	L Middle Frontal Gyrus
70	18	-12	20	R Caudate

71	-38	-18	40	L Postcentral Gyrus
72	12	-10	78	R Superior Frontal Gyrus
73	2	12	70	R Pre-Supplementary Motor Area
74	-12	-40	66	L Postcentral Gyrus
75	30	-22	12	R Posterior Insula
76	-14	-2	16	L Caudate
77	-18	30	60	L Superior Frontal Gyrus
78	-30	-80	26	L Superior Lateral Occipital Cortex
79	-58	-12	48	L Postcentral Gyrus
80	34	-68	-50	R Cerebellum VIIb
81	-60	-10	-36	L Anterior Inferior Temporal Gyrus
82	-50	-68	46	L Superior Lateral Occipital Cortex
83	-32	-60	44	L Intraparietal Sulcus

Table S7. List of peak coordinates for EMO-Meta, extracted with a minimum distance of 15 mm (from Fig. S6)

Node	Х	Υ	Z	Brain Structure
1	20	-4	-18	R Amygdala
2	28	-94	-6	R Occipital Pole
3	-22	-6	-14	L Amygdala
4	-22	-96	-6	L Occipital Pole
5	42	12	28	R Inferior Frontal Gyrus
6	-42	-54	-22	L Mid Fusiform Gyrus
7	40	-50	-26	R Mid Fusiform Gyrus
8	-18	-32	-2	L Thalamus
9	-50	-48	4	L Posterior Superior Termporal Sulcus
10	-54	18	32	L Middle Frontal Gyrus

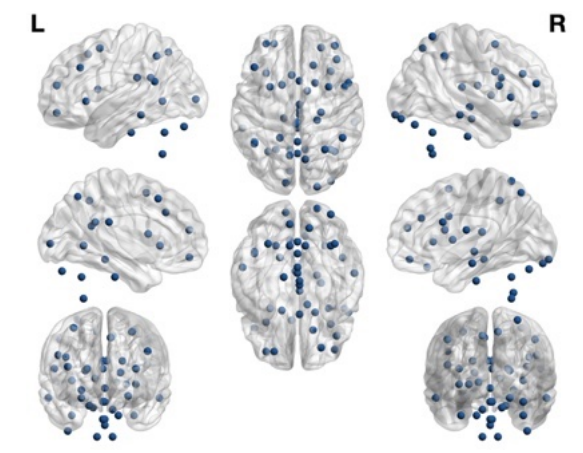


Figure S7. WM Network Nodes.

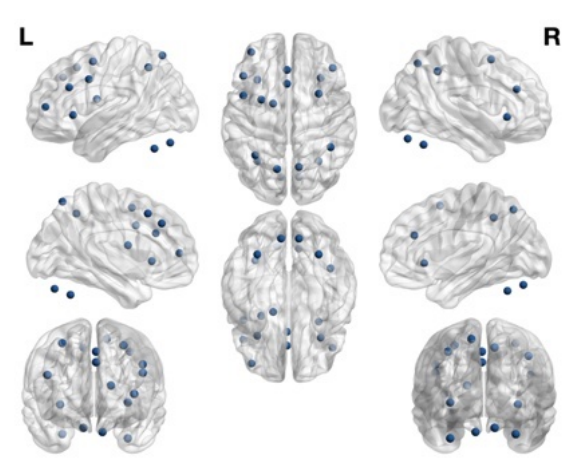


Figure S8. WM Meta-Analysis Network Nodes.

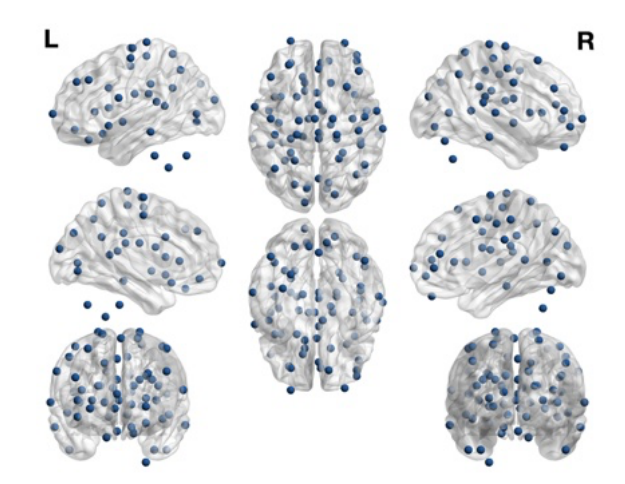


Figure S9. SOCIAL Network Nodes.

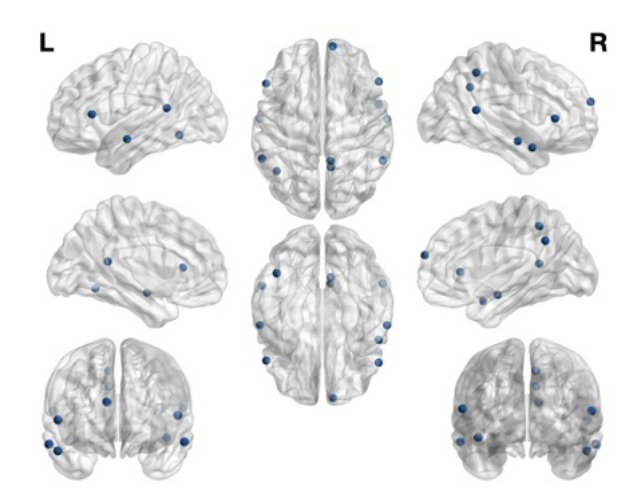


Figure S10. SOCIAL Meta-Analysis Network Nodes

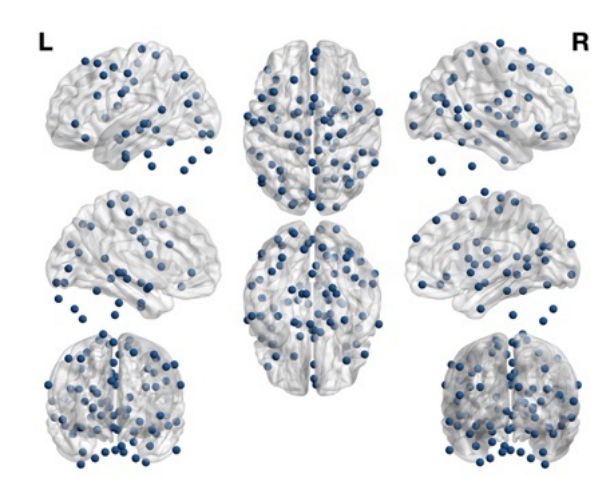


Figure S11. EMO Network Nodes

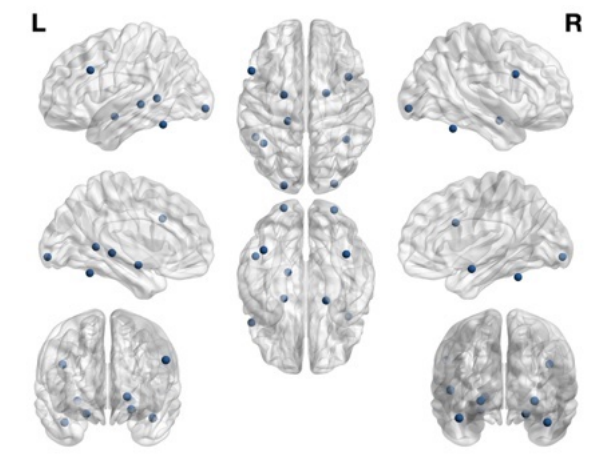


Figure S12. EMO Meta-Analysis Network Nodes

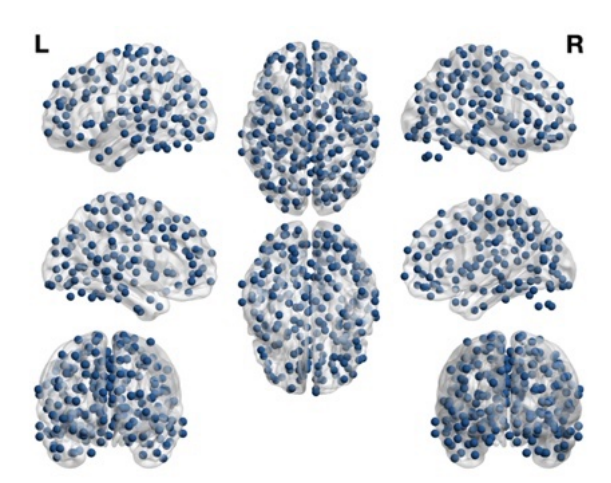


Figure S13. Whole-brain Power nodes.

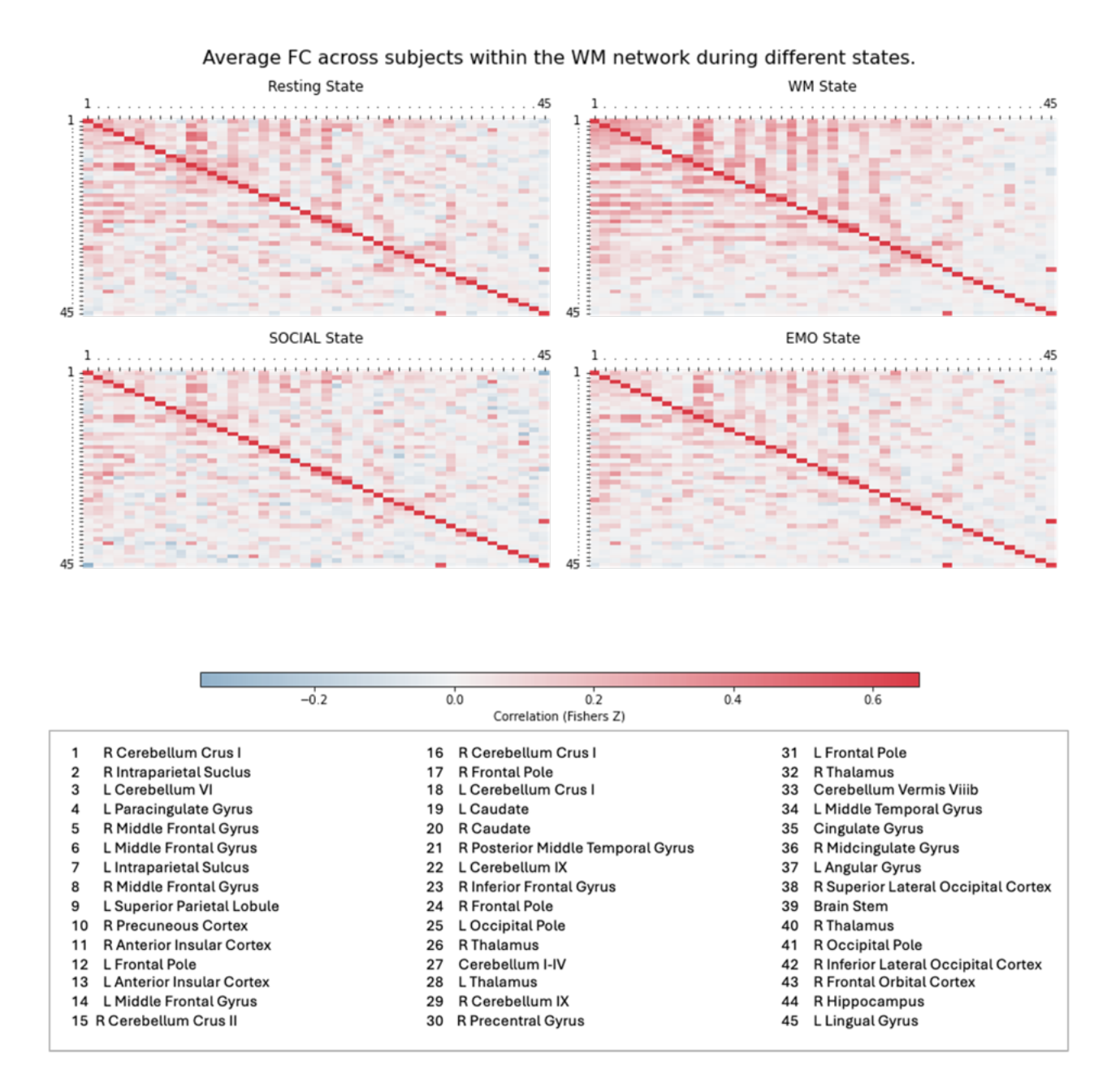


Figure S14) Heatmap of FC within the WM network averaged across participants in the four different states. FC reflects the Fisher Z- transformed Pearson correlation coefficients between all network nodes. Anatomical labels and coordinates of the nodes can be found in table S2-, node numbers are in the same order as in the table.

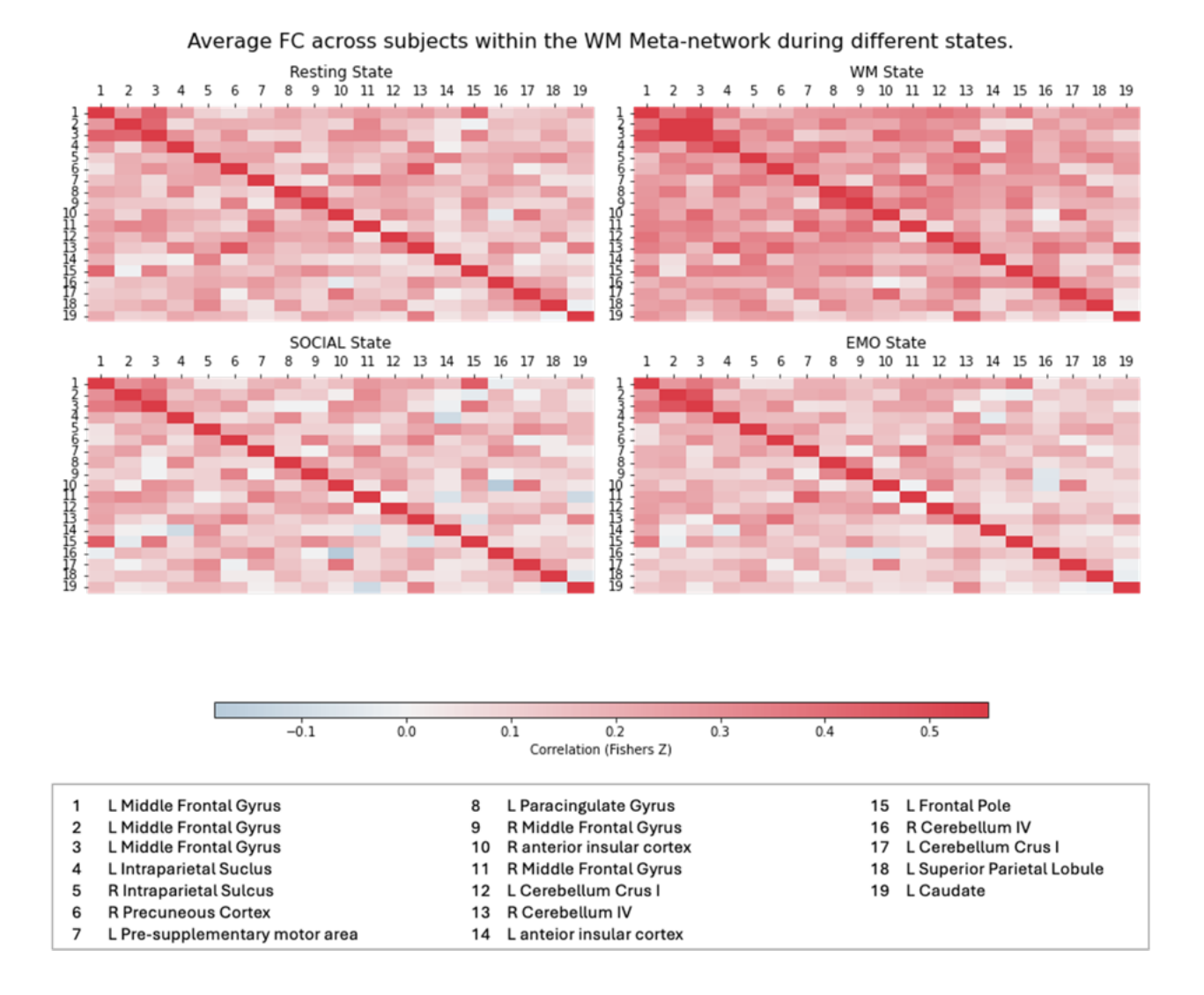


Figure S15) Heatmap of FC within the WM-meta network averaged across participants during the four different states. FC reflects the Fisher Z- transformed Pearson correlation coefficients between all network nodes. Anatomical labels and coordinates of the nodes can be found in table S2-, node number correspond to the node number in the table.

Average FC across subjects within the SOCIAL network during different states. Resting State WM State SOCIAL State **EMO State** Correlation (Fishers Z) L Occipital Pole 23 L Intracalcarine Cortex 45 R Precentral Gyrus L Superior Parietal Lobule R Middle Frontal Gyrus 46 L Parietal Opercular Cotex 24 R Superior Parietal Lobule L Caudate R Precentral Gyrus R Superior Lateral Occipital Cortex 26 L Planum Polare 48 L Anterior Insular Cortex 4 L Frontal Pole 5 L Cuneal Cortex 27 L Lingual Gyrus 49 R Frontal Operculum Cortex R Parietal Opercular Cortex 6 L Precentral Gyrus 28 50 7 R Lingual Gyrus 29 R Anterior Cingulate Gyrus 51 R Middle Frontal Gyrus R Precuneous Cortex L Postcentral Gyrus L Medial Frontal Obital Cortex 31 R Precentral Gyrus R inferior Lateral Occipital Cortex R Superior Frontal Gyrus 10 R Precuneous Cortex R Precentral Gyrus R medial frontal orbital cortex 32 54 L Frontal Orbital Cortex R Posterior Cingulate Gyrus R Precentral Gyrus 33 55 11 Cerebellum Vermis VI R Frontal Pole L Inferior Parietal Lobule 12 34 56 R Inferior Parietal Lobules R Supplementary Motor Area 13 35 57 R Intraparietal Sulcus R Lateral Frontal Orbital Cortex R Caudate R Inferior Parietal Lobule 14 36 58 15 L Frontal Pole 37 R Postcentral Gyrus 59 L Intraparietal Sulcus 16 Septum 38 R Thalamus 60 L Middle Frontal Gyrus R Frontal Pole R Precentral Gyrus R posterior Middle Temporal Gyrus 17 61 R Planum Polare 40 L Intraparietal Sulcus 62 L Cerebellum Crus I 18 L Precentral Gyrus L Posterior Middle Temporal Gyrus 41 L Supplementary Motor Area 63 19

Figure S16) Heatmap of FC within the SOCIAL network averaged across participants during the four different states. FC reflects the Fisher Z- transformed Pearson correlation coefficients between all network nodes. Anatomical labels and coordinates of the nodes can be found in table S3, node number correspond to the node number in the table.

L Medial Frontal Obital Cortex

R Anterior Insular Cortex

R posterior Superior Temporal Gyrus

42

43

L Cerebellum VIIIb

R Cerebellum Crus I

L Cerebellum VI

64

65

L Supplementary Motor Area

R Anterior Cingulate Gyrus

22 L Precentral Gyrus

20

21



Figure S17) Heatmap of FC within the SOCIAL-meta network averaged across participants during the four different states. FC reflects the Fisher Z- transformed Pearson correlation coefficients between all network nodes. Anatomical labels and coordinates of the nodes can be found in table S3, node number correspond to the node number in the table.

Average FC across subjects within the EMO network during different states. Resting State EMO State SOCIAL State -0.2 0.0 Correlation (Fishers Z) R Occipital Pole R Superior Temporal Gyrus R Precentral Gyrus R Mid Fusiform Gyrus 30 R Middle Temporal Gyrus R Basal Forebrain L Occipital Pole R Middle Temporal Gyrus L Cerebellum Crus I R Posterior Fusiform Gyrus 32 R Cerebellum Crus II R Caudate 5 R Amygdala 33 R Frontal Medial Cortex **Cuneal Cortex** 61 L Amygdala R Middle Frontal Gyrus L Precentral Gyrus 6 34 62 L inferior lateral Occipital Cortex 35 L Posterior Superior Termporal Sulcus R Postcentral Gyrus 63 L Mid Fusiform Gyrus 36 R Intraparietal Sulcus 64 L Postcentral Gyrus 9 R Inferior Frontal Gyrus 37 L Frontal Pole 65 L Caudate 10 L Intracalcarine Cortex 38 L Middle Temporal Gyrus R Postcentral Gyrus R Thalamus 39 R Precuneus 67 L Precentral Gyrus L Cerebellum Crus II 40 Midcingulate Cortex L Posterior Superior Temporal Gyrus L Middle Frontal Gyrus R Frontal Pole 41 R superior lateral Occipital Cortex 14 R Parahippocampal Gyrus R Caudate 42 R Frontal Pole L Middle Frontal Gyrus 43 R medial superior Frontal Gyrus 71 L Postcentral Gyrus 15 R Superior Lateral Occipital Cortex R Inferior Frontal Gyrus R Superior Frontal Gyrus 16 44 72 R Pre-Supplementary Motor Area L Thalamus 45 L Cerebellum VIIb 17 73 L Superior Temporal Gyrus L Postcentral Gyrus 18 L Parahippocampus 46 74 19 R Intracalcarine Cortex 47 R Parieto-occipital sulcus 75 R Posterior Insula 20 R Posterior Superior Termporal Sulcus 48 R Thalamus 76 L Caudate R Parahippocampal Gyrus 77 L Superior Frontal Gyrus L Hippocampus 49

Figure S18) Heatmap of FC within the EMO network averaged across participants during the four different states. FC reflects the Fisher Z- transformed Pearson correlation coefficients between all network nodes. Anatomical labels and coordinates of the nodes can be found in table S4, node number correspond to the node number in the table.

L Middle Frontal Gyrus

L Middle Frontal Gyrus

R Middle Frontal Gyrus

R Precentral Gyrus

R Putamen

R Occipital Pole

L Precentral Gyrus

L Superior Lateral Occipital Cortex

L Superior Lateral Occipital Cortex

81 L Anterior Inferior Temporal Gyrus

L Postcentral Gyrus

R Cerebellum VIIb

L Intraparietal Sulcus

82

50

51

52

53

54

55

56

L Frontal Orbital Cortex

Cerebellum Vermis IX

28 L Superior Lateral Occipital Cortex

L Hypothalamus

R Cerebellum X

R Lingual Gyrus

L Cerebellum X

25

26

27



Figure S19) Heatmap of FC within the EMO-meta network averaged across participants during the four different states.. FC reflects the Fisher Z- transformed Pearson correlation coefficients between all network nodes. Anatomical labels and coordinates of the nodes can be found in table S4, node number correspond to the node number in the table.

Average FC across subjects within the Power nodes during different states. Resting State WM State 264 SOCIAL State SOCIAL State 264 SOCIAL State 264

Figure S20) Heatmap of FC within the Power nodes during the four different states averaged across participants. FC reflects the Fisher Z- transformed Pearson correlation coefficients between all network nodes.

0.2 0.4 Correlation (Fishers Z)

0.6

0.8

1.0

-0.4

-0.2

0.0

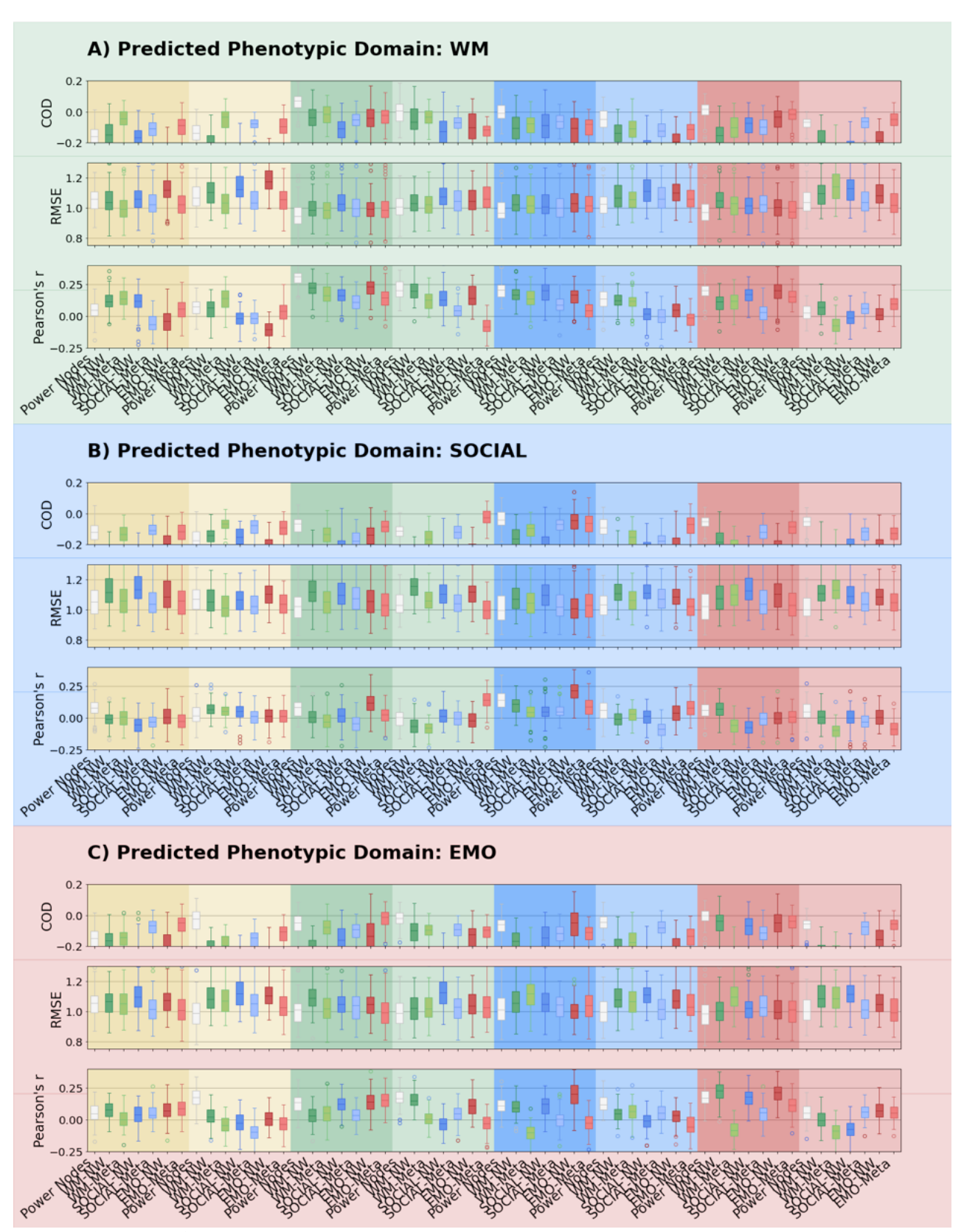


Figure S21) PLS 100 x leave-30%-out CV

Boxplots of the distribution of prediction accuracies from PLS 100 x leave-30%-out CV for WM, SOCIAL, and EMO domain, for coefficient of determination (COD) / model fit, RMSE and Pearson's r.

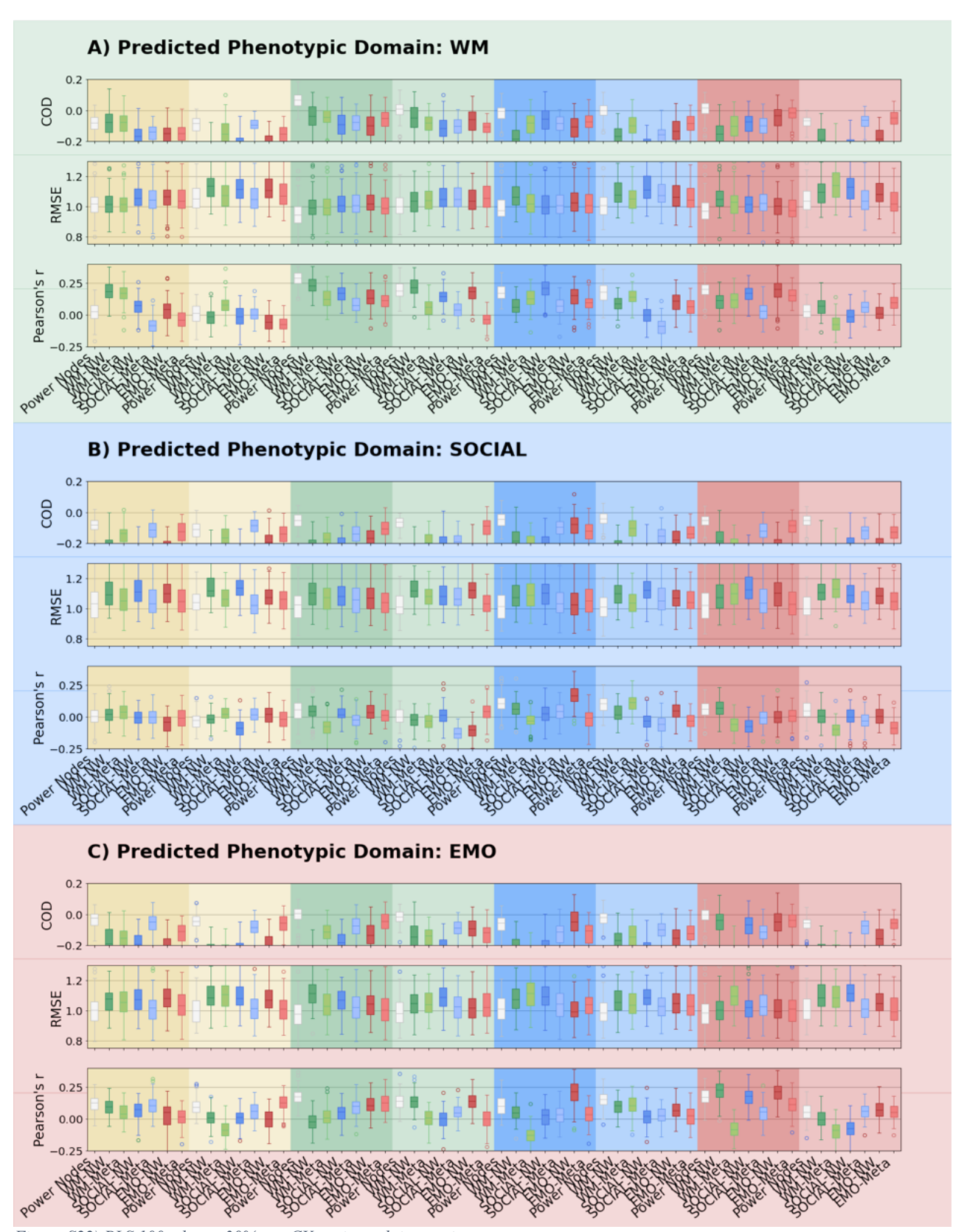


Figure S22) PLS 100 x leave-30%-out CV – trimmed time series

Boxplots of the distribution of prediction accuracies from PLS 100 x leave-30%-out CV - trimmed time series for WM, SOCIAL, and EMO domain, for coefficient of determination (COD) / model fit, RMSE and Pearson's r.

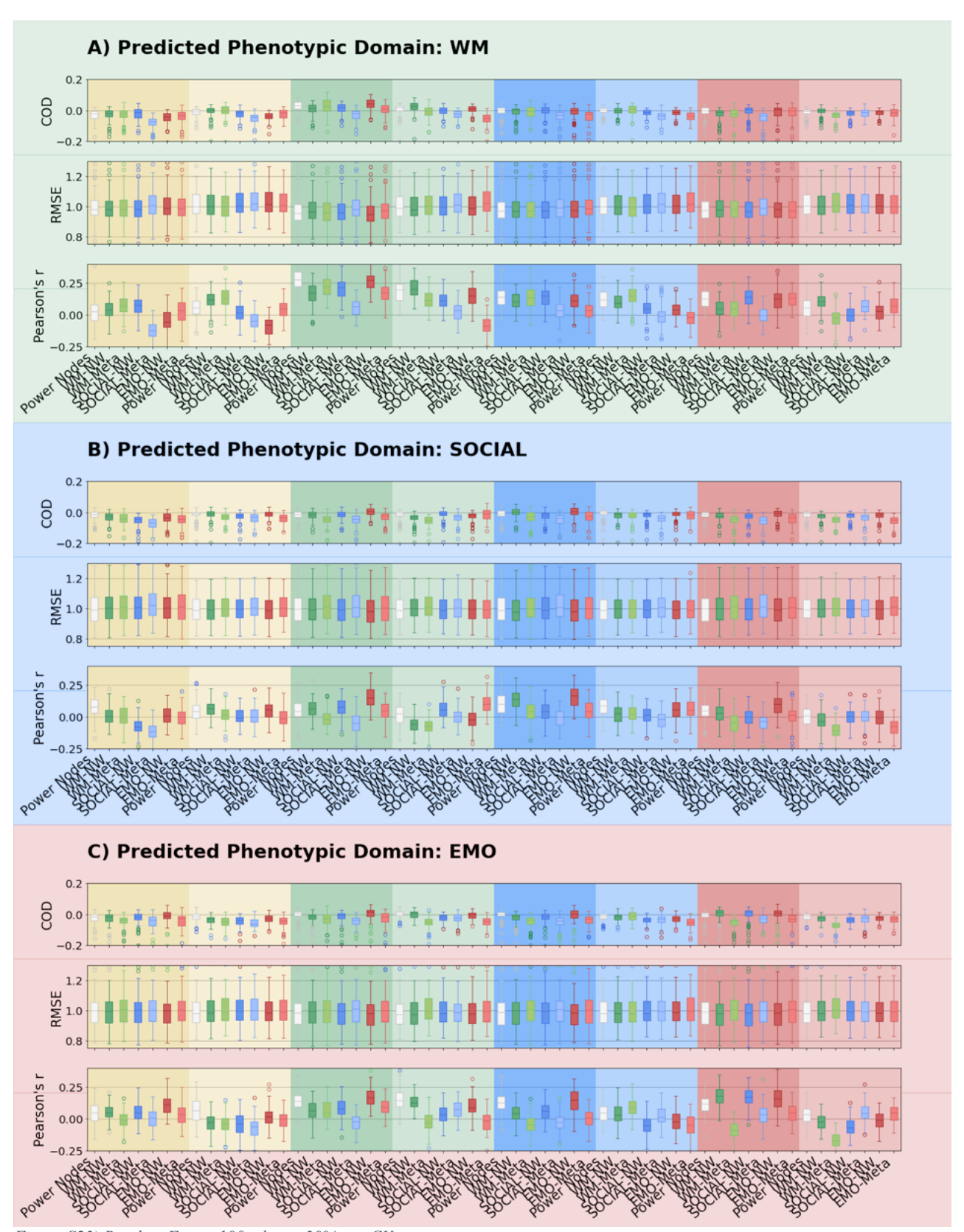


Figure S23) Random Forest 100 x leave-30%-out CV

Boxplots of the distribution of prediction accuracies from Random Forest 100 x leave-30%-out CV for WM, SOCIAL, and EMO domain, for coefficient of determination (COD) / model fit, RMSE and Pearson's r.

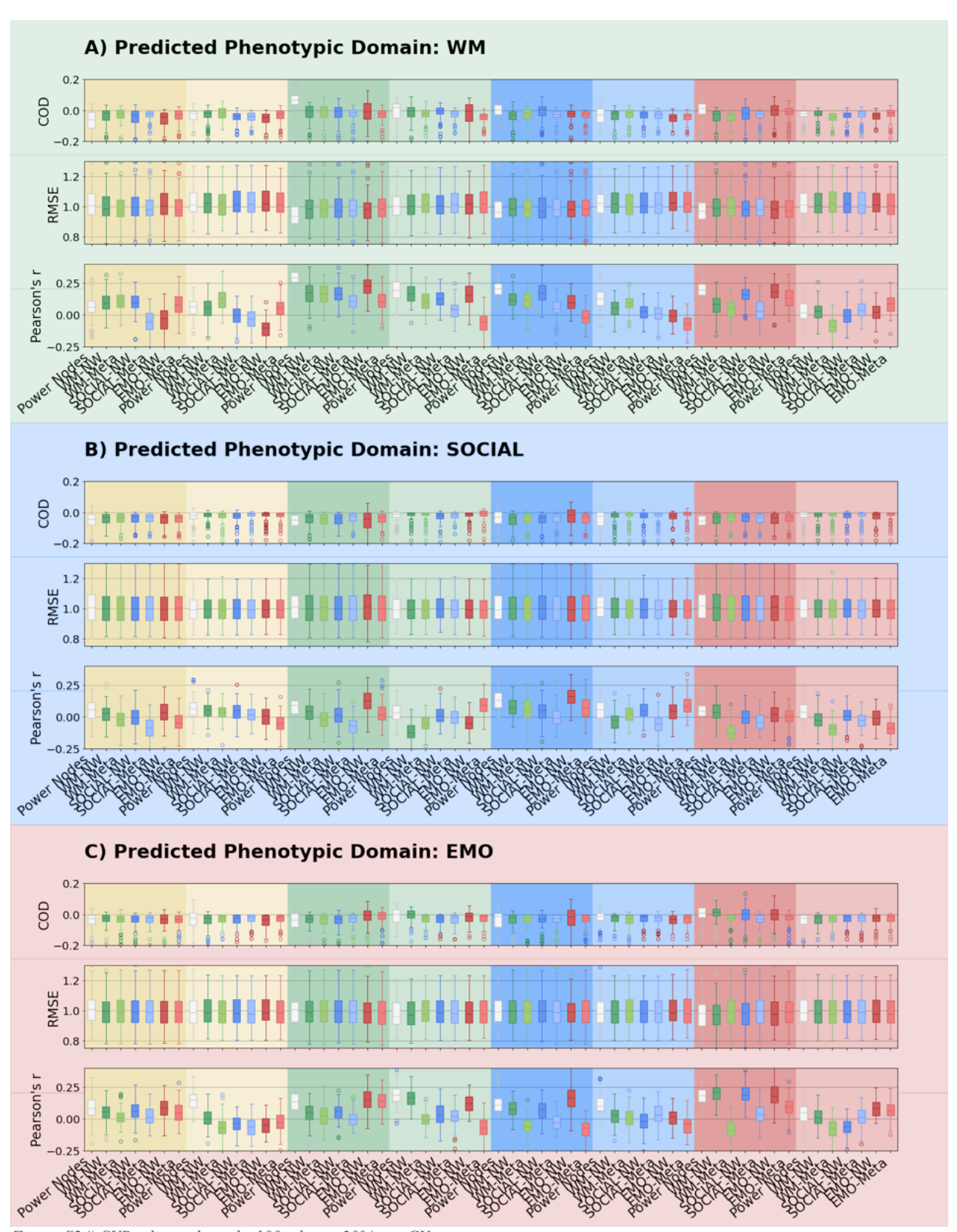


Figure S24) SVR – linear kernel - 100 x leave-30%-out CV

Boxplots of the distribution of prediction accuracies from SVR – linear kernel - $100 \, x$ leave-30%-out CV for WM, SOCIAL, and EMO domain, for coefficient of determination (COD) / model fit, RMSE and Pearson's r.

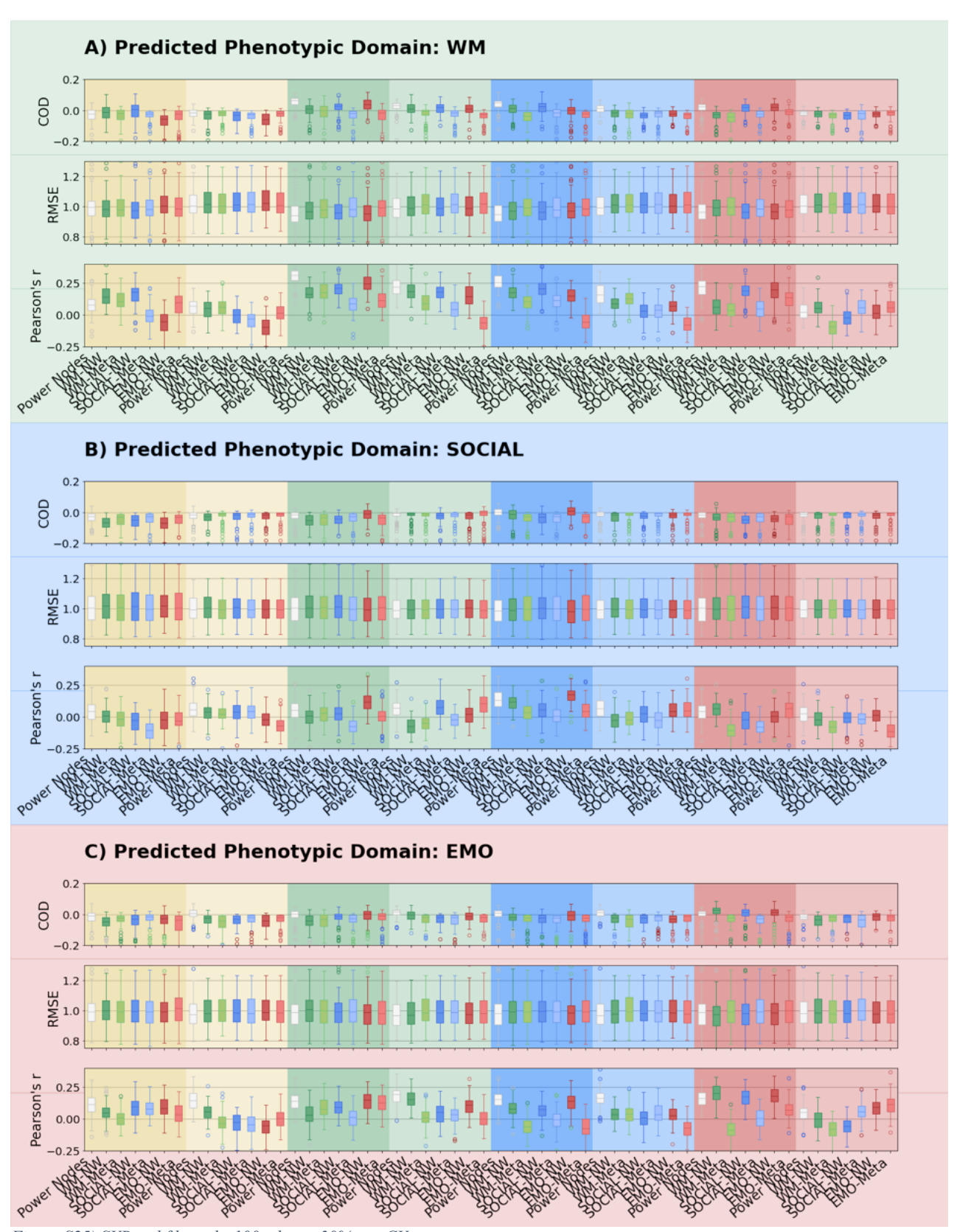


Figure S25) SVR – rbf kernel - 100 x leave-30%-out CV

Boxplots of the distribution of prediction accuracies from SVR - RBF kernel - 100 x leave-30%-out CV for WM, SOCIAL, and EMO domain, for coefficient of determination (COD) / model fit, RMSE and Pearson's r.

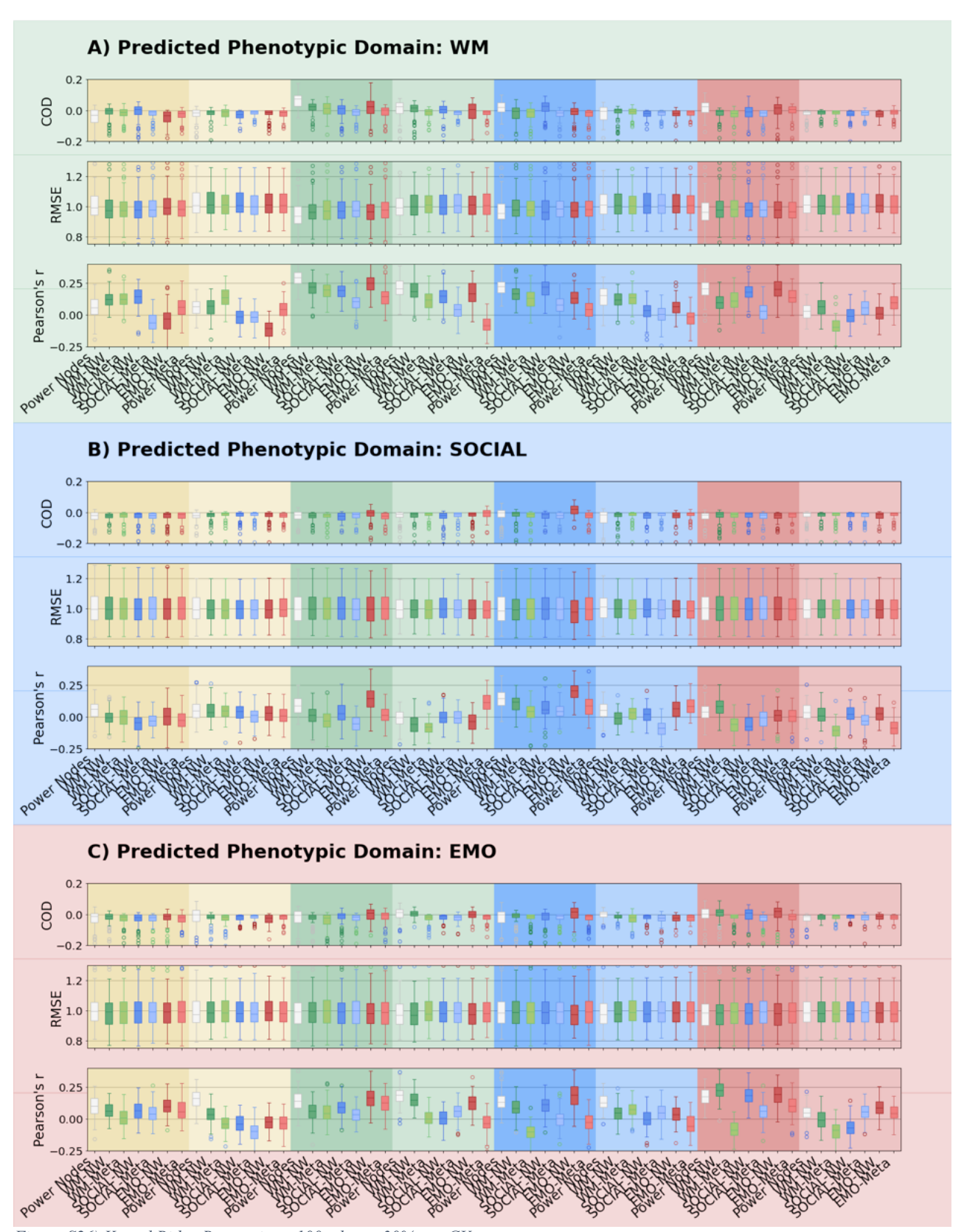


Figure S26) Kernel Ridge Regression - 100 x leave-30%-out CV

Boxplots of the distribution of prediction accuracies from Kernel Ridge Regression - $100 \, x$ leave- 30%-out CV for WM, SOCIAL, and EMO domain, for coefficient of determination (COD) / model fit, RMSE and Pearson's r.

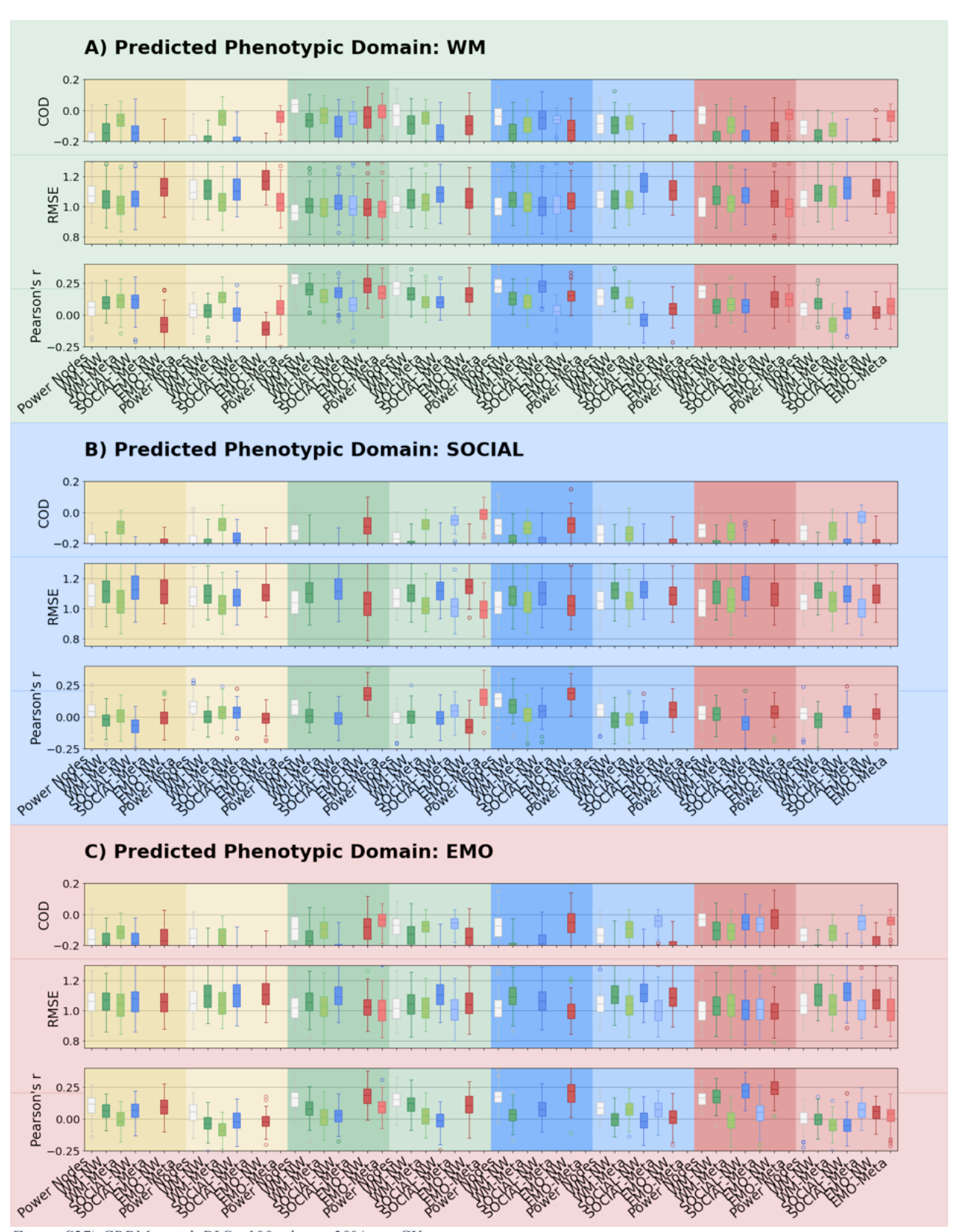


Figure S27) CBPM – with PLS - 100 x leave-30%-out CV

Boxplots of the distribution of prediction accuracies from CBPM – with PLS - $100 \, x$ leave-30%-out CV for WM, SOCIAL, and EMO domain, for coefficient of determination (COD) / model fit, RMSE and Pearson's r.

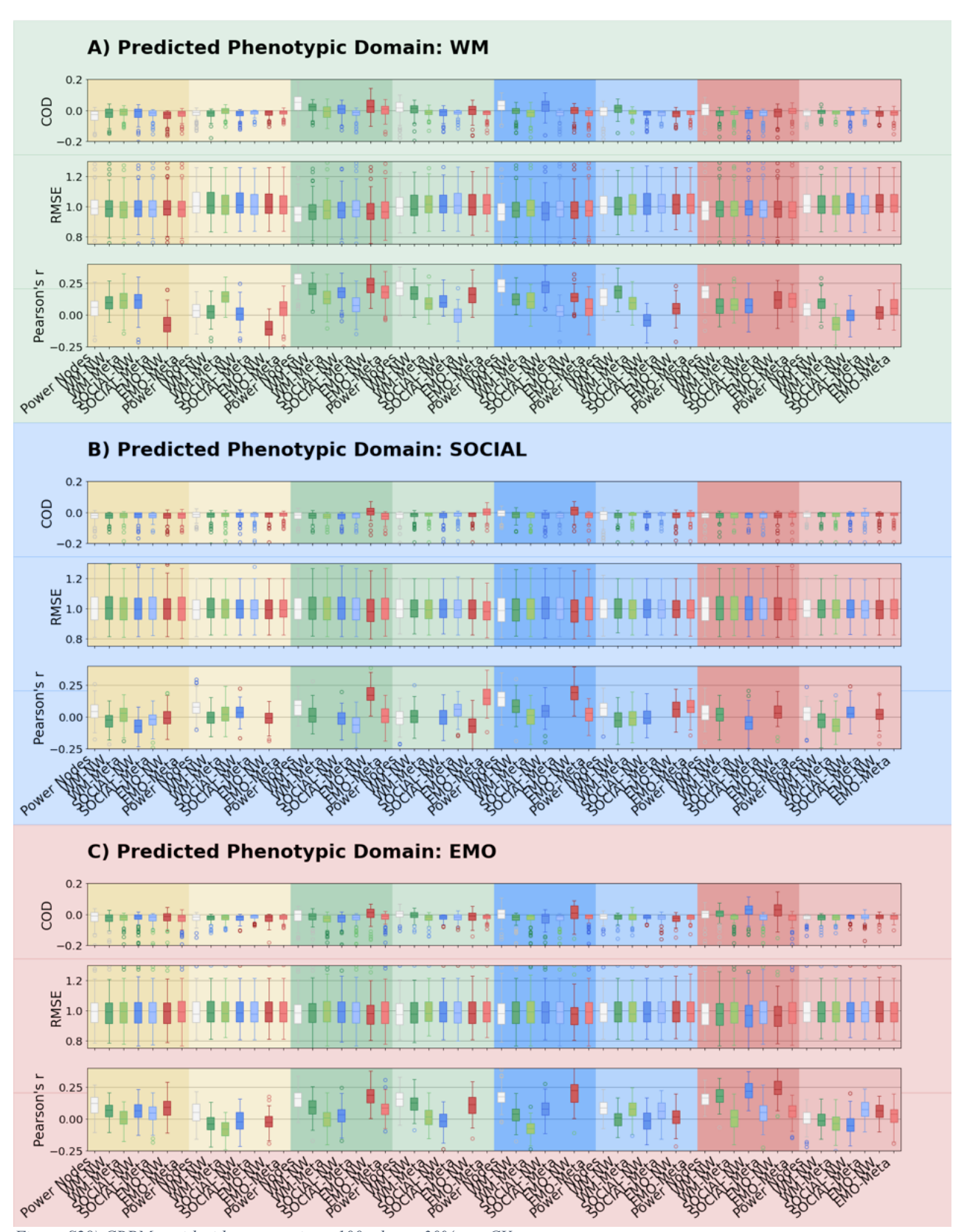


Figure S28) CBPM – with ridge regression - 100 x leave-30%-out CV

Boxplots of the distribution of prediction accuracies from CBPM – with ridge regression - $100 \, x$ leave-30%-out CV for WM, SOCIAL, and EMO domain, for coefficient of determination (COD) / model fit, RMSE and Pearson's r.

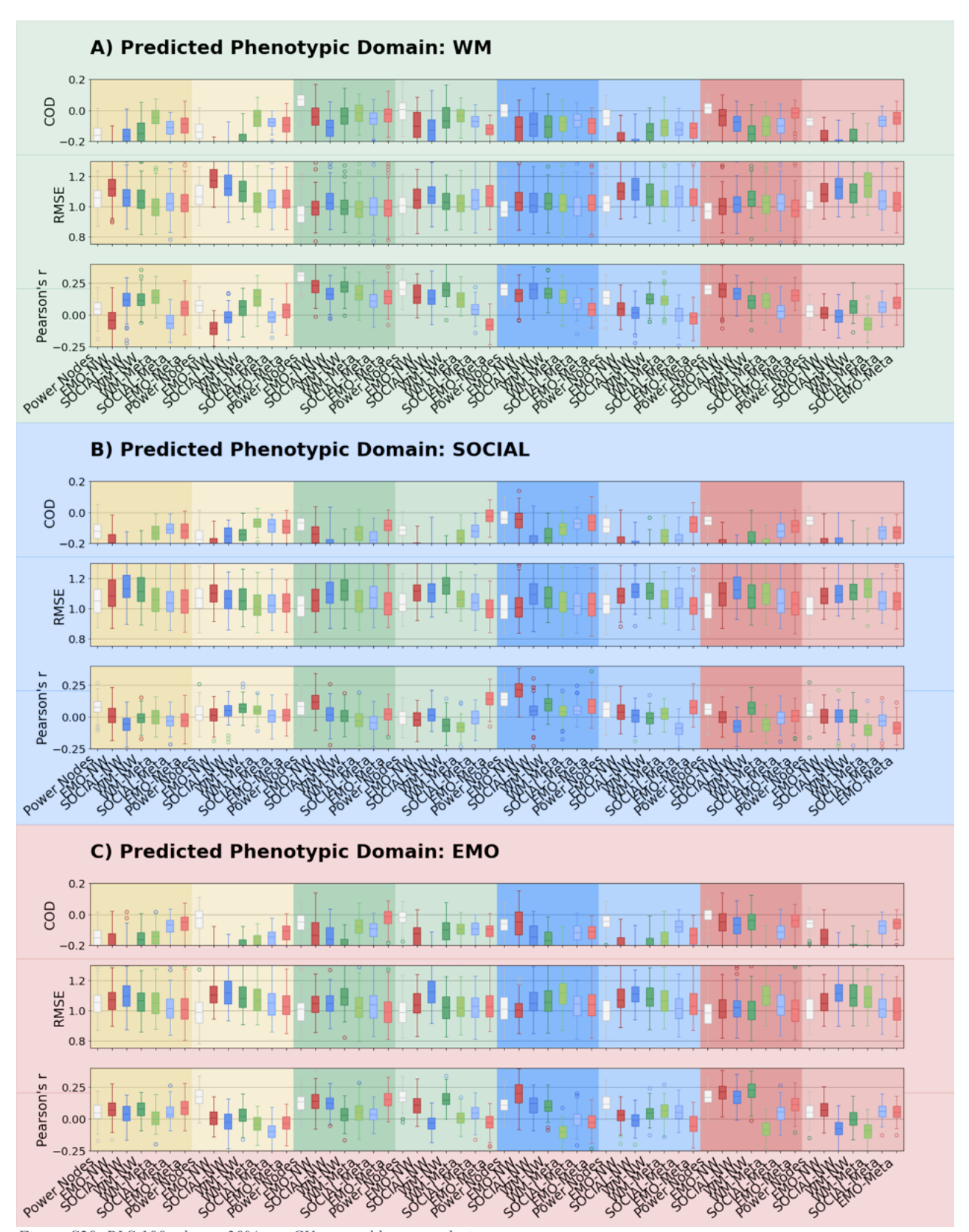


Figure S29. PLS 100 x leave-30%-out CV - sorted by network size

Boxplots of the distribution of prediction accuracies from PLS 100 x leave-30%-out CV for WM, SOCIAL, and EMO domain, for coefficient of determination (COD) / model fit, RMSE and Pearson's r – sorted by network size from large to small: Power (264 nodes), EMO-NW (84 nodes), SOCIAL-NW (66 nodes), WM-NW (49 nodes), WM-meta-NW (19 nodes), SOCIAL-meta-NW (11 nodes) to EMO-meta-NW (10 nodes)

Supplemental References

- Babakhanyan, I., McKenna, B. S., Casaletto, K. B., Nowinski, C. J., & Heaton, R. K. (2018).
 National Institutes of Health Toolbox Emotion Battery for English- and Spanish-speaking adults: Normative data and factor-based summary scores. *Patient Related Outcome Measures*, 9, 115–127. https://doi.org/10.2147/PROM.S151658
- Barch, D. M., Burgess, G. C., Harms, M. P., Petersen, S. E., Schlaggar, B. L., Corbetta, M., Glasser, M. F., Curtiss, S., Dixit, S., Feldt, C., Nolan, D., Bryant, E., Hartley, T., Footer, O., Bjork, J. M., Poldrack, R., Smith, S., Johansen-Berg, H., Snyder, A. Z., ... WU-Minn HCP Consortium. (2013). Function in the human connectome: Task-fMRI and individual differences in behavior. *NeuroImage*, 80, 169–189.
 https://doi.org/10.1016/j.neuroimage.2013.05.033
- Castelli, F., Happé, F., Frith, U., & Frith, C. (2000). Movement and Mind: A Functional Imaging Study of Perception and Interpretation of Complex Intentional Movement Patterns.

 NeuroImage, 12(3), 314–325. https://doi.org/10.1006/nimg.2000.0612
- Cognition Measures. (n.d.). Retrieved May 11, 2022, from

 https://www.healthmeasures.net/explore-measurement-systems/nih-toolbox/intro-to-nih-toolbox/cognition
- Emotion Measures. (n.d.). Retrieved May 11, 2022, from https://www.healthmeasures.net/explore-measurement-systems/nih-toolbox/intro-to-nih-toolbox/emotion
- Finn, E. S., Shen, X., Scheinost, D., Rosenberg, M. D., Huang, J., Chun, M. M., Papademetris, X., & Constable, R. T. (2015). Functional connectome fingerprinting: Identifying individuals using patterns of brain connectivity. *Nature Neuroscience*, 18(11), 1664–1671. https://doi.org/10.1038/nn.4135
- Gur, R. C., Richard, J., Hughett, P., Calkins, M. E., Macy, L., Bilker, W. B., Brensinger, C., & Gur,
 R. E. (2010). A cognitive neuroscience-based computerized battery for efficient
 measurement of individual differences: Standardization and initial construct validation.

- Journal of Neuroscience Methods, 187(2), 254–262. https://doi.org/10.1016/j.jneumeth.2009.11.017
- Gur, R. C., Sara, R., Hagendoorn, M., Marom, O., Hughett, P., Macy, L., Turner, T., Bajcsy, R., Posner, A., & Gur, R. E. (2002). A method for obtaining 3-dimensional facial expressions and its standardization for use in neurocognitive studies. *Journal of Neuroscience Methods*, 115(2), 137–143. https://doi.org/10.1016/S0165-0270(02)00006-7
- Hariri, A. R., Tessitore, A., Mattay, V. S., Fera, F., & Weinberger, D. R. (2002). The Amygdala Response to Emotional Stimuli: A Comparison of Faces and Scenes. *NeuroImage*, *17*(1), 317–323. https://doi.org/10.1006/nimg.2002.1179
- Kogler, L., Müller, V. I., Werminghausen, E., Eickhoff, S. B., & Derntl, B. (2020). Do I feel or do I know? Neuroimaging meta-analyses on the multiple facets of empathy. *Cortex*, 129, 341–355. https://doi.org/10.1016/j.cortex.2020.04.031
- Müller, V. I., Cieslik, E. C., Laird, A. R., Fox, P. T., Radua, J., Mataix-Cols, D., Tench, C. R., Yarkoni, T., Nichols, T. E., Turkeltaub, P. E., Wager, T. D., & Eickhoff, S. B. (2018). Ten simple rules for neuroimaging meta-analysis. *Neuroscience & Biobehavioral Reviews*, 84, 151–161. https://doi.org/10.1016/J.NEUBIOREV.2017.11.012
- Müller, V. I., Höhner, Y., & Eickhoff, S. B. (2018). Influence of task instructions and stimuli on the neural network of face processing: An ALE meta-analysis. *Cortex*, *103*, 240–255. https://doi.org/10.1016/j.cortex.2018.03.011
- Nadeau, C., & Bengio, Y. (1999). Inference for the generalization error. *Advances in Neural Information Processing Systems*, 12.
- Reid, A. T., Bzdok, D., Genon, S., Langner, R., Müller, V. I., Eickhoff, C. R., Hoffstaedter, F., Cieslik, E.-C., Fox, P. T., Laird, A. R., Amunts, K., Caspers, S., & Eickhoff, S. B. (2016).

 ANIMA: A data-sharing initiative for neuroimaging meta-analyses. *NeuroImage*, *124*, 1245–1253. https://doi.org/10.1016/j.neuroimage.2015.07.060

- Rottschy, C., Langner, R., Dogan, I., Reetz, K., Laird, A. R., Schulz, J. B., Fox, P. T., & Eickhoff, S. B. (2012). Modelling neural correlates of working memory: A coordinate-based meta-analysis. *NeuroImage*, 60(1), 830–846. https://doi.org/10.1016/j.neuroimage.2011.11.050
- Salsman, J. M., Butt, Z., Pilkonis, P. A., Cyranowski, J. M., Zill, N., Hendrie, H. C., Kupst, M. J.,
 Kelly, M. A. R., Bode, R. K., Choi, S. W., Lai, J.-S., Griffith, J. W., Stoney, C. M.,
 Brouwers, P., Knox, S. S., & Cella, D. (2013). Emotion assessment using the NIH Toolbox.
 Neurology, 80(11 Suppl 3), S76-86. https://doi.org/10.1212/WNL.0b013e3182872e11
- Shen, X., Finn, E. S., Scheinost, D., Rosenberg, M. D., Chun, M. M., Papademetris, X., & Constable, R. T. (2017). Using connectome-based predictive modeling to predict individual behavior from brain connectivity. *Nature Protocols*, 12(3), 506–518. https://doi.org/10.1038/nprot.2016.178
- Wheatley, T., Milleville, S. C., & Martin, A. (2007). Understanding Animate Agents: Distinct Roles for the Social Network and Mirror System. *Psychological Science*, *18*(6), 469–474. https://doi.org/10.1111/j.1467-9280.2007.01923.x

6 Summary and general discussion

With this dissertation I aimed to investigate how inter-individual differences in cognitive and socio-affective processes are related to structural brain anatomy and functional connectivity and how heritability and task state impact brain-behaviour relationships as influencing factors. First, I investigated the phenotypic and morphological association of cognition and affect in the brain, as well as their shared genetic variance. I then assessed the predictability of task states and network specificity.

With my first study I was able to show phenotypic relationships with both affect and cognition and brain structure in the left superior frontal cortex. Decomposing the phenotypic correlations into genetic and environmental components showed that the associations were accounted for by shared genetic effects between the traits. Yet, my second study revealed that individual behaviour can only moderately be explained by network interactions. The results indicate, that interactions within *a priori* networks are less predictive than global effects. However, a slight benefit of predictions based on FC from task versus resting state was observed for performance in the cognitive domain, indicating state specificity.

6.1 Cognition and affect - integrated dimensions

Intelligence or cognition is a very well-studied and delineated concept. Reliable measures have been developed (Akshoomoff et al., 2013; Heaton et al., 2014), capturing different aspects of cognition such as fluid reasoning and crystallized knowledge, including executive function, working memory, processing speed, attention, episodic memory, and language. In the first study, I used these measures to analyse crystallised and fluid intelligence, assessed with the National Institute of Health (NIH) toolbox for Assessment of Neurological and Behavioral Function® (neuroscienceblueprint.nih.gov). This measurement has been shown to capture interindividual differences reliably (Akshoomoff et al., 2013; Gershon et al., 2013). However in the second study, to investigate the influence of task states, I used the cognitive process of working memory, which in this dataset was assessed with a 2back task. Unfortunately, the simplicity of the task leads to a ceiling effect, where many participant solve the task successfully, leading to a low variance. This has been, however, mitigated by introducing reaction time into an inverse efficiency score. Nevertheless the moderate predictability of task states could be related to the low variance within both the cognitive score, as well as a within the task states.

Emotion or affect has gained scientific attention later and has seen struggles being investigated due to the elusive nature (Barrett, 2012; Lindquist et al., 2012). However, emotion and trait affect influence what we notice, learn (Mather & Sutherland, 2011; Tyng et al., 2017), remember (Cahill & McGaugh, 1998; Mather & Sutherland, 2011)

and even how we decide (Bechara et al., 2000). Several tests have been developed to assess emotion and affect. In the first study, self-reports were used to capture trait affect from the Emotion Battery of the NIH Toolbox (Pilkonis et al., 2013; Salsman et al., 2013, 2014). For the second study an emotional face matching task was performed, which has been developed and tested to reliably activate the amygdala. However, only little variance of individual emotion processing abilities is captured. This has been, again, mitigated by introducing reaction time into an inverse efficiency score. Nevertheless, it would be interesting to see a similar study setup to investigate state and network specificity, however with different, more complex tasks.

Despite cognition and affect being seen as separate constructs for a long time and therefore being studied separately, an integration is inevitable. This can be seen with the word "emotional intelligence", the ability to use and regulate emotions. But also with social cognition or theory of mind, which has been investigated in the second study, showing a combination of both emotional interpretation and social inference.

While cognitive functions have traditionally been attributed to higher-order cortical regions—such as the lateral and medial prefrontal, temporal, and parietal cortices—affective processes have historically been associated with evolutionarily older, subcortical structures, including the amygdala, basal ganglia, and hypothalamus. However, as outlined above, recent research increasingly investigates the integration of affect and cognition across both cortical and subcortical systems, challenging the historical dichotomy between emotional and cognitive brain networks. In line with that, both my studies showed on the one hand a convergence phenotypically, as well as in the superior frontal gyrus (study 1), as well as no network-specificity and only moderate state-specificity for cognition (study 2), suggesting potential overlapping networks and functions.

6.1.1 Brain morphology and heritability (study 1)

The modular approach on cognition and affect has already been challenged by several researchers such as (Barrett et al., 2011; Lindquist et al., 2012; Pessoa, 2008), arguing, that cognition and emotion are deeply intertwined in both brain and behaviour. In this dissertation, by using anatomic data and twin modelling, I build on this by demonstrating that cognitive and affective traits are not only theoretically connected, but phenotypically and genetically associated, pointing toward a shared neural infrastructure in the superior frontal gyrus. This convergence underlines previous findings (Barrett & Satpute, 2013), while furthering this integration through heritability modelling, showing a shared phenotypic and genetic association with cortical thickness in the left superior frontal cortex. This convergence indicates the prefrontal cortex as not just essential for cognitive function, but a hub where emotional and cognitive traits are co-constructed. The discovery of a brain region

simultaneously relating to cognitive and affective traits, while further driving these associations genetically, strongly indicates that cognition and emotion are integrated within the brain. Therefore, this biologically stable marker has further implications for understanding trait-level vulnerabilities, also in mental health.

6.1.2 Functional connectivity and predictability of task states (study 2)

The finding of a shared phenotypic and genetic association between cognition and trait affect in the superior frontal cortex is rooted in quantifiable structural morphology providing trait-level and heritability insights. In a next step, I put a stronger focus on the effects of state and the relationship to brain function, in contrast to brain structure. Thus, these results led me to develop the research of cognition and emotion into a more dynamic approach, by complementing it with functional connectivity in resting-state und task-based fMRI.

Unlike structural markers, functional connectivity reflects state-dependent and network-based dynamics. Therefore, in my second study I explored whether functional connectivity could predict inter-individual differences within cognition (represented through WM), and emotion, complemented with social cognition. Moving from structural morphology and heritability to functional connectivity and machine learning prediction, allowed me to investigate the influence of state on brain-behaviour relationships.

Here, I found that, overall, FC patterns showed limited ability to predict individual behavioural performance. The predictive power was modest, though comparable to other studies applying a similar approach (Dubois et al., 2018; Greene et al., 2018; Ooi et al., 2022). However, slightly better predictions were achieved using task-based FC compared to resting-state FC, particularly in the working memory domain, which extend results from previous studies, showing that FC from task-based fMRI carry more behaviourally relevant and individual information (Finn et al., 2015; Finn & Bandettini, 2021; Greene et al., 2018). Despite the modest predictive power, the stronger prediction performance of task-based compared to resting-state FC supports the idea that contextual activation enhances signal relevance by being more reflective of individual differences. While in my study this was only observed for working memory, it stands to investigate, whether an improvement could be seen within a larger sample (through increase of statistical power) or with different task capturing the emotion domain (through capturing more emotional variance).

6.1.3 Complementary results

With these two studies I investigated how the behavioural and brain morphometric data provide trait-level and heritable foundations, revealing a stable hub of

convergence between cognition and affect in the superior frontal cortex. Further, I approached functional connectivity with machine learning predictions offering insights into large-scale patterns in cognitive and emotional functioning. Here, task-based connectivity yielded better prediction performance (compared to resting-state FC, in working memory prediction) implying the importance of state and network interactions within interindividual variation. However, no significant difference in prediction performance between the different domains could be observed, which could potentially indicate individual variability similarities in FC of cognitive and socio-affective processing.

Encompassing both studies, I applied several analyses, leveraging the power of multimodal integration. With the analyses on both structural and functional data I offer complimentary insights. While the analysed structure in combination with the heritability analysis reveals stable traits and genetic boundaries within which one can change and develop, functional analysis reveals how a person behaves and feels in the moment. Therefore, my results show that cognition and affect are both stable and flexible within our behaviour, as well as our brain, revealing insights important for our understand within the layered inter-individual brain-behaviour relationships. With this dissertation I present the results of a genetically driven overlap between cognition and affect in the superior frontal cortex, while the influence of state showed moderate predictability only in cognition but none for the socio-affective domain. This is in line with the latest research endeavours and important for future individualised neuroscience. In sum, by examining structure and function and investigating different influencing factors of brain-behaviour relationships one gets a more nuanced picture about the integration of cognition and affect in the human brain.

6.2 Limitations and opportunities

Despite the faceted and broad approach, there are some limitations to be acknowledged. First of all, both studies used the openly available Human Connectome Project. Openly available large datasets such as the HCP used here, or the Adolescent Brain Cognitive Development Study (ABCD), and the UK Biobank are tremendously valuable and have transformed and furthered research in neuroscience. They play an important role in the standardization of protocols and data collection, and in the promotion of reproducibility through transparency, replicability and validation of findings. Further, the varied data sampling within these datasets allows for the multimodal analysis of complex research questions as done here. Importantly, the large sample sizes increase statistical power, through which robust correlations (study 1) and the application machine learning models (study 2) are only possible.

While the HCP is a densely sampled dataset enabling the research of complex research questions, it also shows only a small fraction of the population: the age range is

between 22 and 37 years, with all healthy subjects from the USA, with a slightly higher IQ than the population average. While this sample was chosen consciously in an effort to establish potential brain-behaviour relationships within a healthy and constrained sample, it anyhow constrains the results to only a section of the population. For both studies it would be beneficial to repeat the analyses in different samples in order to test for generalisability. However, these very specific research questions addressed in this dissertation could for now unfortunately only be answered with the HCP dataset, as they allow for twin-based heritability testing (study 1), and further offer a wide variety of in- and out-of-scanner tests and questionnaires allowing for the analysis and comparison of FC predictability between different behaviour performances (study 2). Yet, the extensive testing comes at the cost of potentially rather superficial and short tasks. This includes the tasks performed in the scanner as well as outside. Most of the task developed for fMRI induce a robust activation of targeted brain areas instead of allowing for strong interindividual variability. Further, tasks performed both inside and outside the scanner are often optimized for stable group-average effects. In both studies this needs to be factored into the interpretation of the findings.

Furthermore, the widespread use of these datasets increases the risk of false positive findings. Since numerous researchers are conducting a multitude of independent analyses within these datasets, statistically significant results may arise by chance. Publication bias adds to this problem, as positive findings are more likely to be published, skewing the literature towards overstated effects. Therefore, it was especially important to me to publish the results of the second paper as transparently as possible, without overstating the findings and acknowledging the moderate prediction performance.

As mentioned above, it would be valuable to test the generalisability of these findings using independent samples. Since there are so far no suitable large openly available datasets, it could be interesting to test the findings in smaller datasets, as well as in harmonised data from several smaller datasets. Such a data pool could also be used to inform synthetic data. Synthetic data could offer an exciting opportunity to train machine learning models, especially in areas where there is notoriously insufficient data (J. Wang et al., 2023), such as rare diseases, diseases with difficulties to be scanned in an MRI scanner, or areas where data privacy protection is an issue (Vaden et al., 2020).

Further, it is important to mention that although multimodal analyses are highly promising, technical nuances and methodological limitations, and therefore meaningful interpretation, depends on having (or inquiring) domain-specific expertise. This has been especially evident in the work on the second paper applying machine learning for behavioural performance prediction based on FC. Several landmark papers used oversimplified assessments of prediction performance,

painting a more optimistic picture of the achievements. For my publication it was therefore important to offer a critical and transparent assessment of the findings.

Moreover, potential avenues to develop these findings presented here, despite the multimodal approach within the papers, are manifold. Within the first paper the research focus between brain-behaviour relationships and the genetic drivers, could be extended to investigate the heritability of functional task activation and connectivity. Based on studies performed in the same dataset, it would be expected to be in line with our current findings and show that not only brain structure, but also FC is heritable (Colclough et al., 2017; Ge et al., 2017). However, a potential convergence between cognition and affect and FC has not been investigated. Furthermore, in the second paper, only FC was used to predict behavioural performance. While one of the goals of the second paper—to improve interpretability of machine learning features—would be hindered, it would nevertheless be interesting to see if a combination between structural and functional data or even genetic or EEG data could improve prediction performance. Finally, since the network used in the second paper were based on *a priori* defined delineations, future work could adopt and compare different individualised parcellations (such as different approaches developed by (Beckmann et al., 2005; Kong et al., 2019; Mueller et al., 2013; D. Wang et al., 2015)). Within the scope of my research, I have applied the approach by (Kong et al., 2019). However, preliminary results revealed only a marginal improvement in prediction performance for the specific networks and behavioural targets. Therefore, I assume that even individualised a priori defined networks may not significantly improve prediction performance and therefore interpretability of relevant features. Instead, machine-learning appropriate *post-hoc* analyses of whole-brain FC predictions (Tian & Zalesky, 2021) might offer greater potential to identify biologically relevant features.

6.3 Relevance and impact

The research and investigation of cognition and affect is not only of theoretical interest, but is essential in everyone's daily life, as well as fundamental in different mental disorders. Many cognitive and neural processes are expected to operate in similar ways in both healthy individuals and those with neurological or psychiatric disorders. With my dissertation, using a healthy and constrained sample, I aimed to apply different analyses to contribute new insights for precision neuroscience, by providing a deeper understanding of the interplay between cognition and affect, and individual variability in brain and behaviour.

Therefore, in line with previous studies showing structural association with cognition and emotion in the superior frontal cortex (Engen & Anderson, 2018; Okon-Singer et al., 2015), I extend these findings in study 1 by providing evidence for shared genetic

effects between the traits. It therefore reinforces the importance of integrated theories (Barrett, 2012; Pessoa, 2008) and provides a basis for investigating shared risk factors in mental health disorders. Further, study 2 extended the already extensive research of task-based FC compared to resting-state FC comparison for behavioural prediction within the cognitive domain (e.g. (Avery et al., 2020; Greene et al., 2018; Jiang et al., 2020)), by the socio-affective domain. Although the prediction performance was moderate, an additional important contribution was the transparent acknowledgment and reporting of these limitations. Moreover, the undetected differences in prediction performance between unrelated FC and behavioural score (e.g. prediction of working memory score from FC yielded from emotion recognition task), might also suggest that cognitive and emotional processes are interconnected at the neural level to allow for clearly separable predictive patterns.

Finally, in order to improve interpretability of machine learning features, I defined *a priori* networks based on meta-analyses and from large individual task-fMRI studies. Therefore, I computed GLM for all tasks, and further conducted three separate meta-analyses for working-memory (n-back task), emotion recognition and social cognition. These meta-analytically defined networks are openly available via the ANIMA-database (Reid et al., 2016); https://anima.fz-juelich.de/studies/Kraljevic_NetStateSpec_2024).

6.4 Conclusion

In sum, with my dissertation I provide an integrative model of how cognition and affect relate to the human brain. By combining insights from structural anatomy, heritability modelling, and functional connectivity-based prediction, my results reveal that these traditionally distinct domains share common neural substrates, while also being dynamically shaped through context-sensitive activation and connectivity.

The identification of the superior frontal cortex as a heritable anatomical hub for both cognitive and affective traits emphasizes the stability of this integration at the trait level. In contrast, the moderate, yet comparable, predictability of task-based FC shows the influence of brain state and network dynamics in shaping individual behaviour, while also promoting a transparent and critical assessment of multi-modal analyses.

7 References

- Adolphs, R., Damasio, H., Tranel, D., & Damasio, A. R. (1996). Cortical systems for the recognition of emotion in facial expressions. *The Journal of Neuroscience: The Official Journal of the Society for Neuroscience, 16*(23), 7678–7687. https://doi.org/10.1523/JNEUROSCI.16-23-07678.1996
- Adolphs, R., Tranel, D., Damasio, H., & Damasio, A. (1995). Fear and the human amygdala. *The Journal of Neuroscience*, 15(9), 5879–5891. https://doi.org/10.1523/JNEUROSCI.15-09-05879.1995
- Akshoomoff, N., Beaumont, J. L., Bauer, P. J., Dikmen, S. S., Gershon, R. C., Mungas, D., Slotkin, J., Tulsky, D., Weintraub, S., Zelazo, P. D., & Heaton, R. K. (2013). NIH Toolbox Cognition Function Battery (CFB): Composite Scores of Crystallized, Fluid, and Overall Cognition. *Monographs of the Society for Research in Child Development*, 78(4), 119–132. https://doi.org/10.1111/mono.12038
- Alloway, T., & Alloway, R. (2009). The efficacy of working memory training in improving crystallized intelligence. *Nature Precedings*. https://doi.org/10.1038/npre.2009.3697.1
- Avery, E. W., Yoo, K., Rosenberg, M. D., Greene, A. S., Gao, S., Na, D. L., Scheinost, D., Constable, T. R., & Chun, M. M. (2020). Distributed Patterns of Functional Connectivity Predict Working Memory Performance in Novel Healthy and Memory-impaired Individuals. *Journal of Cognitive Neuroscience*, 32(2), 241–255. https://doi.org/10.1162/jocn_a_01487
- Baddeley, A. (2012). Working Memory: Theories, Models, and Controversies. *Annual Review of Psychology*, 63(1), 1–29. https://doi.org/10.1146/annurev-psych-120710-100422
- Baltes, P. B., Staudinger, U. M., & Lindenberger, U. (1999). LIFESPAN PSYCHOLOGY: Theory and Application to Intellectual Functioning. *Annual Review of Psychology*, *50*(1), 471–507. https://doi.org/10.1146/annurev.psych.50.1.471
- Barbey, A. K., Colom, R., & Grafman, J. (2014). Distributed neural system for emotional intelligence revealed by lesion mapping. *Social Cognitive and Affective Neuroscience*, 9(3), 265–272. https://doi.org/10.1093/scan/nss124
- Barrett, L. F. (2012). Emotions are real. *Emotion*, *12*(3), 413–429. https://doi.org/10.1037/a0027555
- Barrett, L. F., Mesquita, B., & Gendron, M. (2011). Current Directions in Psychological Science: Context in Emotion Perception. *SAGE*, *20*(5), 286–290. https://doi.org/10.1177/0963721411422522
- Barrett, L. F., & Satpute, A. B. (2013). Large-scale brain networks in affective and social neuroscience: Towards an integrative functional architecture of the brain. *Current Opinion in Neurobiology*, 23(3), 361–372. https://doi.org/10.1016/j.conb.2012.12.012
- Basten, U., Hilger, K., & Fiebach, C. J. (2015). Where smart brains are different: A quantitative meta-analysis of functional and structural brain imaging studies

- on intelligence. *Intelligence*, 51, 10–27. https://doi.org/10.1016/J.INTELL.2015.04.009
- Bechara, A., Damasio, H., & Damasio, A. R. (2000). Emotion, Decision Making and the Orbitofrontal Cortex. *Cerebral Cortex*, 10(3), 295–307. https://doi.org/10.1093/cercor/10.3.295
- Bechara, A., Damasio, H., Damasio, A. R., & Lee, G. P. (1999). Different Contributions of the Human Amygdala and Ventromedial Prefrontal Cortex to Decision-Making. *The Journal of Neuroscience*, 19(13), 5473–5481. https://doi.org/10.1523/JNEUROSCI.19-13-05473.1999
- Beckmann, C. F., DeLuca, M., Devlin, J. T., & Smith, S. M. (2005). Investigations into resting-state connectivity using independent component analysis. *Philosophical Transactions of the Royal Society B: Biological Sciences*, 360(1457), 1001–1013. https://doi.org/10.1098/rstb.2005.1634
- Biswal, B., Zerrin Yetkin, F., Haughton, V. M., & Hyde, J. S. (1995). Functional Connectivity In The Motor Cortex Of Resting Human Brain Using Echo-Planar MRI. *Magnetic Resonance in Medicine*, 34(4), 537–541. https://doi.org/10.1002/mrm.1910340409
- Bouchard, T. J., & Loehlin, J. C. (2001). Genes, Evolution, and Personality. *Behavior Genetics*, *31*(3), 243–273. https://doi.org/10.1023/A:1012294324713
- Bradley, M. M., & Lang, P. J. (2002). Measuring Emotion: Behavior, Feeling, and Physiology. In R. D. Lane, L. Nadel, & G. L. Ahern (Eds.), *Cognitive Neuroscience of Emotion* (pp. 242–276). Oxford University Press.
- Bruell, J. H. (1970). Heritability of Emotional Behavior. In P. Black (Ed.), *Physiological Correlates of Emotion* (pp. 23–36). Academic Press.
- Bzdok, D., Schilbach, L., Vogeley, K., Schneider, K., Laird, A. R., Langner, R., & Eickhoff, S. B. (2012). Parsing the neural correlates of moral cognition: ALE meta-analysis on morality, theory of mind, and empathy. *Brain Structure and Function*, *217*(4), 783–796. https://doi.org/10.1007/s00429-012-0380-y
- Cahill, L., & McGaugh, J. L. (1998). Mechanisms of emotional arousal and lasting declarative memory. *Trends in Neurosciences*, 21(7), 294–299. https://doi.org/10.1016/S0166-2236(97)01214-9
- Calder, A. J., Keane, J., Manes, F., Antoun, N., & Young, A. W. (2000). Impaired recognition and experience of disgust following brain injury. *Nature Neuroscience*, *3*(11), 1077–1078. https://doi.org/10.1038/80586
- Cattell, R. B. (1943). The measurement of adult intelligence. *Psychological Bulletin*, 40(3), 153–193. https://doi.org/10.1037/h0059973
- Cattell, R. B. (1963). Theory of fluid and crystallized intelligence: A critical experiment. *Journal of Educational Psychology*, 54(1), 1–22. https://doi.org/10.1037/h0046743
- Chauhan, P., Rathawa, A., Jethwa, K., & Mehra, S. (2021). The Anatomy of the Cerebral Cortex. In P. Ryszard (Ed.), *Cerebral Ischemia* (pp. 1–16). Exon Publications.

- https://doi.org/10.36255/exonpublications.cerebralischemia.2021.cerebralc ortex
- Colclough, G. L., Smith, S. M., Nichols, T. E., Winkler, A. M., Sotiropoulos, S. N., Glasser, M. F., Van Essen, D. C., & Woolrich, M. W. (2017). The heritability of multi-modal connectivity in human brain activity. *eLife*, *6*, e20178. https://doi.org/10.7554/eLife.20178
- Cole, M. W., Bassett, D. S., Power, J. D., Braver, T. S., & Petersen, S. E. (2014). Intrinsic and Task-Evoked Network Architectures of the Human Brain. *Neuron*, *83*(1), 238–251. https://doi.org/10.1016/j.neuron.2014.05.014
- Colom, R., Privado, J., García, L. F., Estrada, E., Cuevas, L., & Shih, P.-C. (2015). Fluid intelligence and working memory capacity: Is the time for working on intelligence problems relevant for explaining their large relationship? Personality and Individual Differences, 79, 75–80. https://doi.org/10.1016/j.paid.2015.01.051
- Damasio, H., Grabowski, T., Frank, R., Galaburda, A. M., & Damasio, A. R. (1994). The Return of Phineas Gage: Clues About the Brain from the Skull of a Famous Patient. *Science*, *264*(5162), 1102–1105. https://doi.org/10.1126/science.8178168
- Damasio, H., Grabowski, T. J., Tranel, D., Hichwa, R. D., & Damasio, A. R. (1996). A neural basis for lexical retrieval. *Nature*, *380*(6574), 499–505. https://doi.org/10.1038/380499a0
- Desmet, P. (2018). Measuring Emotion: Development and Application of an Instrument to Measure Emotional Responses to Products. In M. Blythe & A. Monk (Eds.), *Funology 2* (pp. 391–404). Springer International Publishing. https://doi.org/10.1007/978-3-319-68213-6_25
- Diener, E., & Emmons, R. A. (1984). The independence of positive and negative affect. *Journal of Personality and Social Psychology*, 47(5), 1105–1117. https://doi.org/10.1037/0022-3514.47.5.1105
- Dubois, J., Galdi, P., Han, Y., Paul, L. K., & Adolphs, R. (2018). Resting-State Functional Brain Connectivity Best Predicts the Personality Dimension of Openness to Experience. *Personality Neuroscience*, 1. https://doi.org/10.1017/pen.2018.8
- Engen, H. G., & Anderson, M. C. (2018). Memory Control: A Fundamental Mechanism of Emotion Regulation. *Trends in Cognitive Sciences*, *22*(11), 982–995. https://doi.org/10.1016/j.tics.2018.07.015
- Fernandez-Pujals, A. M., Adams, M. J., Thomson, P., McKechanie, A. G., Blackwood, D. H. R., Smith, B. H., Dominiczak, A. F., Morris, A. D., Matthews, K., Campbell, A., Linksted, P., Haley, C. S., Deary, I. J., Porteous, D. J., MacIntyre, D. J., & McIntosh, A. M. (2015). Epidemiology and Heritability of Major Depressive Disorder, Stratified by Age of Onset, Sex, and Illness Course in Generation Scotland: Scottish Family Health Study (GS:SFHS). *PLOS ONE*, *10*(11), e0142197. https://doi.org/10.1371/journal.pone.0142197

- Finn, E. S., & Bandettini, P. A. (2021). Movie-watching outperforms rest for functional connectivity-based prediction of behavior. *NeuroImage*, *235*, 117963. https://doi.org/10.1016/j.neuroimage.2021.117963
- Finn, E. S., Shen, X., Scheinost, D., Rosenberg, M. D., Huang, J., Chun, M. M., Papademetris, X., & Constable, R. T. (2015). Functional connectome fingerprinting: Identifying individuals using patterns of brain connectivity. *Nature Neuroscience*, *18*(11), 1664–1671. https://doi.org/10.1038/nn.4135
- Fischl, B. (2012). FreeSurfer. *NeuroImage*, *62*(2), 774–781. https://doi.org/10.1016/j.neuroimage.2012.01.021
- Fischl, B., & Dale, A. M. (2000). Measuring the thickness of the human cerebral cortex from magnetic resonance images. *Proceedings of the National Academy of Sciences*, 97(20), 11050 LP 11055. https://doi.org/10.1073/pnas.200033797
- Fjell, A. M., Grydeland, H., Krogsrud, S. K., Amlien, I., Rohani, D. A., Ferschmann, L., Storsve, A. B., Tamnes, C. K., Sala-Llonch, R., Due-Tønnessen, P., Bjørnerud, A., Sølsnes, A. E., Håberg, A. K., Skranes, J., Bartsch, H., Chen, C.-H., Thompson, W. K., Panizzon, M. S., Kremen, W. S., ... Walhovd, K. B. (2015). Development and aging of cortical thickness correspond to genetic organization patterns. *Proceedings of the National Academy of Sciences*, 112(50), 15462–15467. https://doi.org/10.1073/pnas.1508831112
- Fusar-Poli, P., Placentino, A., Carletti, F., Landi, P., Allen, P., Surguladze, S., Benedetti, F., Abbamonte, M., Gasparotti, R., Barale, F., Perez, J., McGuire, P., & Politi, P. (2009). Functional atlas of emotional faces processing: A voxel-based meta-analysis of 105 functional magnetic resonance imaging studies. *Journal of Psychiatry and Neuroscience*, 34(6), 418.
- Ge, T., Holmes, A. J., Buckner, R. L., Smoller, J. W., & Sabuncu, M. R. (2017). Heritability analysis with repeat measurements and its application to resting-state functional connectivity. *Proceedings of the National Academy of Sciences*, 114(21), 5521–5526. https://doi.org/10.1073/pnas.1700765114
- Gershon, R. C., Slotkin, J., Manly, J. J., Blitz, D. L., Beaumont, J. L., Schnipke, D., Wallner-Allen, K., Golinkoff, R. M., Gleason, J. B., Hirsh-Pasek, K., Adams, M. J., & Weintraub, S. (2013). IV. NIH TOOLBOX COGNITION BATTERY (CB): MEASURING LANGUAGE (VOCABULARY COMPREHENSION AND READING DECODING). Monographs of the Society for Research in Child Development, 78(4), 49–69. https://doi.org/10.1111/mono.12034
- Geschwind, D. H., & Rakic, P. (2013). Cortical Evolution: Judge the Brain by Its Cover. *Neuron*, 80(3), 633–647. https://doi.org/10.1016/j.neuron.2013.10.045
- Glasser, M. F., Smith, S. M., Marcus, D. S., Andersson, J. L. R., Auerbach, E. J., Behrens, T. E. J., Coalson, T. S., Harms, M. P., Jenkinson, M., Moeller, S., Robinson, E. C., Sotiropoulos, S. N., Xu, J., Yacoub, E., Ugurbil, K., & Van Essen, D. C. (2016). The Human Connectome Project's neuroimaging approach. *Nature Neuroscience*, 19(9), Article 9. https://doi.org/10.1038/nn.4361

- Glasser, M. F., Sotiropoulos, S. N., Wilson, J. A., Coalson, T. S., Fischl, B., Andersson, J. L., Xu, J., Jbabdi, S., Webster, M., Polimeni, J. R., Van Essen, D. C., & Jenkinson, M. (2013). The minimal preprocessing pipelines for the Human Connectome Project.

 NeuroImage,

 NeuroImage,

 https://doi.org/10.1016/j.neuroimage.2013.04.127
- Greene, A. S., Gao, S., Scheinost, D., & Constable, R. T. (2018). Task-induced brain state manipulation improves prediction of individual traits. *Nature Communications*, 9(1), Article 1. https://doi.org/10.1038/s41467-018-04920-3
- Gross, J. J. (2015). Emotion Regulation: Current Status and Future Prospects. *Psychological Inquiry*, 26(1), 1–26. https://doi.org/10.1080/1047840X.2014.940781
- Haier, R. J., Jung, R. E., Yeo, R. A., Head, K., & Alkire, M. T. (2004). Structural brain variation and general intelligence. *NeuroImage*, *23*(1), 425–433. https://doi.org/10.1016/j.neuroimage.2004.04.025
- Heaton, R. K., Akshoomoff, N., Tulsky, D., Mungas, D., Weintraub, S., Dikmen, S., Beaumont, J., Casaletto, K. B., Conway, K., Slotkin, J., & Gershon, R. (2014). Reliability and validity of composite scores from the NIH Toolbox Cognition Battery in adults. *Journal of the International Neuropsychological Society : JINS*, 20(6), 588–598. https://doi.org/10.1017/S1355617714000241
- Hillman, E. M. C. (2014). Coupling Mechanism and Significance of the BOLD Signal: A Status Report. *Annual Review of Neuroscience*, *37*(1), 161–181. https://doi.org/10.1146/annurev-neuro-071013-014111
- Hofmann, W., Schmeichel, B. J., & Baddeley, A. D. (2012). Executive functions and self-regulation. *Trends in Cognitive Sciences*, 16(3), 174–180. https://doi.org/10.1016/J.TICS.2012.01.006
- Hogstrom, L. J., Westlye, L. T., Walhovd, K. B., & Fjell, A. M. (2013). The Structure of the Cerebral Cortex Across Adult Life: Age-Related Patterns of Surface Area, Thickness, and Gyrification. *Cerebral Cortex*, 23(11), 2521–2530. https://doi.org/10.1093/cercor/bhs231
- Hornak, J., Bramham, J., Rolls, E. T., Morris, R. G., O'Doherty, J., Bullock, P. R., & Polkey, C. E. (2003). Changes in emotion after circumscribed surgical lesions of the orbitofrontal and cingulate cortices. *Brain*, 126(7), 1691–1712. https://doi.org/10.1093/brain/awg168
- Hunt, E. (2001). Intelligence: Historical and Conceptual Perspectives. In N. J. Smelser & P. B. Baltes (Eds.), *International Encyclopedia of the Social & Behavioral Sciences* (pp. 7658–7663). Pergamon. https://doi.org/10.1016/B0-08-043076-7/01631-4
- Jansen, A. G., Mous, S. E., White, T., Posthuma, D., & Polderman, T. J. C. (2015). What Twin Studies Tell Us About the Heritability of Brain Development, Morphology, and Function: A Review. *Neuropsychology Review*, *25*(1), 27–46. https://doi.org/10.1007/s11065-015-9278-9
- Jiang, R., Zuo, N., Ford, J. M., Qi, S., Zhi, D., Zhuo, C., Xu, Y., Fu, Z., Bustillo, J., Turner, J. A., Calhoun, V. D., & Sui, J. (2020). Task-induced brain connectivity promotes the

- detection of individual differences in brain-behavior relationships. *NeuroImage*, 207, 116370. https://doi.org/10.1016/j.neuroimage.2019.116370
- Jones, H. E., & Conrad, H. S. (1933). The growth and decline of intelligence: A study of a homogeneous group between the ages of ten and sixty. *Genetic Psychology Monographs*.
- Kendall, K. M., Van Assche, E., Andlauer, T. F. M., Choi, K. W., Luykx, J. J., Schulte, E. C., & Lu, Y. (2021). The genetic basis of major depression. *Psychological Medicine*, 51(13), 2217–2230. https://doi.org/10.1017/S0033291721000441
- Kober, H., Barrett, L. F., Joseph, J., Bliss-Moreau, E., Lindquist, K., & Wager, T. D. (2008). Functional grouping and cortical–subcortical interactions in emotion: A meta-analysis of neuroimaging studies. *NeuroImage*, *42*(2), 998–1031. https://doi.org/10.1016/j.neuroimage.2008.03.059
- Kong, R., Li, J., Orban, C., Sabuncu, M. R., Liu, H., Schaefer, A., Sun, N., Zuo, X.-N., Holmes, A. J., Eickhoff, S. B., & Yeo, B. T. T. (2019). Spatial Topography of Individual-Specific Cortical Networks Predicts Human Cognition, Personality, and Emotion. *Cerebral Cortex*, 29(6), 2533–2551. https://doi.org/10.1093/cercor/bhy123
- Krapohl, E., Rimfeld, K., Shakeshaft, N. G., Trzaskowski, M., McMillan, A., Pingault, J.-B., Asbury, K., Harlaar, N., Kovas, Y., Dale, P. S., & Plomin, R. (2014). The high heritability of educational achievement reflects many genetically influenced traits, not just intelligence. *Proceedings of the National Academy of Sciences of the United States of America*, 111(42), 15273–15278. https://doi.org/10.1073/pnas.1408777111
- Langner, R., Leiberg, S., Hoffstaedter, F., & Eickhoff, S. B. (2018). Towards a human self-regulation system: Common and distinct neural signatures of emotional and behavioural control. *Neuroscience and Biobehavioral Reviews*, *90*(May), 400–410. https://doi.org/10.1016/j.neubiorev.2018.04.022
- Lindquist, K. A., Wager, T. D., Kober, H., Bliss-Moreau, E., & Barrett, L. F. (2012). The brain basis of emotion: A meta-analytic review. *The Behavioral and Brain Sciences*, *35*(3), 121–143. https://doi.org/10.1017/S0140525X11000446
- Little, D. R., Lewandowsky, S., & Craig, S. (2014). Working memory capacity and fluid abilities: The more difficult the item, the more more is better. *Frontiers in Psychology*, *5*. https://doi.org/10.3389/fpsyg.2014.00239
- Lykken, D., & Tellegen, A. (1996). Happiness Is a Stochastic Phenomenon. *Psychological Science*, 7(3), 186–189. https://doi.org/10.1111/j.1467-9280.1996.tb00355.x
- Martinez, D. (2019). Immediate and long-term memory and their relation to crystallized and fluid intelligence. *Intelligence*, 76, 101382. https://doi.org/10.1016/j.intell.2019.101382
- Mather, M., & Sutherland, M. R. (2011). Arousal-Biased Competition in Perception and Memory. *Perspectives on Psychological Science*, 6(2), 114–133. https://doi.org/10.1177/1745691611400234

- Mueller, S., Wang, D., Fox, M. D., Yeo, B. T. T., Sepulcre, J., Sabuncu, M. R., Shafee, R., Lu, J., & Liu, H. (2013). Individual Variability in Functional Connectivity Architecture of the Human Brain. *Neuron*, *77*(3), 586–595. https://doi.org/10.1016/J.NEURON.2012.12.028
- Müller, V. I., Höhner, Y., & Eickhoff, S. B. (2018). Influence of task instructions and stimuli on the neural network of face processing: An ALE meta-analysis. *Cortex*, 103, 240–255. https://doi.org/10.1016/j.cortex.2018.03.011
- Nes, R. B., & Roysamb, E. (2015). The heritability of subjective well-being: Review and meta-analysis. In M. Pluess (Ed.), *Genetics of Psychological Well-being: The Role of Heritability and Genetics in Positive Psychology* (pp. 75–96). Oxford University Press.
- Nummenmaa, L., Glerean, E., Hari, R., & Hietanen, J. K. (2014). Bodily maps of emotions. *PNAS Proceedings of the National Academy of Sciences of the United States of America*, 111(2), 646–651. https://doi.org/10.1073/pnas.1321664111
- Okon-Singer, H., Hendler, T., Pessoa, L., & Shackman, A. J. (2015). The neurobiology of emotion-cognition interactions: Fundamental questions and strategies for future research. *Frontiers in Human Neuroscience*, 9. https://doi.org/10.3389/fnhum.2015.00058
- Ooi, L. Q. R., Chen, J., Zhang, S., Kong, R., Tam, A., Li, J., Dhamala, E., Zhou, J. H., Holmes, A. J., & Yeo, B. T. T. (2022). Comparison of individualized behavioral predictions across anatomical, diffusion and functional connectivity MRI. *NeuroImage*, *263*, 119636. https://doi.org/10.1016/j.neuroimage.2022.119636
- Palomero-Gallagher, N., & Zilles, K. (2019). Cortical layers: Cyto-, myelo-, receptor- and synaptic architecture in human cortical areas. *NeuroImage*, 197, 716–741. https://doi.org/10.1016/j.neuroimage.2017.08.035
- Panizzon, M. S., Fennema-Notestine, C., Eyler, L. T., Jernigan, T. L., Prom-Wormley, E., Neale, M., Jacobson, K., Lyons, M. J., Grant, M. D., Franz, C. E., Xian, H., Tsuang, M., Fischl, B., Seidman, L., Dale, A., & Kremen, W. S. (2009). Distinct Genetic Influences on Cortical Surface Area and Cortical Thickness. *Cerebral Cortex*, 19(11), 2728–2735. https://doi.org/10.1093/cercor/bhp026
- Pessoa, L. (2008). On the relationship between emotion and cognition. *Nature Reviews Neuroscience*, *9*(2), 148–158. https://doi.org/10.1038/nrn2317
- Pilkonis, P. A., Choi, S. W., Salsman, J. M., Butt, Z., Moore, T. L., Lawrence, S. M., Zill, N., Cyranowski, J. M., Kelly, M. A. R., Knox, S. S., & Cella, D. (2013). Assessment of self-reported negative affect in the NIH Toolbox. *Psychiatry Research*, *206*(1), 88–97. https://doi.org/10.1016/j.psychres.2012.09.034
- Plomin, R., & Deary, I. J. (2015). Genetics and intelligence differences: Five special findings. *Molecular Psychiatry*, *20*(1), 98–108. https://doi.org/10.1038/mp.2014.105
- Reid, A. T., Bzdok, D., Genon, S., Langner, R., Müller, V. I., Eickhoff, C. R., Hoffstaedter, F., Cieslik, E.-C., Fox, P. T., Laird, A. R., Amunts, K., Caspers, S., & Eickhoff, S. B. (2016). ANIMA: A data-sharing initiative for neuroimaging meta-analyses.

- *NeuroImage*, 124, 1245–1253. https://doi.org/10.1016/j.neuroimage.2015.07.060
- Rosenbaum, R. S., Köhler, S., Schacter, D. L., Moscovitch, M., Westmacott, R., Black, S. E., Gao, F., & Tulving, E. (2005). The case of K.C.: Contributions of a memory-impaired person to memory theory. *Neuropsychologia*, *43*(7), 989–1021. https://doi.org/10.1016/J.NEUROPSYCHOLOGIA.2004.10.007
- Rottschy, C., Langner, R., Dogan, I., Reetz, K., Laird, A. R., Schulz, J. B., Fox, P. T., & Eickhoff, S. B. (2012). Modelling neural correlates of working memory: A coordinate-based meta-analysis. *NeuroImage*, 60(1), 830–846. https://doi.org/10.1016/j.neuroimage.2011.11.050
- Salazar Kämpf, M., Adam, L., Rohr, M. K., Exner, C., & Wieck, C. (2023). A Meta-Analysis of the Relationship Between Emotion Regulation and Social Affect and Cognition. *Clinical Psychological Science*, 11(6), 1159–1189. https://doi.org/10.1177/21677026221149953
- Salsman, J. M., Butt, Z., Pilkonis, P. A., Cyranowski, J. M., Zill, N., Hendrie, H. C., Kupst, M. J., Kelly, M. A. R., Bode, R. K., Choi, S. W., Lai, J.-S., Griffith, J. W., Stoney, C. M., Brouwers, P., Knox, S. S., & Cella, D. (2013). Emotion assessment using the NIH Toolbox. *Neurology*, 80(11 Suppl 3), S76-86. https://doi.org/10.1212/WNL.0b013e3182872e11
- Salsman, J. M., Lai, J.-S., Hendrie, H. C., Butt, Z., Zill, N., Pilkonis, P. A., Peterson, C., Stoney, C. M., Brouwers, P., & Cella, D. (2014). Assessing psychological well-being: Self-report instruments for the NIH Toolbox. *Quality of Life Research*, *23*(1), 205–215. https://doi.org/10.1007/s11136-013-0452-3
- Salthouse, T. A. (2019). Trajectories of normal cognitive aging. *Psychology and Aging*, *34*(1), 17–24. https://doi.org/10.1037/pag0000288
- Schmaal, L., Hibar, D. P., Sämann, P. G., Hall, G. B., Baune, B. T., Jahanshad, N., Cheung, J. W., Van Erp, T. G. M., Bos, D., Ikram, M. A., Vernooij, M. W., Niessen, W. J., Tiemeier, H., Hofman, A., Wittfeld, K., Grabe, H. J., Janowitz, D., Bülow, R., Selonke, M., ... for the ENIGMA-Major Depressive Disorder Working Group. (2017). Cortical abnormalities in adults and adolescents with major depression based on brain scans from 20 cohorts worldwide in the ENIGMA Major Depressive Disorder Working Group. *Molecular Psychiatry*, *22*(6), 900–909. https://doi.org/10.1038/mp.2016.60
- Scoville, W. B., & Milner, B. (1957). Loss of recent memory after bilateral hippocampal lesions. *Journal of Neurology, Neurosurgery, and Psychiatry*, *20*(1), 11.
- Shine, J. M., Bissett, P. G., Bell, P. T., Koyejo, O., Balsters, J. H., Gorgolewski, K. J., Moodie, C. A., & Poldrack, R. A. (2016). The Dynamics of Functional Brain Networks: Integrated Network States during Cognitive Task Performance. *Neuron*, *92*(2), 544–554. https://doi.org/10.1016/j.neuron.2016.09.018
- Spearman, C. (1904). 'General Intelligence,' Objectively Determined and Measured. *The American Journal of Psychology*, 15(2), 201–292. https://doi.org/10.2307/1412107

- Stuss, D. T., Floden, D., Alexander, M. P., Levine, B., & Katz, D. (2001). Stroop performance in focal lesion patients: Dissociation of processes and frontal lobe lesion location. *Neuropsychologia*, *39*(8), 771–786. https://doi.org/10.1016/S0028-3932(01)00013-6
- Tian, Y., & Zalesky, A. (2021). Machine learning prediction of cognition from functional connectivity: Are feature weights reliable? *NeuroImage*, *245*, 118648. https://doi.org/10.1016/j.neuroimage.2021.118648
- Tucker-Drob, E. M. (2009). Differentiation of cognitive abilities across the life span. *Developmental Psychology*, 45(4), 1097–1118. https://doi.org/10.1037/a0015864
- Tyng, C. M., Amin, H. U., Saad, M. N. M., & Malik, A. S. (2017). The Influences of Emotion on Learning and Memory. *Frontiers in Psychology*, 8, 1454. https://doi.org/10.3389/fpsyg.2017.01454
- Vaden, K. I., Gebregziabher, M., Dyslexia Data Consortium, & Eckert, M. A. (2020). Fully synthetic neuroimaging data for replication and exploration. *NeuroImage*, *223*, 117284. https://doi.org/10.1016/j.neuroimage.2020.117284
- Wang, D., Buckner, R. L., Fox, M. D., Holt, D. J., Holmes, A. J., Stoecklein, S., Langs, G., Pan, R., Qian, T., Li, K., Baker, J. T., Stufflebeam, S. M., Wang, K., Wang, X., Hong, B., & Liu, H. (2015). Parcellating cortical functional networks in individuals. *Nature Neuroscience*, 18(12), 1853–1860. https://doi.org/10.1038/nn.4164
- Wang, J., Dvornek, N. C., Staib, L. H., & Duncan, J. S. (2023). Learning Sequential Information in Task-Based fMRI for Synthetic Data Augmentation. In A. Abdulkadir, D. R. Bathula, N. C. Dvornek, S. T. Govindarajan, M. Habes, V. Kumar, E. Leonardsen, T. Wolfers, & Y. Xiao (Eds.), *Machine Learning in Clinical Neuroimaging* (Vol. 14312, pp. 79–88). Springer Nature Switzerland. https://doi.org/10.1007/978-3-031-44858-4_8
- Warrier, V., Grasby, K. L., Uzefovsky, F., Toro, R., Smith, P., Chakrabarti, B., Khadake, J., Mawbey-Adamson, E., Litterman, N., Hottenga, J.-J., Lubke, G., Boomsma, D. I., Martin, N. G., Hatemi, P. K., Medland, S. E., Hinds, D. A., Bourgeron, T., & Baron-Cohen, S. (2018). Genome-wide meta-analysis of cognitive empathy: Heritability, and correlates with sex, neuropsychiatric conditions and cognition. *Molecular Psychiatry*, *23*(6), 1402–1409. https://doi.org/10.1038/mp.2017.122
- Wheatley, T., Milleville, S. C., & Martin, A. (2007). Understanding Animate Agents: Distinct Roles for the Social Network and Mirror System. *Psychological Science*, *18*(6), 469–474. https://doi.org/10.1111/j.1467-9280.2007.01923.x
- Yeo, B. T. T., Krienen, F. M., Sepulcre, J., Sabuncu, M. R., Lashkari, D., Hollinshead, M., Roffman, J. L., Smoller, J. W., Zöllei, L., Polimeni, J. R., Fischl, B., Liu, H., Buckner, R. L., Thomas Yeo, B. T., Krienen, F. M., Sepulcre, J., Sabuncu, M. R., Lashkari, D., Hollinshead, M., ... Buckner, R. L. (2011). The organization of the human cerebral cortex estimated by intrinsic functional connectivity. *Journal of Neurophysiology*, *106*(3), 1125–1165. https://doi.org/10.1152/jn.00338.2011

8 Acknowledgements

I would first like to thank Prof. Dr. Simon Eickhoff for the opportunity to study in his institute, first as a master student and then for my PhD. I'm greatly appreciative of the support, guidance, and motivation throughout my studies. Thank you for allowing me the freedom to pursue the research I was interested in and for the continued helpful feedback. I would also like to thank Prof. Dr. Gerhard Jocham for his support and assistance as my secondary supervisor during my PhD project.

A particular thanks goes to Dr. Veronika Müller and Dr. Robert Langner for assisting me in all aspects of my PhD. Thank you for your patience and hands-on help when needed. Your supervision has helped me to become an independent researcher. Also, I would like to thank Dr. Kaustubh Patil, for his never-ending support with server-related issues or machine learning difficulties—your patience, understanding and knowledge is admirable.

An additional thanks goes to all my colleagues from INM-7, especially from my working group, Edna, Sofie, Federico, Lya, Marisa, Lennart, Vincent, Martin, Georgios, Kevin, Eliana, Gianna, Vera, Lisa H, Lisa W, Kyesam, Mostafa, Hanwen, Meike, Neville—you all have always been kind, supporting, motivating, funny and made my PhD more enjoyable. Big thanks also to the support system of the INM-7, with Julia, Anna and Ute at the centre, thanks for always being there to help, chat, laugh.

A special thanks goes to: Jean, ohne den nicht nur die Doktorarbeit, sondern auch Master und Bachelor ganz anders gewesen wären. Mit dir ein Büro zu teilen war das Beste und ich vermisse unsere Kaffeepausen jetzt schon. Ich kann mir einen Arbeitsplatz ohne dich gar nicht vorstellen. Mit wem soll ich mich jetzt vor Lachen krümmen? Ich weiß jedoch, dass du immer da bist, wenn ich dich brauche.

Ein großer Dank geht an meine tollen Freunde Claire, Anne, Hannah, Klara, Pauline, Tobi, Theresa. Ihr habt immer an mich geglaubt, mich unterstützt und Verständnis mit mir gehabt.

Konrad, danke, dass du mich immer in meinen Entscheidungen unterstützt, mir beim Durchdenken und Entscheiden hilfst, mit mir die tollsten Workations (Danke, Corona) und Urlaube verbringst. Du stellt immer wieder sicher, schöne Momente im Alltag zu haben und bringst mir immer wieder "life" in die work-life-balance, wenn ich es brauche.

Ein riesengroßer Dank geht an meine Eltern, die viel aufbringen mussten, um meiner Schwester Iva und mir ein besseres und sicheres Leben zu ermöglichen. Weil ein "Danke" nicht ausdrücken kann wie ich fühle, und insbesondere nicht, ako nije na našem: Hvala mojim roditeljima, Vlatki i Mariju Kraljević. Koji su sve od sebe dali da svojoj djeci omoguće dobar život. Hvala najboljoj sestri na svijetu: Ivi Kraljević. Vi ste uvijek vjerovali u mene, sve pokušali da mi olakšate ovaj rad i znam da vam nije uvijek

palo lako vidjeti da mi ne možete oduzeti stres i rad, nego da ja to moram uspjeti. Ali svi smo znali, da ću ja to uspjeti, jer se vodi rezilijentnost u našoj obitelj. Volim vas.